

DEVELOPMENT OF NOVEL FLUORESCENT SENSORS FOR THE SCREENING OF EMERGING CHEMICAL POLLUTANTS IN WATER

Report to the
Water Research Commission

by

H Montaseri, SA Nsibande and PBC Forbes
Chemistry Department, University of Pretoria

WRC Report No. 2752/1/19
ISBN 978-0-6392-0090-3

October 2019



Obtainable from

Water Research Commission

Private Bag X03

GEZINA, 0031

orders@wrc.org.za or download from www.wrc.org.za

DISCLAIMER

This report has been reviewed by the Water Research Commission (WRC) and approved for publication. Approval does not signify that the contents necessarily reflect the views and policies of the WRC nor does mention of trade names or commercial products constitute endorsement or recommendation for use.

EXECUTIVE SUMMARY

BACKGROUND

Emerging chemical pollutants (ECPs) are chemicals which do not have a regulatory status (specifically in this case with respect to water quality legislation in South Africa), but which may have an adverse effect on human health and the environment. Sources and environmental pathways of ECPs in surface waters have been increasingly associated with waste and wastewaters arising from industrial, agricultural and municipal activities. The ECPs of current concern globally include a wide range of compounds including phthalates, pesticides, polychlorinated biphenyls (PCBs), polycyclic aromatic hydrocarbons (PAHs) and Bisphenol A, in addition to disinfectants, pharmaceuticals and hormones. The **four target ECPs** from these compound classes included in this study were **acetaminophen, triclosan, atrazine and polycyclic aromatic hydrocarbons** (PAHs).

Data relating to the occurrence of ECPs in South African waters is currently very limited, which can be ascribed in part to the high cost of performing the complex analyses involved. In this project we addressed this shortcoming by further developing **novel fluorescence sensors for target ECPs** of relevance to South Africa, as a follow-on study from our previous work in this regard (WRC Project K5/2438).

Screening techniques have the advantage of allowing for a large sample set to be analysed, thus trends in time and place can be established. This is possible due to the speed and low cost which screening methods present. Samples which screen positive can then be targeted for comprehensive, quantitative analysis (such as by LC-MS/MS), if required. We therefore sought to develop sensitive and selective novel fluorescence sensors by utilising **quantum dot (QD) nanomaterials** in conjunction with a polymer matrix to immobilise the QDs and to pre-concentrate the target ECPs.

AIMS

The aims of the project were thus to:

1. Investigate the effects of various parameters, such as pH and contact time, on the fluorescence sensing of the selected ECPs.
2. Determine the effects of potential interfering compounds on the selectivity and fluorescence sensing capability of the QD sensors.
3. Develop methods to functionalise the QD materials via MIP overcoating and to investigate the impact thereof on the selectivity of the fluorescence sensors towards the target ECPs.
4. Optimize the methodology to immobilize the QDs in siloxane polymers in order to generate solid fluorescence sensor prototypes.
5. Test and optimize the fluorescence sensor prototypes for the target compounds in real water samples (tap water and river water).

STATE OF KNOWLEDGE ON THE TOXICOLOGICAL LEVELS OF THE TARGET ANALYTES

The current state-of-knowledge regarding the toxicological levels of the target compounds was investigated, focussing on toxicity threshold values of vulnerable organisms and applicable guideline values, where available. These are compared to typical reported environmental concentrations of the target compounds in surface waters.

Triclosan (TCS) is a biocide which is routinely added to a wide range of personal care, veterinary, industrial and household products. It can persist in the environment and show toxicity towards various organisms. The continuous exposure of aquatic organisms to TCS and its bioaccumulation potential have led to detectable levels of this biocide in a wide array of aquatic species. Mammalian systemic toxicity studies have shown that TCS is neither acutely toxic, mutagenic, carcinogenic, nor a developmental toxicant, while endocrine disruption related to thyroid hormone homeostasis disruption and possibly the reproductive axis has been noted. Moreover, there is strong evidence that aquatic species such as algae, invertebrates and certain types of fish are much more sensitive to TCS than mammals. Specifically, algae is highly sensitive indicator organism that may be impacted by TCS occurrences in surface waters at levels of 200-2,800 ng L⁻¹, where the worldwide concentration has been found to range from 1.4-40,000 ng L⁻¹. The Minnesota Department of Health (MDH) has developed a guidance value of 50 ppb (50,000 ng L⁻¹) for triclosan in drinking water, whilst the Canadian Federal Water Quality Guideline for the protection of aquatic life from adverse effects of triclosan is 380 ng L⁻¹.

Acetaminophen (AC), or paracetamol, is an over-the-counter analgesic. Although acetaminophen is removed from wastewater by chemical oxidation processes, it has been detected in surface waters, wastewater and drinking water throughout the world. Concentrations of acetaminophen in surface water of over 10,000 ng L⁻¹ have been reported, including in Africa (107,000 ng L⁻¹ in Kenya and 59,000 ng L⁻¹ in South Africa) which are higher than the predicted no-effect concentration (PNEC) of 9200 ng L⁻¹. Hence, AC might represent a threat for non-target organisms. A guidance value of 200 ppb (200,000 ng L⁻¹) for acetaminophen in drinking water has been set by the MDH.

Polycyclic aromatic hydrocarbons (PAHs) are ubiquitous environmental contaminants, which are emitted from combustion processes. However, PAHs generally have low solubility in water and are therefore typically found at very low concentrations in this matrix, and are rather associated with the sediments. Some local studies have shown that PAHs occur at very low concentrations in local water systems with mean concentrations ranging from 0.035-532 µg L⁻¹. However, even at these low concentrations, some PAH compounds like benzo[a]pyrene are of concern as they have an LC50 of ~4 µg L⁻¹ with respect to cladoceran species. The reviewed literature showed that PAH exposure can lead to various toxicities leading to negative effects on some aquatic organisms.

Atrazine is a commonly used herbicide that has been frequently detected in local water systems. The typical concentrations that have been previously reported in WRC studies range from 0.01-0.19 µg L⁻¹. In this context, it is important to note that the World Health Organization (WHO) has set the guideline limit for atrazine in

drinking water at 0.1 mg L^{-1} and the reported concentrations are well below this limit. However, it is also important to note that some studies have reported carcinogenic effects at much lower concentrations in the range of $50\text{-}649 \text{ ng L}^{-1}$. The negative toxicological effects that atrazine can potentially cause to aquatic organisms result in it being a contaminant of environmental concern.

Recent reports have thus highlighted the **widespread occurrence of the target contaminants in surface waters**, as well as their related **potential toxic effects to aquatic organisms**. In water systems a mixture of compounds is invariably present, therefore the risk of additive and synergistic toxic effects cannot be ignored. Local hotspots of elevated concentrations of contaminants near sources may also occur, which are outside the ranges of expected environmental levels reported in the literature. It is therefore important to monitor the levels of the target compounds in South African water systems as widely as possible in order to effectively and proactively manage our resources and to minimize potential negative toxicological effects.

OPTIMIZATION AND APPLICATION OF QUANTUM DOT BASED FLUORESCENCE SENSORS

Different quantum dot materials were fabricated for application as fluorescence sensors for the detection of the target emerging chemical pollutants. Various parameters are crucial for fluorescence sensor development and they needed to be optimized in order to realize the full potential and performance of the sensor material. These parameters include contact time (or incubation time) with target analyte, excitation wavelength during fluorescence measurements, the concentration of the sensor solution, the ratio of analyte-to-sensor solutions, etc.

Aqueous L-Cysteine (L-Cys) capped CdSe/ZnS quantum dots were synthesized and applied as a fluorescence sensor for **acetaminophen**. The L-Cys-CdSe/ZnS QDs were of a zinc blende crystal structure and displayed excellent fluorescence intensity and photostability and provided a photoluminescence quantum yield of 77%. The fluorescence of L-Cys-CdSe/ZnS QDs was enhanced by the introduction of AC allowing for the development of a simple and rapid method for AC detection. Under optimal conditions, $F-F_0$ was linearly proportional to AC concentration from $3.0\text{-}100 \text{ nmol L}^{-1}$ with a **detection limit of 1.6 nmol L^{-1}** . Some related pharmaceutical compounds including epinephrine hydrochloride (EP), L-ascorbic acid (AA), uric acid (UA), dopamine hydrochloride (DA) and 4-aminophenol (4-AP) did not result in a large interference with the sensing of AC. The probe was also successfully applied in the determination of AC in tap and river water matrices.

Core-shell structured CdSe/ZnS fluorescent QDs were synthesized based on organometallic synthesis and a ligand exchange reaction to cap glutathione (GSH) on the surface for **triclosan sensing**. The **GSH-CdSe/ZnS QDs** showed excellent photostability and a photoluminescence quantum yield of 89%. The fluorescence of the GSH-CdSe/ZnS QDs was enhanced by the introduction of TCS likely based on fluorescence resonance energy transfer from TCS to the QDs, thus allowing for its use as a “turn on” fluorescence probe for the detection and determination of TCS. A linear response was observed in the TCS concentration range of $10\text{-}300 \text{ nmol L}^{-1}$ with a **limit of detection of 3.7 nmol L^{-1}** . The probe displayed good recoveries (94-118%) for the determination of TCS in tap and river water samples.

The fluorescent nanoparticles that were fabricated for **atrazine pesticide** were **CdSeTe/ZnS QDs**, while for **PAHs, graphene quantum dots (GQDs)** were prepared. Upon interaction of the CdSeTe/ZnS sensor with

atrazine, the fluorescence was quenched linearly within the $2-10 \times 10^{-7} \text{ mol L}^{-1}$ range and the **LOD was determined to be $1.8 \times 10^{-7} \text{ mol L}^{-1}$** . The QDs were able to interact with **PAHs** through π - π interaction and for phenanthrene the sensor showed a linear response over $1-5 \times 10^{-7} \text{ mol L}^{-1}$ and the **LOD was found to be $2.5 \times 10^{-8} \text{ mol L}^{-1}$** . The studies showed that a very small amount of the prepared QD materials (0.5 mg L^{-1}) was required to prepare a responsive sensor solution. This is due to the inherently highly fluorescent properties of QDs and has the added advantage of lowering the costs of employing the sensor materials. Further, the results show that a **short contact time is required (5 min)** between the sensor solution and analyte to give a measurable fluorescence response.

FUNCTIONALISATION OF QUANTUM DOTS

Molecularly imprinted polymers (MIPs) are synthetic polymeric materials possessing specific recognition sites complementary in size, shape and functional groups to the template molecule (target). During the molecular imprinting process, functional monomers are located around the template molecules by non-covalent interaction or reversible covalent interaction, followed by polymerization and template removal. The target molecule can then be selectively distinguished from other analytes based on the resulting cavities. We thus used MIPs to functionalise QDs in order to **combine the selectivity of MIPs with the sensitivity of QDs**.

Specifically, a molecularly imprinted coating with **acetaminophen as template molecule** was grafted onto L-Cys-CdSe/ZnS quantum dots using 3-aminopropyltriethoxysilane as the functional monomer and tetraethyl orthosilicate as the cross-linker via an adapted Stöber method, in order to develop a selective and sensitive fluorescence sensor for the determination of AC in water samples. The resulting MIP@QDs were characterized by Fourier-transform infrared spectroscopy, high resolution transmission electron microscopy, and fluorescence spectrophotometry which confirmed the polymer coating. The fluorescence quenching of the sensor provided good linearity over the AC concentration range of $1.0-300 \text{ nmol L}^{-1}$ with a **detection limit of 0.34 nmol L^{-1}** and the sensor showed good photostability over 5 days. The recoveries of AC in water samples at various spiking levels varied from 95% to 114%.

AC-templated MIP@QDs were prepared and used as a homogenous fluorescence sensing platform for the determination of AC in aqueous media under optimized conditions of 0.8 mg MIP@QDs in 3.0 mL^{-1} with an **incubation time of 14 min**. The functional groups ($-\text{NH}_2$) of the silica shell interact with the AC molecules via hydrogen bonding during the synthesis process. After removing AC molecules via solvent extraction, imprinted binding cavities remained in the nanoparticle material that enabled rebinding of the AC molecules selectively.

AC could be detected at low levels based on the fluorescence quenching of MIP@QDs likely through the mechanism of charge transfer induced energy transfer from the MIP@QDs to AC, allowing for the application of the fluorescence sensor to AC monitoring in real water samples. A simple sensor for AC molecules is thus reported which detects this analyte selectively and can be applied to improve water quality, as AC can accumulate in water systems and cause long term health effects, even at low concentrations.

A **CdSeTe/ZnS@MIP fluorescence sensor for the pesticide atrazine** was synthesized and characterized using various techniques to confirm functionalization of the core/shell QDs with the MIP polymer. Application of the sensor towards atrazine detection showed a linear response (fluorescence quenching) with increasing atrazine concentration in the range from $2-20 \times 10^{-7} \text{ mol L}^{-1}$. The **detection limit of $0.80 \times 10^{-7} \text{ mol L}^{-1}$** is within the concentration range expected in environmental water samples. The $-\text{COOH}$ functional groups on the MIP

monomer units were responsible for interaction with atrazine via hydrogen bonding, and due to size exclusion, the sensor was selective for atrazine compared to analogous compounds. When applied in real water samples spiked with atrazine satisfactory recoveries were obtained ranging from 92-118%.

IMMOBILIZATION OF QUANTUM DOTS

The development of luminescence based sensing devices ideally requires **immobilization** of the sensing indicators, in this case the quantum dots, onto or into **solid supports** to form active solids for working in flowing solutions and allowing for re-use. Forming such active materials also brings the advantage of **reducing the potential for leaching** of the QDs into the solution while equilibrium with the target analyte is being established. The immobilization process, however, may reduce the luminescence efficiencies of the QDs due to aggregation, oxidation and poor adhesion on the support material. The challenge therefore, is to retain the properties of the QDs after the immobilization process.

Here we focus on immobilising QDs into **polydimethylsiloxane** (PDMS) because of its advantages which include low cost, non-toxicity, flexibility, as well as its ability to absorb organic non-polar analytes. We therefore fabricated thin films of PDMS embedded with QDs and studied the properties of the resulting PDMS-QD material with the intention to use it to detect ECP compounds in future work. We therefore obtained a turnkey complete spin coater assembly consisting of the spin coater, vacuum pump, degassing assembly, chemicals and consumables in order to assist in achieving these aims.

Unfortunately the first spin coater which was delivered was found to be faulty after much trouble shooting, which delayed progress initially. The supplier subsequently sent a new spin coater, which was successfully commissioned and allowed for the preparation of excellent quality thin films in which QDs were homogeneously embedded. Both **red fluorescing and blue fluorescing thin films** were thus prepared, based on use of **CdSeTe/ZnS QDs and graphene QDs** respectively. The CdSeTe/ZnS@PDMS thin film was **tested for atrazine detection** and an enhanced fluorescence signal was found.

OVERALL CONCLUSIONS

Reliable and robust analytical techniques are needed for the detection of **ECPs in surface waters**. A fluorescence probe monitoring approach utilising **quantum dots offers an alternative sensing technique** to traditional methods, with **clear advantages** including easy operation, low cost, a fast and simple experimental process, and high sensitivity towards different molecular structures with different emission wavelengths. We successfully used MIPs to functionalise the QDs in order to **combine the selectivity of MIPs with the sensitivity of QDs**.

The synthesised fluorescent QD@PDMS thin films hold great potential in designing **reusable rapid field monitoring sensors for targeted ECP compounds in water systems**. The sensitivity and stability of QDs combined with the inertness, flexibility, and ability of PDMS to pre-concentrate analytes will open doors for designing sensitive and robust fluorescence sensors for routine monitoring of ECPs.

RECOMMENDATIONS

The development of South African guideline values or water quality limits for ECPs should receive attention from policy makers in order to safeguard human health. The Department of Health and the Department of Water and Sanitation are encouraged to partner with the Water Research Commission to invest in the further development and ultimate use of novel monitoring technologies which can enhance and complement the current status quo regarding water management.

As a result of the positive outcomes of this project, further work on the optimization studies of the sensor materials is recommended, particularly with respect to the testing thereof for real water samples in which the presence of the target ECPs has been confirmed by traditional (chromatographic-mass spectrometric) methods. A portable sensor device should also be developed based on these sensor materials, to allow for on-site real-time monitoring of ECPs in surface waters. A non-targeted screening method based on a mixture of different QDs should be investigated, as well additional compound class type sensors, to enable early detection of overall change in water quality with respect to ECPs.

ACKNOWLEDGEMENTS

The Project Team acknowledges the financial support of this project which was provided by the Water Research Commission, as well as the guidance and support provided by the WRC Project Manager, Dr Eunice Ubomba-Jaswa.

Reference Group	Affiliation
Dr E Ubomba-Jaswa	Water Research Commission
Prof N Casey	University of Pretoria
Dr J Dabrowski	Confluent Environmental
Dr D Odusanya	Department of Water Affairs
Others	
Dr Shankara Radhakrishnan	University of Pretoria

Co-funding from the Photonics Initiative of South Africa (Grant PISA-15-DIR-06) and the National Research Foundation of South Africa (postgraduate student bursary for Sifiso Nsibande) is gratefully acknowledged. We also thank the Laboratory for Microscopy and Microanalysis, University of Pretoria (UP), for assistance with the microscopy analyses and Wiebke Grote of UP for the XRD measurements.

This page was intentionally left blank

CONTENTS

EXECUTIVE SUMMARY	i
ACKNOWLEDGEMENTS	vii
CONTENTS	ix
LIST OF FIGURES	xii
LIST OF TABLES	xv
ACRONYMS & ABBREVIATIONS	xvi
CHAPTER 1: INTRODUCTION	1
1.1 BACKGROUND TO THE PROJECT	1
1.2 AIMS OF THE PROJECT	1
1.3 SCOPE AND LIMITATIONS	2
1.4 CONTRIBUTIONS OF INDIVIDUAL CHAPTERS TO THE OBJECTIVES OF THE PROJECT	2
CHAPTER 2: State of knowledge on the toxicological levels of the target analytes	3
2.1 INTRODUCTION	3
2.2 TRICLOSAN	3
2.2.1 Sources of triclosan	4
2.2.2 Environmental occurrence and concentrations of triclosan in water resources	5
2.2.3 Toxicity considerations.....	9
2.2.3.1 Toxicity threshold of triclosan	10
2.2.4 Legal limits of triclosan.....	16
2.3 ACETAMINOPHEN.....	16
2.3.1 Sources of acetaminophen	17
2.3.2 Environmental occurrence & concentrations of acetaminophen in water sources	18
2.3.3 Toxicity threshold of acetaminophen	20
2.3.4 Legal limits of acetaminophen	23
2.4 POLYCYCLIC AROMATIC HYDROCARBONS	23
2.4.1 Sources and occurrence	23
2.4.2 Toxicity of PAHs.....	25
2.4.3 Guideline limits for PAHs	28
2.5 PESTICIDES: ATRAZINE.....	29
2.5.1 Sources and occurrence of atrazine in the environment	29
2.5.2 Toxicity of atrazine	31
2.5.3 Legal limits for atrazine in water	32
2.6 CONCLUSION	32
CHAPTER 3: The optimization and application of quantum dot based fluorescence sensors	35
3.1 INTRODUCTION	35
3.2 ACETAMINOPHEN.....	37
3.2.1 Determination of acetaminophen with L-Cys capped CdSe/ZnS QDs	37
3.2.2 Optimization of the determination of acetaminophen	38
3.2.2.1 Effect of aqueous L-Cys-CdSe/ZnS QDs concentration	38
3.2.2.2 Effect of incubation time	39
3.2.2.3 Stabilization of fluorescence intensity	40
3.2.2.4 Fluorescence behavior of L-Cys-CdSe/ZnS QDs in the presence of AC.....	41
3.2.2.5 Calibration curve, limit of detection and limit of quantification.....	42
3.2.2.6 Proposed mechanism.....	43
3.2.2.7 Determination of Förster distance	44

3.2.2.8	Effect of potential interfering analytes on the fluorescence of L-Cys-CdSe/ZnS QDs	44
3.2.2.9	Analytical application	47
3.3	TRICLOSAN	47
3.3.1	Determination of TCS with GSH capped CdSe/ZnS QDs	47
3.3.2	Optimization of the determination of triclosan	48
3.3.2.1	Effect of aqueous GSH-CdSe/ZnS QDs concentration	48
3.3.2.2	Effect of incubation time	49
3.3.2.3	Stabilization of fluorescence intensity	50
3.3.2.4	Fluorescence behavior of GSH capped CdSe/ZnS QDs in the presence of TCS	51
3.3.2.5	Calibration curve, limit of detection and limit of quantification	52
3.3.2.6	Proposed mechanism	54
3.3.2.7	Determination of Förster distance	55
3.3.2.8	Effect of potential interfering analytes on GSH-CdSe/ZnS QDs	55
3.3.2.9	Analytical application	58
3.4	ATRAZINE	59
3.4.1	Introduction	59
3.4.2	Materials & Methods	60
3.4.2.1	Materials	60
3.4.2.2	Preparation of CdSeTe/ZnS QDs	60
3.4.2.3	Procedure for detection of atrazine	60
3.4.3	Results and discussion	61
3.4.3.1	TEM	61
3.4.3.2	FTIR	62
3.4.3.3	XRD	62
3.4.3.4	Fluorescence and absorption properties	63
3.4.3.5	Optimisation	64
3.4.3.6	Fluorescence behaviour of L-Cys-CdSeTe/ZnS in the presence of atrazine	65
3.5	POLYCYCLIC AROMATIC HYDROCARBONS	67
3.5.1	Introduction	67
3.5.2	Materials and methods	68
3.5.2.1	Preparation of GQDs from graphite	68
3.5.2.2	Preparation of GQDs from citric acid	68
3.5.2.3	Sensing experiments	69
3.5.3	Results & Discussion	69
3.5.3.1	FT-IR characterization	69
3.5.3.2	HRSEM	70
3.5.3.3	Powder XRD and Raman spectroscopy	70
3.5.3.4	Fluorescence and absorption	72
3.5.3.5	Application for PAH sensing	75
3.6	CONCLUSION	78
CHAPTER 4: The functionalisation of Quantum dots		80
PART A – MOLECULARLY IMPRINTED POLYMER CAPPED CORE/SHELL QUANTUM DOTS FOR ACETAMINOPHEN DETECTION		80
4.1	INTRODUCTION	80
4.2	EXPERIMENTAL	82
4.2.1	Reagents and materials	82
4.2.2	Characterization	82
4.2.3	Synthesis of MIP-capped L-Cys-CdSe/ZnS QDs	83
4.2.4	Optimization experiments	83
4.2.5	Sample analysis	83

4.3	RESULTS AND DISCUSSION	84
4.3.1	Characterization of MIP- and NIP-Capped CdSe/ZnS QDs	84
4.3.1.1	FT-IR analysis	84
4.3.1.2	TEM analysis	85
4.3.2	Optimization of sensing variables	87
4.3.2.1	Concentration of MIP@QDs	87
4.3.2.2	Effect of incubation time	88
4.3.2.3	Photostability study	89
4.3.3	Fluorescence sensing of acetaminophen using AC-templated molecularly imprinted polymer-quantum dots	90
4.3.4	Selectivity of the sensor to AC	92
4.3.5	Proposed sensing mechanism of the MIP-capped CdSe/ZnS QDs	93
4.3.6	Practical application and performance comparison	94
	PART B – MOLECULARLY IMPRINTED POLYMER CAPPED CORE/SHELL QUANTUM DOTS FOR ATRAZINE DETECTION	96
4.4	INTRODUCTION	96
4.5	MATERIALS AND METHODS	96
4.5.1	Chemicals	96
4.5.2	Equipment	97
4.5.3	Synthesis of CdSeTe/ZnS QDs	97
4.5.4	Functionalisation of CdSeTe/ZnS QDs with MIPs	98
4.5.5	Procedure for fluorescence sensing of atrazine	98
4.6	RESULTS AND DISCUSSION	100
4.6.1	Characterization	100
4.6.1.1	X-ray diffraction (XRD)	100
4.6.1.2	FT-IR analysis	100
4.6.1.3	TEM analysis	101
4.6.1.4	Optical properties	103
4.6.1.5	Sensing application	104
4.6.1.6	Selectivity of the sensor to atrazine	105
4.6.1.7	Practical application	106
4.7	CONCLUSION	108
	CHAPTER 5: The immobilization of Quantum dots	109
5.1	INTRODUCTION	109
5.2	PREPARATION OF QUANTUM DOT PDMS FILMS	110
5.2.1	Chemicals and equipment	110
5.2.2	Preparation of PDMS@QD films	110
5.2.3	Sensing of atrazine using the PDMS@QDs thin film	111
5.3	RESULTS AND DISCUSSION	111
5.3.1	Previous work	111
5.3.2	Optical properties of the PDMS@QD films	113
5.3.3	Application of PDMS@QD thin films for atrazine sensing	115
5.4	CONCLUSION	117
	CHAPTER 6: CONCLUSIONS & RECOMMENDATIONS	118
6.1	CONCLUSIONS	118
6.2	RECOMMENDATIONS	122
	REFERENCES	123
	APPENDIX: CAPACITY BUILDING & KNOWLEDGE DISSEMINATION	138

LIST OF FIGURES

Figure 2.1: Chemical structure of triclosan.....	3
Figure 2.2: Published environmental occurrence data for triclosan and triclocarban in comparison to available toxicity threshold values for various indicator organisms. Concentrations are presented on a logarithmic scale in parts-per-trillion by volume (ng L^{-1}) or mass (ng kg^{-1}) for liquid and solid matrices, respectively. Concentrations in activated sludge and biosolids are expressed on a dry weight basis. Pore water concentrations were calculated from published environmental monitoring data. Overlap of occurrence data with toxicity threshold values of biota residing in the respective environmental compartment indicate locales of unhealthy conditions allowing for chronic or acute toxic effects. WWTP: wastewater treatment plant (Chalew & Halden, 2009).....	9
Figure 2.3: Structure of acetaminophen	16
Figure 2.4: Schematic diagram showing the possible route routes of pesticide circulation in the environment (adapted from Kosikowska and Biziuk (2010)).....	29
Figure 3.1: Effect of the concentration of aqueous L-Cys-CdSe/ZnS QDs on fluorescence in the absence and presence of 5.0 nmol L^{-1} AC at excitation wavelength 300 nm, where F_0 is the fluorescence intensity without AC and F is the fluorescence intensity with AC.....	39
Figure 3.2: Effect of interaction time on the fluorescence intensity of the L-Cys capped CdSe/ZnS QD-AC system at an excitation wavelength of 300 nm.....	40
Figure 3.3: PL stability of the hydrophilic QDs measured before and after 5 days of exposure to ambient light (300 nm excitation).	41
Figure 3.4: The fluorescence spectra of L-Cys-CdSe/ZnS QDs with different concentrations of acetaminophen at an excitation wavelength of 300 nm.	42
Figure 3.5: Linear graph of $F-F_0$, where F and F_0 are the fluorescence intensities of the QDs with and without different acetaminophen concentrations respectively, versus AC concentration.....	43
Figure 3.6: Florescence spectrum of acetaminophen ($1.0 \times 10^{-5} \text{ mol L}^{-1}$) at excitation wavelength 300 nm (A) and UV-Vis absorption spectrum of L-Cys-CdSe/ZnS QDs (B).	44
Figure 3.7: Effect of other pharmaceutical analytes on the fluorescence emission intensity of the L-Cys-CdSe/ZnS QDs probe at an emission wavelength of 595 nm. The concentration of AC and each of the other analytes was 100 nmol L^{-1} and L-Cys-CdSe/ZnS QDs was $1.0 \text{ mg}/3.0 \text{ mL}$. $F-F_0$ is the fluorescence intensity of QDs in the presence and absence of the analytes. The excitation wavelength was 300 nm. Epinephrine hydrochloride (EP), L-ascorbic acid (AA), uric acid (UA), dopamine hydrochloride (DA), 4-aminophenol (4-AP).	45
Figure 3.8: Effect of the concentration of aqueous GSH-CdSe/ZnS QDs in the presence of 70 nmol L^{-1} TCS. The experimental conditions were excitation wavelength, 300 nm; slit widths of excitation and emission, 5 nm.	49
Figure 3.9: Effect of reaction time on the fluorescence intensity of GSH capped CdSe/ZnS QDs in the presence of 70 nmol L^{-1} TCS. The experimental conditions were GSH-CdSe/ZnS QDs 1.5 mg in 3.0 mL^{-1} ; excitation wavelength, 300 nm; slit widths of excitation and emission, 5 nm.	50
Figure 3.10: PL stability of the hydrophilic QDs measured before and after 5 days of exposure to ambient light. The experimental conditions were GSH-CdSe/ZnS QDs 1.5 mg in 3.0 mL^{-1} ; excitation wavelength, 300 nm; slit widths of excitation and emission, 5 nm.	51

Figure 3.11: The fluorescence spectra of GSH-CdSe/ZnS QDs in the presence of different concentrations of triclosan. The experimental conditions were GSH-CdSe/ZnS QDs 1.5 mg in 3.0 mL ⁻¹ ; excitation wavelength, 300 nm; slit widths of excitation and emission, 5 nm.	52
Figure 3.12: Linear graph of F-F ₀ /F ₀ versus TCS concentration. The experimental conditions were GSH-CdSe/ZnS QDs 1.5 mg in 3.0 mL ⁻¹ ; excitation wavelength, 300 nm; slit widths of excitation and emission, 5 nm.	53
Figure 3.13: Fluorescence spectrum of TCS (1.4×10 ⁻⁵ mol L ⁻¹) at excitation wavelength 310 nm (A) and UV-Vis absorption spectrum of GSH-CdSe/ZnS QDs (B).	55
Figure 3.14: Effect of other analytes on the fluorescence emission intensity of the GSH-CdSe/ZnS QDs probe at an emission wavelength of 598 nm. The concentration of TCS and each of the other analytes was 180 nmol L ⁻¹ and GSH-CdSe/ZnS QDs was 1.5 mg/3.0 mL. F-F ₀ /F ₀ relates to the fluorescence intensity of QDs in the presence and absence of the analytes. The excitation wavelength was 300 nm. Analytes were 2,4,6-trichlorophenol (2,4,6-TCP), 2,3,4-trichlorophenol (2,3,4-TCP), 2,4-dichlorophenol (2,4-DCP), 4-chlorophenol (4-CP), 4-hydroxybenzoic acid (a paraben), Bisphenol A (BPA), and Triclocarban (TCC).....	56
Figure 4.1: FT-IR spectra of AC, L-Cys, L-Cys-CdSe QDs, L-Cys-CdSe/ZnS QDs, MIP@QDs (with template removed) and NIP@QDs.....	85
Figure 4.2: TEM images of (A) L-Cys-CdSe QDs (B) L-Cys-CdSe/ZnS QDs (C) MIP@QDs and (D) NIP@QDs (scale bar 100 nm in all cases).....	86
Figure 4.3: Size distribution histogram of (A) L-Cys-CdSe QDs (B) L-Cys-CdSe/ZnS QDs, (C) MIP@QDs and (D) NIP@QDs.....	87
Figure 4.4: Effect of the MIP@QD concentration on PL quenching efficiency (n=3). The concentration of AC was fixed at 300.0 nmol L ⁻¹ . The experimental conditions were excitation wavelength 350 nm; slit widths of excitation and emission, 5.0 nm.	88
Figure 4.5: Effect of incubation time on relative fluorescence of MIP@QDs with AC (n=3). The experimental conditions were MIP@QDs: 0.8 mg in 3.0 mL ⁻¹ ; AC: 300.0 nmol L ⁻¹ ; excitation wavelength, 350 nm; slit widths of excitation and emission, 5 nm.	89
Figure 4.6; Photostability of MIP@QDs over 40 min (values are the average of three measurements). The experimental conditions were MIP@QDs, 0.8 mg in 3.0 mL ⁻¹ ; excitation wavelength, 350 nm; slit widths of excitation and emission, 5.0 nm.	90
Figure 4.7: Average photostability of MIP@QDs and NIP@QDs over 5 days (n=3). The experimental conditions were MIP@QDs or NIP@QDs, 0.8 mg in 3.0 mL ⁻¹ ; excitation wavelength, 350 nm; slit widths of excitation and emission, 5.0 nm.....	90
Figure 4.8: Fluorescence emission spectra of MIP@QDs (A) and NIP@QDs (B) in the presence of varying concentrations of AC. The experimental conditions were MIP@QDs or NIP@QDs at 0.8 mg in 3.0 mL ⁻¹ ; excitation wavelength, 350 nm; slit widths of excitation and emission, 5 nm. The inset graphs display the corresponding Stern-Volmer plots of MIP@QDs and NIP@QDs with the addition of AC (all results are the average of three replicates).....	92
Figure 4.9: Fluorescence quenching of MIP@QDs and NIP@QDs by different analytes at 300.0 nmol L ⁻¹ . The experimental conditions were MIP@QDs, or NIP@QDs 0.8 mg in 3.0 mL ⁻¹ ; excitation wavelength 350 nm; 5 nm excitation and emission slit widths. L-tryptophan (TRY), ascorbic acid (AA), epinephrine hydrochloride (EP), uric acid (UA), dopamine hydrochloride (DA), ketoprofen (KTP), sulfamethoxazole (SM), diclofenac sodium salt (Dic), estradiol (ES), L-3,4-dihydroxyphenylalanine (L-Dopa) and 4-aminophenol (4-AP) (results are the average of three replicates).....	93
Figure 4.10: UV/Vis absorption spectrum of AC (A) and MIP@QDs (B) and fluorescence emission spectrum of MIP coated QDs (C).	94

Figure 4.11: Schematic illustration of the synthesis of hydrophobic CdSeTe/ZnS QDs through stepwise hot injection of organometallic precursors. The reaction was continuously purged with argon while monitoring time and temperature. Water soluble QDs were obtained after ligand exchange with L-cysteine.....	97
Figure 4.12: Schematic illustration of simultaneous silica encapsulation and vinyl modification of the L-Cys CdSeTe/ZnS QDs.....	98
Figure 4.13: Schematic illustration of the binding of atrazine (template) carboxyl groups to MAA through hydrogen bonding (green dotted lines) on the MIP matrix and the specific site cavities left after removal of the template.	99
Figure 4.14: The theoretical interaction of atrazine with MAA monomers through hydrogen bonding. The numbers are the theoretical hydrogen bond lengths in Å (Han et al., 2017).....	99
Figure 4.15: Powder X-ray diffraction patterns for CdSeTe QDs, CdSeTe/ZnS QDs, CdSeTe/ZnS-MPS and CdSeTe/ZnS@MIP showing the characteristic zinc blende crystal structure which was retained after polymerization.....	100
Figure 4.16: FTIR spectra of CdSeTe QDs, CdSeTe/ZnS QDs, CdSeTe/ZnS-MPS and CdSeTe/ZnS@MIP.	101
Figure 4.17: TEM images showing spherically shaped CdSeTe (A) and CdSeTe/ZnS (B) QDs dispersed in water. The insets show statistical size distributions with Gaussian fits (black curves). The average particle size (mean ± HWHM) for the core was 3.1 ± 0.1 nm while the core/shell was 5.0 ± 0.5 nm. Images in (C) show the CdSeTe/ZnS@MIP material with the QDs imbedded inside the polymer's fiber-like network.	102
Figure 4.18: Fluorescence emission spectra of CdSeTe QD at 575 nm, CdSeTe/ZnS QD at 605 nm, and CdSeTe/ZnS@MIP at 599 nm. The excitation wavelength was 363 nm for all measurements.....	103
Figure 4.19; Absorption spectra (dotted lines) of CdSeTe QDs, CdSeTe/ZnS QDs and CdSeTe/ZnS@MIP along with corresponding emission spectra.	104
Figure 4.20; The fluorescence spectra of L-Cys-CdSeTe/ZnS@MIP in the presence of varying concentrations of atrazine ($2-20 \times 10^{-7}$ mol L ⁻¹). The inset shows the linear response of F_0/F versus atrazine concentration where F_0 is the fluorescence intensity of CdSeTe/ZnS@MIP without atrazine and F is the fluorescence intensity after interaction with atrazine ($n = 3$).	105

LIST OF TABLES

Table 2.1: Environmental concentrations of triclosan (SCCS, 2010).....	6
Table 2.2: Effects of TCS on freshwater (FW) and marine (SW) organisms (Dann & Hontela, 2011).	12
Table 2.3: Acute toxicity data for triclosan (Brausch & Rand, 2011).....	13
Table 2.4: Chronic toxicity data of triclosan (Brausch & Rand, 2011).....	14
Table 2.5: Environmental concentrations of acetaminophen.	19
Table 2.6: Effects of acetaminophen on different organisms	22
Table 2.7: Natural and anthropogenic sources of polycyclic aromatic hydrocarbons (PAHs).	24
Table 2.8: The 16 PAHs included in the U.S. EPA priority pollutant list (Manoli & Samara, 1999).	24
Table 2.9: Typical range of PAH concentrations in runoff and river water in South Africa (Chimuka et al., 2015).	25
Table 2.10: PAHs and their toxic equivalency factors (TEFs) expressed relative to BaP (Nisbet & LaGoy, 1992).	26
Table 2.11: Carcinogenic classification of PAH compounds by different agencies (ATSDR, 2012).....	27
Table 2.12: Existing water quality standards for PAHs. (Adapted from U.S. EPA, 2010).....	28
Table 2.13: Physicochemical properties of atrazine.....	30
Table 2.14: Concentration ($\mu\text{g L}^{-1}$) of atrazine sampled over four seasons in drinking water in areas across South Africa. Average concentrations are indicated (n=3) (Patterton, 2013).....	31
Table 2.15: Guideline values for atrazine and its metabolites in drinking water (WHO, 2011).....	32
Table 3.1: Comparison of some analytical methods for the determination of AC in water.	43
Table 3.2: Chemical structures of potentially interfering analytes.....	46
Table 3.3: Analytical results for the determination of recoveries of AC spiked in tap and river water samples using L-Cys-CdSe/ZnS QDs.....	47
Table 3.4: Comparison of some analytical methods for the determination of TCS in water samples.....	54
Table 3.5: Chemical structures of potentially interfering analytes.....	57
Table 3.6: Analytical results for the determination of TCS in tap and river water samples using GSH-capped CdSe/ZnS QDs.	59
Table 4.1: Spiked recovery results for the determination of AC in water samples using 2 mL of 0.8 mg of MIP@QDs in 3 mL of Millipore water and 200 μL of AC standard solution (n=3).....	94
Table 4.2: Comparison of the proposed fluorescence method with other recently reported methods for AC determination in water samples.....	95
Table 4.3: Comparison of the performance of the CdSeTe/ZnS@MIP sensor with other sensors for atrazine detection.	107

ACRONYMS & ABBREVIATIONS

AA	L-ascorbic acid
AC	Acetaminophen
ACE	Associated Chemical Enterprises
ADI	Acceptable daily intake
AIBN	2,2'azobisisobutyronitrile
amPA5	Amphiphilic pillar [5] arene
amPA5-RGO	Amphiphilic pillar [5] arene (amPA5) functionalized reduced graphene oxide
AO	Acridine orange
APIs	Active pharmaceutical ingredients
APTES	3-aminopropyltriethoxysilane
BAP	Benzo[a]pyrene
BAW	Bio-mimetic bulk acoustic wave
BLD	Below limit of detection
BLQ	Below limit of quantification
BPA	Bisphenol A
BRI	Biomarker response index
CNTs@TCS-MIPs	Carbon nanotubes@ triclosan-imprinted polymers
CS/CPE	Chitosan modified carbon paste electrode
CV	Cyclic voltammetry
CZE-UV	Capillary zone electrophoresis with UV detection
DA	Dopamine hydrochloride
Dic	Diclofenac sodium salt
DPV	Differential pulse voltammetry
DWMCL	Drinking water maximum contaminant level
ECOSAR	Ecological structure-activity relationships
ECPs	Emerging chemical pollutants
EDCs	Endocrine disrupting chemicals
EGDMA	Ethylene glycol dimethacrylate
ELS	Early life stage
EP	Epinephrine hydrochloride
ES	Estradiol
FRET	Förster resonance energy transfer
FW	Freshwater
FWA	Freshwater acute values
FWC	Freshwater chronic values
FWQG	Federal water quality guideline
GC-MS	Gas chromatography-mass spectrometry
GO	Graphene oxide

GQDs	Graphene quantum dots
GSH	Glutathione
GSI	Gonadosomatic index
HHOO	Human health organism only values
HHS	United States Department of Health and Human Services
HHWO	Human health water + organism values
HIS	Hepatosomatic index
HPLC-DAD	High-performance liquid chromatography-diode array detector
HPLC-MS/MS	High performance liquid chromatography-electron spray ionization-tandem mass spectrometry
HPLC-UV	High performance liquid chromatography-ultraviolet detection
HRTEM	High resolution transmission electron microscopy
IARC	International Agency for Research on Cancer
KTP	Ketoprofen
LC-ESI-MS/MS	Liquid chromatography/tandem mass spectrometry with electrospray ionization
L-cys	L-cysteine
LED	Light emitting diode
LOD	Limit of detection
LOEC	Lowest observed effect concentration
LOELs	Lowest observed effects levels
LOQ	Limit of quantification
MAA	Mercaptoacetic acid
MCL	Maximum contaminant level
MCLG	Maximum contaminant level goal
MDH	Minnesota Department of Health
MDL	Method limit of detection
MIC	Minimum inhibitory concentration
MIPs	Molecularly imprinted polymers
MPS	3-mercaptopropyl)trimethoxysilane
M-TCS	Methyl triclosan
MWCNT/PE/surfactant	Multi-walled carbon nanotubes/paste electrode in the presence of a surfactant
NAPQI	N-acetyl-p-benzoquinone imine
NC	Nanocrystal
NHGWS	New Hampshire ambient groundwater quality standards
NHSWS	New Hampshire surface water quality standards
NIH	National Institutes of Health
NIP	Non-imprinted polymers
NOAEL	Non-observed adverse effect level
NOEC	No-observed effects concentration
NPs	Nanoparticles

NSAID	Non-steroidal anti-inflammatory drug
nZnO-MWCNT/GCE	Nano-zinc oxide-multiwalled carbon nanotube/glassy carbon electrode
OA	Oleic acid
ODE	Octadec-1-ene
OLEC	Organoleptic effect (taste and odor) criteria
PAA	Poly(acrylic acid)
PAHs	Polycyclic aromatic hydrocarbons
PBDEs	Polybrominated diphenyl ethers
PBT	Persistence, bioaccumulation and ecotoxicity
PCBs	Polychlorinated biphenyls
PDMS	Polydimethylsiloxane
PEC	Predicted environmental concentration
p(HEMAGA)	Poly(2-hydroxyethylmethacrylate-methacryloylamidoglutamic acid)
PMAA	Polymethylmethacrylate
PNEC	Predicted no-effect concentration
PPCPs	Pharmaceutical and personal care products
PVP	Poly(vinyl pyrrolidone)
QDs	Quantum dots
SM	Sulfamethoxazole
SPR	Surface plasmon resonance
STPs	Sewage treatment plants
SW	Surface water
SWA	Saltwater acute values
SWC	Saltwater chronic values
SWV	Square wave voltammetry
TCC	Triclocarban
TCS	Triclosan
TEFs	Toxic equivalency factors
TEOS	Tetraethyl orthosilicate
TOPO	Trioctylphosphine oxide
TP	Toxicity potential
TRY	L-tryptophan
UA	Uric acid
U.S. EPA	United States Environmental Protection Agency
U.S. FDA	United States Food and Drug Agency
VTG	Vitellogenin
WHO	World Health Organization
WHP	Weighted hazard potential
WQC	U.S. EPA national recommended water quality criteria
WWTPs	Wastewater treatment plants
XRD	X-ray diffraction

2,3,4-TCP	2,3,4-trichlorophenol
2,4-DCP	2,4-dichlorophenol
2,4,6-TCP	2,4,6-trichlorophenol
4-AP	4-aminophenol
4-CP	4-chlorophenol
4-VP	4-vinylpyridine

This page was intentionally left blank

CHAPTER 1: INTRODUCTION

1.1 BACKGROUND TO THE PROJECT

There are varying definitions regarding emerging chemical pollutants (ECPs). In this study, we define ECPs based on the definition of Liu et al. (2014), in that ECPs are chemicals which do not have a regulatory status (specifically with respect to water quality legislation in South Africa), but which may have an adverse effect on human health and the environment (Liu et al., 2014). Sources and environmental pathways of these ECPs have been increasingly associated with waste and wastewaters arising from industrial, agricultural and municipal activities (Gavrilescu et al., 2014). The ECPs of current concern globally include a wide range of compounds including phthalates, pesticides, polychlorinated biphenyls (PCBs), polycyclic aromatic hydrocarbons (PAHs) and Bisphenol A, in addition to disinfectants, pharmaceuticals and hormones (Gavrilescu et al., 2014). The four target ECPs from these compound classes included in this study are acetaminophen, triclosan, atrazine and polycyclic aromatic hydrocarbons (PAHs).

Data relating to the occurrence of ECPs in South African waters is currently very limited, which can be ascribed in part to the high cost of performing the complex analyses involved. In this project we addressed this shortcoming by further developing novel fluorescence sensors for target ECPs of relevance to South Africa, as a follow-on study from our previous work in this regard (WRC Project K5/2438).

Screening techniques have the advantage of allowing for a large sample set to be analysed, thus trends in time and place can be established. This is possible due to the speed and low cost which screening methods present. Samples which screen positive can then be targeted for comprehensive, quantitative analysis (such as by LC-MS/MS), if required. We have developed sensitive and selective novel fluorescence sensors by utilising quantum dot (QD) nanomaterials in conjunction with a polymer matrix to immobilise the QDs and to pre-concentrate the target ECPs. This approach also lends itself to the development of a non-targeted screening method based on a mixture of different QDs or compound class type sensors, to enable early detection of overall change in water quality with respect to ECPs.

1.2 AIMS OF THE PROJECT

The aims of the project were:

1. To investigate the effects of various parameters, such as pH and contact time, on the fluorescence sensing of the selected ECPs.
2. To determine the effects of potential interfering compounds on the selectivity and fluorescence sensing capability of the QD sensors.

3. To develop methods to functionalise the QD materials via MIP overcoating and to investigate the impact thereof on the selectivity of the fluorescence sensors towards the target ECPs.
4. To optimize the methodology to immobilize the QDs in siloxane polymers in order to generate solid fluorescence sensor prototypes.
5. To test and optimize the fluorescence sensor prototypes for the target compounds in real water samples (tap water and river water).

1.3 SCOPE AND LIMITATIONS

This study focused on four target ECPs from the range of compound classes which are considered as ECPs, namely acetaminophen, triclosan, atrazine and polycyclic aromatic hydrocarbons (PAHs). The water matrices included were tap and river water.

1.4 CONTRIBUTIONS OF INDIVIDUAL CHAPTERS TO THE OBJECTIVES OF THE PROJECT

Chapter 2 provides the state-of-knowledge regarding the toxicological levels of these target compounds, focussing on toxicity threshold values of vulnerable organisms and applicable legal limits, where available. These are compared to typical reported environmental concentrations of the target compounds in surface waters.

Chapter 3 covers the optimization and application of water-soluble CdSe/ZnS quantum dots for the sensing of two emerging chemical contaminants, namely triclosan and acetaminophen. The fluorescent nanoparticles that were fabricated for pesticides are CdSeTe/ZnS QDs, while for PAHs graphene quantum dots (GQDs) were prepared.

In Chapter 4, the high sensitivity of QDs was integrated with the selectivity of MIPs via the preparation of QD-based MIP composites. Specifically, a CdSeTe/ZnS@MIP fluorescence sensor was developed for atrazine and a L-Cys-CdSe/ZnS@MIP sensor material was synthesised for acetaminophen.

Chapter 5 outlines the *in situ* immobilization of the QDs into polydimethylsiloxane thin films by spin coating technology.

An overall conclusion and suggested future research are provided in Chapter 6.

This project contributed substantially to capacity building and the knowledge gained and generated in conducting this research has resulted in a number of outputs, as detailed in the Appendix.

CHAPTER 2: STATE OF KNOWLEDGE ON THE TOXICOLOGICAL LEVELS OF THE TARGET ANALYTES

2.1 INTRODUCTION

There are varying definitions regarding emerging chemical pollutants (ECPs). In this study, we define ECPs based on the definition of Liu et al. (2014), in that ECPs are chemicals which do not have a regulatory status (specifically with respect to water quality legislation in South Africa), but which may have an adverse effect on human health and the environment (Liu et al., 2014). Sources and environmental pathways of these ECPs have been increasingly associated with waste and wastewaters arising from industrial, agricultural and municipal activities (Gavrilescu et al., 2014). The ECPs of current concern globally include a wide range of compounds including phthalates, pesticides, polychlorinated biphenyls (PCBs), polycyclic aromatic hydrocarbons (PAHs) and Bisphenol A, in addition to disinfectants, pharmaceuticals and hormones (Gavrilescu et al., 2014). The four target ECPs from these compound classes included in this study are acetaminophen, triclosan, atrazine and polycyclic aromatic hydrocarbons. This report provides the state-of-knowledge regarding the toxicological levels of these target compounds, focussing on toxicity threshold values of vulnerable organisms and applicable legal limits, where available. These are compared to typical reported environmental concentrations of the target compounds in surface waters.

2.2 TRICLOSAN

Triclosan, 5-chloro-2-(2,4-dichlorophenoxy) phenol (Fig. 2.1), with the commercial name Irgasan DP300, has been used in a variety of consumer products (Bhargava & Leonard, 1996; Jones et al., 2000). The chemical structure of triclosan (TCS) is similar to polychlorinated biphenyls (PCBs), polybrominated diphenyl ethers (PBDEs), bisphenol A, dioxins and thyroid hormones molecules with two aromatic rings (Allmyr et al., 2008; Crofton, Paul, DeVito, & Hedge, 2007).

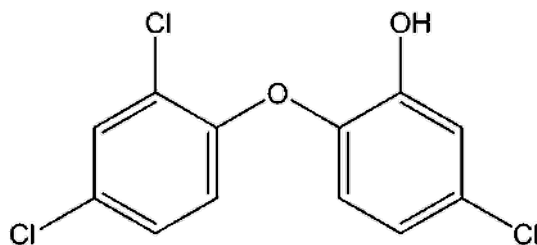


Figure 2.1 Chemical structure of triclosan.

TCS is a fairly small molecule, with a molecular weight of 289.54 g mol⁻¹ and a diameter of about 7.4 Å (Rossner, Snyder, & Knappe, 2009) and has a solubility of <10⁻⁶ g mL⁻¹ in water (Du Preez & Yang, 2003). The partition coefficient of TCS (log P_{ow} = 4.76), suggests that it is lipophilic, where the partition coefficient is a ratio of solubility between two liquids, in this case octanol and water. Values of the pK_a

for TCS have been reported in the range of 7.9-8.1 (Son, Ko & Zoh, 2009). The soil organic carbon coefficient (K_{oc}) of TCS has been calculated to equal 13,400 at pH 7; 6,020 at pH 8, and 934 at pH 9 (Chalew & Halden, 2009).

2.2.1 Sources of triclosan

Triclosan (TCS) has been used for more than 35 years as an antimicrobial and antifungal agent. Its widespread addition to numerous household products results in substantial release to sewage treatment plants. Although TCS does not appear to resist sewage treatment, with removal of as much as 95.5% from sewage treatment plants reported (Sabaliunas et al., 2003), the United States monitoring survey revealed that TCS was commonly detected in surface water at a frequency of 57.6% and at concentrations as high as 2300 ng L⁻¹ (Kolpin et al., 2002). Triclosan bioaccumulates to a much greater degree in algae than methyl triclosan (M-TCS) (Coogan et al., 2007). One possible explanation for differences in TCS bioaccumulation is due to potential ionization of TCS. Under typical environmental conditions, TCS may be completely protonated (pH = 5.4) or totally deprotonated (pH = 9.2) in surface waters, based on a pK_a value of 7.8 (Young et al., 2008). Based on these results, at higher pHs TCS would be expected to accumulate more, whereas at lower pHs M-TCS would be expected to accumulate to higher levels (Brausch & Rand, 2011).

The ubiquitous use of TCS has resulted in its presence in wastewater, sediments and many water sources (Zhao et al., 2013) where it has the potential to affect ecosystems as it may kill algae, for example (Tatarazako et al., 2004). There have also been several human health concerns attributed to TCS, as it can accumulate in the body over time and may result in long-term health risks (Allmy et al., 2008). TCS may also degrade in the aquatic environment to more toxic products. The most concerning degradation products are dioxins, which are known carcinogens and can mutate DNA and cause birth defects in offspring (Geyer et al., 2002).

Triclosan is susceptible to oxidative degradation by ozone and chlorine in the presence of sunlight and to biodegradation by microorganisms (SCCS, 2010). It has been found that biodegradation is an efficient mechanism for triclosan removal from wastewater and also that biodegradation under aerobic conditions provides higher removal efficiency in comparison to anaerobic conditions (McAvoy et al., 2002).

Wastewater treatment achieves average triclosan removal efficiencies in the range of 58-99% (NICNAS, 2009), depending on the technical capabilities of the sewage treatment systems (Bester, 2003; Federle, Kaiser, & Nuck, 2002; Kanda et al., 2003; Lindström et al., 2002; Lishman et al., 2006; Lopez-Avila & Hites, 1980; McAvoy et al., 2002; Singer et al., 2002a; Thompson et al., 2005). Approximately 50% of the incoming mass of triclosan, which is produced by activated sludge treatment together with aerobic biosolid digestion in conventional wastewater treatment plants (WWTPs), persists and becomes sequestered in biosolids. As a result, major pathways of biocide released into the environment are WWTP effluent discharge into surface waters and the application of biosolids to land (Chalew & Halden, 2009).

Cleavage of the ether bond and chlorination of the phenolic bond were identified as the main degradation pathways for triclosan during wastewater treatment (Canosa et al., 2005). Five main products were found upon reaction of triclosan with free chlorine including 2,4-dichlorophenol (2,4-DCP), 2,4,6-trichlorophenol (2,4,6-TCP) and tetra- and penta-chlorinated species. 2,4,6-TCP is a known endocrine disruptor, and may cause cancer, birth defects and developmental disorders in offspring, whilst 2,4-DCP may be fatal if large amounts are absorbed by the body (Canosa et al., 2005). Treatment with ozone during municipal sewage treatment was efficient in the removal of triclosan (Dodd *et al.*, 2009; Suarez *et al.*, 2007; Wert, Rosario-Ortiz, & Snyder, 2009). Although chloramines can be employed, chlorine is a stronger oxidant and has been shown to be more effective at oxidizing pharmaceuticals and endocrine disrupting chemicals (EDCs) in a comparative study where phenolic compounds, including triclosan, exhibited greater than 95% removal by chlorination under the conditions tested (Snyder *et al.*, 2007). The reaction mechanism of phenolic compounds with free chlorine proceeds via an electrophilic substitution pathway, with a mixture of substituted products at the ortho and para positions. Further chlorine addition results in cleavage of the aromatic ring (Lee & Morris, 1962; Snyder *et al.*, 2007). It is noteworthy to mention that phototransformation also can remove triclosan from wastewaters (Tixier *et al.*, 2002).

2.2.2 Environmental occurrence and concentrations of triclosan in water resources

Several recent studies have clearly demonstrated the widespread presence of triclosan in the environment, especially in wastewater, wastewater treatment plant effluents, rivers and in sediments in various countries.

A study in the United States identified triclosan as one of the top seven contaminants in surface water, with a maximum concentration of 2,300 ng L⁻¹ (Kolpin *et al.*, 2002). The worldwide concentration range of triclosan in water has been found to range from 1.4-40,000 ng L⁻¹ in surface waters, 20-86,161 ng L⁻¹ in wastewater influent, 23-5,370 ng L⁻¹ wastewater effluent, <0.001-100 ng L⁻¹ in sea water, sediment (lake/river/other surface water) <100-53,000 µg·kg⁻¹ dry weight (dw); sediment (marine) 0.02-35 µg·kg⁻¹ dw, biosolids from WWTP 20-33,000 µg·kg⁻¹ dw, activated/digested sludge 580-15,600 µg·kg⁻¹ dw; and pore water from 0.201-328.8 µg·L⁻¹ (Dhillon *et al.*, 2015; SCCS, 2010).

Triclosan is a frequent contaminant of aquatic and terrestrial environments and it is detected at a concentration ranging from parts-per-trillion in surface water to parts-per-million in biosolids. The elevated concentration of triclosan in biosolids and aquatic sediments may be attributed to the high usage, strong sorption to organic matter and environmental persistence of this compound (Chalew & Halden, 2009). The half-life of TCS depends on the specific environmental compartment and prevailing conditions (Bester, 2005).

Environmental concentrations of triclosan reported in the published literature are summarised in Table 2.1.

Table 2.1 Environmental concentrations of triclosan (SCCS, 2010)

Environmental Matrix	Triclosan concentration	Country	Reference
River water	Average 140 ng L ⁻¹ Max 2300 ng L ⁻¹ 1.4-74.0 ng L ⁻¹	USA	(Kolpin et al., 2002)
Seawater	Average 15 ng L ⁻¹ Median 10 ng L ⁻¹	Switzerland	(Lindström et al., 2002)
River water	600-40,000 ng L ⁻¹	USA	(Lopez-Avila & Hites, 1980)
Lake sediment	<D.L – 100,000 µg kg ⁻¹ d.w.		
Wastewater effluents	42-213 ng L ⁻¹		
Receiving water	1198 ng L ⁻¹	Switzerland	(Singer et al., 2002b)
Activated sludge	580 µg kg ⁻¹ d.w.		
Sewage influent	600-1300 ng L ⁻¹	Switzerland	(Lindström et al., 2002)
Sewage effluent	100-650 ng L ⁻¹		
Streams	<D.L – 140 ng L ⁻¹	USA	(Kolpin et al., 2004)
Sewage influent	380 ng L ⁻¹	Sweden	(Bendz et al., 2005)
Sewage effluent	160 ng L ⁻¹		
Streams with known input of raw wastewater	Median 120 ng L ⁻¹ Max 1600 ng L ⁻¹	USA	(Glassmeyer et al., 2005)
River water	8.8-26.3 ng L ⁻¹	USA	(Zhang et al., 2007)
Wastewater influent	6100 ng L ⁻¹	USA	(Halden & Paull, 2005)
Wastewater effluent	35 ng L ⁻¹		
River and coastal water	4.1-117 ng L ⁻¹	China	(Chau, Wu, & Cai, 2008)
WWTP outfall	120 ng L ⁻¹	USA	(Coogan et al., 2007)
WWTP outfall	112 ng L ⁻¹	USA	(Coogan & Point, 2008)
Wastewater effluent (activated sludge)	240-410 ng L ⁻¹		
Wastewater effluent (trickling filters)	1600-2700 ng L ⁻¹	USA	(McAvoy et al., 2002)
Digested sludge	530-15600 µg kg ⁻¹ d.w.		
Wastewater effluent	Median 106 ng L ⁻¹ Mean 108 ng L ⁻¹	Canada	(Lishman et al., 2006)

Environmental Matrix	Triclosan concentration	Country	Reference
Wastewater influent	Max 324 ng L ⁻¹	USA	(Waltman, Venables, & Waller, 2006)
	Median 1860 ng L ⁻¹		
	Mean 1930 ng L ⁻¹		
	Max 4010 ng L ⁻¹		
Wastewater effluent	30-250 ng L ⁻¹		
Wastewater influent	2700-26800 ng L ⁻¹		
Wastewater influent	70 ng L ⁻¹	USA	(Heidler & Halden, 2007)
Wastewater influent	4700 ng L ⁻¹		
Digested sludge	30,000 µg kg ⁻¹ d.w.		
Wastewater effluent	83-1283 ng L ⁻¹	Spain	(Kantiani et al., 2008)
Wastewater influent	231-12,500 ng L ⁻¹		
Wastewater effluent	190 ng L ⁻¹	Canada	(Fair et al., 2009)
Wastewater influent	2830-3440 ng L ⁻¹		
Wastewater effluent	180-5,370 ng L ⁻¹	USA	(Kumar et al., 2010)
Wastewater influent	5,213-32,639 ng L ⁻¹		
Wastewater effluent	43-59 ng L ⁻¹		
Wastewater influent	1100-1300 ng L ⁻¹	Germany	(Bester, 2003)
Sewage sludge	1000-1300 µg kg ⁻¹ d.w.		
Wastewater effluent	Max 3100 ng L ⁻¹	UK	(Kanda et al., 2003)
Wastewater effluent	Average 69.2 ng L ⁻¹ LOD 17.4 ng L ⁻¹		
Wastewater effluent	340-1100 ng L ⁻¹	UK	(Sabaliunas et al., 2003)
Wastewater influent	7500-21900 ng L ⁻¹		
Wastewater effluent	<700 ng L ⁻¹	UK	(Thompson et al., 2005)
Wastewater effluent	23-434 ng L ⁻¹	Australia	(Ying & Kookana, 2007)
	Median 108 ng L ⁻¹		
	90-16790 µg kg ⁻¹ d.w.		
Biosolid from WWTP	Median 2320 µg kg ⁻¹ d.w.		

Environmental Matrix	Triclosan concentration	Country	Reference
Seawater	0.0008-6.87 ng L ⁻¹	Germany	(Xie et al., 2008)
Sea water	50 ng L ⁻¹		
Sediment	10 µg kg ⁻¹ d.w.	Japan	(Okumura & Nishikawa, 1996)
Marine	10 µg kg ⁻¹ d.w.		
River sediment	4.4 and 35.7 µg kg ⁻¹ d.w.		
Biosolid from WWTP	5400 µg kg ⁻¹ d.w.	Spain	(Morales et al., 2005)
River Sediment	Max 80 µg kg ⁻¹ d.w. Average 70 µg kg ⁻¹ d.w.	USA	(Miller et al., 2008)
Biosolid from WWTP	3300-5970 µg kg ⁻¹ d.w.	Canada	(Chu & Metcalfe, 2007)
Biosolid from WWTP	1170-32900 µg kg ⁻¹ d.w. Median 10200 µg kg ⁻¹ d.w.	USA	(Kinney et al., 2006)
Biosolid from WWTP	90-7060 µg kg ⁻¹ d.w.		
Soil	0.16-1.02 µg kg ⁻¹ d.w.	USA	(Cha & Cupples, 2009)
Pore water	201-273300 ng L ⁻¹ (calculated)	USA	(Chalew & Halden, 2009)

Typical environmental concentration ranges for TCS in water systems are also shown in Fig. 2.2, which relates these to toxicological threshold values for various aquatic species.

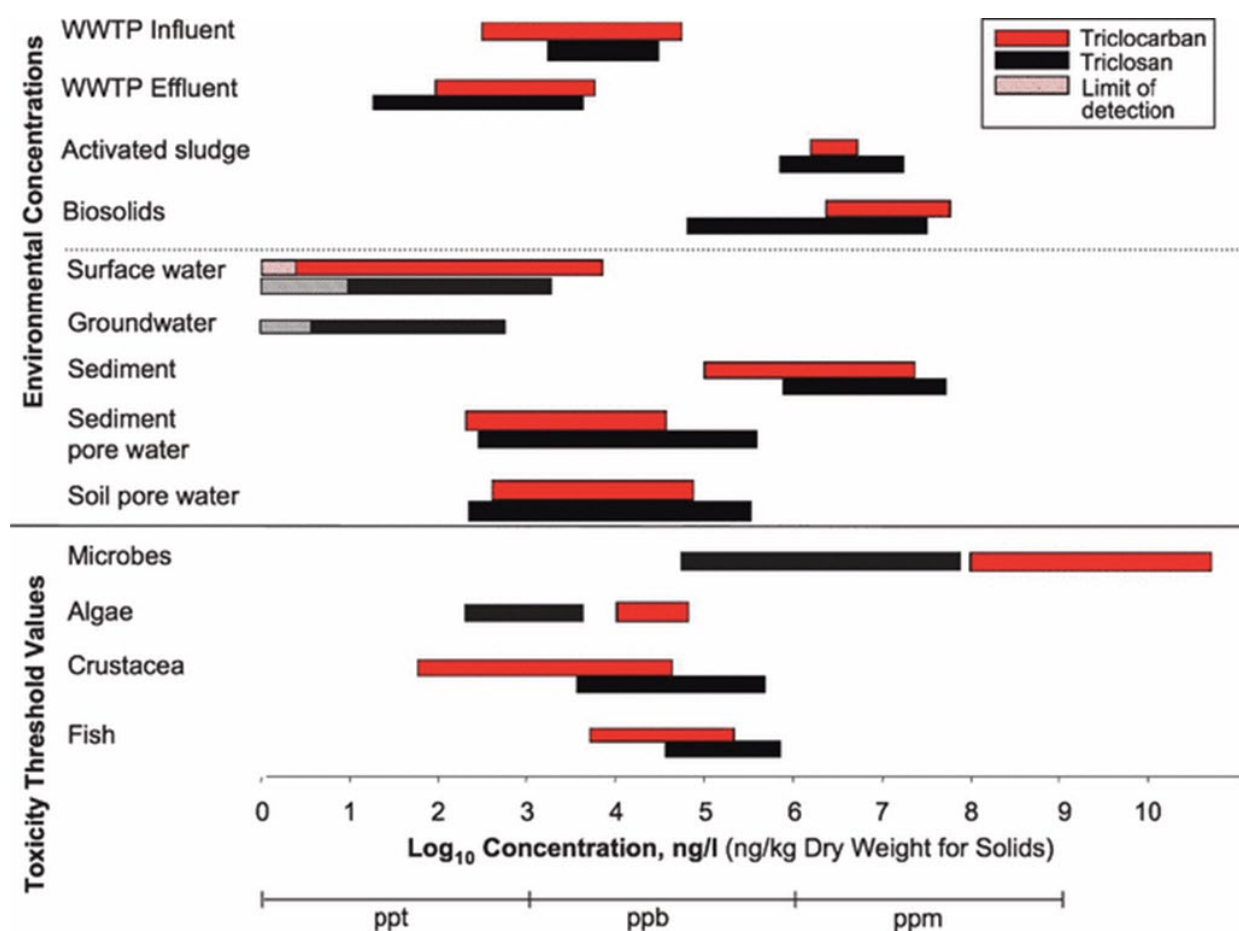


Figure 2.2 Published environmental occurrence data for triclosan and triclocarban in comparison to available toxicity threshold values for various indicator organisms. Concentrations are presented on a logarithmic scale in parts-per-trillion by volume (ng L^{-1}) or mass (ng kg^{-1}) for liquid and solid matrices, respectively. Concentrations in activated sludge and biosolids are expressed on a dry weight basis. Pore water concentrations were calculated from published environmental monitoring data. Overlap of occurrence data with toxicity threshold values of biota residing in the respective environmental compartment indicate locales of unhealthy conditions allowing for chronic or acute toxic effects. WWTP: wastewater treatment plant (Chalew & Halden, 2009).

2.2.3 Toxicity considerations

Fish, algae and crustaceans may be affected by elevated levels of biocides in surface waters, the concentrations of which are influenced by raw and treated sewage (Fig. 2.2). Minimum inhibitory concentration (MIC) threshold values for microbes with respect to TCS may be exceeded in activated sludge and biosolids which is a vital implication for the health and fertility of agricultural soils treated with biosolids. Multiple generations of various organisms have been exposed to TCS at concentrations expected to trigger acute and chronic effects or possibly adaptation (Chalew & Halden, 2009).

Fish may be affected by environmental biocide exposures in surface waters heavily impacted by raw and treated sewage but biocide concentrations typically present in surface waters show little if any overlap with fish toxicity threshold values. Algae and crustacea are highly sensitive indicator organisms that may be impacted by biocide occurrences in surface waters receiving raw and treated sewage. TCS

has been detected in surface waters at concentrations exceeding the no-observed effects concentration (NOEC) of algae, whilst crustacea may be adversely affected by TCS levels in sediment pore water (Chalew & Halden, 2009).

A study examined the toxicity ranking of five pharmaceutical and personal care products (PPCPs) including triclosan and acetaminophen. Bivalve *Dreissena polymorpha* in fresh water were exposed to different environmentally relevant concentrations of the PPCPs (290 and 154 ng L⁻¹ for triclosan and acetaminophen, respectively) over 96 hrs and the biological response of eight biomarkers was integrated into a simple biomarker response index (BRI). It was found that triclosan demonstrated dramatic effects. It induced primary lesions to hemocyte DNA following only 24 hrs of exposure ($p < 0.01$) with a clear time-dependent relationship (Parolini, Pedriali, & Binelli, 2013) while 96 h of exposure to acetaminophen produced only minor effects on cellular and genetic endpoints. The relative toxicities of the compounds were found to be triclosan > trimethoprim > ibuprofen > diclofenac = acetaminophen (Parolini et al., 2013).

2.2.3.1 Toxicity threshold of triclosan

Ecotoxicity data are essential for the interpretation of biocide occurrences in the environment. Common measures of toxicity can be divided into acute and chronic effects. Threshold values for acute toxicity of TCS in fish have been determined to range from 260,000 to 440,000 ng L⁻¹ whereas chronic effect thresholds were in the range of 34,000-290,000 ng L⁻¹ (Orvos et al., 2002; Tatarazako et al., 2004). Acute toxicity threshold values in crustacea were determined to range from 185,000-390,000 ng L⁻¹ and chronic toxicity in crustacea was observed at levels as low as 6,000-182,000 ng L⁻¹ (Samsøe-Petersen, Winther-Nielsen, & Madsen, 2003; Tatarazako et al., 2004). Concentrations toxic to algae also are in the parts-per-billion range, with values of 200-2,800 ng L⁻¹ for TCS (Samsøe-Petersen et al., 2003; Yang et al., 2008). Inhibitory effects on microorganisms were shown to begin at levels ranging from 25,000-80,000,000 ng L⁻¹ for TCS (Farré et al., 2008; Stasinakis et al., 2007; Stickler & Jones, 2008).

A chronic predicted no effect concentration (PNEC) for TCS is 1,550 ng L⁻¹ which was determined by aquatic risk assessment. This study was based on a predicted environmental concentration (PEC) for TCS in U.S. surface waters of no more than 850 ng L⁻¹, resulting from modeling output using a worst-case scenario precluding in-stream removal of the compound (Capdevielle et al., 2008). Moreover, as the concentration of TCS increases, there is a possibility of adaption of bacterial strains by developing resistance (Stickler & Jones, 2008).

Researchers in Spain conducted another environmental risk assessment for 26 PPCPs (de García et al., 2014). They employed Microtox acute ecotoxicity tests and activated sludge respirometry assays. The U.S. EPA Ecological Structure-Activity Relationships (ECOSARTM) QSAR program was also utilized to predict the estimated ecotoxicological effects. Based on the results of ecotoxicity tests, triclosan was found to be very toxic to different species. Furthermore, evaluation of persistence, bioaccumulation and ecotoxicity (PBT) revealed that triclosan is persistent and toxic but not bioaccumulative (de García, García-Encina, & Irusta-Mata, 2011).

Triclosan has been shown to exert deleterious effects towards different somatic and reproductive mammalian cells at extracellular concentrations of $<1,000,000$ - $5,000,000$ ng L⁻¹. It also had adverse effects in cells that are non-renewable (pancreatic β -cells). Triclosan is a mitochondrial toxic chemical which may cause unexpected long-term toxic effects depending on its tissue distribution and elimination (Ajao et al., 2015).

Acute toxicity of TCS was investigated using the bacterium *Vibrio fischeri*, the phytoplankton species *Dunaliella tertiolecta*, and three life stages of the grass shrimp *Palaemonetes pugio* by DeLorenzo et al. (2008). They found acute aqueous toxicity values (96 h LC50) were $305,000$ ng L⁻¹ for adult shrimp, $154,000$ ng L⁻¹ for larvae, and $651,000$ ng L⁻¹ for embryos. The presence of sediment decreased triclosan toxicity in adult shrimp (24 h LC50s were $620,000$ ng L⁻¹ with sediment, and $482,000$ ng L⁻¹ without sediment). The bacterium showed more sensitivity to TCS compared to the grass shrimp, with a 15 min aqueous LC50 value of $53,000$ ng L⁻¹ and a 15 min spiked sediment LC50 value of 616 μ g kg⁻¹. The most sensitive species were the phytoplankton with a 96 h EC50 value of $3,550$ ng L⁻¹. Accumulation of methyl-triclosan after a 14-day exposure to $100,000$ ng L⁻¹ triclosan in adult grass shrimp indicated formation of this metabolite in a seawater environment and its potential to bioaccumulate in higher organisms. Furthermore, the low detected concentration of TCS in surface water (1 ng L⁻¹) suggested that TCS has low acute toxicity risk to estuarine organisms. Toxicity of TCS in aquatic organisms reported over the last 10 years is summarised in Table 2.2. Acute and chronic toxicity data relating to triclosan are also provided in Tables 2.3 and 2.4.

Table 2.2 Effects of TCS on freshwater (FW) and marine (SW) organisms (Dann & Hontela, 2011).

Test species	Life stage	System type	Route of exposure	Test duration	TCS exposure	Endpoint	Reference
Algae Phytoplankton (<i>Dunaliella tertiolecta</i>)	-	SW	Water (static)	Acute (96 h)	3,500 ng L ⁻¹	EC50 (population density)	(Delorenzo & Fleming, 2008)
Invertebrates (<i>Chironomus tentans</i>)	-	FW	Water (renewal)	10 days	400,000 ng L ⁻¹	LC50	(Dussault et al., 2008)
Invertebrates (<i>Hyalella Azteca</i>)	Embryo				200,000 ng L ⁻¹		
Grass shrimp (<i>Palaemonetes pugio</i>)	Larvae	SW	Water (renewal)	Acute (96 h)	154,000 ng L ⁻¹	LC50	(Delorenzo et al., 2008)
	Adult				305,000 ng L ⁻¹		
Crustacean (<i>Thamnocephalus platyurus</i>)	-	FW	Water (static)	Acute (24 h)	470,000 ng L ⁻¹	LC50	(Kim et al., 2009)
	Hemocytes		<i>In vitro</i>	Acute (30 min)	1 µ M	↓lysosomal membrane stability Altered hemocyte and digestive gland function	(Canesi et al., 2007)
Bivalve (<i>Mytilus galloprovincialis</i>)	Whole animal	SW	Injection	Acute (24 h)	2.9 µg kg ⁻¹		
Zebra mussel (<i>Dreissena polymorpha</i>)	Hemocytes	FW	<i>In vitro</i>	Acute (60 min)	0.1 µ M	Genotoxicity	(Binelli et al., 2009)
			<i>In vivo</i>	Acute (96 h)	1 M		
Medaka (<i>Oryzias latipes</i>)	Eggs	SW	In ovo injection	1 day postfertilization	4.2 ng egg ⁻¹	EC50 (survival)	(Nassef et al., 2010)
Medaka (<i>Oryzias latipes</i>)	Adult	SW	Water (renewal)	Acute (96 h)	1700,000 ng L ⁻¹	LC50	(Nassef et al., 2009)
Medaka (<i>Oryzias latipes</i>)	Larvae	FW	Water (static)	Acute (96 h)	600,000 ng L ⁻¹	LC50	(Kim et al., 2009)
Fathead minnow (<i>Pimephales promelas</i>)	Full life cycle	FW	Water (TCS in mixture)	-	100 and 300 ng L ⁻¹ mixture of products	No effects F ₀ ; ↑ larval deformities in F ₁	(Parrott & Bennie, 2009)

Test species	Life stage	System type	Route of exposure	Test duration	TCS exposure	Endpoint	Reference
Zebrafish (<i>Danio rerio</i>)	Embryo	FW	24-Well microplates	Acute (96 h)	420,000 ng L ⁻¹	LC50; teratogenic effects	(Oliveira et al., 2009)
	Adult				340,000 ng L ⁻¹	LC50	
Amphibians Bullfrog (<i>Acris crepitans Blanchardii</i>)	Larvae				367,000 ng L ⁻¹		
Amphibians Bullfrog (<i>Bufo woodhousii Woodhousii</i>)	Stage 30				152,000 ng L ⁻¹		(Palenske, Nallani, & Dzialowski, 2010)
Amphibians Bullfrog (<i>Rana sphenoccephala</i>)	-	FW	Water	Acute (96 h)	562,000 ng L ⁻¹	LC50	
Amphibians Bullfrog (<i>Xenopus laevis</i>)	Stage 41				343,000 ng L ⁻¹		

Table 2.3 Acute toxicity data for triclosan (Brausch & Rand, 2011)

Species	Trophic group	Endpoint/duration	LC50 (ng L ⁻¹)	Reference
<i>D. magna</i>	Invertebrate	48 h	390,000	(Orvos et al., 2002)
<i>Ceriodaphnia dubia</i>	Invertebrate	24, 48 h (pH = 7.0)	200,000, ~125,000,000	(Orvos et al., 2002)
		24 h	360,000	
<i>Pimephales promelas</i>	Fish	48 h	270,000	(Orvos et al., 2002)
		72 h	270,000	
		96 h	260,000	
		24h	440,000	
<i>Lepomis macrochirus</i>	Fish	48 h	410,000	(Orvos et al., 2002)
		96 h	370,000	
<i>Oryzias latipes</i>	Fish	96 h	602,000 (larvae), 399,000 (embryos)	(Ishibashi et al., 2004)
<i>Xenopus laevis</i>	Amphibian	96 h	259,000	(Palenske et al., 2010)
<i>Acris blanchardii</i>	Amphibian	96 h	367,000	(Palenske et al., 2010)
<i>Bufo woodhousii</i>	Amphibian	96 h	152,000	(Palenske et al., 2010)
<i>Rana sphenoccephala</i>	Amphibian	96 h	562,000	(Palenske et al., 2010)

Species	Trophic group	Endpoint/duration	LC50 (ng L ⁻¹)	Reference
<i>Pseudokirch-neriella subcapitata</i>	Algae	72 h Growth	530	(Yang et al., 2008)

Table 2.4 Chronic toxicity data of triclosan (Brausch & Rand, 2011)

Species	Trophic group	Endpoint/duration	LOEC (ng L ⁻¹)	NOEC (ng L ⁻¹)	Reference
<i>D. magna</i>	Invert.	21 d Survival, Reproduction	Repro. = 200,000 (LOEC)	Surv. = 200,000 (NOEC)	(Orvos et al., 2002)
		7 d Survival		50,000	
<i>C. dubia</i>	Invert.	Reproduction	-	6,000	(Orvos et al., 2002)
<i>C. dubia</i>	Invert.	7 d Survival, Reproduction	LC25 = 170,000	-	(Tatarazako et al., 2004)
<i>Chironomus riparius</i>	Invert.	28 d Survival, Emergence	-	440,000	(Memmert, 2006)
<i>Chironomus tentans</i>	Invert.	10 d Survival, Growth	LC25 = 100,000	-	(Dussault et al., 2008)
<i>Hyalella azteca</i>	Invert.	10 d Survival, Growth	LC25 = 60,000		(Dussault et al., 2008)
<i>O. mykiss</i>	Fish	96 d ELS Hatching	No Effect		(Orvos et al., 2002)
		Survival	71,300	-	
<i>O. latipes</i>	Fish	14 d Hatching	213,000	-	(Ishibashi et al., 2004)
		21 d Growth	200,000		
		Fecundity	No Effect		
<i>O. latipes</i>	Fish	HSI and GSI,	200,000	-	(Ishibashi et al., 2004)
		VTG	20,000		
<i>O. latipes</i>	Fish	14 d Hatchability	LC25 = 290,000	-	(Tatarazako et al., 2004)
<i>Gambusia affinis</i>	Fish	35 d Sperm Count, VTG	101,300	-	(Raut & Angus, 2010)
<i>Danio rerio</i>	Fish	9 d Hatchability	LC25 = 160,000		(Tatarazako et al., 2003)
<i>Xenopus laevis</i>	Amphibian	21 d Metamorphosis	No effect (200,000)	-	(Fort et al., 2009)
<i>Rana catesbeiana</i>	Amphibian	18 d Development	300,000	-	(Veldhoen et al., 2006)

Development of novel fluorescent sensors for the screening of emerging chemical pollutants in water

Species	Trophic group	Endpoint/duration	LOEC (ng L ⁻¹)	NOEC (ng L ⁻¹)	Reference
<i>Rana pipiens</i>	Amphibian	24 d Survival	230,000	-	(Fraker & Smith, 2004)
		Growth	2,300		
<i>Bufo americanus</i>	Amphibian	14 d Survival, Growth	No effect (230,000)	-	(Smith & Burgett, 2005)
<i>S. capricornutum</i>	Algae	96 h Growth	EC50 = 4,460	EC25 = 2,440	(Orvos et al., 2002)
<i>S. subspicatus</i>	Algae	96 h Biomass	EC50 = 1,200	EC50 = 500	(Orvos et al., 2002)
		Growth Rate	EC50 = 1,400	EC50 = 690	
<i>S. costatum</i>	Algae	96 h Growth Rate	EC50 ≥ 66,000	EC25 > 66,000	(Orvos et al., 2002)
<i>A. flos-aquae</i>	Algae	96 h Biomass	EC50 = 970	EC25 = 670	(Orvos et al., 2002)
<i>P. subcapitata</i>	Algae	72 h Growth	EC25 = 3,400	200	(Tatarazako et al., 2004; Yang et al., 2008)
<i>N. pelliculosa</i>	Algae	96 h Growth Rate	EC50 = 19,100	EC25 = 10,700	(Orvos et al., 2002)
<i>Natural algal assemblage</i>	Algae	96 h Biomass	120	-	(Wilson et al., 2003)
<i>Closterium ehrenbergii</i>	Algae	96 h Growth	-	250,000	(Ciniglia et al., 2005)
<i>Dunaliella tertiolecta</i>	Algae	96 h Growth	-	1,600	(DeLorenzo & Fleming, 2008)
<i>L. gibba</i>	Plant	7 d Growth	EC50 ≥ 62,500	EC25 ≥ 62,500	(Orvos et al., 2002)
<i>S. herbacea</i>	Plant	28 d Seed Germination	100,000 germination	-	(Stevens et al., 2009)
		Morphology	10,000 morphology		
<i>E. prostrata</i>	Plant	28 d Seed Germination	No effect	-	(Stevens et al., 2009)
		Morphology	1000,000		
<i>B. frondosa</i>	Plant	28 d Seed Germination	100,000	-	(Stevens et al., 2009)
		Morphology	10,000		

LOEC: lowest observed effect concentration; NOEC: no observed effect concentration; ELS: Early Life Stage; HIS: Hepatosomatic Index; GSI: Gonadosomatic Index; VTG: Vitellogenin.

2.2.4 Legal limits of triclosan

Triclosan is an anti-microbial and preservative agent added to personal care products (toothpaste, detergent, soap, shampoos, skin care creams and lotions) at a typical concentration in the range of 0.1-0.3% (w/w) which is regulated by the European Community Cosmetic Directive or the U.S. Food and Drug Agency (U.S. FDA) in Europe and the USA, respectively (Rodricks et al., 2010; Sabaliunas et al., 2003). The content of TCS in household products should not exceed 0.3% (w/w) (Allmyr et al., 2006). The Minnesota Department of Health (MDH) developed a guidance value of 50 ppb for triclosan in drinking water. A person drinking water at or below this level, would have little or no risk of any health effects from triclosan ("Toxicological Summary: Triclosan," 2010). The Canadian Federal Water Quality Guideline for the protection of aquatic life from adverse effects of triclosan is 380 ng L⁻¹ (Canadian Environmental Protection Act, 2017).

2.3 ACETAMINOPHEN

Paracetamol or acetaminophen (N-acetyl-p-aminophenol) with log K_{ow} 0.46 (Westerhoff et al., 2005) (Fig. 2.3) is an acylated aromatic amide that was first introduced by Von Mering in 1893 as an antipyretic/analgesic medicine used for fever, headaches, and other minor pain (Wu, Zhang, & Chen, 2012). It has a pK_a of 9.38 with a solubility of 1.4×10⁴ mg L⁻¹ in water at 25°C (Achilleos et al., 2008). The high solubility and hydrophilicity of acetaminophen result in its accumulation in the aquatic environment. It has been detected in surface waters, wastewater, and drinking water throughout the world (Thomas et al., 2007).

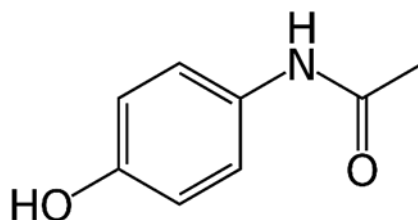


Figure 2.3 Structure of acetaminophen

Acetaminophen (AC) unlike other common analgesics, such as aspirin and ibuprofen, has relatively little anti-inflammatory activity. As a result, it is not considered to be a non-steroidal anti-inflammatory drug (NSAID). Acute overdoses of paracetamol can cause potentially fatal liver damage, and in some individuals, a normal dose can cause the same, the risk of which can be heightened by alcohol consumption. Recent studies have suggested that excessive doses and/or excessively high plasma concentrations of AC may be associated with hepatotoxicity (Barker, de Carle, & Anuras, 1977). It has been demonstrated that 58-68% of paracetamol and its metabolites are excreted from the body during therapeutic use (Muir et al., 1997). Hu et al. reported that microorganisms play a pivotal role in acetaminophen degradation in the environment under various conditions (Hu et al., 2012).

Although the detected concentrations of pharmaceuticals are typically in the nanogram to microgram-per-liter range (Huber et al., 2005), a variety of potential adverse effects, including acute and chronic

damage, accumulation in tissues, reproductive damage, inhibition of cell proliferation and behavioral changes, have been documented at these low levels (Escher et al., 2011; Phillips et al., 2010).

2.3.1 Sources of acetaminophen

Acetaminophen is frequently prescribed or purchased over the counter, and falls within the pharmaceutical and personal care products (PPCPs) subclass of organic contaminants. Countries reported to have the largest consumption values for AC are the United States (5790 tons in 2002), France (3303 tons in 2005) (Weber et al., 2016) and Germany (622 tons in 2001) (Huschek et al., 2004). Pharmaceutical compounds are continuously introduced into the aquatic environment from hospital waste, consumer use and disposal, as well as from manufacturing facilities (Langford & Thomas, 2009). In spite of the fact that the detected concentrations thereof are low, a wide variety of potential deleterious effects, including acute and chronic toxicity to the aquatic environment (Crane, Watts, & Boucard, 2006), accumulation in tissues (Schultz et al., 2010) and inhibition of cell proliferation (Pomati et al., 2006) have been reported even at these low levels. The continuous introduction of acetaminophen into the environment can also negate its high transformation rates (Petrović, Gonzalez, & Barceló, 2003): acetaminophen is usually easily biodegraded in biological wastewater treatment plants (WWTPs) (Ternes, 2006; Wu et al., 2012) although maximum concentrations of acetaminophen in surface waters of 10,000 ng L⁻¹ have been found (Daughton & Ternes, 1999).

In many cases, WWTPs are unable to efficiently remove PPCP compounds, which are thus adsorbed by the sludge of primary and secondary wastewater treatment processes, or they remain in the treated wastewater, leading to their distribution in surface and groundwater, sediments and/or tissues of exposed wildlife. In order to avoid possible harm to humans, there is an increasing need to develop fast and sensitive methods for detecting low concentrations of PPCPs in natural water, wastewater and drinking water systems (U.S. EPA, 2015).

The primary sources of pharmaceuticals entering surface water are from treated or untreated municipal wastewater effluent discharges into receiving surface water bodies (Buser, Müller, & Theobald, 1998; Buser, Poiger, & Müller, 1999; Daughton, 2001; Heberer et al., 2001; Heberer, Reddersen, & Mechlinski, 2002; Kolpin et al., 2002; Ternes, 1998) and improper disposal of pharmaceutical waste and excess medication by consumers, as well as healthcare and veterinary facilities, into sewers and drains.

Eleven different chlorination products were observed during chlorination of acetaminophen, including the toxic substances N-acetyl-p-benzoquinone imine (NAPQI) and 1,4-benzoquinone. Although they are at very low levels in drinking water and wastewater, their presence along with multiple other pharmaceuticals may be of concern (Bedner & MacCrehan, 2006).

Roberts and Thomas (2006) analyzed wastewater effluent and surface waters for 13 pharmaceuticals. Acetaminophen was detected in raw effluent at concentrations ranging from 11 to 69,570 ng L⁻¹. In this study, the treatment process was found to remove 100% of the acetaminophen present in the raw effluent.

2.3.2 Environmental occurrence & concentrations of acetaminophen in water sources

Acetaminophen is usually easily biodegraded in biological WWTPs (Ternes, 2006; Wu et al., 2012), although maximum concentrations of acetaminophen in surface waters of 10,000 ng L⁻¹ have been found (Kolpin et al., 2002). Acetaminophen is reported as one of the most frequently detected pharmaceuticals in sewage treatment plant effluents, drinking water, and surface water. This compound was detected in 24% of U.S. stream water samples with a maximum detection level of 10,000 ng L⁻¹ (Kolpin et al., 2002).

Acetaminophen is also detected in over 5% of groundwater samples, where it was found to be one of the active pharmaceutical ingredients (APIs) with the highest reported concentrations ranging from 0.3 to 210 ng L⁻¹ (Naidenko et al., 2008; Stackelberg et al., 2007; Togola & Budzinski, 2008; Versteegh, Van Der Aa, & Dijkman, 2007).

Acetaminophen was also observed in wastewater (<10,000 ng L⁻¹) and bio-solids (up to 12 ng g⁻¹) where it was efficiently removed from the wastewater while the bio-solids still contained >50% of the AC (Matongo et al., 2015). The highest concentration of AC in a South Africa study was found near human settlements (Matongo et al., 2015). Environmental concentrations of acetaminophen reported in the published literature are provided in Table 2.5.

Table 2.5 Environmental concentrations of acetaminophen.

Environmental Matrix	Acetaminophen concentration (ng L ⁻¹)	Country	Reference
Surface water	52-290	UK	(Bound & Voulvoulis, 2006)
WWTP influent	130-26,090 Average 10,194		
WWTP effluent	BLQ-5,990 Average 2,102	Spain	(Gros, Petrovic, & Barcelo, 2006)
Surface water	BLD-250 Average 42		
STPs effluent	Median 1,900		
Receiving waters downstream of STPs	Max 3,600 Median 5.0	Canada	(Brun et al., 2006)
WWTP influent	Max 260 Mean 70		
WWTP effluent	Max 160 Mean 60	South Korea	(Han, Hur, & Kim, 2006)
STP influent	29,000-246,000 Mean 134,000		
STP effluent	<LOD-4,300 Mean 220	Spain	(Gómez et al., 2007)
River water	<20		
Wastewater effluent	11-69,570	UK	(Roberts & Thomas, 2006)
Sewage effluents	Max 6,000	Germany	(Ternes, 1998)
WWTP influent	160,000		
River water	Max 107,000	Kenya	(K'Oreje et al., 2016)
Surface water	Max 16,000	Africa	(Weber et al., 2016)
WWTP inlet (wastewater)	5,760		(Matongo et al., 2015)

Environmental Matrix	Acetaminophen concentration (ng L ⁻¹)	Country	Reference
WWTP inlet (bio-solid)	12.08 ng g ⁻¹		
WWTP inside (wastewater)	2,970		
WWTP inside (bio-solid)	8.44 ng g ⁻¹	South Africa (Msunduzi River, KwaZulu-Natal)	
WWTP outlet (wastewater)	<MDL		
WWTP outlet (bio-solid)	7.02 ng g ⁻¹		
WWTP inlet (wastewater)	6,260		
WWTP inlet (bio-solid)	6.99 ng g ⁻¹		
WWTP inside (wastewater)	4,580	South Africa (Umgeni River, KwaZulu-Natal)	(Matongo et al., 2015)
WWTP inside (bio-solid)	7.76 ng g ⁻¹		
WWTP outlet (wastewater)	3,270		
WWTP outlet (bio-solid)	6.70 ng g ⁻¹		
Surface water	<10,000	South Africa (Umgeni River, KwaZulu-Natal)	(Agunbiade & Moodley, 2014)
Inlet wastewater	59,000		
WWTP influent	500-1,200		
WWTP effluent	12-58	Greece	(Kosma, Lambropoulou, & Albanis, 2014)

BLD: Below limit of detection; BLQ: Below limit of quantification; MDL: Method limit of detection; STPs: Sewage Treatment Plants; WWTP: Wastewater Treatment Plants.

2.3.3 Toxicity threshold of acetaminophen

Acetaminophen induces proliferation of cultured breast cancer cells via estrogen receptors without binding to them, but has no estrogenic activity in rodents (Harnagea-Theophilus et al., 1999). The mode of action of acetaminophen is not yet fully elucidated. It seems that this drug acts mainly by inhibiting the cyclooxygenase of the central nervous system and it does not have anti-inflammatory effects, because of the lack of inhibition of peripheral cyclooxygenase involved in inflammatory processes. Adverse effects of acetaminophen are mainly due to formation of hepatotoxic metabolites, primarily *N*-acetyl-*p*-benzoquinone imine, synthesized when the availability of glutathione is diminished in liver cells (Fent, Weston, & Caminada, 2006; Harnagea-Theophilus et al., 1999).

Acetaminophen has detrimental effects especially in over dosage related to the formation of toxic metabolites by oxidative pathways. Toxicity of acetaminophen is usually caused by reactive oxygen

species and can result in multiple effects, ranging from protein denaturation to lipid peroxidation and DNA damage (Antunes et al., 2013).

Morasch and Perazzolo (Morasch et al., 2010; Perazzolo et al., 2010) screened wastewater treatment plant influent and effluent, and raw drinking water samples in Switzerland, for 37 pharmaceuticals including acetaminophen, four hormones, and a number of other micropollutants. All pharmaceuticals were detected in at least one sample of influent or effluent from the wastewater treatment plants. Predicted no-effect concentrations of acetaminophen were exceeded in raw drinking water samples and therefore presented a potential risk to the ecosystem (Morasch et al., 2010).

A separate study (Galus et al., 2013) exposed adult zebrafish (*Danio rerio*) to a pharmaceutical mixture including acetaminophen and to diluted wastewater effluent over a six week period. They observed that chronic exposure of zebrafish to 10,000 ng L⁻¹ acetaminophen markedly decreased fecundity. Liver histology was altered and acetaminophen exposure increased developmental abnormalities (Galus et al., 2013).

Acetaminophen has shown embryotoxic effects on the development, growth, behavior and survival of *D. rerio* larvae of zebrafish embryos. It induces anomalies at different levels of development in a dose-dependent manner (0, 1×10⁶, 5×10⁶, 10×10⁶, 50×10⁶ and 100×10⁶ ng L⁻¹), causing impairment in (1) the early development, (2) hatching, (3) organogenesis (by altering the rate of apoptosis), (4) larval growth and morphometry, (5) tail and tail-fin formation, (6) pigmentation and (7) larval behavior and survival (David & Pancharatna, 2009).

Acute aquatic toxicity of acetaminophen and some other pharmaceuticals was examined on a marine bacterium (*Vibrio fischeri*), a freshwater invertebrate (*Daphnia magna*), and the Japanese medaka fish (*Oryzias latipes*) in Korea (Kim et al., 2007). The acute toxicity results were predicted by a quantitative structure activity relationship model using pH-dependent distribution coefficient and molecular orbital energy parameters of the test pharmaceuticals. The 48 hrs EC50 values for *D magna* and *O. latipes* were 30,100,000 ng L⁻¹ and >160,000,000 ng L⁻¹ respectively while the 15 min EC50 for *V. fischeri* was 567,700,000 ng L⁻¹. The highest predicted environmental concentration (PEC) was also expected for acetaminophen (16,500 ng L⁻¹) due to the highest volume production of AC regarding pharmaceuticals in Korea (1,068,921 kg in 2003). The hazard quotient which was derived from the PEC and predicted no effect concentration (PNEC) for acetaminophen was 1.8 showing potential environmental concerns of this medicine, as hazard quotients exceeding 1 indicate potential effects (Brausch & Rand, 2011).

The effect of several environmental factors such as water pH (7.4, 8.3, and 9.2), temperature (15, 21, and 25°C) and ultraviolet light (continuous irradiation of 15.0 μW cm⁻²) on the toxicity of some pharmaceutical compounds including acetaminophen in water, has been evaluated by Kim et al. (2010) using the freshwater invertebrate *Daphnia magna*. They showed that lower water pH caused greater acute lethal toxicity of acetaminophen due to the higher unionized fraction thereof. AC was markedly more toxic at pH 8.3 compared to pH 9.2 in terms of 48 hrs EC50 ($P < 0.05$). Moreover, enhancement in the temperature of the water led to an increase in the acute toxicity of AC which was attributed to the alteration in toxicokinetics of chemicals, as well as the impact on the physiological mechanisms of the test organism. In the presence of UV-B light, the toxicity of acetaminophen also tended to increase.

The acute toxicity (median lethal concentration, LC50, for a 96-h exposure) of acetaminophen and ibuprofen alone and different mixtures thereof was investigated in green neon shrimp (*Neocaridina denticulata*) (Sung et al., 2014). They revealed that the 96-h LC50 value for acetaminophen was 6,070,000 ng L⁻¹. Furthermore, the 96-h LC50 value for mixtures with high acetaminophen concentration and low ibuprofen concentration indicated enhanced toxicity in *N. denticulate* (LC50 = 4,780,000 ng L⁻¹) compared to acetaminophen and ibuprofen alone. The effects of AC on different organisms are shown in Table 2.6.

Table 2.6 Effects of acetaminophen on different organisms

Taxon	Species	Toxicological endpoint	Ecotoxicity data (ng L ⁻¹)	Reference
Bacteria	<i>V. fischeri</i>	EC50 (5 min)	549,700,000 (534,000,000-565,900,000)	(Kim et al., 2007)
		EC50 (15 min)	567,500,000 (358,600,000-898,100,000)	
Bacteria	<i>V. fischeri</i>	EC50 (30 min)	650,000,000	(Henschel et al., 1997)
Crustacean	<i>D. magna</i>	EC50 (24 h) (immobilization)	293,000,000	(Henschel et al., 1997)
		EC50 (48 h) (immobilization)	50,000,000	
Crustacean	<i>D. magna</i>	EC50 (48 h) (immobilization)	30,100,000 (23,200,000-39,000,000)	(Kim et al., 2007)
		EC50 (96 h) (immobilization)	26,600,000 (19,600,000-33,600,000)	
Fish	<i>O. latipes</i>	LC50 (48 h)	>160,000,000	(Kim et al., 2007)
		LC50 (96 h)	>160,000,000	
Fish	<i>B. rerio (zebra fish)</i>	LC50 (48 h)	378,000,000	(Henschel et al., 1997)
Algae	<i>Scenedesmus subspicatus</i>	EC50 (72 h)	134,000,000	(Henschel et al., 1997)
Ciliates	<i>Tetrahymena pyriformis</i>	EC50 (48 h) (growth inhibition)	112,000,000	(Henschel et al., 1997)

Taxon	Species	Toxicological endpoint	Ecotoxicity data (ng L ⁻¹)	Reference
Green neon shrimp	<i>Neocaridina denticulata</i>	LC50 (96 h) (exposure)	6,070,000 (5,330,000-7,840,000)	(Sung et al., 2014)

Some authors reported the presence of AC in effluents at concentrations below to 20 ng L⁻¹ (Roberts & Thomas, 2006) to 4,300 ng L⁻¹ (Gómez et al., 2007), although in surface waters values can reach 78,170 ng L⁻¹ (Grujić, Vasiljević, & Laušević, 2009), which is higher than the predicted no-effect concentration (PNEC) of 9,200 ng L⁻¹ (Carlsson et al., 2006). Hence, AC might present a threat to non-target organisms.

2.3.4 Legal limits of acetaminophen

Based on available information, the Minnesota Department of Health (MDH) developed a guidance value of 200 ppb for acetaminophen in drinking water. MDH considers the liver to be the organ most sensitive to acetaminophen exposure ("Toxicological Summary for: Acetaminophen," 2010).

2.4 POLYCYCLIC AROMATIC HYDROCARBONS

2.4.1 Sources and occurrence

Polycyclic aromatic hydrocarbons (PAHs) are a class of organic compounds with fused benzene rings which are of environmental concern because of their negative health effects. PAHs are produced from a wide variety of sources (Table 2.7) and hence they are one of the classes of pollutants which are of global concern (Manoli & Samara, 1999; Sojinu et al., 2010). Table 2.8 details relating to the U.S. EPA priority PAH compounds. These compounds can be introduced into environmental water systems through various ways after wet or dry deposition from the atmosphere following their release from sources including industrial combustion activities, biomass burning, and vehicular emissions. A comprehensive review on the occurrence and typical concentration ranges of PAHs in South African water systems is provided by Chimuka et al. (2015) and are presented in Table 2.9. Clearly these compounds occur at low concentrations in runoff and river water, but continuous exposure may incur human health effects.

PAHs generally have low solubility in water, where high molecular weight PAHs like benzo[a]pyrene have the lowest solubility (0.0057 mg L⁻¹ at 25°C) and lower molecular weight naphthalene having the highest solubility (31.69 mg L⁻¹ at 25°C) as shown in Table 2.8. Removal of PAHs from water systems can be achieved either by using traditional methods like destructive oxidation with ozone or by using adsorption technology with adsorbents like activated carbon (Zeledón-Toruño et al., 2007).

Table 2.7 Natural and anthropogenic sources of polycyclic aromatic hydrocarbons (PAHs).

Natural	Anthropogenic
Natural petroleum	Petroleum Spills
Vegetative Decay	Pesticide Formulations
Rare Minerals	Sewage Sludge
Plant Synthesis	PAH-contaminated Media
Fires	Road Dust
Volcanic Eruptions	Vehicles (Internal combustion)
	Jet Aircrafts
	Incineration
	Wood Burning
	Cigarette Smoke
	Cooking Plants
	Other Industries/Processes
	Miscellaneous Burning

Table 2.8 The 16 PAHs included in the U.S. EPA priority pollutant list (Manoli & Samara, 1999).

PAHs	Structure	Vapor Pressure (Torr)	Solubility in Water (mg L ⁻¹)	K _{ow}	Carcinogenic potency IARC/US EPA* classification
Acenaphthene, Ace		10 ⁻³ -10 ⁻² at 20°C	3.4 at 25°C	21000	
Acenaphthylene, Acy		10 ⁻³ -10 ⁻² at 20°C	3.93	12000	
Fluorene, F		10 ⁻³ -10 ⁻² at 20°C	1.9	15000	
Naphthalene, Np		0.0492	32	2300	
Anthracene, An		2x10 ⁻⁴ at 20°C	0.05-0.07 at 25°C	28000	3
Fluoranthene, Fl		10 ⁻⁶ to 10 ⁻⁴ at 20°C	0.26 at 25°C	340000	3
Phenanthrene, Ph		6.8x10 ⁻⁴ at 20°C	1.0-1.3 at 25°C	29000	3
Benzo[α]anthracene, B[α]An		5x10 ⁻⁹ at 20°C	0.01 at 25°C	4x10 ⁵	2A/B2
Benzo[b]fluoranthene, B[b]Fl		10 ⁻¹¹ to 10 ⁻⁶ at 20°C	-	4x10 ⁶	2B/B2
Benzo[k]fluoranthene, B[k]Fl		9.6x10 ⁻⁷ at 20°C	-	7x10 ⁶	2B
Chrysene, Chry		10 ⁻¹¹ to 10 ⁻⁶ at 20°C	0.002 at 25°C	4x10 ⁵	3/B2
Pyrene, Py		6.9x10 ⁻⁹ at 20°C	0.14 at 25°C	2x10 ⁵	3
Benzo[ghi]perylene, B[ghi]Pe		~10 ⁻¹⁰	0.00026 at 25°C	10 ⁷	3
Benzo[α]pyrene, B[α]Py		5x10 ⁻⁹	0.0038 at 25°C	10 ⁶	2A/B2
Dibenzo[α,h]anthracene, dB[α,h]An		~10 ⁻¹⁰	0.0005 at 25°C	10 ⁶	2A/B2
Indeno[1,2,3-cd]pyrene, I[1,2,3-cd]Py		~10 ⁻¹⁰		5x10 ⁷	2B/B2

2A/B2: Probably carcinogenic to humans/Probable human carcinogen; 2B: Possibly carcinogenic to humans;

3: Not classifiable as to human carcinogenicity; Blank: Not tested for human carcinogenicity;

*IARC: International Agency for Research on Cancer; U.S. EPA: U.S. Environmental Protection Agency.

Table 2.9 Typical range of PAH concentrations in runoff and river water in South Africa (Chimuka et al., 2015).

PAH	Runoff water	River water
	Range ($\mu\text{g L}^{-1}$)	Range ($\mu\text{g L}^{-1}$)
Indene	1.3-10.1	0.8-3.3
Azulene	9.5-134	Nd
Dibenzo thiophene	0.6-67.5	0.3-9.4
Anthracene	6.7-230	6.7-53.5
Fluoranthene	3.4-251	3.6-24.2
Pyrene	7.2-2,500	0.1-52.4
Mean values	4.78-532.1	2.3-28.56
	Jukskei River water ²	River and Dam water ²
Naphthalene	0.025-0.145	0.022-0.239
Acenaphthene	0.036-0.239	0.053-0.407
Phenanthrene	0.119-0.197	0.053-0.616
Fluoranthene	0.046-0.201	0.021-0.890
Pyrene	0.030-0.104	0.024-0.089
Mean values	0.051-0.177	0.035-0.480

1 = samples taken from the Thohoyandou area, Limpopo Province

2 = samples taken from Eastern, Central and Western areas of Johannesburg

2.4.2 Toxicity of PAHs

The exposure to various PAH compounds can lead to various toxicities in organisms. In order to perform risk assessments of exposure to the various PAHs, Nisbet and LaGoy (1992) assigned Toxic Equivalency Factors (TEFs) to the different PAH compounds and these are shown in Table 2.10. These TEFs are measured relative to the carcinogenicity of benzo[a]pyrene (BaP) and are used to assess the potential health risk for each PAH exposure. It is, however, important to note that PAHs rarely occur as a single compound in the environment (including in water), but rather as mixtures whose toxic effects can be additive or synergistic.

Table 2.10 PAHs and their toxic equivalency factors (TEFs) expressed relative to BaP (Nisbet & LaGoy, 1992).

PAH compounds	TEF
Dibenzo[ah]anthracene	5
Benzo[a]pyrene	1
Benzo[a]anthracene	0.1
Benzo[b]fluoranthene	0.1
Phenanthrene	0.001
Indeno[1,2,3-cd]pyrene	0.1
Anthracene	0.01
Benzo[ghi]perylene	0.01
Chrysene	0.01
Acenaphthene	0.001
Acenaphthylene	0.001
Fluoranthene	0.001
Fluorene	0.001
Pyrene	0.001
Naphthalene	0.01

The toxicity of PAHs to aquatic organisms is enhanced by their metabolism and photooxidation into derivative compounds. Thus they become more toxic in the presence of UV light which facilitates their derivatization (Abdel-Shafy & Mansour, 2016). Animals can absorb PAHs through dermal contact, inhalation and ingestion pathways and once in their systems, PAHs can cause adverse effects like tumors, and can affect reproduction, development and immunity (Abdel-Shafy & Mansour, 2016).

A study by Engraff et al. (2011) demonstrated the importance of considering PAH mixtures when studying toxicity in aquatic systems. This is because it is not common for PAH contamination to consist of only a single compound, but usually a mixture of PAHs. The use of single PAH compounds for risk assessments can lead to an underestimation of the risk since the effect of compound mixtures can be additive or synergistic.

Ikenaka et al. (2013) conducted exposure experiments to investigate the acute toxicity of benzo[a]pyrene on cladoceran species (*Ceriodaphnia reticulata* and *Daphnia magna*) and its impact on zooplankton communities. They found the LC50 to be 4.3 and 4.7 $\mu\text{g L}^{-1}$ for *C. reticulata* and *D. magna* respectively. The study further showed that B[a]P induced a decrease in zooplankton abundance when concentrations of 5 and 10 $\mu\text{g L}^{-1}$ were used with <4 days residence time.

Some PAHs have been reported to have possible carcinogenic effects to aquatic animals and humans (ATSDR, 2012). Different environmental agencies have classified a number of PAH compounds in this regard as shown in Table 2.11. Some studies in animals have revealed that certain PAHs also can affect the hematopoietic and immune systems and can produce reproductive, neurologic, and developmental effects (Szczeklik et al., 1994; Zhao, 1990).

Table 2.11 Carcinogenic classification of PAH compounds by different agencies (ATSDR, 2012).

Agency	PAH Compound(s)	Carcinogenic Classification
U.S. Department of Health and Human Services (HHS)	benz(a)anthracene, benzo(b)fluoranthene, benzo(a)pyrene, dibenz(a,h)anthracene, and indeno(1,2,3-c,d)pyrene.	Known animal carcinogens
International Agency for Research on Cancer (IARC)	benz(a)anthracene and benzo(a)pyrene.	Probably carcinogenic to humans
	benzo(a)fluoranthene, benzo(k)fluoranthene, and ideno(1,2,3-c,d)pyrene.	Possibly carcinogenic to humans
	anthracene, benzo(g,h,i)perylene, benzo(e)pyrene, chrysene, fluoranthene, fluorene, phenanthrene, and pyrene.	Not classifiable as to their carcinogenicity to humans
U.S. Environmental Protection Agency (EPA)	benz(a)anthracene, benzo(a)pyrene, benzo(b)fluoranthene, benzo(k)fluoranthene, chrysene, dibenz(a,h)anthracene, and indeno(1,2,3-c,d)pyrene.	Probable human carcinogens
	acenaphthylene, anthracene, benzo(g,h,i)perylene, fluoranthene, fluorene, phenanthrene, and pyrene	Not classifiable as to human carcinogenicity

2.4.3 Guideline limits for PAHs

Due to the low solubilities of most PAHs in water, they are typically found at very low concentrations, hence there are not many regulations relating to their maximum contaminant level (MCL) in water. The U.S. EPA, however, has a number of standards that can be used to assess environmental contamination of PAHs in water systems (shown in Table 2.12) but only benzo(a)pyrene, a known carcinogen, has a MCL value of $<0.2 \mu\text{g L}^{-1}$ in drinking water. Locally in South Africa there are currently no regulatory values for PAHs in water systems, hence they are considered ECPs.

Table 2.12 Existing water quality standards for PAHs (adapted from U.S. EPA, 2010).

Parameter ($\mu\text{g/l}$)	WQC ($\mu\text{g/l}$)		DWMCL/ MCLG	NHSWS		NHSWS		NHGWS
	HHWO	HHOO		FWA	FWC	HHWO	HHOO	
Napthalene				2300	620			20
Fluorene	1100	5300					1300	14000
Benzo(a)anthracene	0.0038	0.018				0.0044	0.049	0.05
Benzo(a) pyrene	0.0038	0.018	0.2/zero			0.0044	0.049	0.2
Benzo(a) fluoranthene	0.0038	0.018				0.0044	0.049	0.05
Benzo(k) fluoranthene	0.0038	0.018				0.0044	0.049	0.5
Chrysene	0.0038	0.018				0.0044	0.049	5
Dibenzo(a,h) anthracene	0.0038	0.018				0.0044	0.049	0.005
Indeno(1,2,3-cd) pyrene	0.0038	0.018				0.0044	0.049	0.05
Acenaphthene	670	990		1700	520	20	20	420
Acenaphthylene								420
Anthracene	8300	40000				9600	110000	2100
Benzo(ghi) perylene								210
Fluoranthene	130	140		3980				280
Phenanthrene								210
Pyrene	830	4000				960	11000	210

DWMCL: EPA Drinking Water MCLs/Other Standard, EPA 822-R-02-038, summer 2002

FWA: Freshwater Acute Values (CMC or Criteria Maximum Concentration)

FWC: Freshwater Chronic Values (CCC or Criterion Continuous Concentration)

HHOO: Human Health Organism Only Values

HHWO: Human Health Water + Organism Values

MCLG: Maximum Contaminant Level Goal

NHGWS: New Hampshire Ambient Groundwater Quality Standards, Env.-Wm 1403.05, 2/23/99

NHSWS: New Hampshire Surface Water Quality Standards, Env.-Ws 1703.21, 12/03/99

WQC: EPA National Recommended Water Quality Criteria, EPA-822-R-02-047, November 2002

2.5 PESTICIDES: ATRAZINE

2.5.1 Sources and occurrence of atrazine in the environment

Atrazine (6-chloro-4-N-ethyl-2-N-propan-2-yl-1,3,5-triazine-2,4-diamine) is a widely used herbicide for controlling annual broad-leaved weeds and grasses in pre- or post-emergent crops like maize, sorghum and sugar cane. It kills weeds by inhibiting the photosynthetic electron transport, but the target crop is tolerant to atrazine because of rapid detoxification (MacBean, 2012). The use of atrazine in agriculture can result in contamination of non-target surrounding water resources through various pathways that are shown in Fig. 2.4 and the physiochemical properties of atrazine are provided in Table 2.13.

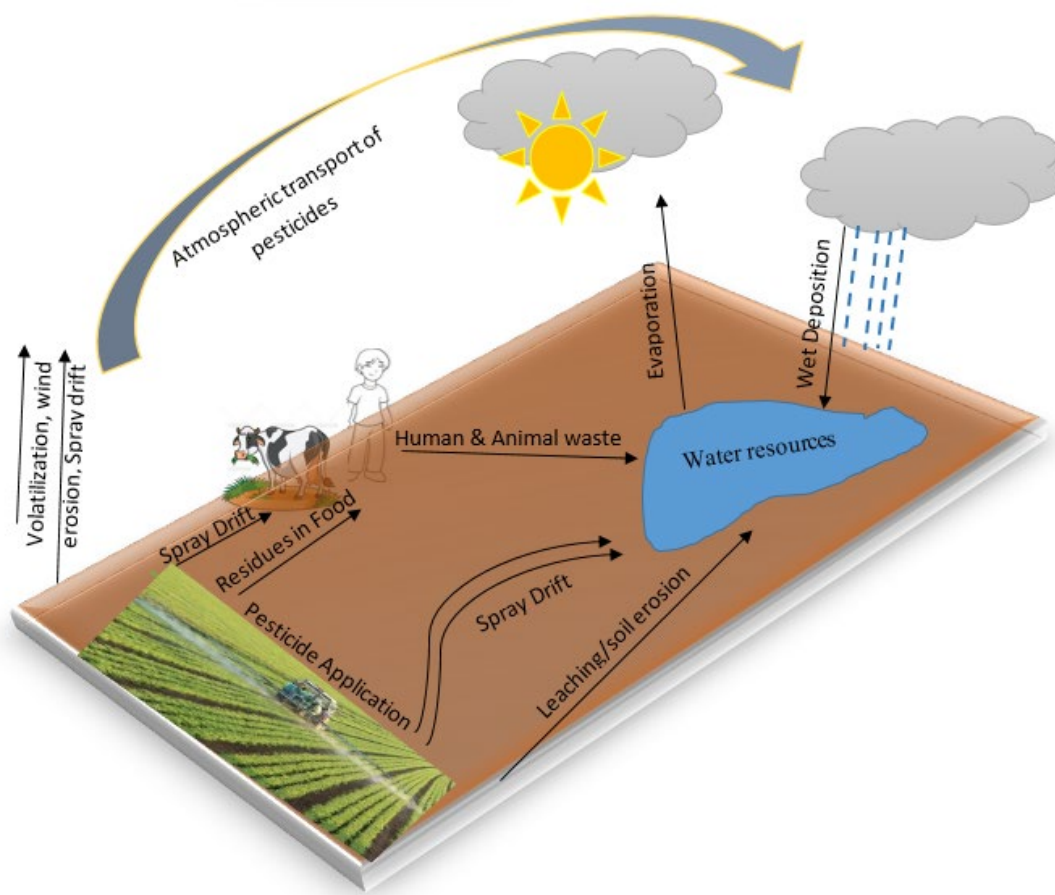


Figure 2.4 Schematic diagram showing the possible routes of pesticide circulation in the environment (adapted from Kosikowska and Biziuk (2010)).

Table 2.13 Physiochemical properties of atrazine

Property	Value
Molecular Weight [#]	215.7 g mol ⁻¹
Molecular formula [#]	C ₈ H ₁₄ ClN ₅
Form [#]	Colourless powder
Melting point [#]	175.8°C
Boiling point [#] (at 101 kPa)	205.0°C
Vapour pressure [#] (at 25°C)	3.85×10 ⁻² mPa
K _{ow} log P [#]	2.5 (25°C)
Henry's constant [#]	1.5×10 ⁻⁴ Pa m ³ mol ⁻¹
Density [#] (at 22°C)	1.23 g cm ⁻³
Solubility: in water (at 22°C, pH 7) [#]	33 mg L ⁻¹
K _d [*]	2.60
Log K _{SA} [*]	7.18
Deposition potential, Φ (%)	17.60

K_{SA}: volatilization potential from soil to air

K_d: distribution coefficient from soil and soil-water partitioning

K_{ow}: octanol-water partition coefficient

[#]MacBean (2012)

^{*}Ratola et al. (2014)

Because of its high annual use in agriculture, atrazine has been one of the most frequently detected pesticides in freshwater systems in many parts of the world. For example, Gilliom (2007) found that atrazine was the most frequently detected pesticide in US surface and groundwater systems. A similar assertion has been made for European groundwater (Gavrilescu et al., 2014). In South Africa, atrazine has also been shown to have the largest number of seasonal occurrences as shown in Table 2.14 (Patterton, 2013).

A WRC study by Dabrowski et al. (2014) dealing with the prioritization of pesticides that are used in South Africa, featured atrazine as the highest ranked pesticide among 25 priority pesticides. This ranking and prioritization was based on a weighted hazard potential (WHP) – a prioritization index which is directly proportional to the pesticide's toxicity potential (TP) and total quantity of use.

Several studies have found atrazine in South African freshwater systems (Dabrowski et al., 2013; Du Preez et al., 2005; Pick, van Dyk, & Botha, 1992) due to its high use.

Table 2.14 Concentration ($\mu\text{g L}^{-1}$) of atrazine sampled over four seasons in drinking water in areas across South Africa. Average concentrations are indicated ($n=3$) (Patterton, 2013).

Sampling sites	Summer	Autumn	Winter	Spring
Bloemfontein North tap	0.02	0.15	0.01	0.02
Bloemfontein South tap	0.01	0.19	0.02	0.15
Bloemfontein	0.02	0.02	0.01	0.01
Cape Town	0.00	0.00	0.00	0.00
Durban	0.02	0.02	0.00	0.01
Johannesburg	0.03	0.15	0.11	0.12
Pietermaritzburg	0.02	0.02	0.02	0.02
Port Elizabeth	0.01	0.00	0.00	0.00
Pretoria	0.04	0.16	0.00	0.01

2.5.2 Toxicity of atrazine

Once in water systems, atrazine can have harmful effects on aquatic life, such as endocrine disrupting activity (Giusi *et al.*, 2006; Hayes *et al.*, 2010; Hrouzková & Matisová, 2012). Alarmingly, some studies have shown atrazine to be an endocrine disruptor in human cells (Fan *et al.*, 2007; Sanderson *et al.*, 2000). Atrazine can be quite persistent in water, as a study in Lake Superior in Canada, suggested that the half-life of atrazine in lakes was over 10 years (Thurman & Cromwell, 2000). This stability can lead to negative effects on aquatic organisms. For example, a study by Hayes *et al.* (2010) showed that atrazine exposure demasculinized (chemically castrated) male African clawed frogs (*Xenopus laevis*) leading to suppressed mating behaviors and reduced spermatogenesis. Studies by Santos and Martinez (2012) showed exposure to 2-10 $\mu\text{g L}^{-1}$ of atrazine resulted in biochemical changes and DNA damage to Neotropical fish species (*Prochilodus lineatus*).

Ingestion of 100 g of atrazine by humans was observed to have catastrophic results. According to literature such exposure may lead to coma, heart and peripheral vessel damage, and renal failure, resulting in death (Corporation, Substances, & Registry, 2003; Ellenhorn *et al.*, 1997). Other delayed, fatal consequences include leukaemia and brain cancer (Bingham, Cohrssen, & Powell, 2001). Exposure to atrazine also had other critical carcinogenic risks. Tumours of the reproductive organs were often related to atrazine exposure (Bingham *et al.*, 2001; Corporation *et al.*, 2003). Several studies on lymph cancer also showed an association with atrazine exposure. Alarmingly, one study by Van Leeuwen *et al.* (1999) revealed an association between stomach cancer and atrazine exposure in the range 50-649 ng L^{-1} , which is well below the EPA's MCL of 3 $\mu\text{g L}^{-1}$ for drinking water. Other critical effects revolve around vulnerabilities of women during pregnancy and on the foetus or infants. These effects include foetal development aberrations like growth retardation, a decrease in gestation age, and gastroschisis (Chevrier *et al.*, 2011; Munger *et al.*, 1997; Ochoa-Acuña *et al.*, 2009; Waller *et al.*, 2010). Lower birth weight was also directly associated with perinatal mortality in the U.S. (Paneth, 1995).

Moderate effects of exposure include a decrease in sperm concentration and motility, known as oligospermia (Swan, 2006). Minor side effects of atrazine exposure included fatigue, dizziness, nausea, and skin irritation (Corporation et al., 2003; Ellenhorn *et al.*, 1997).

2.5.3 Legal limits for atrazine in water

The World Health Organization (WHO) has derived guideline values for atrazine and its metabolites and these are shown in Table 2.15. Typical atrazine concentrations rarely exceed $2 \mu\text{g L}^{-1}$ which is well below the $0.1 \mu\text{g L}^{-1}$ guideline limit for atrazine in drinking water. The acceptable daily intake for atrazine and its chloro-s-triazine metabolites is between 0-0.02 mg kg^{-1} body weight based on luteinizing hormone surge suppression and subsequent disruption of the estrous cycle seen at 3.6 mg kg^{-1} body weight per day in a 6 month study in rats. Hydroxyatrazine is another atrazine metabolite and the WHO has set its guideline limit in drinking water to 0.2 mg L^{-1} which was identified on the basis of kidney toxicity at 7.8 mg kg^{-1} body weight per day in a 24 month study on rats, using a safety factor of 25, based on kinetic considerations.

Table 2.15 Guideline values for atrazine and its metabolites in drinking water (WHO, 2011)

Compound	Guideline		Guideline value derivation
	Value (mg L^{-1})	ADI	
Atrazine	0.1	0-0.02 mg kg^{-1} body weight based on the NOAEL for atrazine of 1.8 mg kg^{-1} body weight per day.	Allocation to water : 20% of upper limit of ADI Body weight : 60 kg adult Consumption : 2 litres per day
Chloro-s-triazine metabolites	0.1	0-0.02 mg kg^{-1} body weight based on the NOAEL for atrazine of 1.8 mg kg^{-1} body weight per day.	
Hydroxyatrazine	0.2	0-0.04 mg kg^{-1} body weight based on the NOAEL of 1.0 mg kg^{-1} body weight per day.	

ADI: acceptable daily intake

NOAEL: non-observed adverse effect level

2.6 CONCLUSION

The reviewed literature has shown that the target compounds included in this study (namely triclosan, acetaminophen, PAHs and atrazine) are constantly being released into the environment from various sources, mainly through human activities. A number of studies have also demonstrated that these substances have potential negative effects on the health of aquatic organisms and humans. Exposure

to some of these compounds has been shown to disrupt reproductive cycles in some animals and has also been linked to carcinogenic effects. This, therefore, shows the importance of continuous monitoring and regulation of these compounds in the environment, including water resources, especially in water scarce countries such as South Africa.

Triclosan is a biocide which is routinely added to a wide range of personal care, veterinary, industrial and household products. It can persist in the environment and shows toxicity towards various organisms. The continuous exposure of aquatic organisms to TCS and its bioaccumulation potential have led to detectable levels of this biocide in a wide array of aquatic species. Mammalian systemic toxicity studies have shown that TCS is neither acutely toxic, mutagenic, carcinogenic, nor a developmental toxicant, while endocrine disruption related to thyroid hormone homeostasis disruption and possibly the reproductive axis has been noted. Moreover, there is strong evidence that aquatic species such as algae, invertebrates and certain types of fish are much more sensitive to TCS than mammals. Specifically, algae is highly sensitive indicator organism that may be impacted by TCS occurrences in surface waters at levels of 200-2,800 ng L⁻¹, where the worldwide concentration has been found to range from 1.4-40,000 ng L⁻¹. The Minnesota Department of Health (MDH) has developed a guidance value of 50 ppb (50,000 ng L⁻¹) for triclosan in drinking water, whilst the Canadian Federal water quality guideline (FWQG) for the protection of aquatic life from adverse effects of triclosan is 380 ng L⁻¹.

Acetaminophen, or paracetamol, is an over-the-counter analgesic. Although acetaminophen is removed from wastewater by chemical oxidation processes, it has been detected in surface waters, wastewater and drinking water throughout the world. Concentrations of acetaminophen in surface water of over 10,000 ng L⁻¹ have been reported, including in Kenya and South Africa (107,000 ng L⁻¹ and 59,000 ng L⁻¹, respectively) which are higher than the predicted no-effect concentration (PNEC) of 9200 ng L⁻¹. Hence, AC might represent a threat to non-target organisms. A guidance value of 200 ppb (200,000 ng L⁻¹) for acetaminophen in drinking water has been set by the MDH.

PAHs are known to have generally low solubility in water hence they are typically found at very low concentrations in this medium, although they are ubiquitous environmental pollutants arising from combustion processes. Local studies have shown that PAHs occur in water systems at mean concentrations ranging from 0.035-532 µg L⁻¹. However, even at these low concentrations they are of concern, as some PAH compounds like benzo[a]pyrene have been shown to have LC50 of around 4 µg L⁻¹ towards cladoceran species. The reviewed literature shows that PAH exposure can lead to various toxicities leading to negative effects on some aquatic organisms.

The target pesticide, atrazine, is a commonly used herbicide that has been frequently detected in local water systems. The typical concentration that has been previously reported in WRC studies for this compound ranges from 0.01-0.19 µg L⁻¹. In this context, it is important to note that the World Health Organization has set the guideline limit for atrazine in drinking water to 0.1 mg L⁻¹ and the reported concentrations are well below this limit. However, it is also important to note that some studies have reported carcinogenic effects at much lower concentrations of 50-649 ng L⁻¹. Other negative

toxicological effects that atrazine can cause to aquatic organisms have also been highlighted in the literature, making it a contaminant of environmental concern.

It needs to be remembered that ecotoxicity testing of compounds merely provides indications of acute effects *in vivo* in specific organisms of different trophic levels after short-term exposure, and only rarely after long-term (chronic) exposures (Fent, 2001). The results may thus not accurately reflect potential environmental toxic effects induced by long-term exposure to low levels of these pollutants. Moreover, in water systems a mixture of compounds is invariably present, therefore the risk of additive and synergistic toxic effects cannot be ignored. Local hotspots of elevated concentrations of contaminants near sources may also occur, which are outside the ranges of expected environmental levels reported in the literature. It is therefore important to monitor the levels of the target compounds in South African water systems as widely as possible in order to effectively and proactively manage our resources and to minimize potential negative toxicological effects.

CHAPTER 3: THE OPTIMIZATION AND APPLICATION OF QUANTUM DOT BASED FLUORESCENCE SENSORS

3.1 INTRODUCTION

Quantum dots (QDs) are semiconductor crystalline nanomaterials that have unique electronic and optical properties due to quantum confinement effects (Murphy & Coffey, 2002). They have a number of attractive properties that make them suitable as analytical sensors, including high fluorescence quantum yields, independence of emission to the excitation wavelength, size-dependent fluorescence, narrow spectral line widths, and stability against photobleaching (William *et al.*, 2006). Furthermore, their utilization can be advantageous over larger particles because of their large surface to volume ratios, their surface activity, and their strong adsorption affinity to other nanoparticles. Importantly, QDs have size-dependent optical properties, which means their absorption and emission properties can be tuned by changing the particle size, shape and surface structure (Zhang *et al.*, 2003).

QDs also have unique physico-chemical properties that pertain to the combination of their crystalline metalloid core structure and composition and quantum-size confinement (Hardman, 2006). When the size of the exciton, known as the exciton Bohr radius, (r_{Bohr} ($\sim 1\text{-}5\text{ nm}$)), exceeds the physical size of the semiconductor nanocrystal (D), the quantum confinement effect of QDs occurs which provides size-dependent emission (Wilson *et al.*, 1993). Furthermore, QDs are photo electrochemically active which make them reliable optical labels in environmental analysis (Liu *et al.*, 2014b).

The mechanisms involved in QD-based sensing are involve energy transfer and charge transfer. Förster resonance energy transfer (FRET) is a non-radiative energy transfer between donor and acceptor fluorophores in which QDs may act as an energy donor by being size-tuned in order to provide overlap with the acceptor (Stanisavljevic *et al.*, 2015). Although there are numerous applications reported where QDs serve as an energy donor, few publications report mechanisms related to QDs as acceptor (Sapsford *et al.*, 2006).

The photoluminescence (PL) “turn-on” mode is more desirable compared to the “turn-off” mode, as many other factors can also induce the PL “off” state resulting in false positives. The “turn-on” mode can also be utilized for multiplexing in order to use several detectors that uniquely respond to various analytes and to provide lower detection limits (Xu *et al.*, 2011).

In order to obtain high quality semiconductor quantum dots (QDs) suitable for a variety of chemical and biological applications, the hot-injection organometallic synthetic route is the most effective (de Mello Donegá *et al.*, 2005). The reason is due to the flexibility it provides in tuning the optical properties of the QDs and to eliminate as much as possible the presence of surface defects that diminish the optical properties of the QDs. CdSe/ZnS core/shell QDs have been synthesized at high temperature in organic media and stabilized with hydrophobic capping agents including trioctylphosphine oxide (TOPO) and

oleic acid (OA) (Xie *et al.*, 2005). In order to mediate dangling bonds on the surface of the QDs, surface modification has been developed to passivate the QDs. CdSe QDs are typically covered by either a ZnS or CdS shell so the band gap of the core will lie energetically within the band gap of the shell and the exciton will be confined inside the core (Hines & Guyot-Sionnest, 1996; Xie *et al.*, 2005). It has been previously shown that high lattice mismatch (~16%) between ZnS and CdTe may cause incomplete coating of the core QDs with ZnS which also makes the QDs susceptible to degradation (Ithurria *et al.*, 2007). Low lattice mismatch (~12%) for CdSe and ZnS, however, results in less degradation (Yong *et al.*, 2011). Therefore CdSe/ZnS QDs are more stable and less toxic than CdTe/ZnS QDs. Moreover, CdSe/ZnS QDs have exhibited the least cytotoxicity and the most biocompatibility with high sensing ability among CdSe, CdSe/ZnS and CdSe/CdS QDs (Ratnesh & Mehata, 2017). These core/shell QDs have a number of attractive properties that make them suitable as analytical sensors and through surface modification strategies they have found various applications across disciplines. Reviews have thus been published on their application in solar cells (Nozik *et al.*, 2010), as biological labels (Jin *et al.*, 2011), in microelectronics (De Menezes *et al.*, 2005) and in electrochemistry (Huang & Zhu, 2013).

In terms of the use of CdSe/ZnS QDs as fluorescence sensors, a simple method was, for example, deployed based on the increment of the fluorescence intensity of mercaptoacetic acid (MAA)-capped CdSe/ZnS quantum dots for L-cysteine (Cys) detection in three synthetic amino acid mixed solutions and human urine samples over the range of 10-800 nmol L⁻¹ with a limit of detection of 3.8 nmol L⁻¹ (Huang *et al.*, 2009).

In another study, L- and D-carnitine enantiomers were quantitatively determined by chiral cysteine (Cys) capped CdSe/ZnS QDs. The authors noted that although the fluorescence intensity of the QDs decreased in the presence of D-carnitine, there was no evidence for the PL change by L-carnitine. A dramatic quenching was ascribed to the reorganization of Cys molecules on the QD surface (Carrillo-Carrion *et al.*, 2009).

Polymethylmethacrylate (PMMA)-capped CdSe/ZnS quantum dots were also developed for the determination of paeonol in paeonol ointment based on fluorescence quenching of an aqueous solution of the QDs. This quenching effect was due to the interaction of hydroxyl group of paeonol with PMMA via hydrogen bonding which obstructed excitation of electrons from the conduction band to the valence band. The fluorescence intensity of the CdSe/ZnS QDs was quenched in the range of 150.4-1.0×10⁶ nmol L⁻¹ with a LOD of 102.3 nmol L⁻¹ (Dong *et al.*, 2011).

In another study, chiral methyl ester N-acetyl-L-cysteine-CdSe/ZnS QDs were used for the chiral recognition of naproxen, flurbiprofen, aryl propionic acids, ibuprofen and ketoprofen. The QDs showed stability owing to the ligand anchored onto the surface of the QDs by not only the thiolate but also the ester carbonyl group. Quenching of the QDs emission was a possible mechanism for the detection of all the assayed drugs which was attributed to the interaction of the drug with the reorganized ligand on the surface of the QDs (Delgado-Perez *et al.*, 2013). Quantitative determination of both chiral forms of these drugs can be performed in mixtures and pharmaceutical samples.

A set of QDs was synthesized including CdSe with and without a ZnS shell in the size range of 2.0-3.5 nm by Kuzyniak *et al.* They investigated cytotoxic effects of the QDs in the human pancreatic carcinoma cell line BON at QD concentrations below 0.5 μM . CdSe/ZnS QDs with GSH capping showed good tolerability both in living organisms and in cell models and low toxicity. They are therefore a promising candidate for *in vitro* and *in vivo* biomedical applications.

Various parameters are crucial for fluorescence sensor development which need to be optimized in order to realize the full potential and performance of the sensor material. These parameters include contact (or incubation) time with target analyte, excitation wavelength during fluorescence measurements, the concentration of the sensor solution, the ratio of analyte-to-sensor solutions, pH, etc.

Here we report on the optimization and application of water-soluble CdSe/ZnS quantum dots for the sensing of two emerging chemical contaminants, namely triclosan and acetaminophen. The fluorescent nanoparticles that were fabricated for pesticides are CdSeTe/ZnS QDs, while for PAHs graphene quantum dots (GQDs) were prepared.

3.2 ACETAMINOPHEN

In 2012, a simple and sensitive assay of acetaminophen (AC) was proposed by Li *et al.* based on the quenching of the fluorescence intensity of L-cysteine capped CdTe nanoparticles (NPs) in aqueous solution. The method relied on changes in the fluorescence intensity when the target analyte interacts with the surface of QDs. Under optimal experimental conditions, the relative fluorescence intensity ($\Delta I = I_0/I$) of L-cysteine capped CdTe NPs versus the concentration of acetaminophen was linear over the range of 1.5×10^3 - 2.4×10^3 ng L^{-1} with a detection limit of 639.0 ng L^{-1} . The applicability of the method was tested for the analysis of AC pharmaceutical tablets (Li *et al.*, 2012).

Recently, amphiphilic pillar [5] arene (amPA5) functionalized reduced graphene oxide (amPA5-RGO) has been applied as a 'turn on' fluorescence sensing platform for the determination of AC in serum samples. Acridine orange (AO)/acetaminophen was used as signal probe/target molecule. The mechanism was based on competitive host-guest interaction between two analytes leading to a change in fluorescence signal of the dye molecule. The prototype sensor gave a linear response over the concentration range 1.5×10^4 - 6.0×10^5 ng L^{-1} and 6.0×10^5 - 5.0×10^6 ng L^{-1} with a detection limit of 7.6×10^3 ng L^{-1} (Zhao *et al.*, 2017).

3.2.1 Determination of acetaminophen with L-Cys capped CdSe/ZnS QDs

All measurements were performed under the same conditions for the optimization experiments: the excitation and emission slit width of the spectrofluorometer (Horiba Jobin Yvon FluoroMax-4) was 5 nm and the fluorescence intensity was measured at an excitation wavelength of 300 nm. A typical procedure for the detection of AC is described as follows: 1.0 mg of CdSe/ZnS-L-Cys was dissolved in

3 mL Millipore water and a standard solution containing a specific amount of AC was added and the corresponding PL spectrum was recorded after 5 min. AC standard solutions were prepared within the range of 3.0-100 nmol L⁻¹ by dissolution in H₂O. Sensing was carried out by placing 2 mL of QDs solution in a quartz cuvette followed by addition of 500 μL of AC standard solution. It took about 5 min for the stabilization of the PL profile and this PL intensity was set as F. Moreover, the PL intensity of QDs in the presence of 500 μL of water was set as F₀. Through the variation of AC concentration, a series of F-F₀ values were obtained.

Tap water samples for fluorescence measurements were collected from a municipal tap water in Pretoria, South Africa using pre-cleaned glass bottles. River water samples were collected from the LC de Villiers sports grounds of the University of Pretoria. The sample bottles were filled without headspace and immediately placed in cooler boxes filled with icepacks and transferred to the laboratory for storage at 4°C prior to analysis within one week. Before analysis, the collected tap water and river water samples were centrifuged at 4500 rpm for 5 min and filtered using filter paper (110 mm pore size).

3.2.2 Optimization of the determination of acetaminophen

3.2.2.1 Effect of aqueous L-Cys-CdSe/ZnS QDs concentration

Taking into consideration that the concentration of QDs can influence the fluorescence intensity, different concentrations of L-Cys-CdSe/ZnS QDs (1.0, 1.5, 2.0, 2.5, 3.0 mg in 3.0 mL water) were prepared and 5.0 nmol L⁻¹ of AC was added to each. Briefly, 500 μL of a fixed concentration of AC was added to 2 mL of each concentration of QDs and the fluorescence intensity was recorded after 5 min. It was found that high concentrations of aqueous L-Cys-CdSe/ZnS QDs decreased the sensitivity of the system likely due to self-quenching or agglomeration effects, whereas very low concentrations of QDs leads to a narrowing of the linear range. The optimum concentration was found to be 1.0 mg of L-Cys-CdSe/ZnS QDs in 3.0 mL water, indicating an increase in the interaction of AC with QDs in solution (Fig. 3.1).

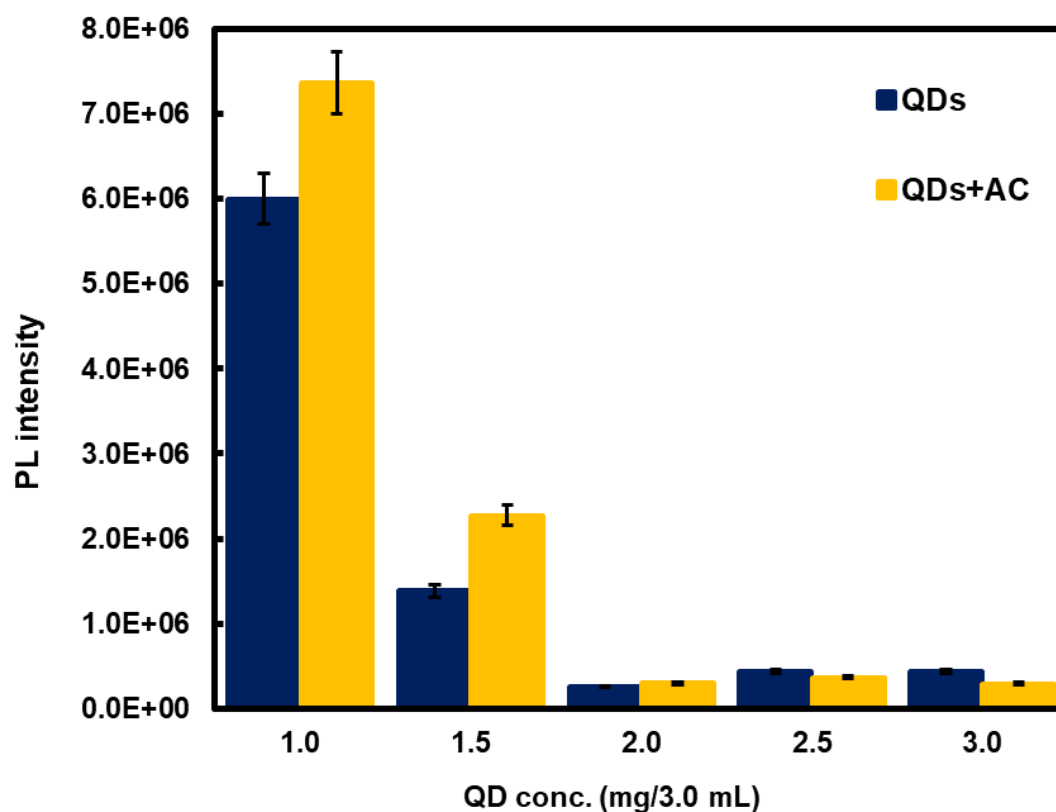


Figure 3.1 Effect of the concentration of aqueous L-Cys-CdSe/ZnS QDs on fluorescence in the absence and presence of 5.0 nmol L^{-1} AC at excitation wavelength 300 nm, where F_0 is the fluorescence intensity without AC and F is the fluorescence intensity with AC.

3.2.2.2 Effect of incubation time

In order to investigate the optimum interaction time of L-Cys-CdSe/ZnS QDs with AC, the fluorescence intensity of the system was tested at different time intervals in the presence of 5.0 nmol L^{-1} AC (Fig. 3.2). The maximum fluorescence intensity was obtained after 5 min, which was thus used in subsequent experiments. A quenching effect of the PL intensity of the QDs was observed after 10 min, indicating a potential reversible interaction. The results show that although AC can be detected within 5 to 35 min of incubation time, shorter incubation time is more suitable due to the appreciable enhancement in fluorescence signal.

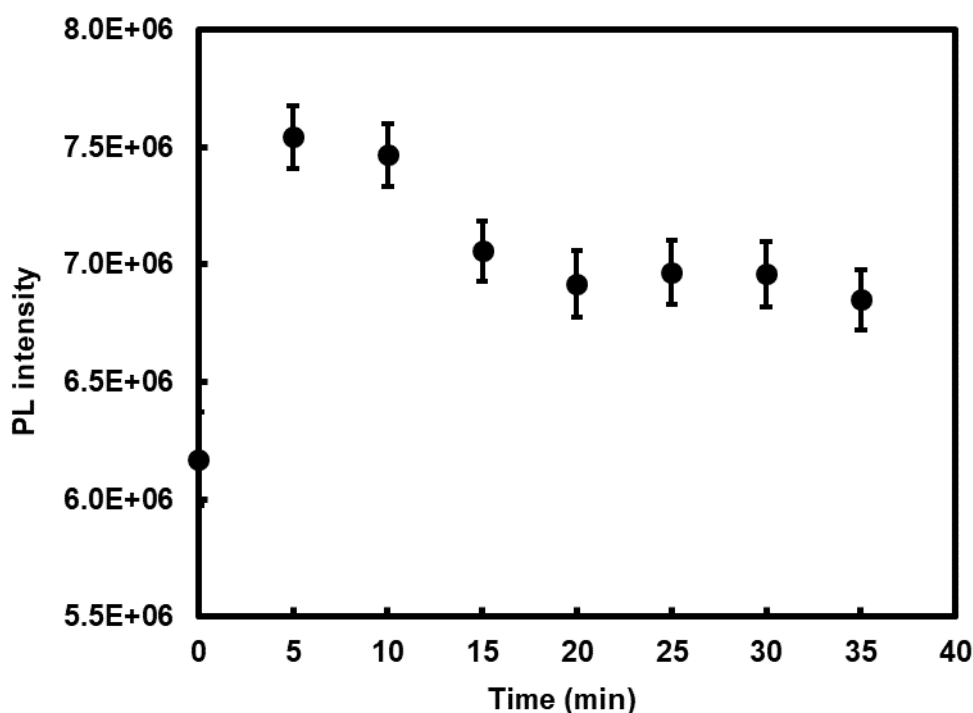


Figure 3.2 Effect of interaction time on the fluorescence intensity of the L-Cys capped CdSe/ZnS QD-AC system at an excitation wavelength of 300 nm.

3.2.2.3 Stabilization of fluorescence intensity

The fluorescence intensity of L-Cys-CdSe/ZnS QDs in Millipore water increased over time and became stable after one day. No major changes in the fluorescence intensity of $1.0 \text{ mg } 3.0 \text{ mL}^{-1}$ QD solutions were noted even after storage for 5 days in solution under ambient light conditions (Fig. 3.3). The red shift in the PL emission of the exposed L-Cys-CdSe/ZnS QDs is an indication that the band gap of the QDs decreased. Aggregation can induce such a red shift in the QD fluorescence which would also be accompanied by PL quenching although quenching in fluorescence intensity may also be attributed to the inability of the thiol ligand to suppress the electron much deeper into the interior of the QDs. The slight decrease in fluorescence intensity between day 1 to day 5 may also be due to desorption of L-Cys from the surface of CdSe/ZnS QDs, as L-Cys acts as a surface passivating agent, which eliminates surface defects (Koneswaran & Narayanaswamy, 2009). Subsequent analytical measurements were thus carried out after the fluorescence intensity of QDs had become stable after one day.

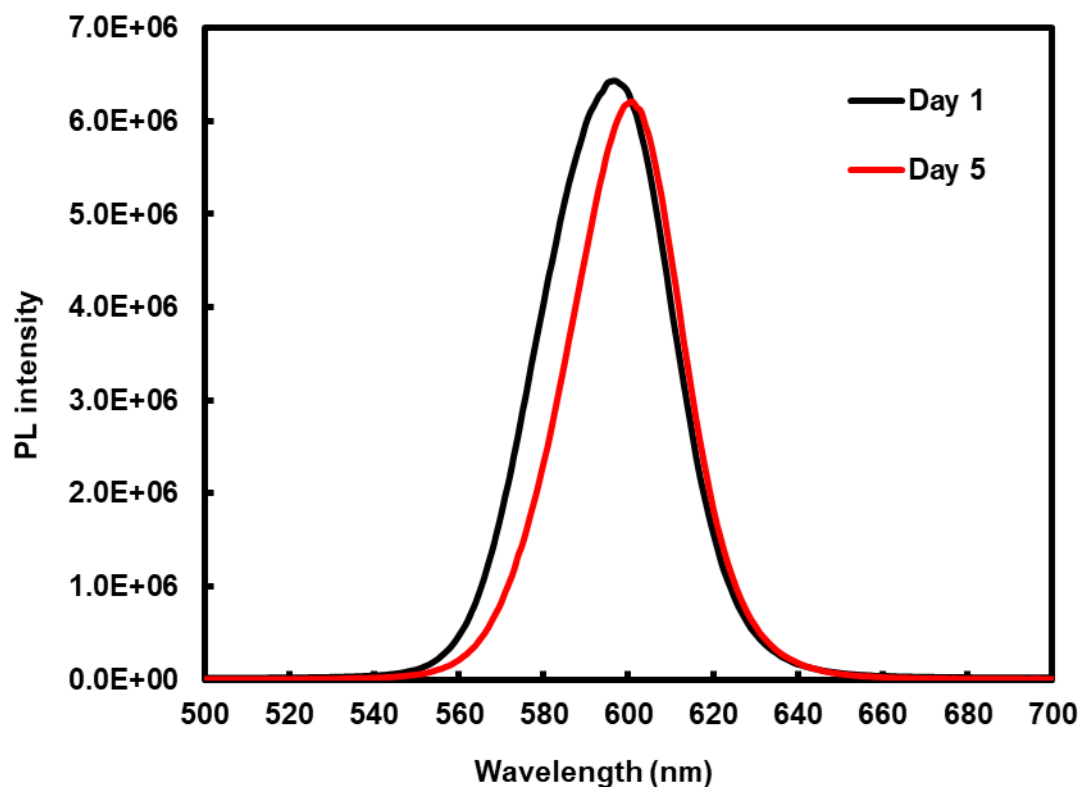


Figure 3.3 PL stability of the hydrophilic QDs measured before and after 5 days of exposure to ambient light (300 nm excitation).

3.2.2.4 Fluorescence behaviour of L-Cys-CdSe/ZnS QDs in the presence of AC

Under optimal conditions (i.e. 1.0 mg 3.0 mL⁻¹ of L-Cys-CdSe/ZnS QDs and 5 min as incubation time), the introduction of acetaminophen to the L-Cys-CdSe/ZnS QDs solution resulted in luminescence enhancement (Fig. 3.4). This signal enhancement could be due to fluorescence resonance energy transfer (FRET) from analyte (donor) to QDs (acceptor), which occurs when the emission band of the donor overlaps with the excitation band of the acceptor, as in this case. The emission of the acceptor enhances and simultaneously the luminescence of the donor quenches (Goldman *et al.*, 2005; Medintz *et al.*, 2003). Here the fluorescence of the donor (AC) was of very weak intensity compared to that of the acceptor (QDs), therefore the quenching of AC fluorescence was not expected to be visible in Fig. 3.4.

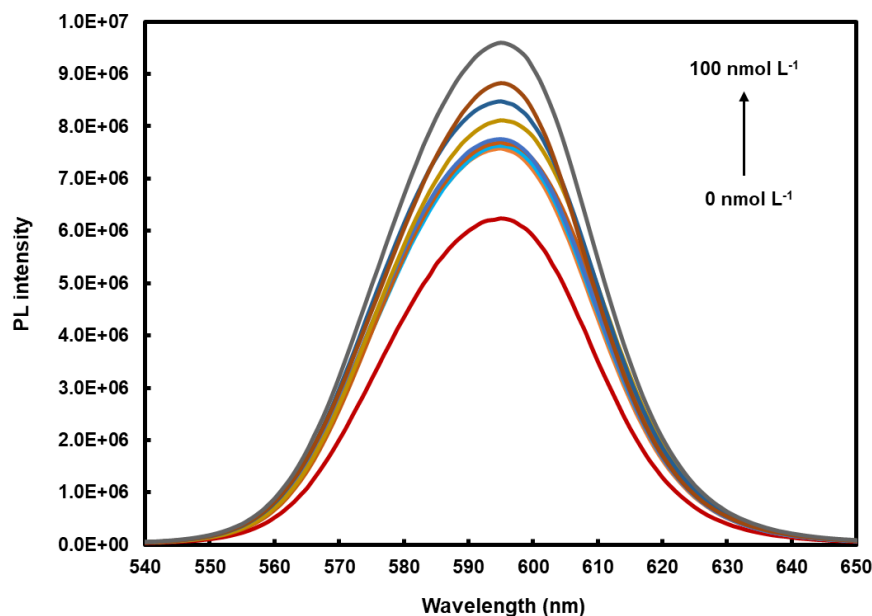


Figure 3.4 The fluorescence spectra of L-Cys-CdSe/ZnS QDs with different concentrations of acetaminophen at an excitation wavelength of 300 nm.

3.2.2.5 Calibration curve, limit of detection and limit of quantification

A plot of fluorescence intensity ($F-F_0$) versus AC concentration is shown in Fig. 3.5, where F_0 and F are the fluorescence intensities of the QDs with and without different acetaminophen concentrations, respectively. A good linear relationship between $F-F_0$ and $[AC]$ was observed from 3.0-100 nmol L^{-1} at an emission wavelength of 595 nm ($r^2 = 0.99$).

The limit of detection (LOD) and quantification (LOQ) are defined as $3\delta/m$ and $10\delta/m$, where δ is the standard deviation of blank measurement ($n=10$) and m is the slope of the calibration curve. LOD and LOQ were found to be 1.6 nmol L^{-1} and 5.3 nmol L^{-1} respectively. The data thus revealed that the proposed method is suitable for the determination of AC at environmentally relevant levels (refer to Chapter 2). The linear range and detection limit of some other methods for the detection of AC in water samples are summarized in Table 3.1 for comparison purposes. The results indicate the potential of our sensor for detecting the low concentrations of AC typically present in water samples.

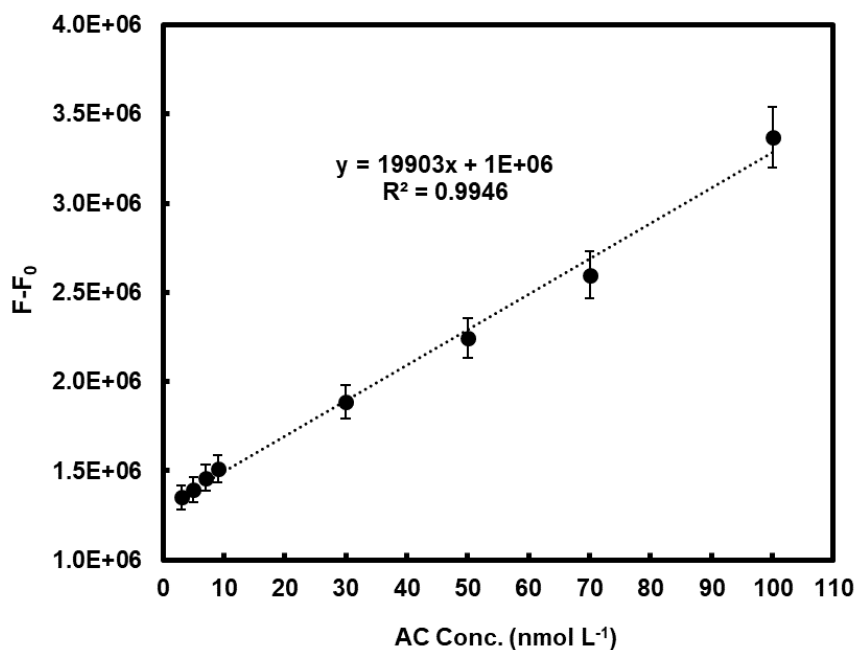


Figure 3.5 Linear graph of $F-F_0$, where F and F_0 are the fluorescence intensities of the QDs with and without different acetaminophen concentrations respectively, versus AC concentration.

Table 3.1 Comparison of some analytical methods for the determination of AC in water.

Detection method	Linear range (nmol L ⁻¹)	Detection limit (nmol L ⁻¹)	Sample matrix	Reference
Biocatalytic spectrophotometry	2,000-1,4000	550	Bottle, tap water and treated wastewater effluent	(Méndez-Albores <i>et al.</i> , 2015)
Differential pulse voltammetry	1,5000-180,000	290	Tap and domestic wastewater	(Gorla <i>et al.</i> , 2016)
Square wave voltammetry		4,400		
LC-ESI-MS/MS	0.027-0.48	-	Surface water	(Kim <i>et al.</i> , 2007)
Fluorescence: L-Cys-CdSe/ZnS QDs	3.0-100	1.6	Tap and river water	This work

LC-ESI-MS/MS: Liquid chromatography/tandem mass spectrometry with electrospray ionization

3.2.2.6 Proposed mechanism

In theory, Förster resonance energy transfer (FRET) is a non-radiative process and if the emission spectra of target compounds overlap with the absorption spectra of the QDs, energy transfer from the analyte to the QDs could occur upon excitation, leading to enhanced QDs fluorescence signals. The rate of energy transfer typically depends on the relative orientation of the transition dipoles, spectral overlap and most importantly the distance between donor and acceptor (Sapsford *et al.*, 2006). In this study, the absorption spectrum of L-Cys-CdSe/ZnS QDs at 450-560 nm (the highest absorbance is at

515 nm) (Fig. 3.6B) overlaps with the emission spectrum of acetaminophen at 350-560 nm (Fig.3.6A). Hence the QDs can absorb the emission energy from acetaminophen leading to the enhancement of the PL emission of QDs, as was observed experimentally.

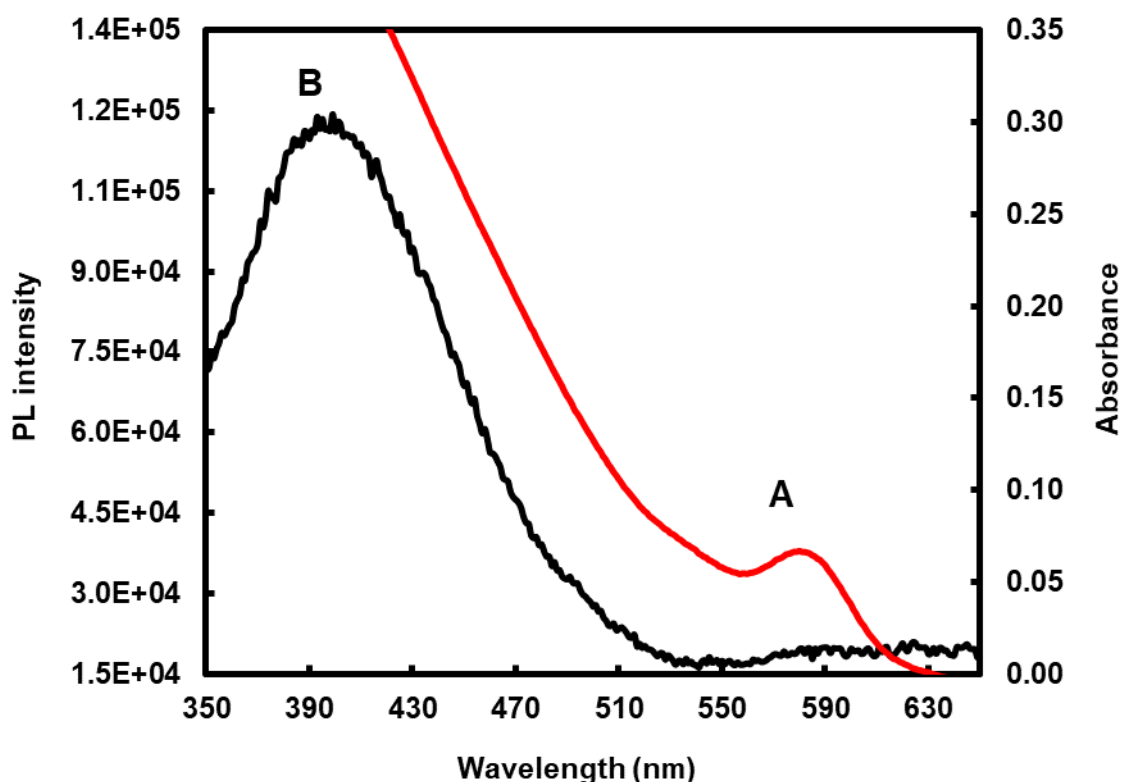


Figure 3.6 Fluorescence spectrum of acetaminophen (1.0×10^{-5} mol L⁻¹) at excitation wavelength 300 nm (A) and UV-Vis absorption spectrum of L-Cys-CdSe/ZnS QDs (B).

3.2.2.7 Determination of Förster distance

The distance between donor and acceptor is also a critical parameter of FRET processes since FRET only occurs over a limited distance. The Förster distance (Å) is the distance between the donor and the acceptor pairs for which efficiency of energy transfer is 50% and depends on the quantum yield of the donor (Lakowicz, 1999). FRET will occur when the overlap between the emission spectrum of the donor and the absorption spectrum of the acceptor is greater than 30% and the distance is less than 10 nm (Elangovan *et al.*, 2002). The Förster distance in the system of L-Cys-CdSe/ZnS QDs-AC was found to be 6.1 nm which was computed using the program PhotochemCAD (Du *et al.*, 1998).

3.2.2.8 Effect of potential interfering analytes on the fluorescence of L-Cys-CdSe/ZnS QDs

The possible effect of other related pharmaceutical analytes was investigated under optimum conditions of 2 mL of 1.0 mg/3.0 mL L-Cys-CdSe/ZnS QDs in the presence of 500 μ L of 100 nmol L⁻¹ of each analyte. 5 min was employed as equilibrium time for each of the fluorescence measurements. Photoluminescence intensity of the L-Cys-CdSe/ZnS QDs was enhanced in the presence of these pharmaceutical analytes (Fig. 3.7). It is thus clear that the prototype QD probe is the most sensitive to AC which provided the highest relative fluorescence intensity whereas the other analytes investigated

did not produce as large a fluorescence enhancement with the QDs (Table 3.2). These compounds therefore do not interfere to a large extent with the detection of AC. Should other structurally related compounds such as ketoprofen and diclofenac sodium be found to interfere with the detection of AC, the selectivity of the QDs sensor could be enhanced by the application of a surface molecular imprinted polymer.

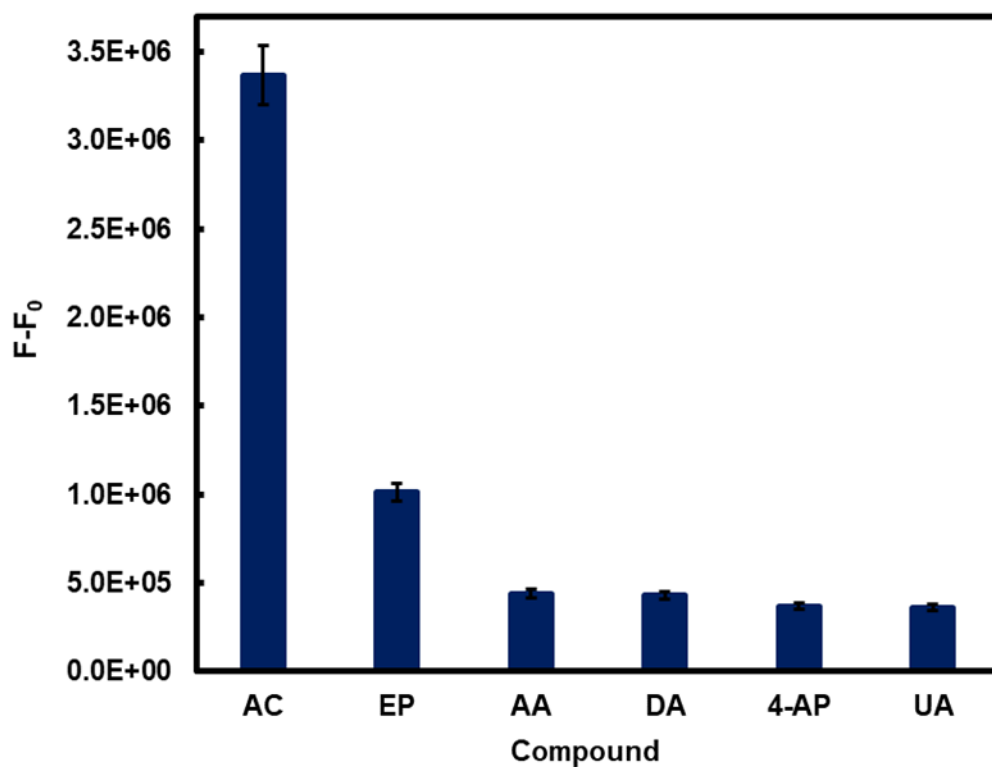


Figure 3.7 Effect of other pharmaceutical analytes on the fluorescence emission intensity of the L-Cys-CdSe/ZnS QDs probe at an emission wavelength of 595 nm. The concentration of AC and each of the other analytes was 100 nmol L⁻¹ and L-Cys-CdSe/ZnS QDs was 1.0 mg/3.0 mL. F-F₀ is the fluorescence intensity of QDs in the presence and absence of the analytes. The excitation wavelength was 300 nm. Epinephrine hydrochloride (EP), L-ascorbic acid (AA), uric acid (UA), dopamine hydrochloride (DA), 4-aminophenol (4-AP).

Table 3.2 Chemical structures of potentially interfering analytes.

Name	Structure
Epinephrine hydrochloride (EP)	
L-ascorbic acid (AA)	
Uric acid (UA)	
Dopamine hydrochloride (DA)	
4-aminophenol (4-AP)	

3.2.2.9 Analytical application

In order to investigate the effectiveness of this fluorescence sensor for AC determinations in real samples, the method was applied to AC in tap and river water samples. As can be seen from Table 3.3, the recoveries of different known amounts of AC spiked in tap water and river water were from 95 to 108% and 90 to 108% respectively. The fluorescence sensing method developed in this study was thus found to be practical and reliable for the determination of AC in the aqueous environment. HPLC-MS/MS analysis was performed as a comparative method which confirmed that the background concentration of AC in the tap and river water samples was below the detection limit (150.0 ng L⁻¹).

Table 3.3 Analytical results for the determination of recoveries of AC spiked in tap and river water samples using L-Cys-CdSe/ZnS QDs.

	AC Spiked (nmol L ⁻¹)	Determined AC (mean ± RSD; n=3, nmol L ⁻¹)	Recovery (%)
Tap water	10	10.1±0.1	101
	50	54.0±0.1	108
	100	95.0±0.2	95
River water	10	10.8±0.7	108
	50	53.0±0.1	106
	100	90.0±0.2	90

3.3 TRICLOSAN

To the best of our knowledge, until now there has been no report on the detection of TCS based on the application of water soluble quantum dots in real water samples. Only one research study has been performed for the extraction of TCS using molecularly imprinted polymers (MIPs), where molecularly imprinted core-shell nanoparticles were synthesized on silica-coated multi-walled carbon nanotubes (MWCNTs) via a sol-gel process so as to extract triclosan from environmental water samples with subsequent HPLC analysis. The binding isotherms of TCS were determined in the concentration range of 34.5-1.4×10⁵ nmol L⁻¹ (Gao *et al.*, 2010).

3.3.1 Determination of TCS with GSH capped CdSe/ZnS QDs

The same conditions were applied for the optimization experiments: the excitation and emission slit width of the spectrofluorometer (Horiba Jobin Yvon FluoroMax-4) was 5 nm and the fluorescence intensity was measured at an excitation wavelength of 300 nm. A typical procedure for the detection of TCS is described as follows: 1.5 mg of GSH-CdSe/ZnS QDs was dissolved in 3 mL Millipore water and a standard solution containing different amounts of TCS was injected and then the corresponding PL

spectra were recorded after different time intervals. TCS standard solutions were prepared within the range of 10-300 nmol L⁻¹ by dissolution in H₂O. Sensing was carried out by placing 2 mL of QDs solution in a quartz cuvette followed by addition of 200 µL of TCS solution standard solution. 5 min was considered as the stabilization time of the PL profile and this PL intensity was set as F. Moreover, the PL intensity of QDs in the presence of 200 µL of water was set as F₀. Through the variation of TCS concentration, a series of F-F₀/F₀ values were obtained.

Municipal tap water samples for fluorescence measurements were collected in Pretoria, South Africa using pre-cleaned glass bottles. River water samples were collected from LC de Villiers sports grounds in Pretoria. The sample bottles were filled and immediately placed in coolers filled with icepacks and transferred to the laboratory for storage at 4°C. Before analysis, the collected tap water and river water samples were centrifuged again at 5000 rpm for 5 min and filtered through filter paper (110 mm pore size).

3.3.2 Optimization of the determination of triclosan

3.3.2.1 Effect of aqueous GSH-CdSe/ZnS QDs concentration

The concentration of GSH-CdSe/ZnS QDs influences the fluorescence intensity and sensitivity of the system. Thus different concentrations of GSH-CdSe/ZnS QDs (1.0, 1.5, 2.0, 2.5, 3.0 mg in 3.0 mL water) were prepared and 70 nmol L⁻¹ of TCS was added to each separately. It was found that high concentrations of aqueous GSH-CdSe/ZnS QDs decreased the sensitivity of the system as self-quenching of QDs occurred (Fig. 3.8) therefore the optimum concentration was found to be 1.5 mg in 3.0 mL water.

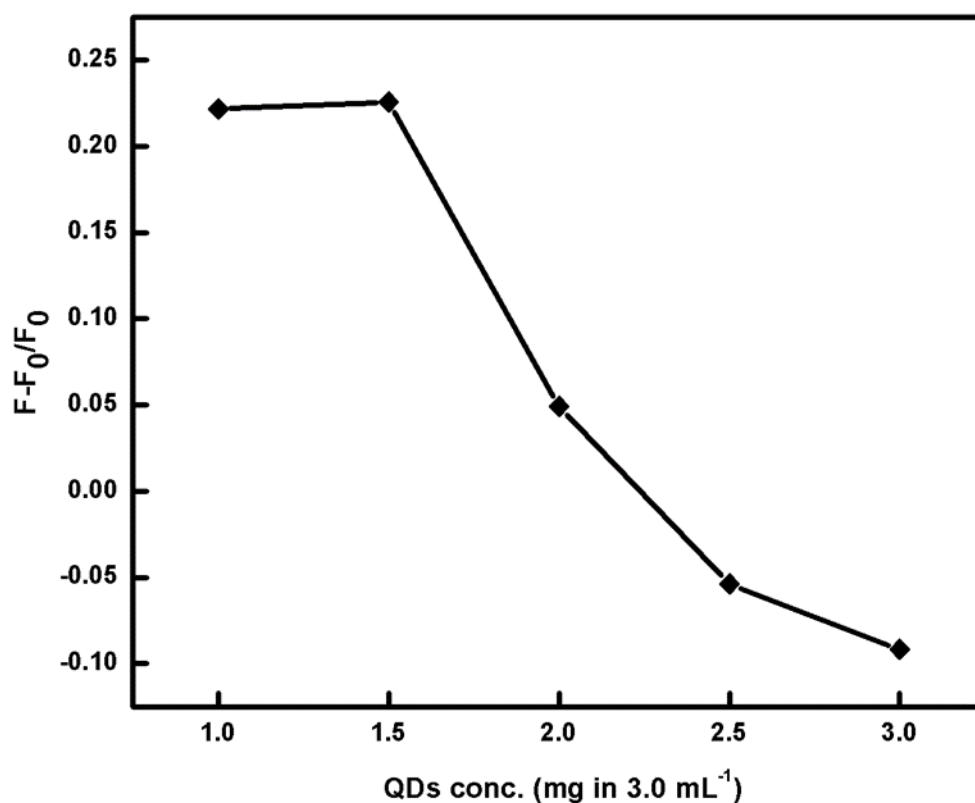


Figure 3.8 Effect of the concentration of aqueous GSH-CdSe/ZnS QDs in the presence of 70 nmol L⁻¹ TCS. The experimental conditions were excitation wavelength, 300 nm; slit widths of excitation and emission, 5 nm.

3.3.2.2 Effect of incubation time

The effect of reaction time on the fluorescence intensity of the GSH capped CdSe/ZnS QDs-TCS system was investigated at different time intervals in the presence of 70 nmol L⁻¹ TCS (Fig. 3.9). The maximum fluorescence intensity was found after 5 min which indicated that the reaction was completed within 5 min at room temperature. Although TCS can be detected within 5 to 30 min of incubation time, a shorter incubation time is more suitable due to the observable enhancement in fluorescence signal. Further studies were thus carried out after 5 min incubation.

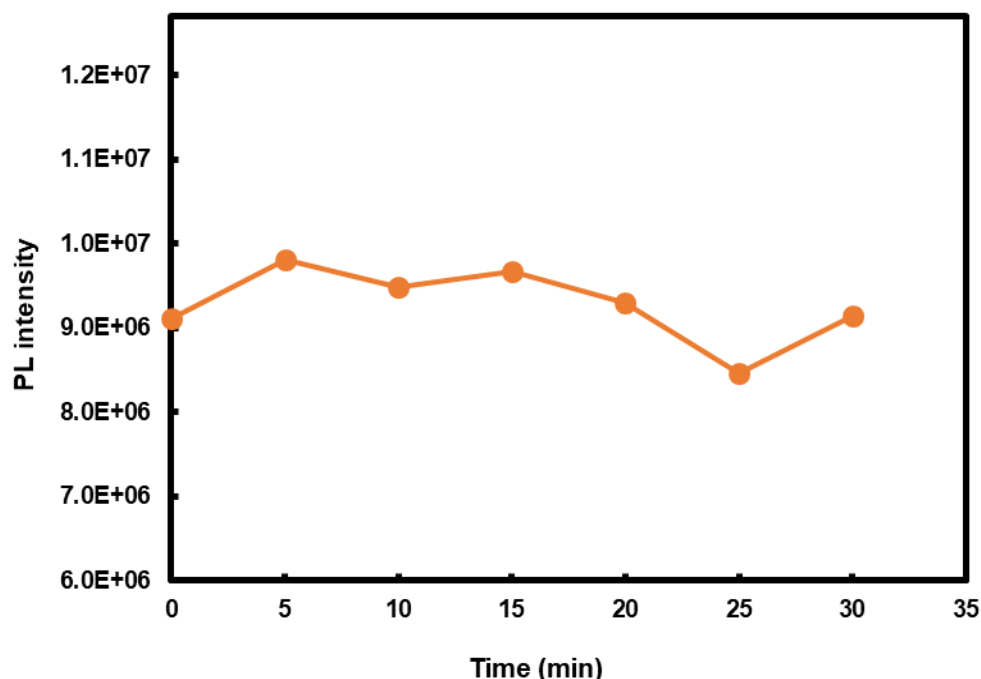


Figure 3.9 Effect of reaction time on the fluorescence intensity of GSH capped CdSe/ZnS QDs in the presence of 70 nmol L⁻¹ TCS. The experimental conditions were GSH-CdSe/ZnS QDs 1.5 mg in 3.0 mL⁻¹; excitation wavelength, 300 nm; slit widths of excitation and emission, 5 nm.

3.3.2.3 Stabilization of fluorescence intensity

The fluorescence intensity of GSH-CdSe/ZnS QDs in Millipore water was slightly increased and became stable after one day compared to freshly prepared QD solutions. The increase of fluorescence intensity of QDs can be attributed to the photo-activation of GSH-capped CdSe/ZnS QDs (Koneswaran & Narayanaswamy, 2009). There were no remarkable changes in the fluorescence intensity of QDs even when stored for 5 days (Fig. 3.10). The slight red shift in the PL emission of the GSH-CdSe/ZnS QDs may be due to a decrease in the band gap of the QDs. Aggregation may also induce PL quenching which would be accompanied by a red shift (1 nm) in the QD fluorescence (Adegoke *et al.*, 2017). Consequently, all analytical measurements were performed after one day to attain stable fluorescence intensity.

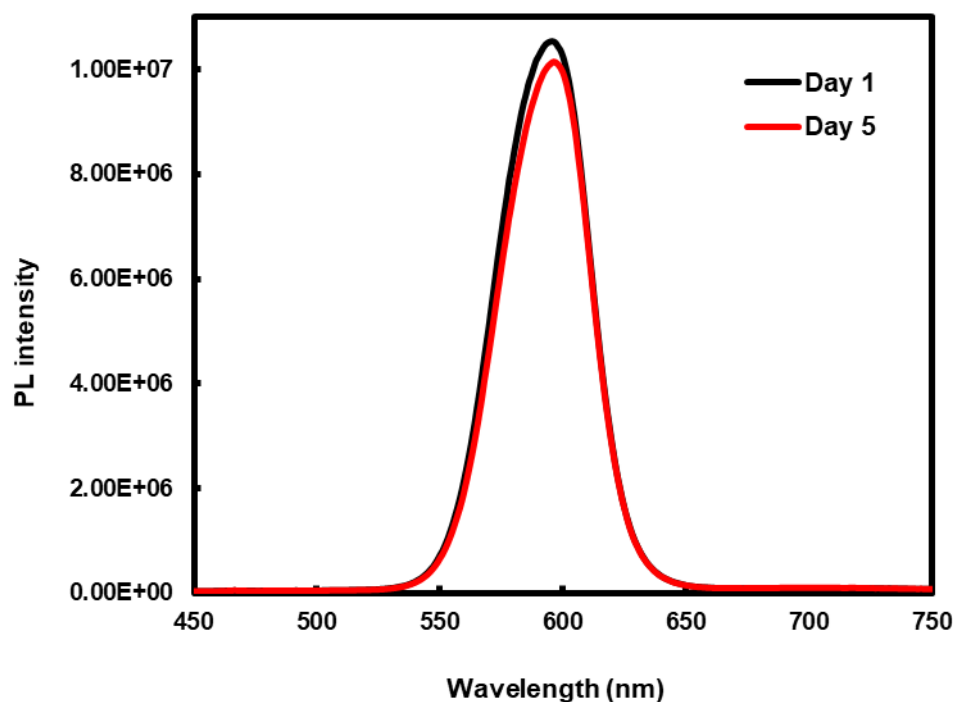


Figure 3.10 PL stability of the hydrophilic QDs measured before and after 5 days of exposure to ambient light. The experimental conditions were GSH-CdSe/ZnS QDs 1.5 mg in 3.0 mL⁻¹; excitation wavelength, 300 nm; slit widths of excitation and emission, 5 nm.

3.3.2.4 Fluorescence behaviour of GSH capped CdSe/ZnS QDs in the presence of TCS

Under optimal conditions, the fluorescence spectra of GSH-CdSe/ZnS QDs with different concentrations of TCS were recorded. It was found that within the concentration range of 10-300 nmol L⁻¹, the intensity of aqueous GSH-CdSe/ZnS QDs enhanced with the introduction of TCS (Fig. 3.11). Förster resonance energy transfer (FRET) from analyte (donor) to QDs (acceptor) was deemed as the possible mechanism in this system. FRET is non-radiative transfer whereby energy transfer from an excited state of the donor (TCS) to a proximal ground state of the acceptor (QDs) through long-range dipole-dipole interactions which can be monitored by quenching or enhancement of acceptor (Lakowicz, 1999). In our experiments, the fluorescence intensity of the acceptor was enhanced while that of the donor was quenched. However, as the fluorescence of the donor (TCS) was of very weak intensity compared to that of the acceptor (QDs), the quenching of the TCS fluorescence was not expected to be visible in Fig. 3.11.

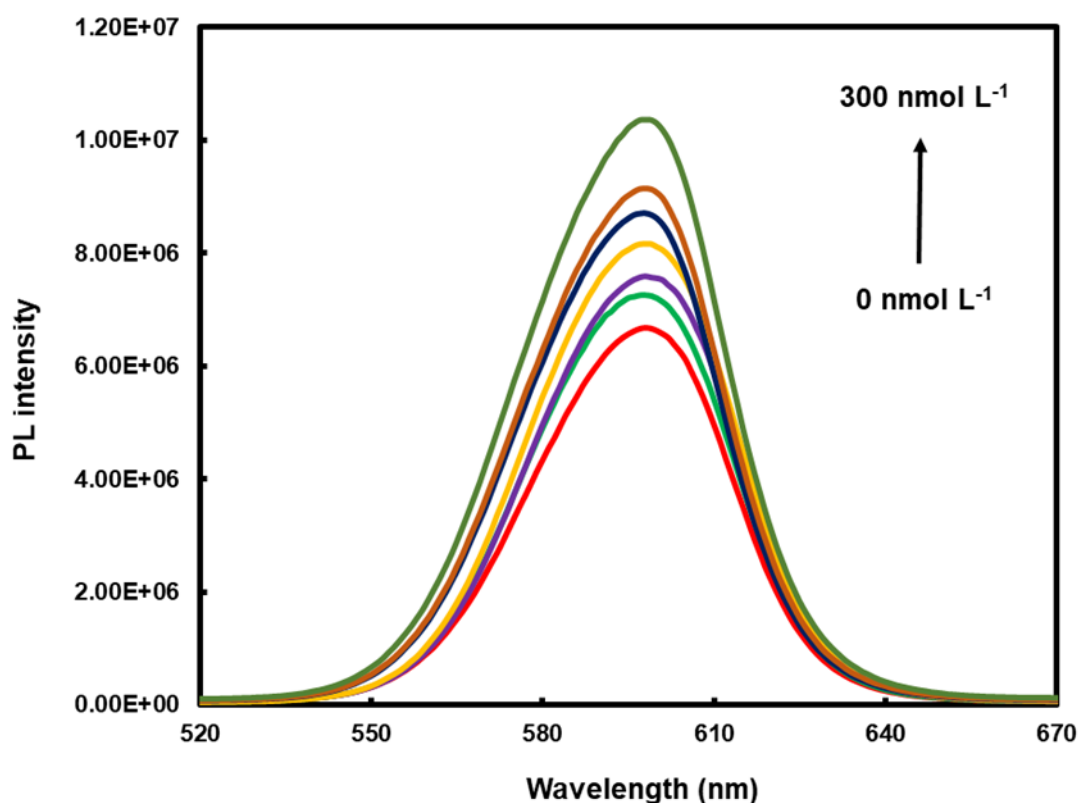


Figure 3.11 The fluorescence spectra of GSH-CdSe/ZnS QDs in the presence of different concentrations of triclosan. The experimental conditions were GSH-CdSe/ZnS QDs 1.5 mg in 3.0 mL⁻¹; excitation wavelength, 300 nm; slit widths of excitation and emission, 5 nm.

3.3.2.5 Calibration curve, limit of detection and limit of quantification

The fluorescence intensity of GSH capped CdSe/ZnS QDs increased linearly in the concentration range of 10-300 nmol L⁻¹ TCS at an emission wavelength of 598 nm ($r^2 = 0.98$) (Fig. 3.12). In comparison, the worldwide concentration range of TCS in water has been found to range from 0.005-140 nmol L⁻¹ in surface waters, 0.07-300 nmol L⁻¹ in wastewater influent, 0.08-18.0 nmol L⁻¹ wastewater effluent, and $<3.5 \times 10^{-6}$ -0.35 nmol L⁻¹ in sea water (Dhillon *et al.*, 2015; SCCS, 2010). The potential applicability of the fluorescence sensing method reported here for the monitoring of TCS in surface and wastewaters is thus evident. Moreover, the detection and quantification limits which were calculated using $3\delta/m$ and $10\delta/m$, where δ is the standard deviation of the blank signal ($n=10$) and m is the slope of the linear range, were found to be 3.7 nmol L⁻¹ and 12.4 nmol L⁻¹ respectively.

Voltammetric methods using nanomaterial electrode systems and chromatography based methods are the most dominant techniques for TCS analysis, as seen in Table 3.4. These methods have disadvantages in terms of environmentally unfriendly solvent use, expensive instrumentation, analytical running costs, long analysis time, complexity, as well as the need for laborious sample pre-treatment and highly skilled technicians and are therefore not ideal for routine screening analysis (Guo *et al.*, 2009).

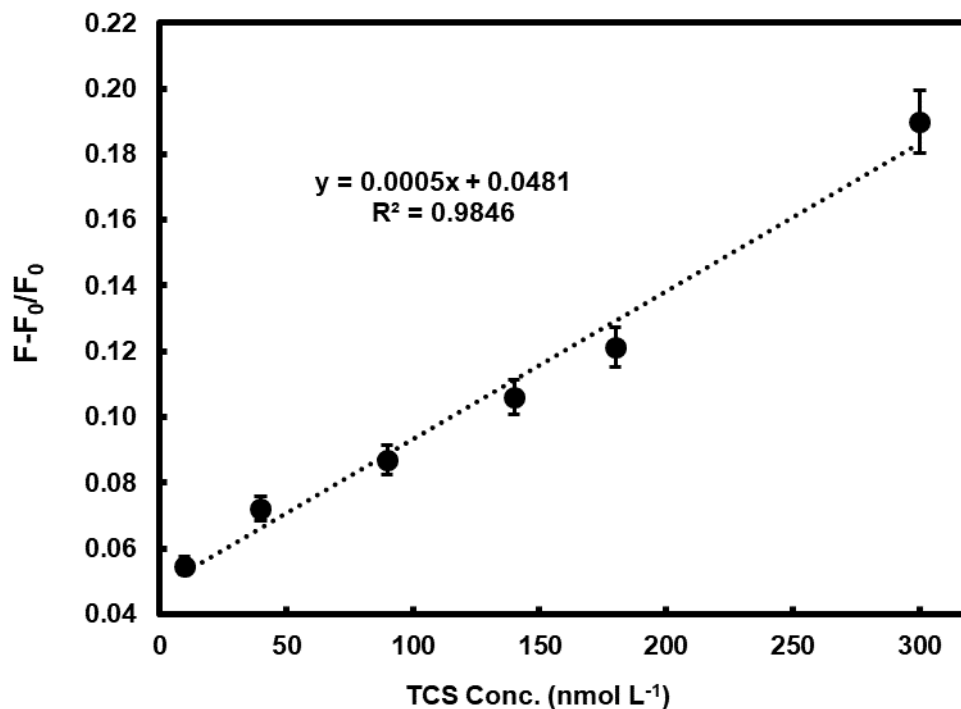


Figure 3.12 Linear graph of $F-F_0/F_0$ versus TCS concentration. The experimental conditions were GSH-CdSe/ZnS QDs 1.5 mg in 3.0 mL⁻¹; excitation wavelength, 300 nm; slit widths of excitation and emission, 5 nm.

Table 3.4 Comparison of some analytical methods for the determination of TCS in water samples.

Detection method	Linear range (nmol L ⁻¹)	Detection limit (nmol L ⁻¹)	Sample matrix	Reference
CNTs@TCS-MIPs/HPLC analysis	34.5-1.4×10 ⁵	-	River and lake water	(Gao <i>et al.</i> , 2010)
GC-MS	0.07-70.0	0.02	River water	(Pintado-Herrera <i>et al.</i> , 2014)
HPLC-UV	0.03-580.2	0.003	Tap water, river water and municipal wastewater	(Kim <i>et al.</i> , 2013)
HPLC-MS/MS	0.002-0.34	0.004	Deionized water	(Shen <i>et al.</i> , 2012b)
		0.005	River water	
nZnO-MWCNT/GCE (CV, DPV and SWV)	5.2-7.0×10 ³	4.5	Tap water	(Moyo <i>et al.</i> , 2015)
Carbon nanoparticles (CV)	1.0×10 ⁴ -1.0×10 ⁵	2.0×10 ⁴	-	(Vidal <i>et al.</i> , 2008)
CZE-UV	70.0-7.0×10 ³	13.8	Tap and river water	(Wang <i>et al.</i> , 2013)
Allylmercaptane modified gold SPR chip and imprinted p(HEMAGA) nanofilm	0.2-3.5	0.06	Wastewater	(Atar <i>et al.</i> , 2015)
Fluorescence: GSH-CdSe/ZnS QDs	10.0-300.0	3.7	Tap and river water	This work

CNTs@TCS-MIPs: Carbon nanotubes@ triclosan-imprinted polymers; CV: Cyclic Voltammetry; CZE-UV: Capillary Zone Electrophoresis with UV detection; DPV: Differential Pulse Voltammetry; GC-MS: Gas Chromatography – Mass Spectrometry; HPLC-UV: High Performance Liquid Chromatography – Ultraviolet Detection; HPLC-MS/MS: High Performance Liquid Chromatography-Electron Spray Ionization-Tandem Mass Spectrometry; nZnO-MWCNT/GCE: Nano-Zinc Oxide-Multiwalled Carbon Nanotube/Glassy Carbon Electrode; [p(HEMAGA)]: poly(2-hydroxyethylmethacrylate-methacryloylamidoglutamic acid); SPR: Surface Plasmon Resonance; SWV: Square Wave Voltammetry.

3.3.2.6 Proposed mechanism

The fluorescence behavior of TCS was recorded at different excitation wavelengths. The highest emission intensity was found at 407 nm at an excitation wavelength of 310 nm (Fig. 3.13A). Energy transfer is a possible mechanism for the fluorescence enhancement because there is overlap between the absorption spectrum of the core/shell QDs (500-600 nm) and the emission spectrum of TCS in the

range 350-600 nm (Fig. 3.13). In general, Förster resonance energy transfer (FRET) is a specific mechanism of non-radiative energy transfer between donor and acceptor molecules which are also called FRET pairs (Stanisavljevic *et al.*, 2015). FRET usually occurs when the overlap of the emission spectrum of the donor and adsorption spectrum of the acceptor is greater than 30% and the distance between them is less than 10 nm (Elangovan *et al.*, 2002). Herein the QDs can absorb the emission energy from TCS leading to the enhancement of the PL emission of QDs, as was observed experimentally.

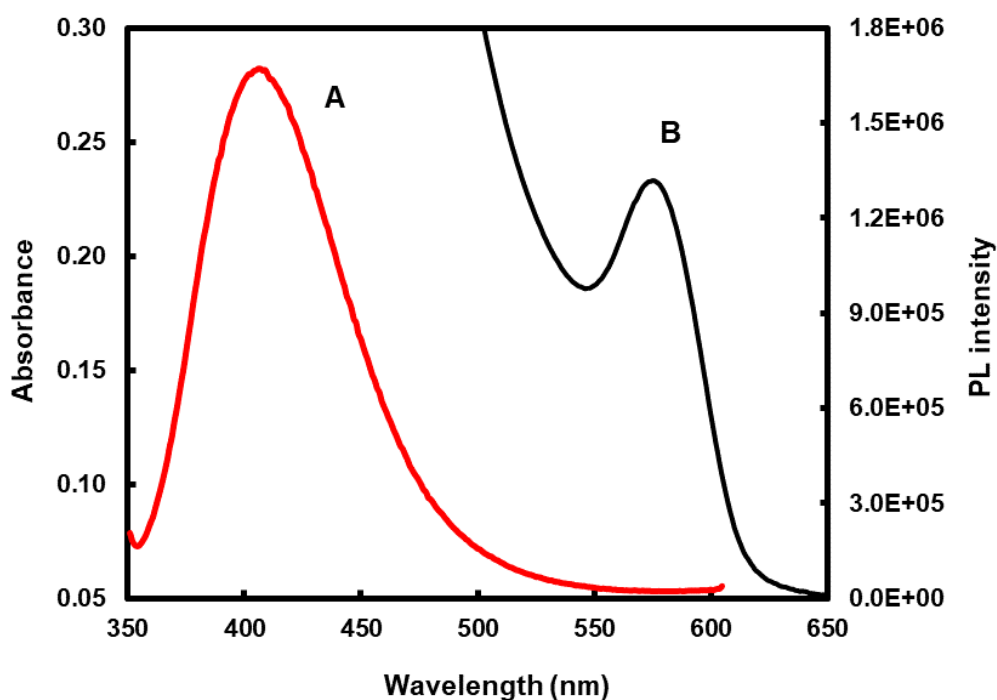


Figure 3.13 Fluorescence spectrum of TCS (1.4×10^{-5} mol L⁻¹) at excitation wavelength 310 nm (A) and UV-Vis absorption spectrum of GSH-CdSe/ZnS QDs (B).

3.3.2.7 Determination of Förster distance

The energy transfer between a donor and acceptor pair relies on the distance between them which can be expressed by Förster distance. It is the distance at which 50% of the excited donor molecules decay by energy transfer while the remainder decay through other radiative or non-radiative channels (Sapsford *et al.*, 2006). The Förster distance in the system of GSH-CdSe/ZnS QDs-TCS was computed using the program PhotochemCAD and was found to be approximately 4.0 nm (Du *et al.*, 1998).

3.3.2.8 Effect of potential interfering analytes on GSH-CdSe/ZnS QDs

To further evaluate the applicability of the fluorescence probe, potential interfering compounds as shown in Table 3.5 were investigated under the optimum conditions of 2 mL of 1.5 mg/3.0 mL GSH-CdSe/ZnS QDs in the presence of 200 μ L of 180.0 nmol L⁻¹ of each analyte. 5 min was employed as equilibrium time for each of the fluorescence measurements. The relative fluorescence intensity of GSH-CdSe/ZnS QDs was enhanced in the presence of each analyte (Fig. 3.14). The highest relative fluorescence intensity was achieved for TCS, thus the probe is most sensitive to this target analyte.

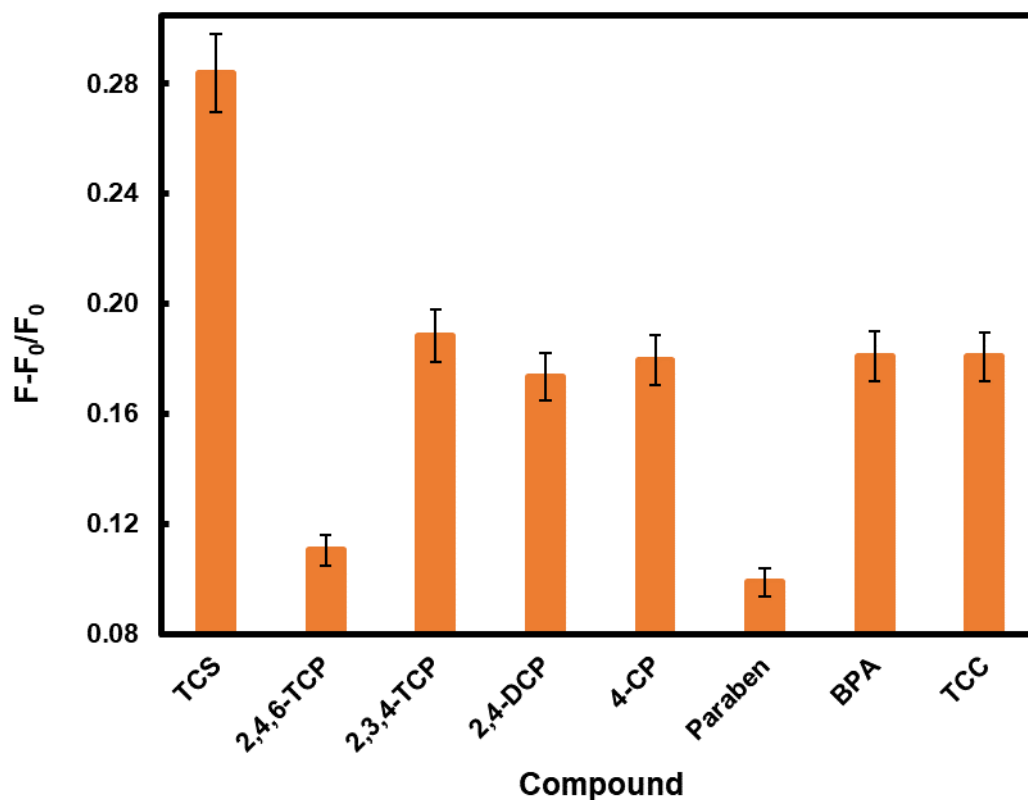
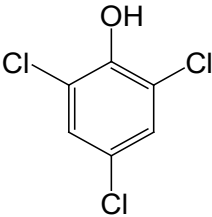
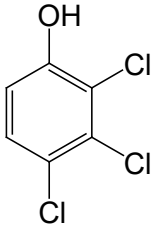
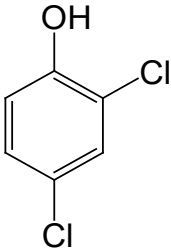
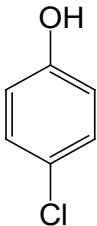
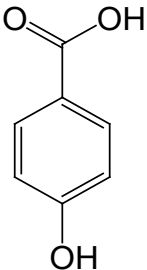
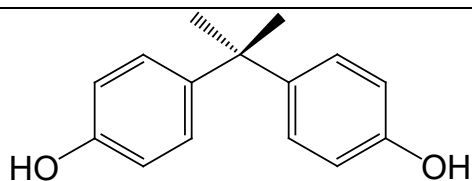


Figure 3.14 Effect of other analytes on the fluorescence emission intensity of the GSH-CdSe/ZnS QDs probe at an emission wavelength of 598 nm. The concentration of TCS and each of the other analytes was 180 nmol L^{-1} and GSH-CdSe/ZnS QDs was $1.5 \text{ mg}/3.0 \text{ mL}$. $F-F_0/F_0$ relates to the fluorescence intensity of QDs in the presence and absence of the analytes. The excitation wavelength was 300 nm. Analytes were 2,4,6-trichlorophenol (2,4,6-TCP), 2,3,4-trichlorophenol (2,3,4-TCP), 2,4-dichlorophenol (2,4-DCP), 4-chlorophenol (4-CP), 4-hydroxybenzoic acid (a paraben), bisphenol A (BPA), and triclocarban (TCC).

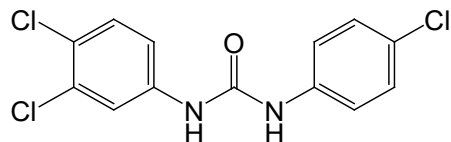
Table 3.5 Chemical structures of potentially interfering analytes.

Name	Structure
2,4,6-trichlorophenol (2,4,6-TCP)	
2,3,4-trichlorophenol (2,3,4-TCP)	
2,4-dichlorophenol (2,4-DCP)	
4-chlorophenol (4-CP)	
4-hydroxybenzoic acid (a paraben)	

Bisphenol A
(BPA)



Triclocarban
(TCC)



3.3.2.9 Analytical application

The feasibility of the prototype sensor was evaluated in real water samples by the addition of different concentrations of TCS to tap and river water. The experimental results are summarized in Table 3.6. The recoveries of different known amounts of TCS spiked in tap water and river water were very good and ranged from 94 to 115% and 98 to 118%, respectively, indicating the applicability of the sensor for quantitative determination of TCS in real water samples. HPLC-MS/MS analysis was performed as a comparative method which confirmed that the background concentration of TCS in the tap and river water samples was also below the detection limit.

Table 3.6 Analytical results for the determination of TCS in tap and river water samples using GSH-capped CdSe/ZnS QDs.

	TCS spiked (nmol L ⁻¹)	Determined TCS (mean±SD; n=3, nmol L ⁻¹)	Recovery (%)
Tap water	20	23±0.3	115
	100	94±0.6	94
	180	183±0.3	102
River water	20	24±0.4	118
	100	107±2.4	107
	180	177±1.2	98

3.4 ATRAZINE

3.4.1 Introduction

In this work, atrazine was selected as a target pesticide for sensor development. Atrazine is used extensively in agriculture for controlling weeds and it may eventually contaminate water systems through leaching, runoff and spray drift. It has been reported to occur in South African water systems in several studies (Dabrowski, 2015a, 2015b; Dabrowski *et al.*, 2013; Dabrowski & Balderacchi, 2013; Dabrowski & Schulz, 2003; Dabrowski *et al.*, 2014; Du Preez *et al.*, 2005; Patterton, 2013). This makes atrazine a priority emerging chemical pollutant (ECP) and warrants the development of sensitive and economical analytical methods which can be used routinely as an alternative to current conventional methods, which are relatively expensive.

In this project, CdSeTe/ZnS quantum dots (QDs) were synthesized and then modified with L-cysteine (L-Cys-CdSeTe/ZnS QDs) to make them water soluble which were used for atrazine detection in water. The choice of a ternary alloyed CdSeTe QD core was because they have been shown to have better chemical stability and increased conduction band edge compared to their binary counterparts (CdSe or CdTe) (Pan *et al.*, 2013). However, since this structure typically has a high density of surface defects possibly due to the susceptibility of Te to oxidation (Yang *et al.*, 2015), it was necessary to overcoat the core with ZnS shell and, subsequently, with L-cysteine to make them water soluble.

3.4.2 Materials & Methods

3.4.2.1 Materials

Trioctylphosphine oxide (TOPO), cadmium oxide, octadec-1-ene (ODE), selenium powder (Se), tellurium powder (Te), zinc oxide, sulphur (S), L-cysteine and oleic acid (OA) were purchased from Sigma-Aldrich. PAH and atrazine standards were also obtained from Sigma-Aldrich. Methanol, absolute ethanol, chloroform, acetone, and potassium hydroxide (KOH) were purchased from Associated Chemical Enterprises (Pty) Ltd. An ultrapure Milli-Q Water System was used for preparation of all standard solutions. All fluorescence measurements were carried out using a Horiba Jobin Yvon FluoroMax-4 spectrofluorometer with both excitation & emission slit widths set at 5 nm.

3.4.2.2 Preparation of CdSeTe/ZnS QDs

The one-pot synthesis of CdSeTe/ZnS QDs was carried out based on a reported procedure for the synthesis of core/shell QDs (Adegoke *et al.*, 2015). 1.3 g of CdO was added into a solution of 50 mL of QDE and 30 mL of OA and the solution was vigorously stirred in a 3-necked flask under argon atmosphere to a temperature of $\sim 260^{\circ}\text{C}$ in order to form a colourless Cd-OA complex. Once the colourless complex solution was formed, a premixed TOPTe solution containing 0.48 g of Te and 1.93 g of TOPO in 25 mL of ODE was added into the solution and this was followed swiftly by the addition of a TOPSe solution containing 0.30 g of Se and 1.93 g of TOPO in 25 mL of ODE. Nucleation and growth of the alloyed core QDs was allowed to proceed for about 15 min after which a ZnO solution containing 0.41 g of ZnO dissolved in 20 mL of OA and 30 mL of ODE was injected into the growth solution and this was followed immediately by the addition of the S precursor which consisted of 0.17 g of S in 30 mL ODE and 20 mL OA. The CdSeTe/ZnS QDs were allowed to react for around 40 min with continuous monitoring of the shell growth, after which the reaction was stopped and they were harvested and dispersed in chloroform.

The QDs were then made hydrophilic by capping them with L-cysteine via a ligand exchange reaction which was performed as follows: A KOH-methanolic-L-cysteine solution was prepared by dissolving 3.0 g of KOH in 40 mL of methanol and 2.0 g of L-cysteine was then dissolved in the solution via ultrasonication. The hydrophobic CdSeTe/ZnS QD solution was then added into the KOH-methanolic-L-cysteine solution followed by the addition of Millipore water. This resulted in the separation of the organic phase from the water-soluble phase. The solution was stirred for 15 min and was then purified by successive washing with acetone, chloroform, water:chloroform:acetone, and finally with acetone. This rigorous purification step was necessary in order to remove the high level of unreacted organic layers embedded on the surface of the QDs.

3.4.2.3 Procedure for detection of atrazine

For atrazine detection the core/shell QDs were used rather than the core QDs because they are considered less toxic due to the ZnS shell which prevents the cadmium core from leaching. 300 μL of L-Cys-CdSeTe/ZnS QDs dissolved in water was mixed with 100 μL of different atrazine standard

solutions (2×10^{-7} - 10×10^{-7} mol L⁻¹). Fluorescence measurements were then carried out using a Horiba Jobin Yvon Fluoromax-4 spectrofluorometer for all experiments. The QDs interact with the atrazine mainly through hydrogen bonding (Fig 3.15) resulting in quenching of the fluorescence intensity of the QDs.

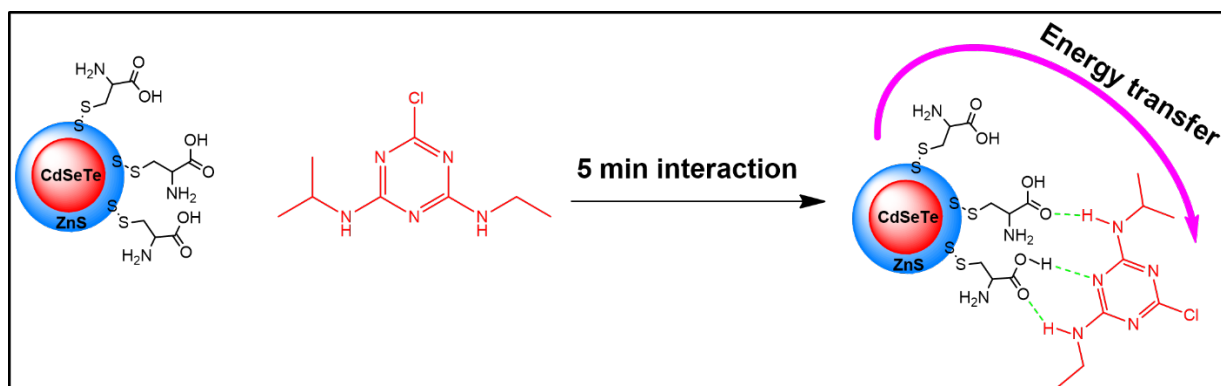


Figure 3.15 Schematic illustration of the interaction of atrazine with the L-cysteine ligands on the QD surface. The interaction is likely through hydrogen bonding, resulting in quenching of the fluorescence intensity of the QD as a consequence of energy transfer.

3.4.3 Results and discussion

3.4.3.1 TEM

TEM analysis was carried out to investigate the particle size and distribution of the different nanoparticles. As shown in Figure 3.16, the L-Cys-CdSeTe core was mono dispersed in water and had an average particle size of 3.1 ± 0.1 nm, while the L-Cys-CdSeTe/ZnS core/shell QDs had an average size of 5.0 ± 0.5 nm, confirming coating of the core with the ZnS shell (≈ 1 nm thickness).

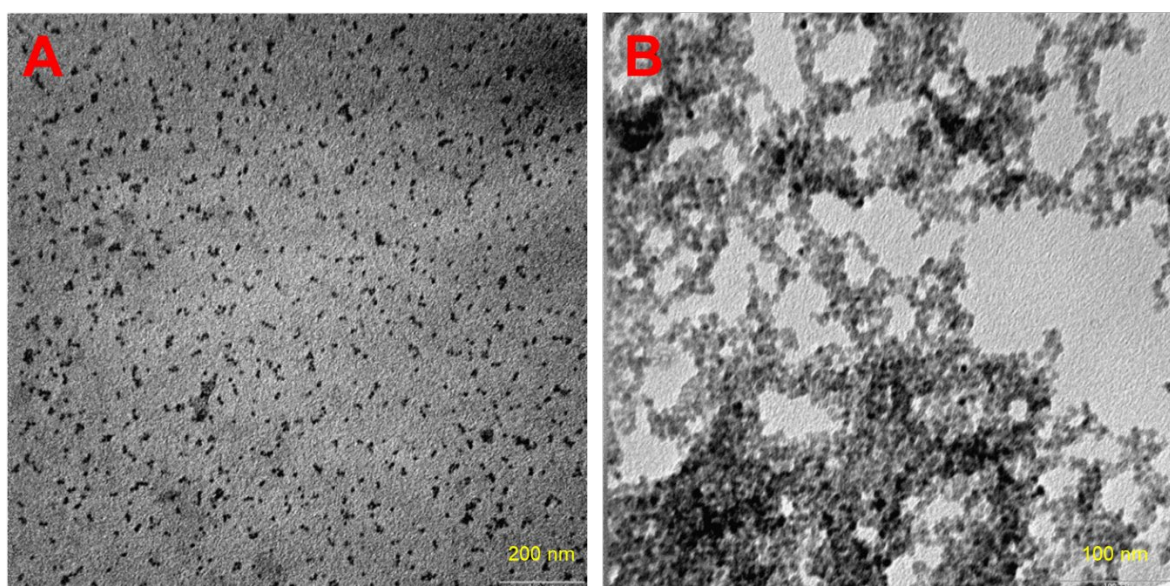


Figure 3.16 TEM images showing particle size and distribution of the L-Cys-CdSeTe QDs (A) and L-Cys-CdSe/ZnS QDs (B). The average size for the core was 3.1 ± 0.1 nm and for the core/shell QDs was 5.0 ± 0.5 nm, thereby confirming the passivation the core with the ZnS shell during synthesis.

3.4.3.2 FTIR

FTIR spectra of L-Cys, core and core/shell QDs are shown in Figure 3.15. The stretching bands for C=O and C-O were observed at 1537 cm^{-1} and 1434 cm^{-1} , respectively. The bands at $2924\text{--}2850\text{ cm}^{-1}$ were attributed to N-H. A broad band $\sim 3500\text{ cm}^{-1}$ was attributed to O-H stretching. This FTIR data, together with disappearance of the S-H band at 2077 cm^{-1} indicated successful functionalization of the QD surface.

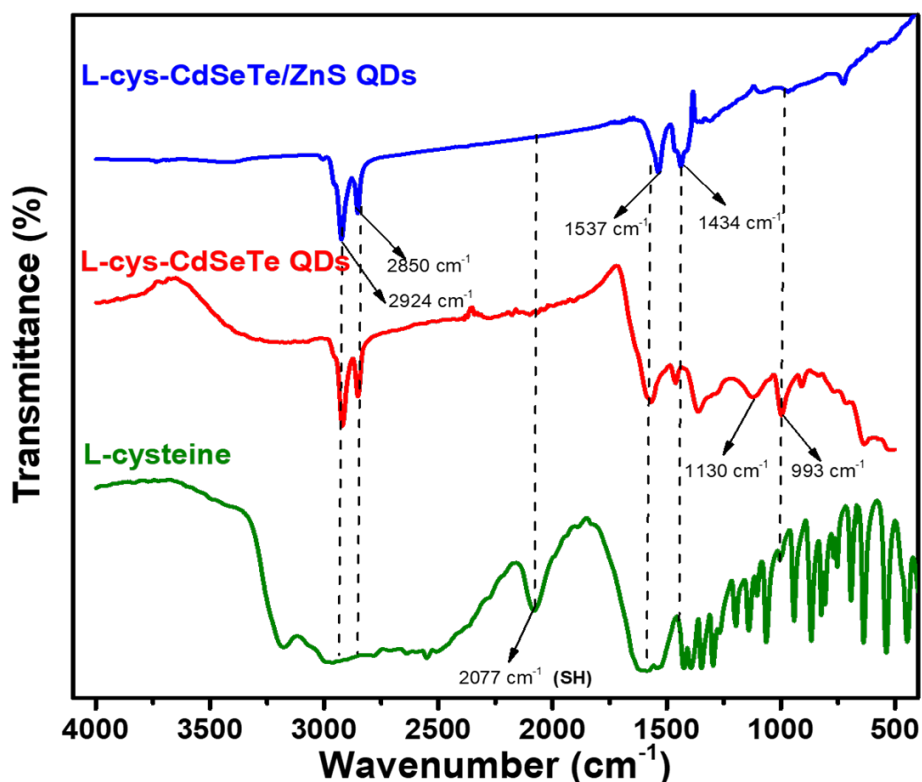


Figure 3.17 FTIR spectra of L-Cys, core and core/shell QDs. The stretching bands for C=O and C-O were observed at 1537 cm^{-1} and 1434 cm^{-1} , respectively. The bands at $2924\text{--}2850\text{ cm}^{-1}$ were attributed to N-H. A broad band $\sim 3500\text{ cm}^{-1}$ was attributed to O-H stretching. This FTIR data, together with disappearance of the S-H band at 2077 cm^{-1} indicate successful functionalization of the QD surface.

3.4.3.3 XRD

The x-ray diffraction patterns shown in Fig 3.18 show the characteristic zinc-blende crystal structure for CdSeTe and CdSeTe/ZnS QDs as indexed at the $\{111\}$, $\{220\}$ and $\{311\}$ lattice planes. This confirms that both the core and core/shell retained their crystalline nature even after ligand exchange with L-cysteine, i.e. the ligands did not interfere with the crystalline structure.

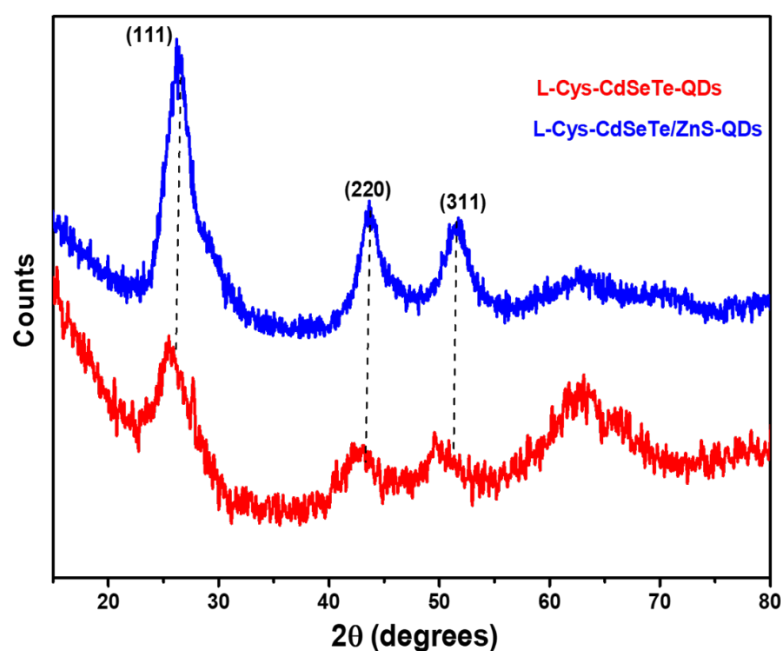


Figure 3.18 Powder XRD spectra of the L-Cys-QDs confirming their crystalline nature. The planes {111}, {220} and {311} correspond to the typical zinc blende structure for both the core & core/shell QDs.

3.4.3.4 Fluorescence and absorption properties

The prepared L-Cys-CdSeTe QDs had high fluorescence intensity at 594 nm as shown in Fig. 3.19 and upon passivation with the ZnS shell the emission slightly redshifted to 608 nm. This can be attributed to an increase in size as confirmed by TEM. This change in PL properties could be due to enhanced quantum confinement upon surface coating which stabilizes the core. The QDs have broad absorption spectra which is typical for QDs.

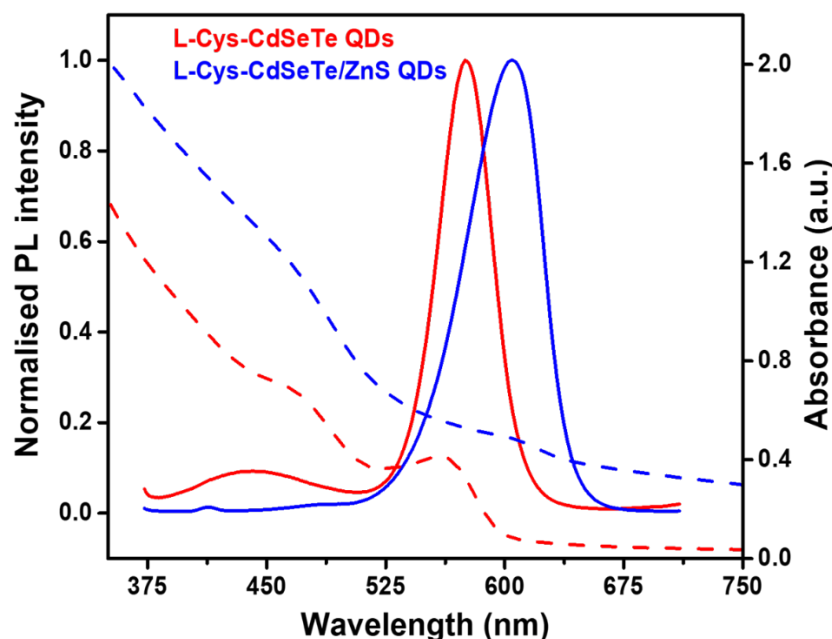
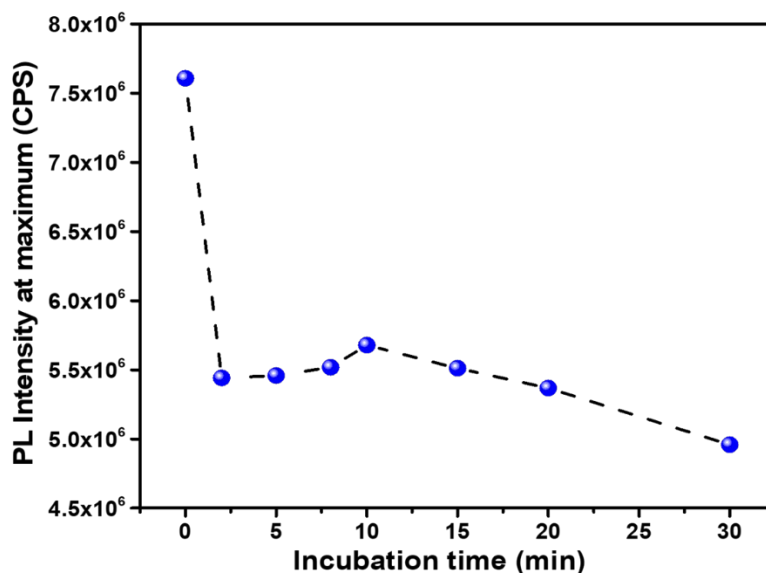


Figure 3.19 Normalized fluorescence (solid lines) and absorption (dashed lines) spectra of L-Cys-CdSeTe (red lines) and L-Cys-CdSeTe/ZnS QDs (blue lines). The core has strong emission

at 594 nm and this shifts to 608 nm for the core/shell due to increase in size. They both have the typical broad absorption spectra.

3.4.3.5 Optimisation

The optimum interaction time (incubation time) of L-Cys-CdSeTe/ZnS QDs with the target analyte was investigated by monitoring the fluorescence intensity at different time intervals in the presence of 10×10^{-7} mol L⁻¹ atrazine. As shown in Fig 3.20, the fluorescence intensity was quenched most up to 5 min and showed less of a decrease with further increase in incubation time. The quenching indicates that the integration of atrazine with the L-Cys ligands on the QD surfaces resulted in energy transfer from the QDs to the atrazine. Thus 5 min incubation time was applied for subsequent sensing experiments. The quick response time is desirable in potential field application of the sensor. Further, the optimal excitation wavelength of the sensor was investigated and exciting at 365 nm was found to be optimal as it give the highest fluorescence intensity.



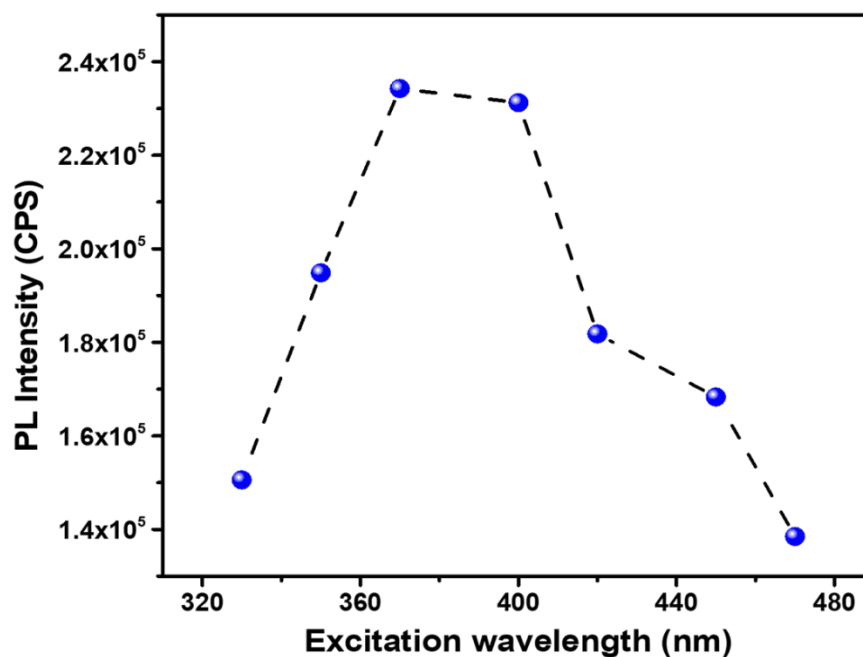


Figure 3.20 Effect of incubation time on the quenching of the fluorescence intensity of L-Cys-CdSeTe/ZnS QDs using $10 \times 10^{-7} \text{ mol L}^{-1}$ atrazine (top) and effect of excitation wavelength on the PL intensity of L-Cys QDs (bottom) where the optimal wavelength was found to be 365 nm.

3.4.3.6 Fluorescence behaviour of L-Cys-CdSeTe/ZnS in the presence of atrazine

To investigate the behaviour of the sensor with different concentrations of atrazine, the core/shell QDs were used rather than the core QDs because of their stability and reduced toxicity following passivation with the ZnS shell which prevents the cadmium core from leaching. Thus, 300 μL of L-Cys-CdSeTe/ZnS QDs dissolved in water was mixed with 100 μL of different atrazine standard solutions (2×10^{-7} - $10 \times 10^{-7} \text{ mol L}^{-1}$). Fluorescence measurements were then carried out using a Horiba Jobin Yvon Fluoromax-4 spectrofluorometer for all experiments. The QDs interact with the atrazine mainly through hydrogen bonding resulting in quenching of the fluorescence intensity of the QDs (Fig. 3.21). Increasing atrazine concentration was found to be linearly proportional to the F_0/F ($R^2 = 0.9277$) within the concentration range 0 - $10 \times 10^{-7} \text{ mol L}^{-1}$, as shown in Fig 3.22. The limit of detection for this system was determined to be $1.8 \times 10^{-7} \text{ mol L}^{-1}$ hence it potentially useful for application in water systems where atrazine can be found at elevated levels.

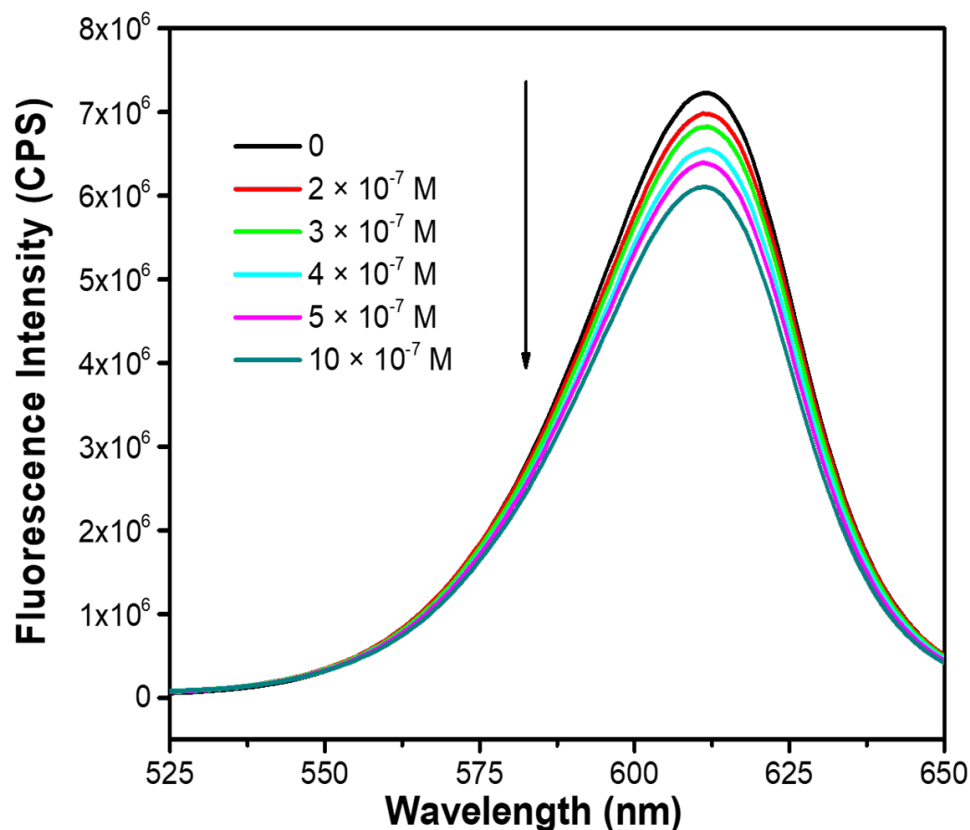


Figure 3.21 Fluorescence emission spectra of L-Cys-CdSeTe/ZnS QDs in the presence of varying atrazine concentrations (2×10^{-7} mol L⁻¹ – 10×10^{-7} mol L⁻¹). The spectra show a decrease in intensity with increase in atrazine concentration.

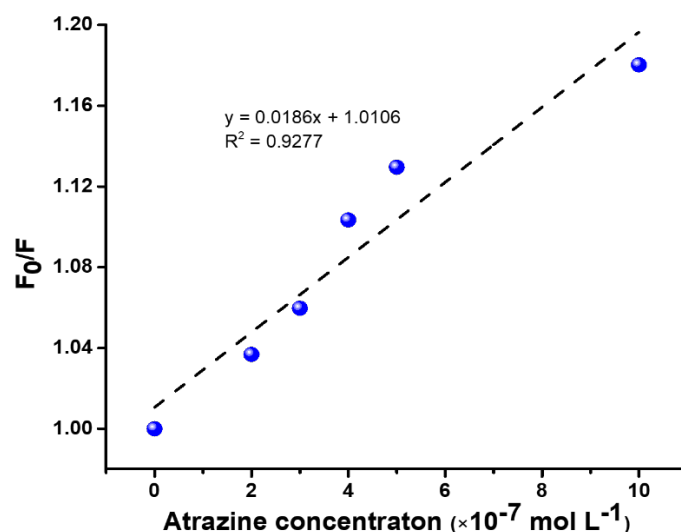


Figure 3.22 Linear calibration curve showing F_0/F vs atrazine concentration. The fluorescence intensity of the QD sensor solution without and with atrazine is denoted F_0 and F , respectively. The limit of detection determined from the slope and blank measurements ($n=9$) was found to be 1.8×10^{-7} mol L⁻¹.

3.5 POLYCYCLIC AROMATIC HYDROCARBONS

3.5.1 Introduction

Graphene QDs (GQDs) can be regarded as small (<20 nm), zero-dimensional pieces of graphene. They have properties of graphene but also quantum confinement and edge effect properties similar to carbon dots (Li *et al.*, 2013). These QDs have certain advantageous properties over semi-conductor quantum dots, including higher photostability, biocompatibility, large surface area, better surface grafting using π - π conjugation and surface groups, and they have very low toxicity (Chong *et al.*, 2014; Shen *et al.*, 2012a; Wang *et al.*, 2016). Because of their low toxicity they have also been widely used for biological applications (Zheng *et al.*, 2015). Thus they have recently found extensive application in designing sensing probes (Benítez-Martínez & Valcárcel, 2015; Lin *et al.*, 2014; Shen *et al.*, 2012a; Sun *et al.*, 2013). Their application in analytical chemistry has mostly been towards metal ions sensing (Ju & Chen, 2015) with few studies reporting their use for organic pollutant detection like pentachlorophenol (Liu *et al.*, 2014a), trinitrotoluene (Fan *et al.*, 2012) and the pesticide tributyltin (Zor *et al.*, 2015).

The fluorescence properties of GQDs arise from the radiative recombination of electron-hole (e-h) pairs in sp^2 aromatic carbon sites. This is because graphene has infinitely large Bohr diameters (distance between electron and hole) and therefore its fragments, i.e. GQDs, of any size, exhibit quantum confinement effects (Zhu *et al.*, 2015). The π - π^* electronic transitions are confined.

GQDs can be prepared using two approaches, namely the 'top-down' approach or the 'bottom-up' approach. The top-down approach involves cutting of large macroscopic carbon materials (e.g. graphite, carbon fibers, graphene oxide, metal-organic frameworks, etc.) into small GQDs pieces, usually through harsh oxidation treatments. On the other hand, the bottom-up approach involves GQDs formation from molecular or atomic carbon precursors (e.g. chlorobenzene, acetic acid, glucose, and even from PAHs) through controlled reactions to obtain desired GQD sizes (Benítez-Martínez & Valcárcel, 2015; Shen *et al.*, 2012a).

The occurrence of PAHs in the environment and the potential negative health effects that they pose requires that they be monitored regularly. Traditionally, chromatographic techniques are used for quantification of PAHs, but these can be expensive especially where routine environmental monitoring is to be done. To overcome this challenge, researchers have been working on using various nanomaterials as sensors and/or platforms for sensitive detection of PAHs. For example, Fe-based magnetic nanoparticles have been widely used as sorbents for pre-concentration of PAHs prior to chromatographic analysis. Here we discuss the preparation of GQDs prepared from a graphite precursor (top-down approach) and from citric acid (CA) (bottom-up approach) and investigate their potential application as fluorescence sensors for PAHs.

3.5.2 Materials and methods

PAH standards were purchased from Sigma-Aldrich. Hydrogen peroxide (H_2O_2), sulfuric acid (H_2SO_4), sodium nitrate (NaNO_3), hydrochloric acid (HCl), graphite powder, potassium hydroxide (KOH) and potassium permanganate (KMnO_4) were purchased from Merck. An ultrapure Milli-Q Water System was used for sample preparation. Fluorescence measurements were carried out using a Horiba Jobin Yvon FluoroMax-4 spectrofluorometer with both excitation and emission slit widths set at 5 nm.

3.5.2.1 Preparation of GQDs from graphite

GQDs were prepared using the top-down approach using graphite as a starting material. Firstly, graphene oxide (GO) was prepared using a modified Hummer's method (Hummers & Offeman, 1958) where 2.5 g of graphite powder and 1.3 g of NaNO_3 were mixed in a 250 mL three-neck round-bottom flask containing 60 mL of H_2SO_4 . This mixture was continuously stirred inside an ice bath to allow thorough dispersion of the graphite powder for about 30 min. Afterwards, 7.5 g KMnO_4 was gradually added and the mixture was left stirring for 2 hrs until it turned greenish. The mixture was then removed from the ice and left to stir at room temperature ($\sim 27^\circ\text{C}$) resulting in the formation of a pasty light-brown coloured mixture. The following day the mixture was again placed in an ice bath and 75 mL Millipore water was slowly added under stirring for 2.5 hrs. The temperature of the solution was then raised to $\sim 60^\circ\text{C}$ and allowed to stir. On the following day, 25 mL of 30% H_2O_2 was added to the reaction mixture followed by centrifuging with 5% HCl and lastly centrifuging with Millipore water. The solid GO was dried in an oven at 65°C to give a dark grey powder with a yield of 5.8 g.

Graphene quantum dots (GQDs) were then prepared from GO using a previously reported method with some modifications (Fan *et al.*, 2015). 1.0 g of GO was added to 40 mL H_2SO_4 and the mixture was stirred in ice until the next day. KMnO_4 was then added and the mixture was allowed to stir at room temperature for about 1 h before raising the temperature to about $\sim 60^\circ\text{C}$ and heating it until the following day. The reaction was then quenched by adding ice-cold water containing small amounts of H_2O_2 and was left at room temperature for about 2 days to allow for settling. The supernatant containing GQDs was carefully pipetted out and used for sensing studies.

3.5.2.2 Preparation of GQDs from citric acid

GQDs were prepared from citric acid (CA) via direct pyrolysis (Dong *et al.*, 2012) as illustrated in Fig. 3.23. Briefly, about 2 g of CA was placed in a beaker and heated to $\sim 200^\circ\text{C}$ on a hot plate. After about 5 min the CA turned into a transparent solution and after a further 15 min of heating it turned pale yellow, suggesting formation of GQDs. The reaction was then stopped followed by slow addition of NaOH (0.25 mol L^{-1}) while stirring vigorously. Lastly, the pH was adjusted to pH 7 and the pale yellow solution thus obtained was stored for further sensing application tests.

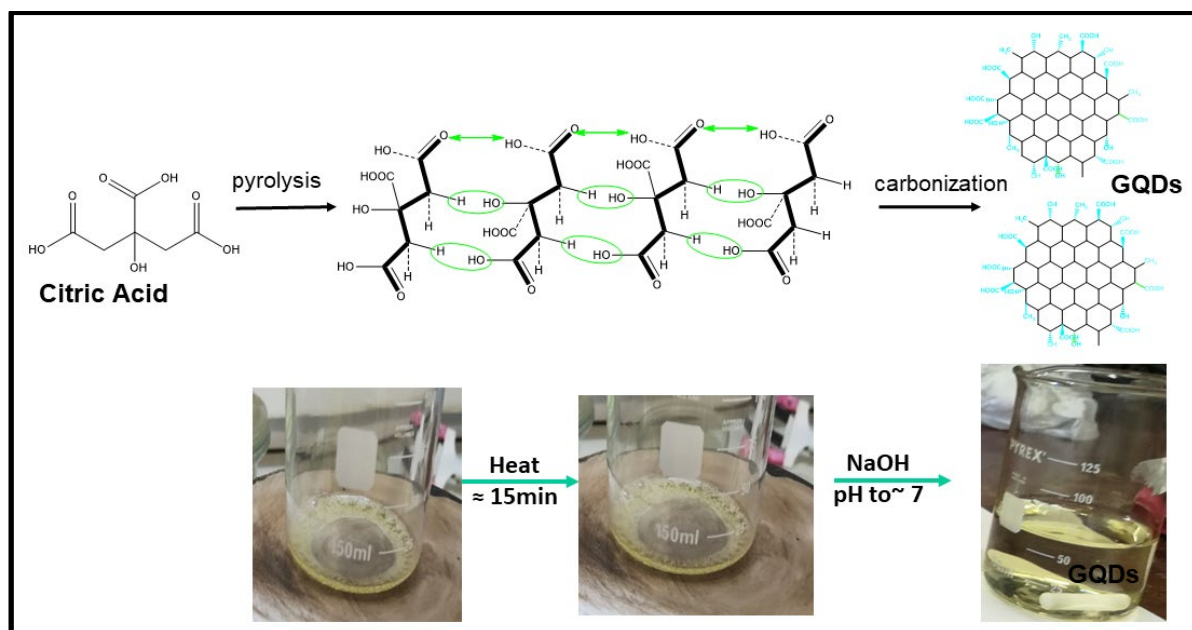


Figure 3.23 Illustration of the preparation of GQDs via pyrolysis of citric acid.

3.5.2.3 Sensing experiments

PAH standard solutions of anthracene, naphthalene, pyrene and phenanthrene were prepared within the $1\text{-}5 \times 10^{-7}$ mol L⁻¹ concentration range by dissolving them in H₂O/EtOH (2:1) mixture. To improve their solubility they were first dissolved in small amounts of toluene.

Sensing was carried out by placing 3 mL of GQDs solution in a quartz cuvette followed by adding 200 μ L of analyte PAH standard solution. The effect of interaction time (incubation time) was determined using 300 μ L of GQDs and 100 μ L of phenanthrene standard solution. The effect of different PAHs at a fixed concentration (1×10^{-7} mol L⁻¹) on the fluorescence intensity of the GQDs probe was also determined. The fluorescence response of the GQDs to phenanthrene concentration was evaluated over the $1\text{-}5 \times 10^{-7}$ mol L⁻¹ concentration range (0, 1×10^{-7} , 2×10^{-7} , 3×10^{-7} , 4×10^{-7} and 5×10^{-7} mol L⁻¹). Excitation was at 340 nm for all measurements.

3.5.3 Results & Discussion

3.5.3.1 FT-IR characterization

Infra-red (IR) analysis was done to confirm formation of GO from graphite. To get the GQDs into powder form, a small amount of the GQDs solution was freeze-dried before IR analysis. The results as shown in Fig 3.24 revealed that GO was successfully made as the characteristic bands for GO were observed. These characteristic bands are: the carbonyl band ($\nu_{\text{C=O}}$ 1723.07 cm⁻¹), the aromatic band ($\nu_{\text{C=C}}$ 1588.81 cm⁻¹), the carboxy band ($\nu_{\text{C-O}}$ 1222.92 cm⁻¹), the epoxy band ($\nu_{\text{C-O}}$ 1222.92 cm⁻¹) and the alkoxy band ($\nu_{\text{C-O}}$ 1046.15 cm⁻¹). The broad band at around 3350 cm⁻¹ is due to O-H stretching vibrations.

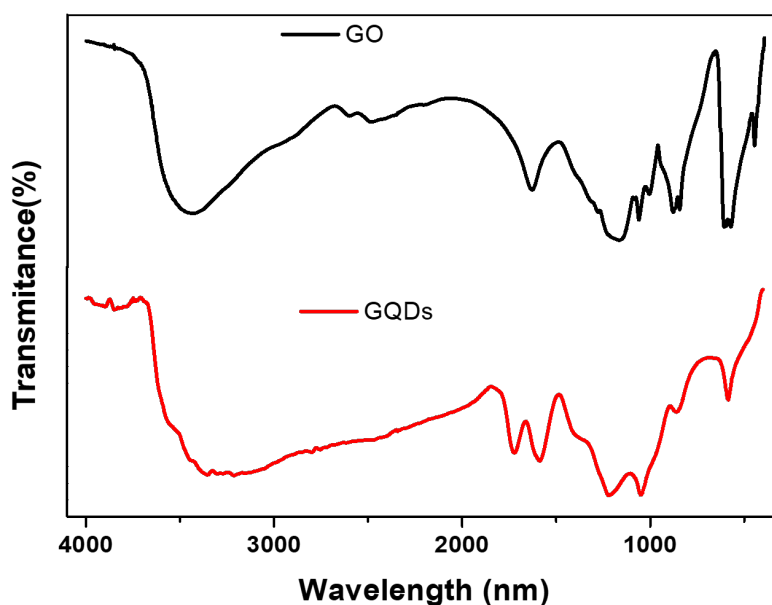


Figure 3.24 FT-IR spectra of graphene oxide (black line) and graphene quantum dots (red line).

3.5.3.2 HRSEM

High resolution scanning electron microscopy (HRSEM) was used to study the morphology of the graphene oxide from exfoliation of graphite precursors. The HRSEM images show that the graphite had characteristic flat carbon sheets stacked into layers (Fig 3.25a) and after exfoliation to graphene oxide the sheets become folded into crumpled silk waves (Fig 3.25b). This transformation is due to the harsh oxidation conditions which the graphite was subjected to.

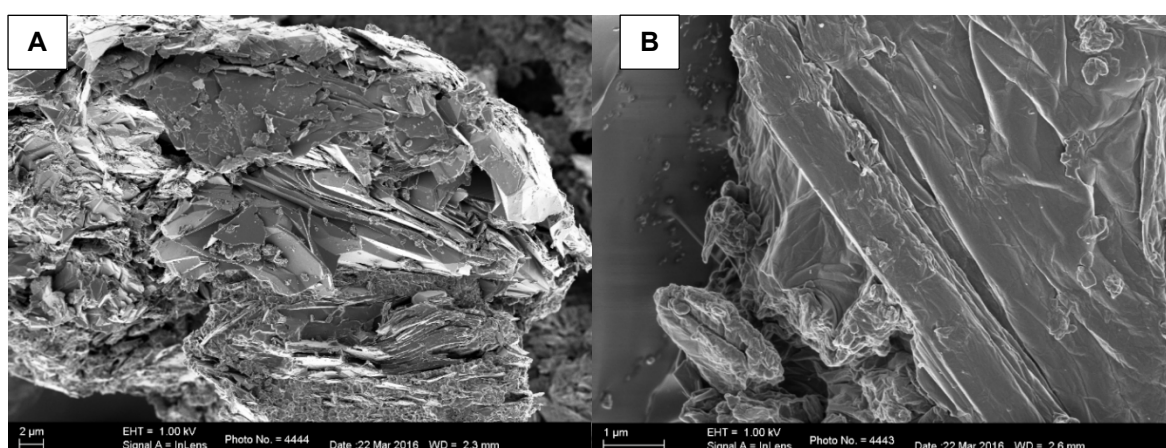


Figure 3.25 HRSEM image of (a) graphite powder (b) GO from exfoliation.

3.5.3.3 Powder XRD and Raman spectroscopy

Powder XRD was used to study the crystal phase nature of both the graphite precursor and the graphene oxide and a clear distinction was observed between the two (Fig 3.26). Graphite had an intense peak at $2\theta = 30.6$ degrees and after converting to graphene oxide the peak diminished. GO had

a weak characteristic peak at $2\theta = 10$ degrees which indicates a loose-layer-like structure. The interlayer spacing of this peak depends on water layers in the gallery space of the materials as well as on the synthesis method employed (Liu *et al.*, 2002). Raman spectroscopy (Fig. 3.27) also confirmed the formation of GO. The characteristic D (1360 cm^{-1}) and G (1600 cm^{-1}) bands were observed for both materials but were more pronounced for GO. This confirmed successful exfoliation of the graphite precursor material. The D band corresponds to the plane termination of disordered graphite containing vibrating carbon atoms while the G band corresponds to vibrating sp^2 bonded carbon atoms (Wei *et al.*, 2013).

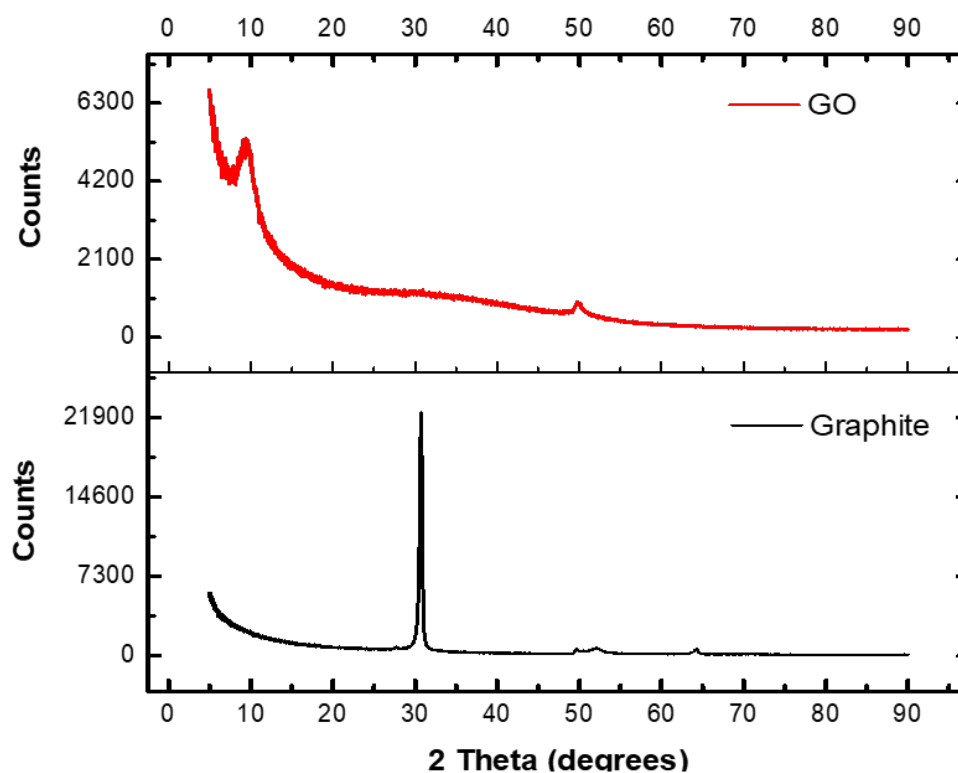


Figure 3.26 X-ray diffraction patterns of graphite (bottom) and graphene oxide derived from graphite (top).

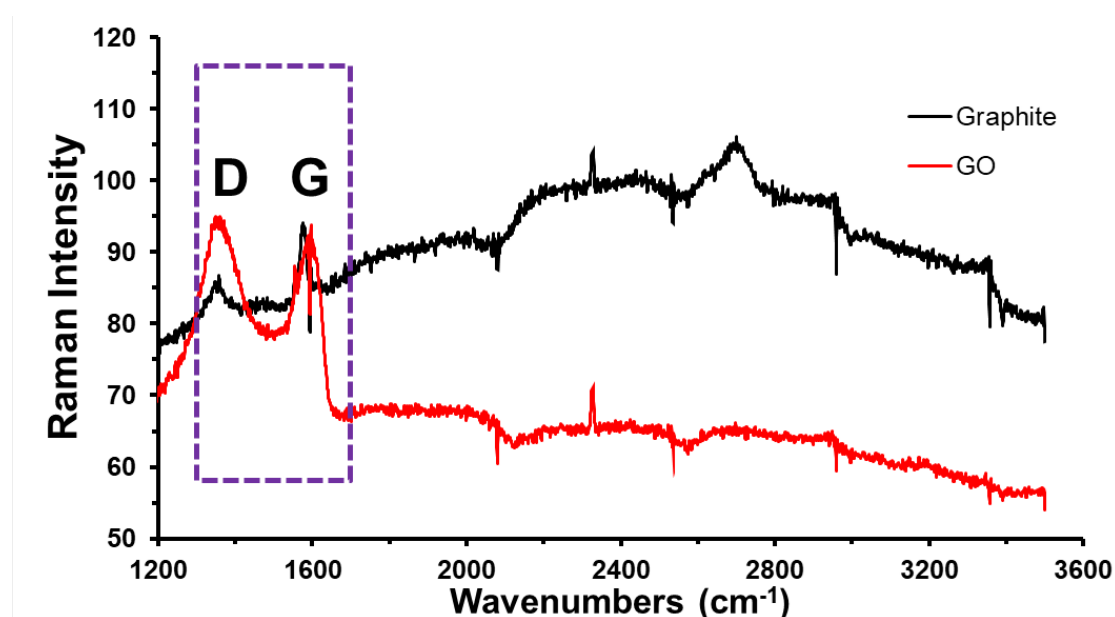


Figure 3.27 Raman spectra of graphite and graphene oxide prepared from graphite.

3.5.3.4 Fluorescence and absorption

The UV-vis absorption and fluorescence emission spectra of GQDs are shown in Fig 3.28. The GQDs had a strong UV absorption peak at 315 nm which is attributed to the $\pi \rightarrow \pi^*$ transition of aromatic sp^2 domains in the graphene structure, and a shoulder around 330 nm which is ascribed to the $n \rightarrow \pi^*$ transition of C=O bonds or other groups on the GQD surface (Zhu *et al.*, 2015). The position and intensities of these characteristic peaks have been shown by Zhang *et al.* (2016) to be dependent on the size distribution of the GQDs, which itself is dependent on the synthetic route.

The emission spectrum on the other hand shows a strong broad asymmetric peak with a tail extending to longer wavelengths. This is indicative of the existence of different singlet ground (S_0) – first-excited state (S_1) transitions (Wang *et al.*, 2014; Zhu *et al.*, 2015).

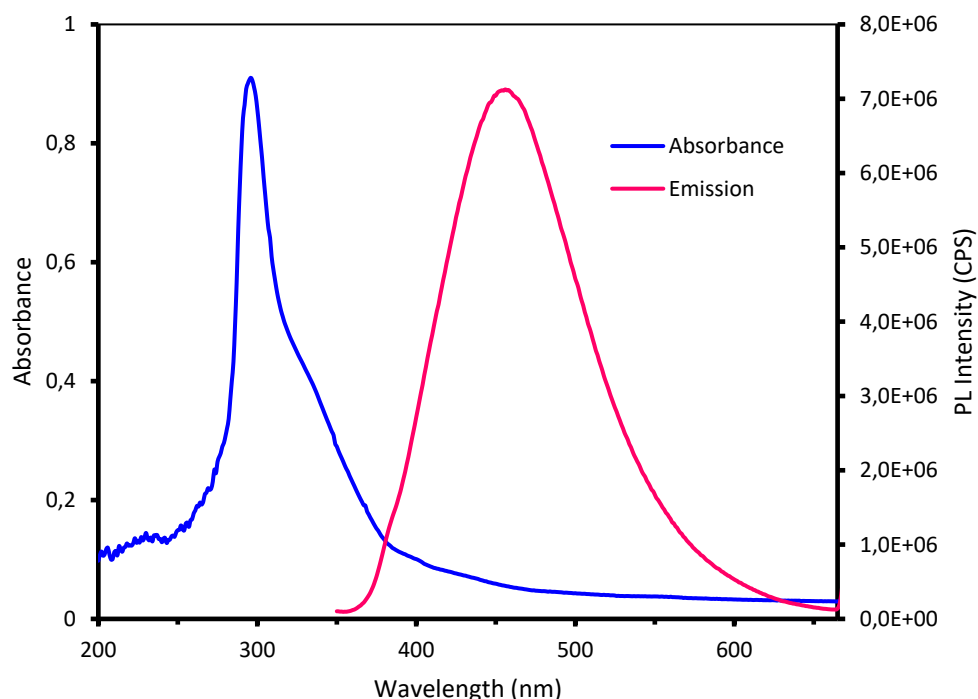


Figure 3.28 Fluorescence emission and UV absorption spectra of GQDs prepared from graphite. The emission peak at 460 nm is broad and asymmetric due surface or edge effects. The strong absorption peak around 330 is due to $\pi \rightarrow \pi^*$ and $n \rightarrow \pi^*$ transitions.

Fig 3.29 and 3.30 show fluorescence emission spectra of the GQDs prepared using the two methods. The intensity of emission peaks was observed to be dependent on the excitation wavelength for GQDs prepared from GO and had a red-shift as the wavelength was changed from 340 to 500 nm, while the emission spectra of GQDs synthesised from CA were independent of excitation wavelength. The behaviour noted for GQDs prepared from GO is common with fluorescent carbon materials and in the case of GQDs it may be due to the presence of differently sized dots, surface chemistry, or emissive traps. Another striking feature is that the peaks are broad and asymmetric, with a tail extending to longer wavelength. This may be due to inhomogeneous chemical structure and different emission centers corresponding to different singlet ground (S_0) – first-excited state (S_1) gaps (Wang *et al.*, 2014; Zhu *et al.*, 2015). The CA synthetic route is favoured due to the more uniform GQD size thus produced.

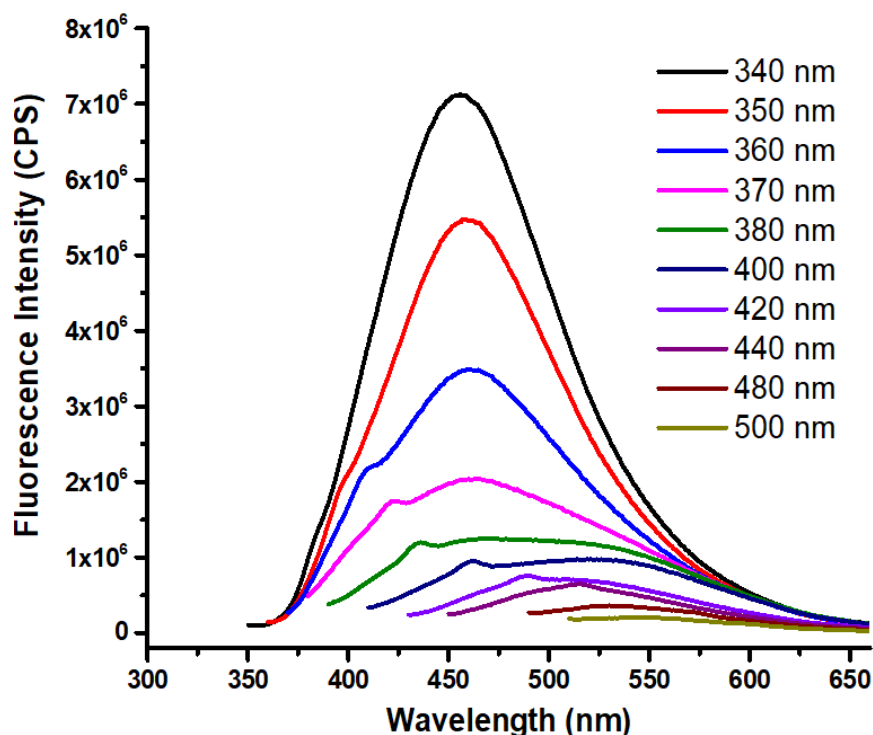


Figure 3.29 Fluorescence spectra of GQDs (synthesized from graphite) at different excitation wavelengths showing a decrease in PL intensity with increasing excitation wavelength.

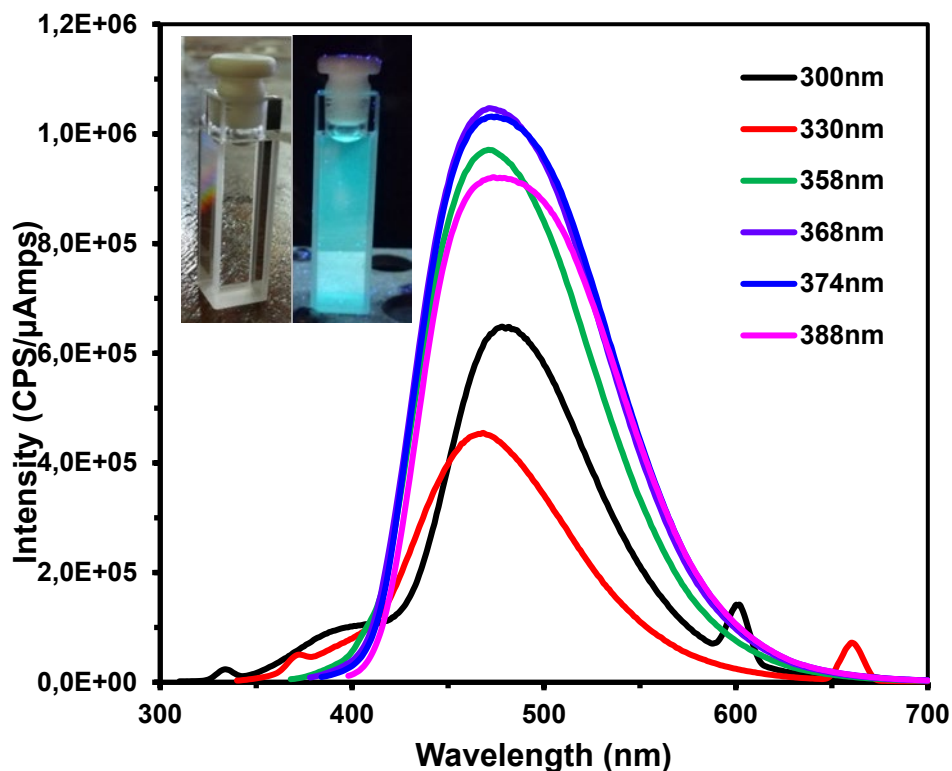


Figure 3.30 Fluorescence spectra of GQDs (synthesized from CA) at different excitation wavelengths. The emission wavelength is independent of excitation wavelength.

3.5.3.5 Application for PAH sensing

The interaction mechanism between graphene materials and PAHs is mainly through adsorption on the planar graphene structure via π - π stacking as illustrated in Fig. 3.31 (Adegoke & Forbes, 2016; Wang *et al.*, 2015). This interaction brings the PAH molecules into close proximity with the GQDs thereby quenching the fluorescence through Foster Resonance Energy Transfer (FRET) (Fan *et al.*, 2012). There was limited additional quenching after 5 min, suggesting that this is a suitable time to allow for equilibration to occur (Fig 3.32). The dispersion of GQDs in solution and their large surface area could be responsible for enhancing this relatively short equilibration time – a desirable feature for fluorescence sensor development.

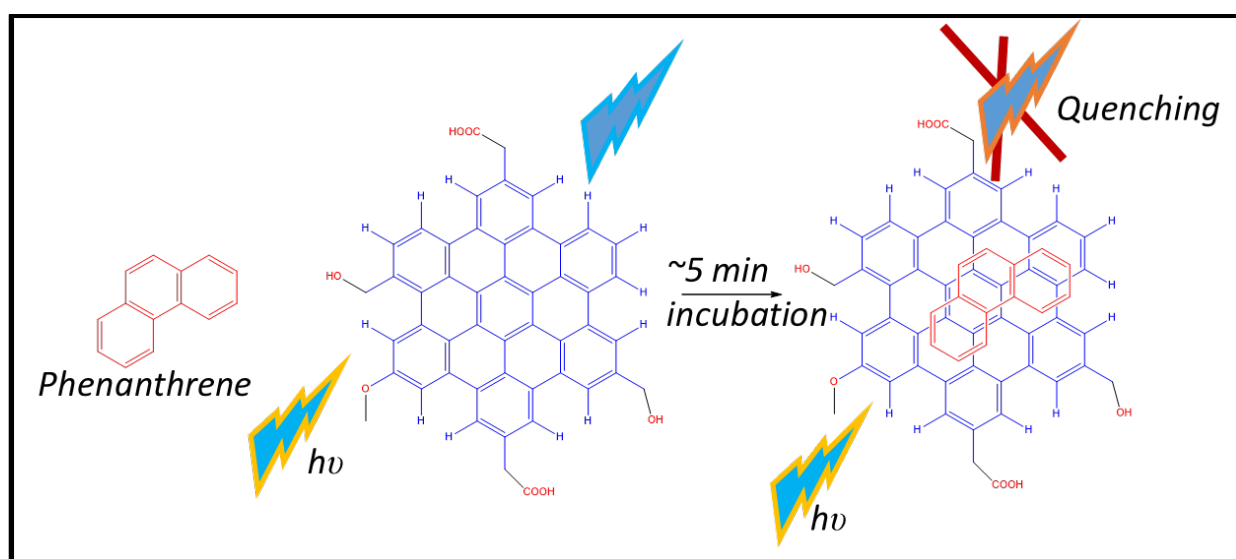


Figure 3.31 Schematic illustration of the interaction of phenanthrene with GQDs via π - π stacking leading to fluorescence quenching.

Four PAH compounds (anthracene, naphthalene, pyrene and phenanthrene) were selected to test the sensitivity of the GQD probe towards PAHs. These PAHs are of environmental and human health concern, and have been listed as priority PAHs by the United States Environmental Protection Agency (U.S. EPA, 2010). Moreover, they have been reported to occur in water systems due to their low molecular weight (Chimuka *et al.*, 2015; Qin *et al.*, 2014; Zhou & Maskaoui, 2003). PAH standard solutions were prepared within the $1\text{--}5 \times 10^{-7}$ mol L⁻¹ concentration range by dissolving them in H₂O/EtOH (2:1) mixture. To improve their solubility they were first dissolved in small amounts of toluene.

Sensing was carried out by placing 3 mL of GQDs solution in a quartz cuvette followed by adding 200 μ L of analyte PAH standard solution. For all the sensing measurements the GQDs and PAHs were allowed an equilibration time of exactly 5 min before taking fluorescence measurements to ensure interaction of the analytes with the sensor. Figure 3.33 shows the effect of different PAHs at a fixed concentration (1×10^{-7} mol L⁻¹) on the fluorescence intensity of the GQDs probe. Phenanthrene had the lowest quenching effect on the probe compared to the other PAHs that were investigated. It was

selected for further sensing studies as a worst case scenario of the PAHs considered, as results are expected to be enhanced (lower LODs) for the other PAHs, which can be tested further in due course.

Figure 3.34 shows the fluorescence signal response of the GQDs as the phenanthrene concentration was changed from $1-5 \times 10^{-7} \text{ mol L}^{-1}$. Signal quenching of GQDs upon interaction with aromatic compounds could be due to either fluorescence resonance energy transfer (FRET) or charge transfer, and a study by (Fan et al., 2012) with TNT (2,4,6-trinitrotoluene) showed that FRET was the more likely mechanism. Fluorescence life-time measurements have to be carried out in order to propose a plausible mechanism in the case of the PAHs. The quenching of the signal could be due to energy transfer from the GQDs to the phenanthrene analyte upon their interaction. Figure 3.35 shows that the signal decreased linearly with increasing phenanthrene concentration ($R^2 = 0.9572$). This shows that the GQDs probe can potentially be used as a sensor for detection of phenanthrene and possibly other PAHs in water.

The limit of detection (LOD) was calculated using the equation $3\delta/K$, where K is the slope of the calibration graph and δ is the standard deviation of blank measurements ($n = 9$). It was found to be $2.53 \times 10^{-8} \text{ mol L}^{-1}$ for phenanthrene – before any optimization. This shows great potential for the sensor for detecting the low concentrations of PAHs reported to occur in South African water systems.

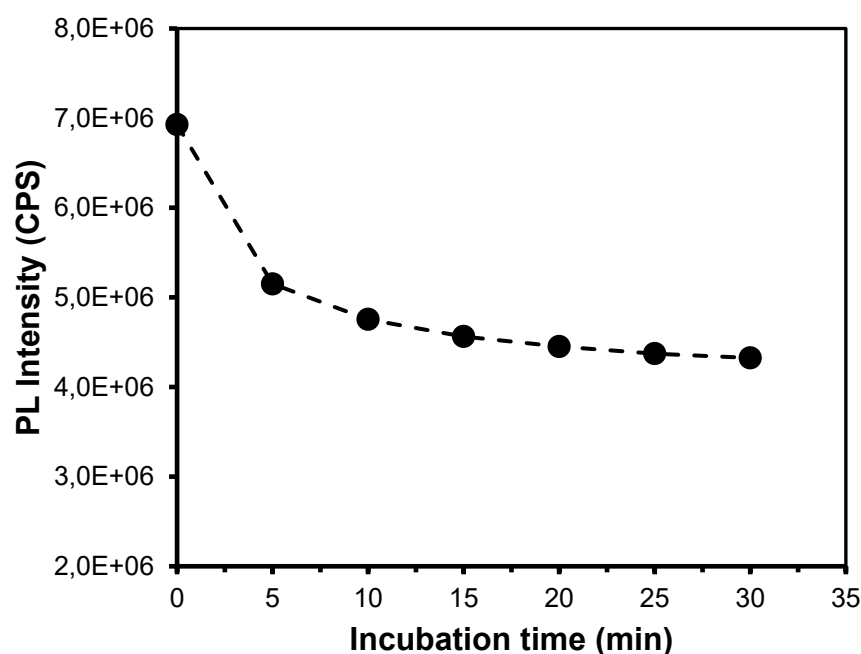


Figure 3.32 Effect of interaction time (incubation time) between 300 μL of GQDs and 100 μL of phenanthrene standard solution. The fluorescence intensity was quenched and became almost constant after 5 min.

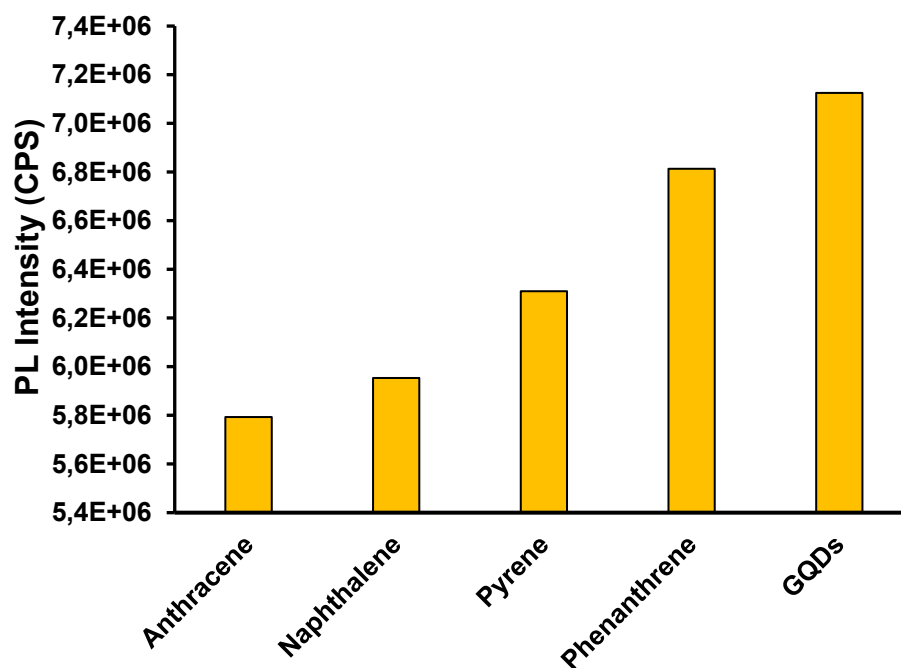


Figure 3.33 Effect of fixed concentration (1×10^{-7} mol L⁻¹) of PAHs on the fluorescence intensity of GQDs. $\lambda_{ex}=340$ nm.

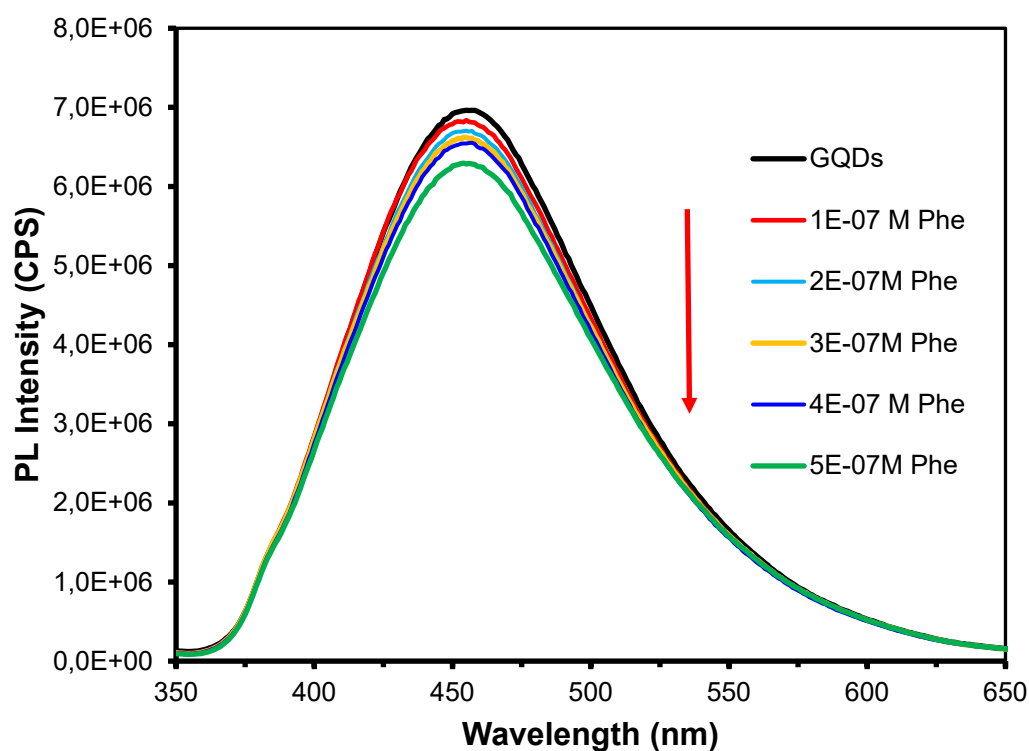


Figure 3.34 Fluorescence detection at increasing concentrations of phenanthrene corresponding to a decrease in PL signal of the GQDs. Phenanthrene concentrations were 0, 1×10^{-7} , 2×10^{-7} , 3×10^{-7} , 4×10^{-7} and 5×10^{-7} mol L⁻¹. Excitation was at 340 nm for all measurements.

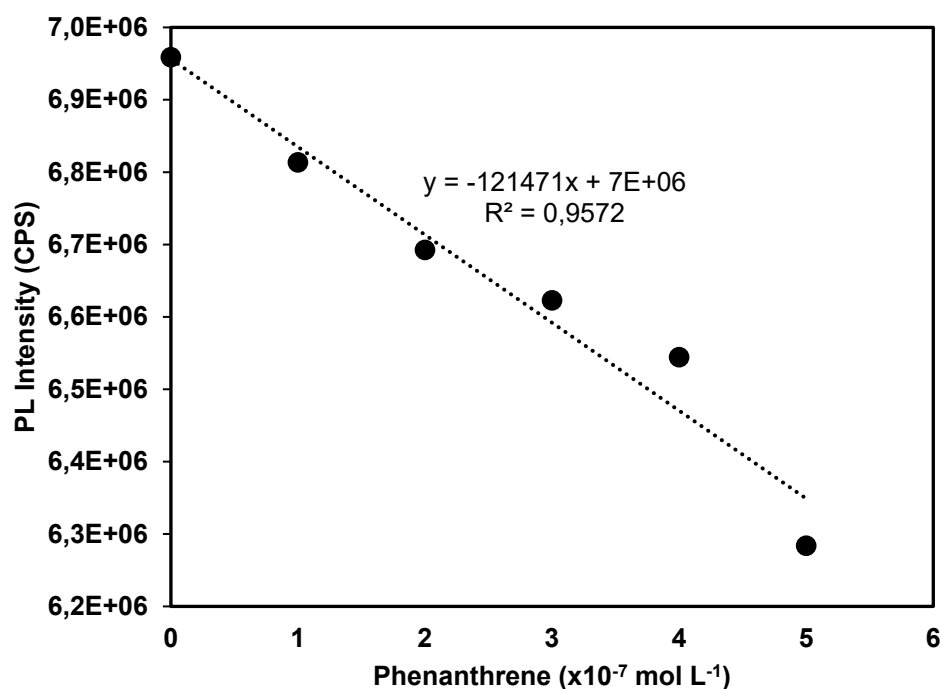


Figure 3.35 Calibration regression curve showing a linear response of the QDs upon interaction with phenanthrene.

3.6 CONCLUSION

Water soluble L-Cys functionalized CdSe/ZnS QDs were used as a fluorescence sensor for the determination of acetaminophen in water samples. The operating mechanism of the designed probes was based on the fluorescence “turn-on” mode. Under optimum conditions, with the addition of acetaminophen to QDs in aqueous solution, the original PL intensity of the QDs was enhanced most likely due to fluorescence resonance energy transfer from analytes to QDs which was found to be linear within the concentration range of 3.0-100 nmol L⁻¹ AC with a detection limit of 1.6 nmol L⁻¹. The method could therefore be applied to detect AC at nanomolar levels, which is environmentally relevant. Other advantages of this method include its simplicity, as well as stability and resistivity of QDs against photobleaching under ambient light conditions. The application of the sensor to additionally related pharmaceuticals (such as ketoprofen, sulfamethoxazole, L-tryptophan, estradiol, L-Dopa and diclofenac sodium salt) may also be possible.

We also designed and synthesized core-shell structured GSH-CdSe/ZnS QDs via a one pot organometallic synthesis method. Transmission electron microscopy images, FTIR spectra and fluorescence spectra confirmed the successful synthesis of QDs and the formation of a GSH coating thereon. The fluorescence of QDs was effectively enhanced by TCS at an emission wavelength of 598 nm over the concentration range of 10-300 nmol L⁻¹ with a detection limit of 3.7 nmol L⁻¹ which confirmed the applicability of the method to detect TCS at nanomolar levels. The turn-on mechanism of the sensing process is likely associated with energy transfer from TCS to the QDs. The good response of this probe

to TCS facilitates its application in the detection and determination of TCS in real water samples in the field of environmental monitoring.

Fluorescence sensor materials for detection of phenanthrene (GQDs) and atrazine (L-Cys-CdSeTe/ZnS QDs) were synthesized and initial tests were carried out to test their performance. Some of the important parameters that are crucial for the performance of the sensors were investigated and optimized. A low concentration of the sensor solution of 0.5 mg L^{-1} was used and appears to give a good response to the target analytes. The interaction time (incubation time) between sensor solutions and target analytes was also investigated and 5 min was found to be sufficient for both atrazine and phenanthrene as a representative PAH compound, respectively. This short interaction time is ideal for application of the sensor in cases where there are a large number of samples to be analysed.

CHAPTER 4: THE FUNCTIONALISATION OF QUANTUM DOTS

PART A – MOLECULARLY IMPRINTED POLYMER CAPPED CORE/SHELL QUANTUM DOTS FOR ACETAMINOPHEN DETECTION

4.1 INTRODUCTION

Acetaminophen (AC) is a common analgesic and antipyretic drug which is prescribed and purchased over the counter for the relief of minor pain such as fever and headaches. AC has no toxic effect in normal therapeutic doses while large doses particularly with simultaneous consumption of alcohol or other drugs can cause nephrotoxicity, skin rashes, inflammation of the pancreas and liver disorders (Lourencao *et al.*, 2009). A few reports have been published regarding the presence of acetaminophen in potable water, such as Frick *et al.* 2001, and on the potential chronic health effects related to long term ingestion of AC in water (Kümmerer, 2001).

Conventional methods for the detection of AC in real water samples are based on electrochemistry (Bouabi *et al.*, 2016), chromatography (Gracia-Lor *et al.*, 2010) and spectrophotometry (Méndez-Albores *et al.*, 2015). A fluorescence probe approach offers an alternative with clear advantages including easy operation, low cost, a fast and simple experimental process, and high sensitivity towards different molecular structures with different emission wavelengths (Li *et al.*, 2009).

Molecularly imprinted polymers (MIPs) are synthetic polymeric materials possessing specific recognition sites complementary in size, shape and functional groups to the template molecule (Holthoff *et al.*, 2011; Yang *et al.*, 2011). In molecular imprinting, functional monomers are located around the template molecules by non-covalent interaction or reversible covalent interaction, followed by polymerization and template removal. So a molecular 'memory' within the imprinted polymer matrix is created, and then the target molecule can be selectively distinguished based on the molecular 'memory' (Fang *et al.*, 2009). In covalent molecularly imprinting, the functional monomer is attached to the template by reversible covalent bonding during polymerisation (Kempe & Mosbach, 1995) while in non-covalent interactions, the functional monomer associates to the template via an intermolecular interaction such as hydrogen bonding or ion-pairing (Yu & Mosbach, 1997). MIPs have been considered as alternatives for natural receptors (Reddy *et al.*, 2013; Yuan *et al.*, 2011) in chemical assays or sensors due to their low cost, long lifetime, their tailor-made recognition sites for target analytes and intrinsic robustness.

The use of QDs is limited when coexisting interfering compounds produce a similar photoluminescence response to the target analyte. Molecularly imprinted polymers (MIPs) are a promising way to enhance

the selectivity of QDs. They are synthetic polymeric materials possessing specific recognition sites complementary to the template molecule in terms of functional groups, size and shape.

In 2012, a simple and sensitive assay of acetaminophen was proposed based on the quenching of the fluorescence intensity of L-cysteine capped CdTe nanoparticles (NPs) in aqueous solution. Under optimal experimental conditions, the relative fluorescence intensity ($\Delta I = I_0/I$) of L-cysteine capped CdTe NPs versus the concentration of acetaminophen was linear over the range of 10-160 nmol L⁻¹ with a detection limit of 4.2 nmol L⁻¹. The applicability of the method was tested for the analysis of AC in pharmaceutical tablets (Li *et al.*, 2012).

A bio-mimetic bulk acoustic wave (BAW) sensor was fabricated using a molecularly imprinted polymer with two functional monomers of 4-vinylpyridine (4-VP) and methacrylic acid (MAA) for the determination of acetaminophen over the linear range of 5.0-100 nmol L⁻¹ with a detection limit of 5.0 nmol L⁻¹. The biosensor was then applied for the determination of acetaminophen in human serum and urine samples (Tan *et al.*, 2001).

Recently, amphiphilic pillar[5]arene (amPA5) functionalized reduced graphene oxide (amPA5-RGO) as a receptor has been applied as a 'turn on' fluorescence sensing platform for the determination of AC in serum samples. The mechanism was based on competitive host-guest interaction between two analytes of acridine orange (AO)/acetaminophen which led to a change in fluorescence signal of the dye molecule. The prototype sensor gave a linear concentration range over 1.0×10²-4.0×10³ and 4.0×10³-3.2×10⁴ nmol L⁻¹ with a detection limit of 50 nmol L⁻¹ (Zhao *et al.*, 2017).

In another study for the simultaneous spectrophotometric determination of acetaminophen and gentamicin in tablets, ampoules and blood serum samples, silver nanoparticles were synthesized and applied over the concentration range of 5.0×10³-1.0×10⁵ nmol L⁻¹ with a detection limit of 1.2×10² nmol L⁻¹ (Bahram *et al.*, 2015).

Until now, various MIP capped CdSe/ZnS QD sensors with different capping agents have been reported for the detection of different contaminants, but not for AC. Lee *et al.* synthesized CdSe/ZnS QDs functionalized using ethylene glycol dimethacrylic acid as the cross-linker and 4-vinylpyridine methacrylic acid as the functional monomer with various templates corresponding to analytes such as caffeine and uric acid. Although they also used caffeine as a template for theobromine, they showed that the imprinted polymers provided more affinity to the corresponding print molecule compared with analogous structures. The quenching of the photoluminescence emission was attributed to the Förster resonance energy transfer (FRET) between quantum dots and template molecules (Lin *et al.*, 2004).

Rhee *et al.* developed a size series of water soluble mercaptopropionic acid capped CdSe/ZnS QDs entrapped in sol-gel membranes for the detection of some polycyclic aromatic hydrocarbons (PAHs). They could detect PAHs at trace levels (10-100 nmol L⁻¹ for anthracene and phenanthrene and 5-50 nmol L⁻¹ for pyrene) due to fluorescence enhancement of the QDs through the mechanism of energy transfer between PAHs and QDs (Duong *et al.*, 2011).

A surface molecular imprinting process using AC as a template was applied to synthesize the fluorescent sensor which places the binding sites in the vicinity of the MIP surface and enhances

selectivity and mass transfer. In comparison with bulk polymerisation which generates MIPs with poor binding capacity and low binding kinetics, the surface imprinting technique facilitates complete removal of the template due to the thin imprinting layers and also provides accessible sites for rebinding of the target analyte leading to high binding capacities, in addition to good synthesis reproducibility (Chen *et al.*, 2016; Yu *et al.*, 2017).

Here, the high sensitivity of QDs was integrated with the selectivity of MIPs via the preparation of a QD-based MIP composite. L-Cys-CdSe/ZnS QDs were synthesized and entrapped in the layers of 3-aminopropyltriethoxysilane (APTES) and tetraethyl orthosilicate (TEOS) through an adapted Stöber method (sol-gel approach) and surface imprinting technique. The sol-gel technique has many advantages over other polymerization techniques, including simple preparation at room temperature, preventing problems associated with thermal and chemical decomposition. Furthermore, environmentally friendly solvents such as Millipore water or ethanol can be used in radical polymerisation instead of toluene, acetonitrile or chloroform (Chen *et al.*, 2016; Chen *et al.*, 2011). AC could be detected at low levels based on the fluorescence quenching of MIP@QDs likely through the mechanism of charge transfer induced energy transfer from the MIP@QDs to AC, allowing for the application of the fluorescence sensor to AC monitoring in real water samples. A simple sensor for AC molecules is thus reported which detects this analyte selectively and can be applied to improve water quality, as AC can accumulate in water systems and cause long term health effects, even at low concentrations.

4.2 EXPERIMENTAL

4.2.1 Reagents and materials

Octadec-1-ene (ODE), trioctylphosphine oxide (TOPO), zinc oxide, cadmium oxide, oleic acid (OA), sulfur powder, L-cysteine (L-Cys), hydrochloric acid, potassium hydroxide, acetaminophen (AC), 3-aminopropyltriethoxysilane (APTES) and tetraethyl orthosilicate (TEOS) were purchased from Sigma Aldrich. Anhydrous ethanol and ammonia solution were purchased from Merck. Potential interfering analytes, namely L-ascorbic acid (AA), dopamine hydrochloride (DA), epinephrine hydrochloride (EP), uric acid (UA), 4-aminophenol (4-AP), L-tryptophan (TRY), ketoprofen (KTP), sulfamethoxazole (SM), estradiol (ES), L-Dopa and diclofenac sodium salt (Dic) were purchased from Sigma Aldrich. An ultrapure Milli-Q Water System (18.0 M Ω .cm at 25°C) was used for sample preparation.

4.2.2 Characterization

A Horiba Jobin Yvon Fluoromax-4 spectrofluorometer was employed to record fluorescence emission spectra. Transmission electron microscopy (TEM) images were taken using a JEOL JEM 2100F operated at 200 kV. The estimated particle size distribution of QDs was determined using ImageJ software (<http://imagej.nih.gov/ij/>, U.S. National Institutes of Health [NIH], Bethesda, Maryland, USA). IR measurements (4000-400 cm⁻¹) in KBr were taken using a Spectrum RXI FT-IR System from Perkin

Elmer. All pH measurements were made with a Metrohm 780 pH-meter that was calibrated with Accsen standards of pH 4.0 and 7.0.

4.2.3 Synthesis of MIP-capped L-Cys-CdSe/ZnS QDs

One pot synthesis was carried out for the preparation of the L-Cys-CdSe/ZnS QDs according to a published method which was detailed in Chapter 3.

Regarding the synthesis of MIP@QDs, 20 mg of AC (template) in ethanol and APTES (functional monomer) were added to a flask followed by stirring. 5 mL of L-Cys-CdSe/ZnS QDs, TEOS (cross linker) and ammonia were then injected into the mixture and stirred for 24 h. Anhydrous ethanol was utilized to purify the resultant MIP-capped CdSe/ZnS QDs until the fluorescence intensity remained constant. Lastly, the MIP-capped CdSe/ZnS QDs (MIP@QDs) were dried under vacuum at room temperature and stored in a desiccator for further use. The non-imprinted polymers (NIP@QDs) were also prepared in the same manner but without the addition of AC to compare with MIP@QDs.

4.2.4 Optimization experiments

Regarding the optimization of the MIP@QDs concentration, different concentrations of MIP@QDs were prepared in 3.0 mL of Millipore water and 200 μL of a standard solution of AC (300 nmol L^{-1}) was then injected to 2 mL of each solution separately. The PL of the resulting solution was then determined.

In order to optimize the incubation time, 0.8 mg of MIP@QDs was dissolved in 3 mL Millipore water and 200 μL of a standard solution containing 300 nmol L^{-1} of AC was injected. The corresponding PL spectra were then recorded after different time intervals. The values of F_0 and F were recorded for each optimization which were the PL intensity of MIP@QDs in the absence and presence of AC respectively. KOH and HCl were used to adjust the pH of Millipore water in the pH optimization experiments. 0.8 mg of MIP@QDs was dissolved in 3 mL Millipore water at different pH values and 200 μL of 300 nmol L^{-1} AC solution was injected to 2 mL of each MIP@QDs solution separately. The corresponding PL spectra were recorded after 14 min which were set as F while the PL intensity of MIP@QDs in the absence of AC was recorded as F_0 .

Intra-day photostability of MIP@QDs and NIP@QDs were performed by recording PL spectra after 10 min intervals for 40 min. In order to examine inter-day photostability, the solution of each polymer was kept in the fridge for 5 days and the corresponding PL spectra were recorded.

4.2.5 Sample analysis

Tap water samples for fluorescence measurements were collected from a municipal tap in Pretoria, South Africa using cleaned glass bottles. River water samples were also collected from the LC de Villiers sports grounds of the University of Pretoria. The sample bottles were filled and immediately placed in cooler boxes containing icepacks and transferred to the laboratory for storage at 4°C prior to analysis. The collected tap and river water samples were centrifuged at 4500 rpm for 5 min and filtered through

110 mm pore size filter paper before analysis to eliminate particulate matter before storage in pre-cleaned glass bottles. As no AC was detected in collected water samples by HPLC-MS/MS, a spiking method (over the concentration range of 10-300 nmol L⁻¹) was adopted with different known amounts of AC dissolved in Millipore water and the AC concentration was determined based on the fluorescence quenching of the MIP@QDs. Sensing was carried out by placing 2 mL of 0.8 mg of MIP@QDs in 3 mL of Millipore water in a quartz cuvette followed by addition of 200 μ L of a standard solution containing different amounts of AC. The PL intensity after 14 min stabilization time was set as F and the PL intensity of MIP@QDs in the absence of AC was set as F₀. Through the variation of AC concentration, a series of F₀/F values were obtained.

4.3 RESULTS AND DISCUSSION

4.3.1 Characterization of MIP- and NIP-Capped CdSe/ZnS QDs

4.3.1.1 FT-IR analysis

In order to confirm that the MIP was well coated onto the QDs, FTIR of MIP@QDs, NIP@QDs, original L-Cys-CdSe core QDs, L-Cys-CdSe/ZnS core/shell QDs, L-Cys and AC were compared (Fig. 4.1). Carboxylic acid and amino groups of L-Cys around 1550-1600 cm⁻¹ and 2900-3420 cm⁻¹ were evident for the L-Cys capped CdSe/ZnS and CdSe QDs, while the S-H group vibration (2550-2750 cm⁻¹) was absent in the spectra of the L-Cys-CdSe/ZnS QDs which is due to the formation of covalent bonds between thiols and the surface of ZnS in the L-Cys capped CdSe/ZnS QDs and the formation of Cd-S bonds in the L-Cys-CdSe QDs. After the coating of MIP onto the surface of the QDs, a strong band at 1046 cm⁻¹ corresponded to the asymmetric stretching vibration of Si-O-Si groups. The bands at 3100-3500 cm⁻¹ and 1630 cm⁻¹ in the spectra of MIP@QDs and NIP@QDs can be due to the stretching and bending vibrations of N-H groups from the APTES. The FT-IR results revealed that APTES and TEOS were successfully grafted onto the surface of the L-Cys-capped CdSe/ZnS QDs.

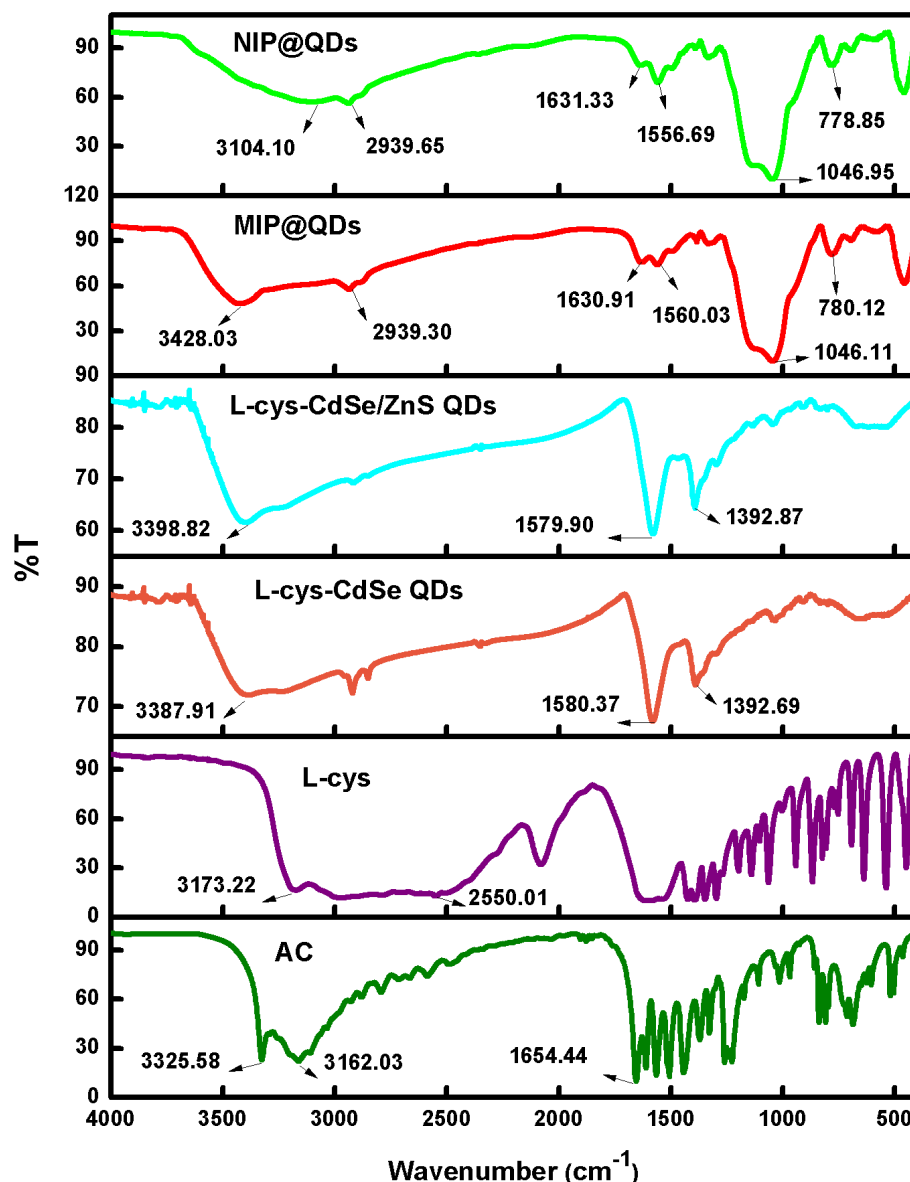


Figure 4.1 FT-IR spectra of AC, L-Cys, L-Cys-CdSe QDs, L-Cys-CdSe/ZnS QDs, MIP@QDs (with template removed) and NIP@QDs.

4.3.1.2 TEM analysis

Modification of the surface of QDs with MIP was further confirmed by TEM analysis. The TEM images of original L-Cys-CdSe QDs, L-Cys CdSe/ZnS QDs, MIP@QDs and NIP@QDs are shown in Fig. 4.2A-D. They all had a nearly spherical morphology and were well dispersed in the aqueous solution. The diameters of MIP@QDs increased after coating with APTES in comparison with core/shell QDs. NIP@QDs particles were also spherical and monodispersed in the solution. As an indirect approach (Cheng *et al.*, 2005), the shell thickness of silica was calculated by subtracting the average particle size of MIP@L-Cys-CdSe/ZnS QDs from L-Cys-CdSe/ZnS QDs which was estimated to be 0.55 nm. The size distribution of L-Cys-CdSe QDs, L-Cys-CdSe/ZnS QDs, MIP@QDs and NIP@QDs are shown in Fig. 4.3A-D.

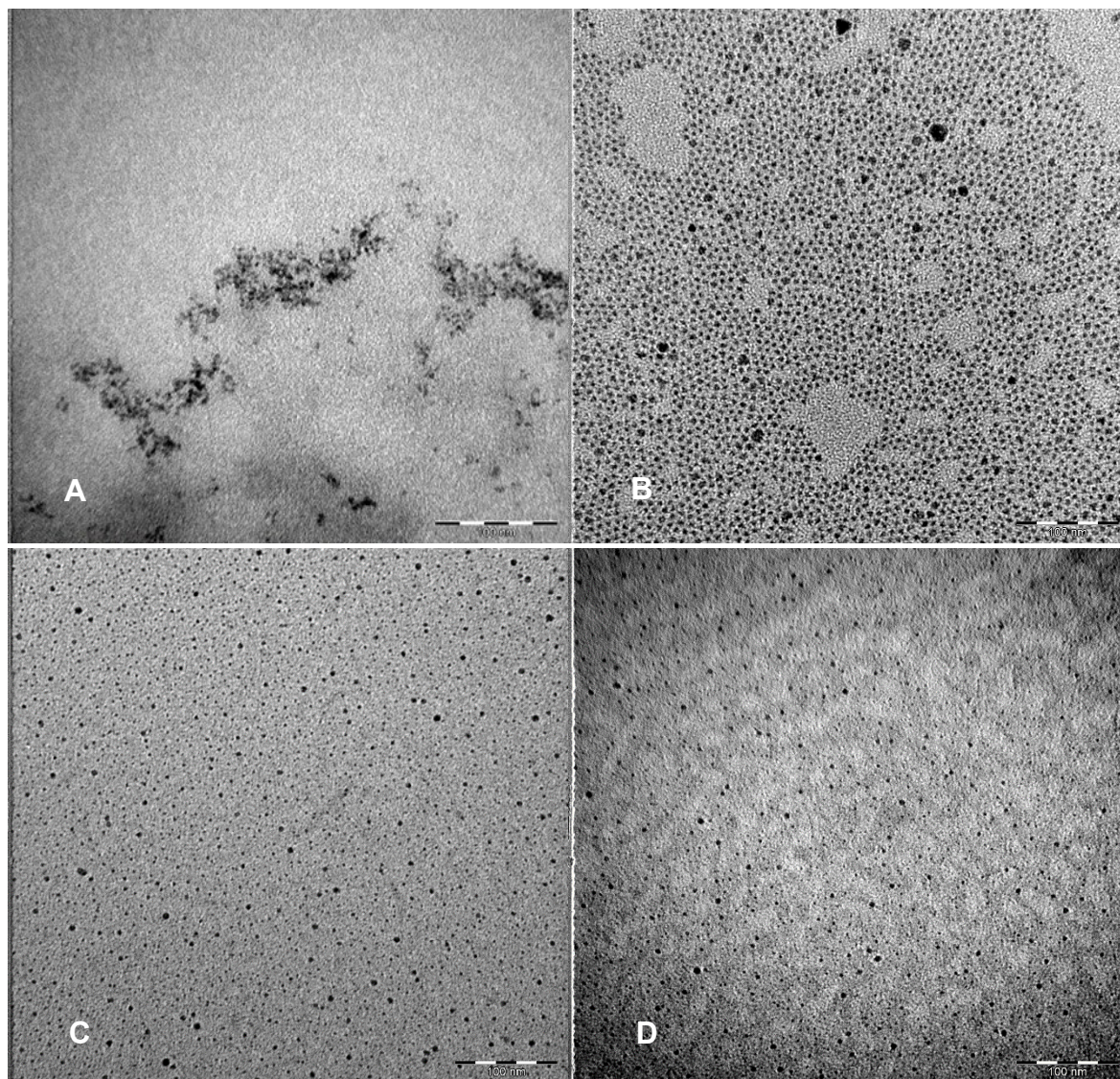


Figure 4.2 TEM images of (A) L-Cys-CdSe QDs (B) L-Cys-CdSe/ZnS QDs (C) MIP@QDs and (D) NIP@QDs (scale bar 100 nm in all cases).

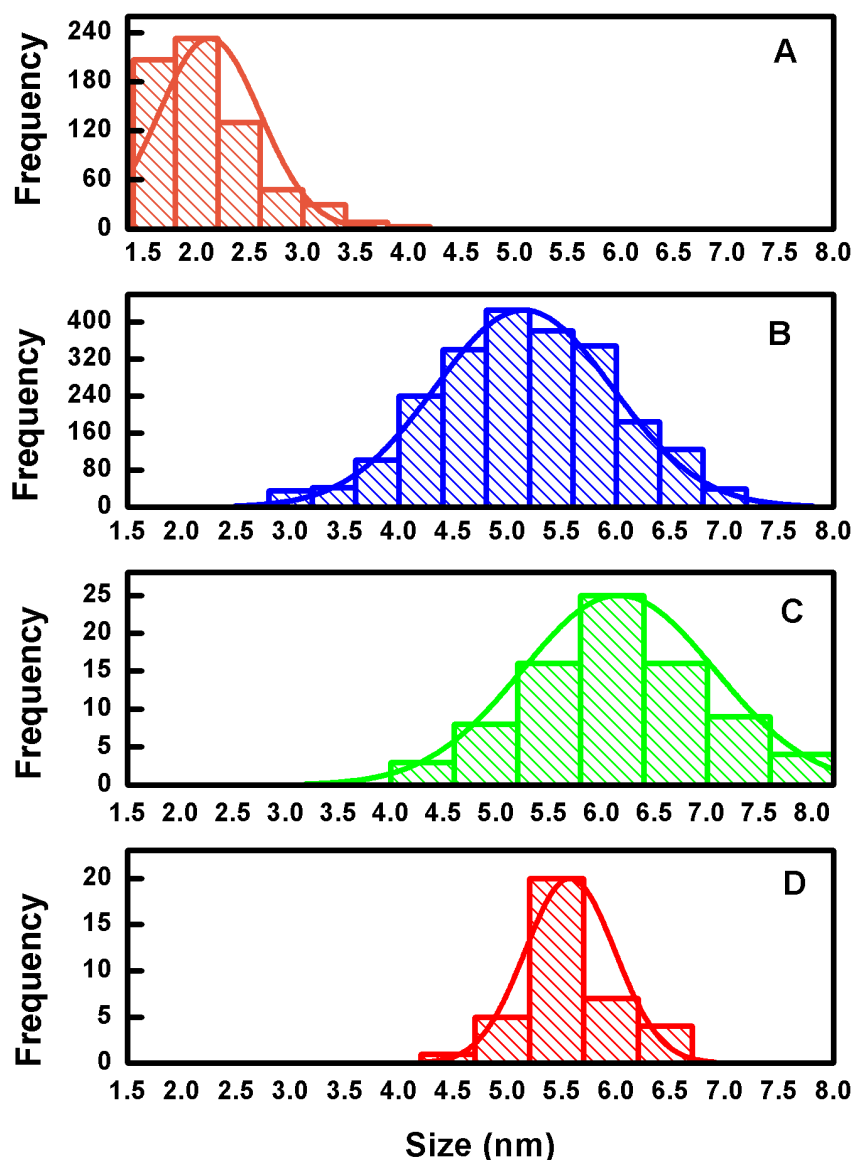


Figure 4.3 Size distribution histogram of (A) L-Cys-CdSe QDs (B) L-Cys-CdSe/ZnS QDs (C) MIP@QDs and (D) NIP@QDs.

4.3.2 Optimization of sensing variables

The aim of this work was to develop a sensor material which is selective and sensitive towards AC molecules. The effects of MIP@QDs concentration, incubation time and pH on the fluorescence quenching of MIP@QDs were thus studied in order to optimize these experimental variables and allow for control thereof in subsequent application experiments.

4.3.2.1 Concentration of MIP@QDs

The amount of MIP@QDs was varied from 0.2 to 1.2 mg in 3.0 mL of Millipore water and a fixed concentration of AC was used. The highest degree of quenching was achieved at the concentration of 0.8 mg in 3.0 mL (Fig. 4.4) which was therefore used for subsequent experiments. At higher

concentrations possible self-quenching occurs thus only concentrations of MIP@QDs below 1.0 mg in 3.0 mL were investigated.

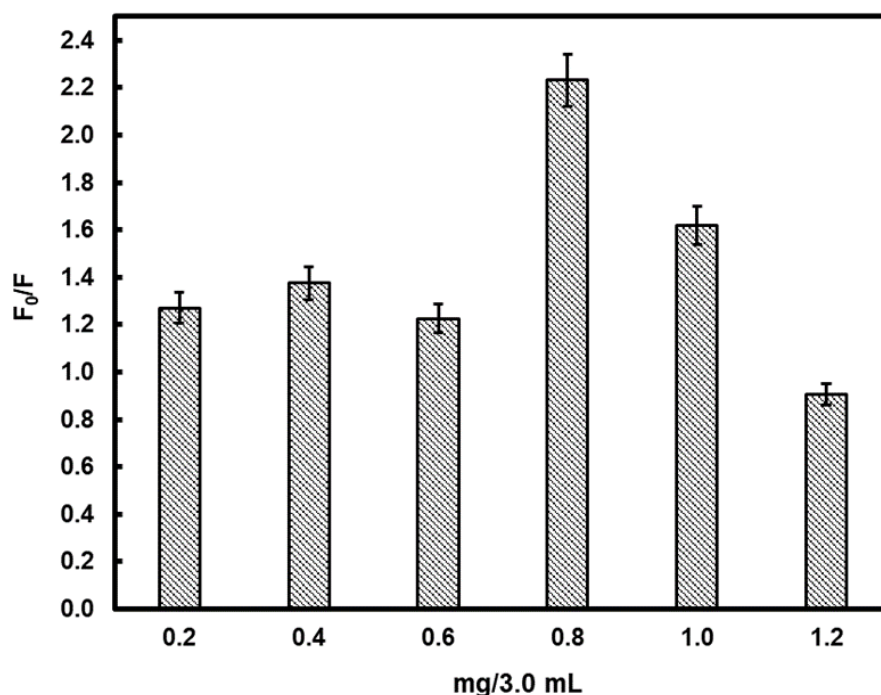


Figure 4.4 Effect of the MIP@QD concentration on PL quenching efficiency (n=3). The concentration of AC was fixed at 300.0 nmol L⁻¹. The experimental conditions were excitation wavelength 350 nm; slit widths of excitation and emission, 5.0 nm.

4.3.2.2 Effect of incubation time

The experimental results for the incubation time of MIP@QDs at a fixed concentration of AC showed a notable increase after 14 min (Fig. 4.5). Fluorescence intensity of MIP@QDs also decreased after 14 min possibly due to self-quenching. The imprinting silica layer was ultrathin which facilitated fast response of the MIP@QDs to AC (Wang *et al.*, 2016a). Therefore 0.8 mg of MIP@QDs in 3.0 mL and an incubation time of 14 min were chosen for subsequent experiments.

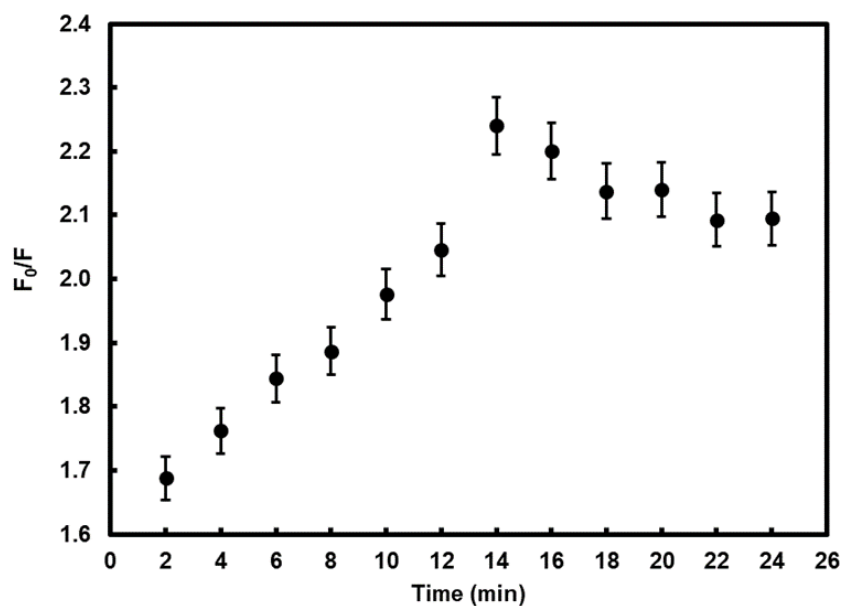


Figure 4.5 Effect of incubation time on relative fluorescence of MIP@QDs with AC (n=3). The experimental conditions were MIP@QDs: 0.8 mg in 3.0 mL⁻¹; AC: 300.0 nmol L⁻¹; excitation wavelength, 350 nm; slit widths of excitation and emission, 5 nm.

4.3.2.3 Photostability study

The photostability of MIP@QDs was investigated over 40 min which did not show a large change in PL intensity (Fig. 4.6). The highest relative fluorescence intensity of MIP@QDs towards AC was achieved after only 14 min.

The stabilities of MIP@QDs and NIP@QDs were then evaluated over 5 days. The FL intensity of MIP@QDs was stable for 2 days, and then declined slightly over the next 3 days, while the change in fluorescence intensity of NIP@QDs over 5 days was minimal (Fig. 4.7). The prototype polymer thus displayed acceptable storage stability over time which indicated effective protection of L-Cys-CdSe/ZnS QDs by the silica layers of the polymer.

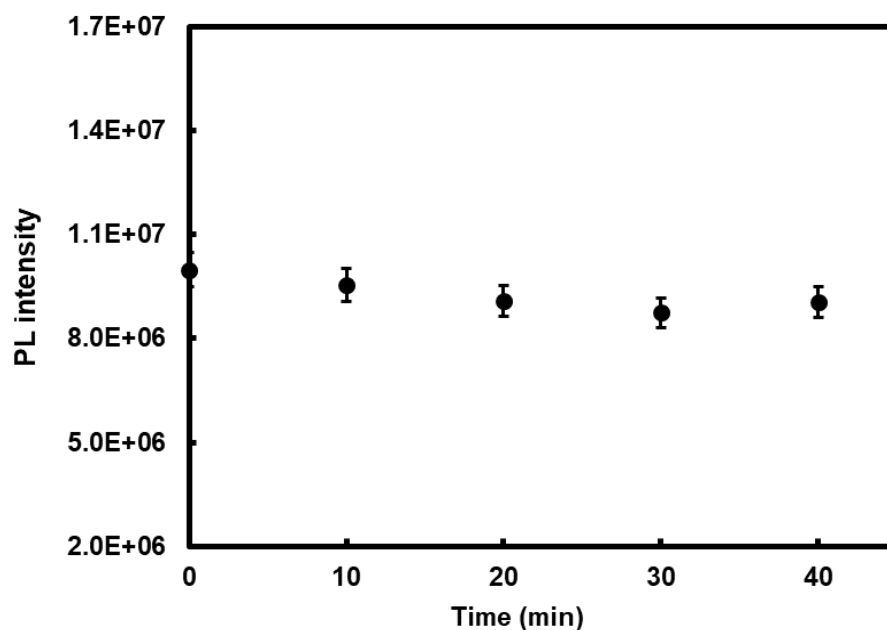


Figure 4.6 Photostability of MIP@QDs over 40 min (values are the average of three measurements). The experimental conditions were MIP@QDs, 0.8 mg in 3.0 mL⁻¹; excitation wavelength, 350 nm; slit widths of excitation and emission, 5.0 nm.

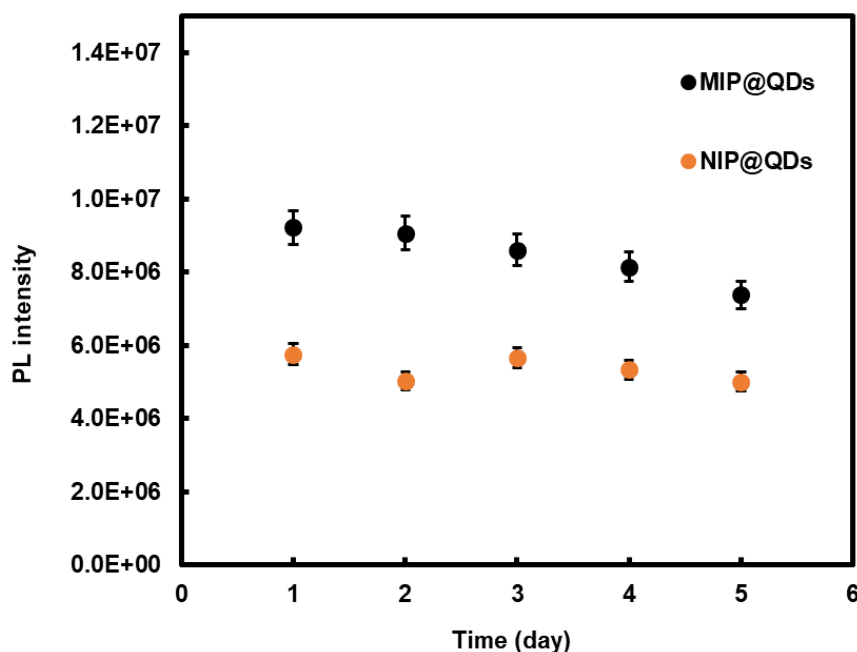


Figure 4.7 Average photostability of MIP@QDs and NIP@QDs over 5 days (n=3). The experimental conditions were MIP@QDs or NIP@QDs, 0.8 mg in 3.0 mL⁻¹; excitation wavelength, 350 nm; slit widths of excitation and emission, 5.0 nm.

4.3.3 Fluorescence sensing of acetaminophen using AC-templated molecularly imprinted polymer-quantum dots

The binding affinity of MIP@QDs and NIP@QDs towards different concentrations of AC was investigated by fluorescence analysis (Fig. 4.8A and B). The quenching mechanism can be described according to the Stern-Volmer equation (Li *et al.*, 2010):

$$\frac{F_0}{F} = 1 + K_{sv} [Q]$$

Here F_0 and F are the fluorescence intensities in the absence and presence of the quencher, respectively, K_{sv} is the quenching constant of the quencher, and $[Q]$ is the concentration of the quencher.

With the introduction of AC, the fluorescence intensity of the MIP@QDs was quenched linearly in the concentration range of 1.0-300 nmol L⁻¹ (Fig. 4.8A) with detection and quantification limits of 0.34 and 1.1 nmol L⁻¹ respectively. The limit of detection (LOD) and quantification (LOQ) are defined by $3\delta/m$ and $10\delta/m$, where δ is the standard deviation of the blank measurement ($n=10$) and m is the slope of the calibration curve. The LOD value is lower than the guidance value of 1.3×10^3 nmol L⁻¹ (200 ppb) for acetaminophen in drinking water given by the Minnesota Department of Health (MDH) ("Toxicological Summary for: Acetaminophen," 2010).

As a comparison, the binding affinity of NIP@QDs was also examined with different concentrations of AC (Fig 4.8B). It was observed that the NIP@QDs could not bind AC as effectively, resulting in lower sensitivity with detection and quantification limits. The decrease of fluorescence intensity of the MIP@QDs was considerably more than for NIP@QDs at the same concentration of AC indicating better quenching efficiency of MIP@QDs and thus an increasing in spectral sensitivity of MIP@QDs to AC. Furthermore, due to the absence of specific recognition cavities in the structure of NIP@QDs, AC could not entrap properly into the polymer and only the QDs located on the proximity of the surface of the NIP@QDs could be quenched. Consequently, the fluorescence intensity of many of the QDs is expected to have remained unchanged (Jia *et al.*, 2017; Wang *et al.*, 2016b).

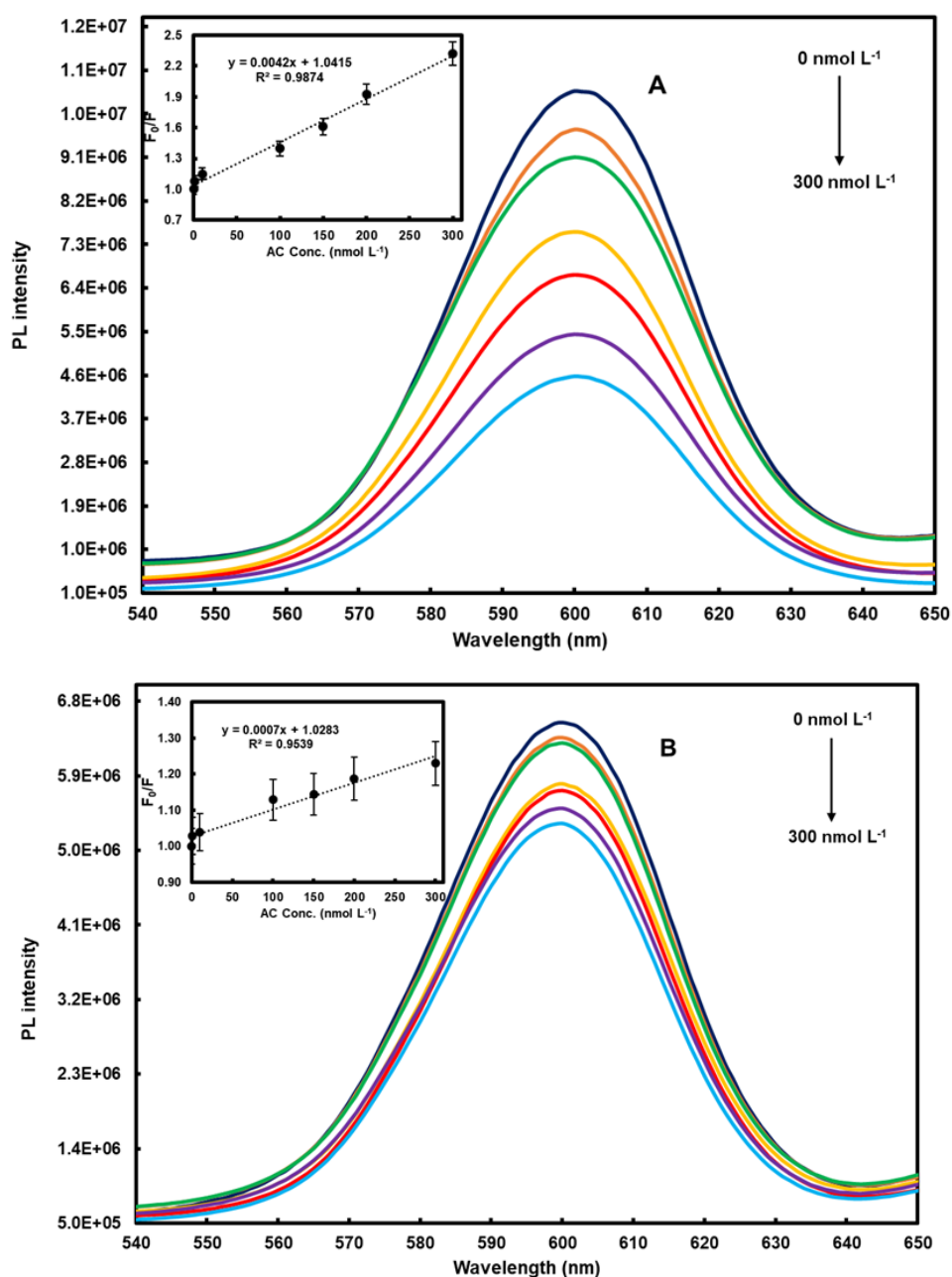


Figure 4.8 Fluorescence emission spectra of MIP@QDs (A) and NIP@QDs (B) in the presence of varying concentrations of AC. The experimental conditions were MIP@QDs or NIP@QDs at 0.8 mg in 3.0 mL^{-1} ; excitation wavelength, 350 nm ; slit widths of excitation and emission, 5 nm . The inset graphs display the corresponding Stern-Volmer plots of MIP@QDs and NIP@QDs with the addition of AC (all results are the average of three replicates).

4.3.4 Selectivity of the sensor to AC

The selectivity of MIP@QDs was examined towards different analytes with similar structures to AC, including vitamins (AA), catecholamines (EP, DA, L-Dopa), aminophenols (4-AP), analgesics and antipyretics (KTP, Dic), antiseptics (SM), essential amino acids (TRY), hormones (ES) and UA. The largest fluorescence quenching was observed for the MIP@QDs in the presence of AC (Fig. 4.9), while

this response was not as large for the other analytes. The imprinted cavities left by the removal of the template thus provided easier access to the recognition sites for AC molecules (Li *et al.*, 2010).

Fig. 4.9 also shows the quenching of NIP@QDs with AC and the other analytes. In this case there was much less of a difference between the sensor response to AC and other competitive compounds, i.e. less selectivity was observed.

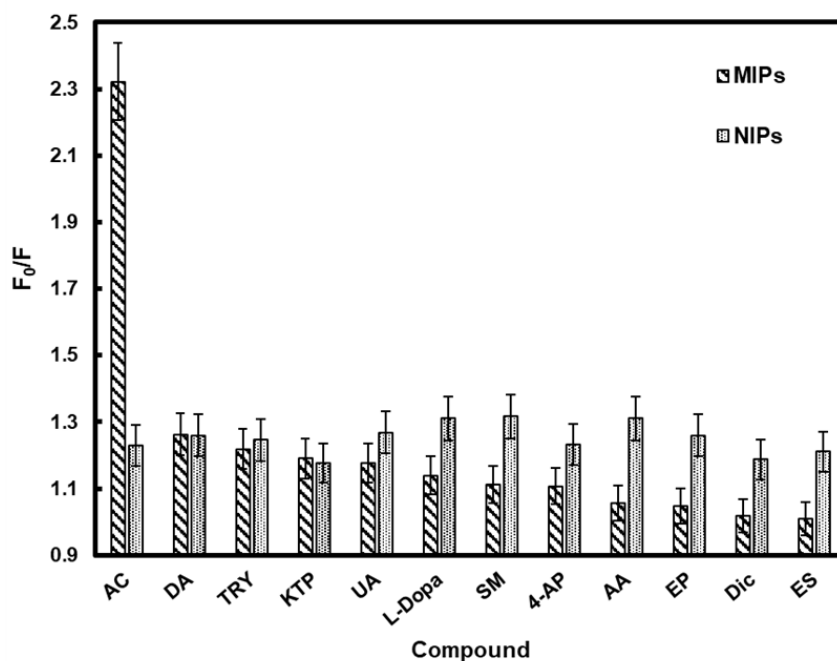


Figure 4.9 Fluorescence quenching of MIP@QDs and NIP@QDs by different analytes at 300.0 nmol L⁻¹. The experimental conditions were MIP@QDs, or NIP@QDs 0.8 mg in 3.0 mL⁻¹; excitation wavelength 350 nm; 5 nm excitation and emission slit widths. L-tryptophan (TRY), ascorbic acid (AA), epinephrine hydrochloride (EP), uric acid (UA), dopamine hydrochloride (DA), ketoprofen (KTP), sulfamethoxazole (SM), diclofenac sodium salt (Dic), estradiol (ES), L-3,4-dihydroxyphenylalanine (L-Dopa) and 4-aminophenol (4-AP) (results are the average of three replicates).

4.3.5 Proposed sensing mechanism of the MIP-capped CdSe/ZnS QDs

Two possible mechanisms have been proposed for the fluorescence quenching of MIP@QDs, namely energy transfer and charge transfer. Fluorescence resonance energy transfer (FRET) from MIP@QDs to AC can be excluded as there is no spectral overlap between the absorption spectra of AC and the fluorescence emission of the MIP@QDs (Fig. 4.10A and C). We therefore conclude that a strong charge transfer interaction took place between the electron-rich aromatic ring (conjugating OH) of AC and electron deficient amino group of APTES.

Such a charge transfer mechanism has been also reported by Jia *et al.* in the case of SiO₂@QDs@mesoporous-MIPs for the fluorescence determination of 2,4-dichlorophenoxyacetic acid over the linear range of 6.6×10²-80×10³ nmol L⁻¹ with a detection limit of 2.1 nmol L⁻¹ (Jia *et al.*, 2017) and Yu *et al.* for the determination of 4-nitrophenol via molecularly imprinted polymer coated thioglycolic acid capped CdTe QDs over the linear range of 2.0×10²-8.0×10³ nmol L⁻¹ with a detection limit of 51 nmol L⁻¹ (Yu *et al.*, 2017).

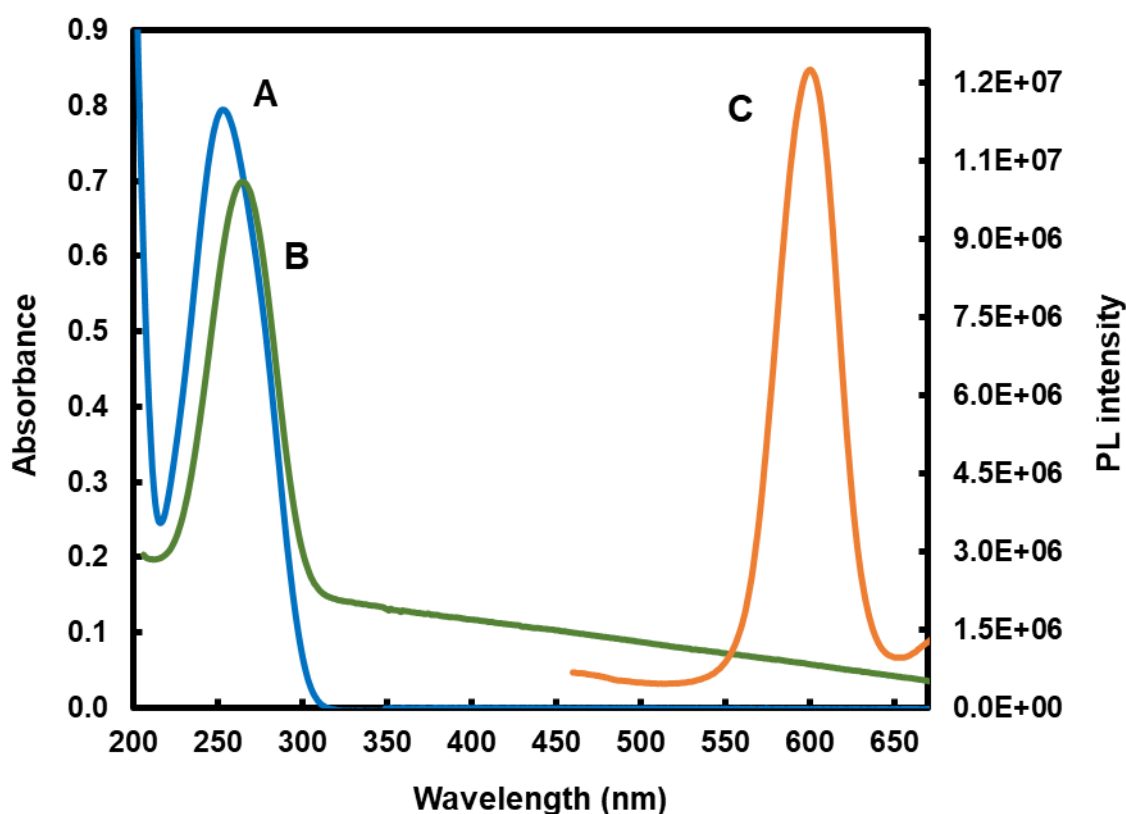


Figure 4.10 UV/Vis absorption spectrum of AC (A) and MIP@QDs (B) and fluorescence emission spectrum of MIP coated QDs (C).

4.3.6 Practical application and performance comparison

The synthesized MIP@QDs were applied to determine AC in real water samples. HPLC-MS/MS analysis was performed as a comparative method which confirmed that the background concentration of AC in the tap and river water samples was below the detection limit. As AC was not present in these samples, they were spiked with three different concentrations of AC. The fluorescence of the MIP@QDs was notably quenched upon addition of the samples, suggesting the existence of imprinted cavities with the size and shape of AC molecules. For each sample, the experiments were conducted three times at three spiking levels and the recoveries varied from 95% to 114% (Table 4.1), indicating the potential application of the prototype sensor for the determination of AC in real water samples.

Although numerous studies have been reported regarding the detection of AC in different matrices, there are limited reports for water samples. However, the performance of the synthesized MIP@QDs AC sensor with that of other reported methods for real water samples are compared in Table 4.2.

Although the linear range is smaller compared to square wave voltammetry, for example, both the selectivity and sensitivity of the developed MIP@QDs sensor have been markedly enhanced compared to other reported methods. As a new material, our developed MIP@QDs fluorescence sensor is thus a promising candidate for the selective and sensitive detection of AC in water.

Table 4.1 Spiked recovery results for the determination of AC in water samples using 2 mL of 0.8 mg of MIP@QDs in 3 mL of Millipore water and 200 μ L of AC standard solution (n=3).

	Spiked AC (nmol L ⁻¹)	Determined AC (mean±RSD; n=3, nmol L ⁻¹)	Recovery (%)
Tap water	50	52.0±0.1	104
	150	146.0±0.4	97
	300	320.0±0.1	107
River water	50	57.0±0.3	114
	150	142.0±0.01	95
	300	301.0±0.1	100

Table 4.2 Comparison of the proposed fluorescence method with other recently reported methods for AC determination in water samples.

Sensor system	Linear range (nmol L ⁻¹)	LOD (nmol L ⁻¹)	Sample matrix	Reference
CS/CPE (SWV)	8.0×10 ² -2.0×10 ⁵ 4.0×10 ⁵ -1.0×10 ⁶	7.1×10 ²	River water	(Bouabi <i>et al.</i> , 2016)
		6.8×10 ²	Seawater	
HPLC-DAD	3.8×10 ¹ -3.9×10 ²	<66.2	Surface water	(Agunbiade & Moodley, 2014)
		390.3	Wastewater influent	
Biocatalytic spectrophotometry	2.0×10 ³ -1.4×10 ⁴	5.5×10 ²	Potable, tap water and treated wastewater effluent	(Méndez-Albores <i>et al.</i> , 2015)
MWCNT/PE/surfactant (DPV)	1.5×10 ⁴ -1.8×10 ⁵	3.0×10 ²	Tap and domestic wastewater	(Gorla <i>et al.</i> , 2016)
MWCNT/PE/surfactant (SWV)	1.5×10 ⁴ -1.2×10 ⁵	4.4×10 ³		
MIP-capped L-Cys CdSe/ZnS QDs	1.0-300.0	0.34	Tap and river water	This work

CS/CPEL: Chitosan modified carbon paste electrode; DPV: Differential pulse voltammetry; HPLC-DAD: High-performance liquid chromatography-diode array detector; LOD: Limit of detection; MWCNT/PE/surfactant: Multi-walled carbon nanotubes/paste electrode in the presence of a surfactant; SWV: Square wave voltammetry.

PART B – MOLECULARLY IMPRINTED POLYMER CAPPED CORE/SHELL QUANTUM DOTS FOR ATRAZINE DETECTION

4.4 INTRODUCTION

Atrazine is used extensively in agriculture for controlling weeds and it may eventually contaminate water systems through leaching, runoff and spray drift. The high global use of atrazine, and pesticides in general, can be attributed to the ever increasing food demand and the need to ensure food security which consequently comes with the risk of environmental contamination. Atrazine has been reported to occur in South African water systems by several WRC studies (Dabrowski, 2015a, 2015b; Dabrowski *et al.*, 2013; Dabrowski & Balderacchi, 2013; Dabrowski & Schulz, 2003; Dabrowski *et al.*, 2014; Du Preez *et al.*, 2005; Patterson, 2013). These reports make a strong case for the prioritisation of atrazine as a priority emerging chemical pollutant (ECP) and warrant the development of sensitive and economical analytical methods which can be used routinely as an alternative to current conventional methods, which are relatively expensive.

In a paper by Nsibande & Forbes (2016) we reviewed different studies on the application of QDs as fluorescence probes for pesticide detection. Different functionalisation strategies were also reviewed but none of the studies had used QDs as fluorescence probes for atrazine detection. Here we demonstrate that by using molecularly imprinted polymers (MIPs), QDs can be applied for the detection of atrazine. Some of the attractive advantages of using MIPs is that they are easy to prepare, cost effective, and have high mechanical and chemical stability, and can be tailored to be selective towards an analyte of interest. The choice of monomer is very important when preparing MIPs as it should be able to interact with the target analyte. The favoured monomer for atrazine MIPs is methacrylic acid (MAA) as it has better imprinting effects and allows for maximum hydrogen bonding with atrazine (Han *et al.*, 2017; Lakshmi *et al.*, 2013). Thus we report on the development of MIP functionalized CdSeTe/ZnS QDs (CdSeTe/ZnS@MIP) for detection of atrazine in water.

4.5 MATERIALS AND METHODS

4.5.1 Chemicals

Cadmium oxide (CdO), octadec-1-ene (ODE), tellurium powder (Te), zinc oxide, sulphur (S), selenium powder (Se), trioctylphosphine oxide (TOPO), L-cysteine, oleic acid (OA), atrazine standard, (3-mercaptopropyl)trimethoxysilane (MPS), methacrylic acid (MAA), ethylene glycol dimethacrylate (EGDMA), and 2,2'azobisisobutyronitrile (AIBN) standard were purchased from Sigma-Aldrich. Methanol, absolute ethanol, chloroform, acetone, and potassium hydroxide (KOH) were purchased from Associated Chemical Enterprises (ACE). Deionized water was supplied by a Milli-Q water system.

4.5.2 Equipment

Fluorescence emission measurements were recorded on a Horiba Jobin Yvon Fluoromax-4 spectrofluorometer. UV-vis absorption spectra were recorded on a Cary Eclipse (Varian) spectrophotometer. Transmission electron microscopy (TEM) images were taken using a JEOL JEM 2100F operated at 200 kV. Powder XRD patterns were obtained using a Bruker, D2 Phaser, Cu(K α) radiation ($\lambda=1.54184$ Å). FT-IR spectra were measured using a Bruker Alpha-T spectrometer.

4.5.3 Synthesis of CdSeTe/ZnS QDs

The synthesis of CdSeTe/ZnS QDs was carried out based on a reported procedure for the synthesis of core/shell QDs (Adegoke & Forbes, 2015) with some modifications. A schematic illustration of the synthesis process is shown in Fig. 4.11. Briefly, CdO was added into a solution of 50 mL of ODE and 30 mL of OA and the solution was vigorously stirred in a 3-necked flask under argon atmosphere to a temperature of $\sim 260^\circ\text{C}$ in order to form a colourless Cd-OA complex. A pre-mixed TOPTe solution containing 0.48 g of Te and 1.93 g of TOPO in ODE was added into the solution and this was followed swiftly by the addition of a TOPSe solution containing 0.30 g of Se and 1.93 g of TOPO in ODE. Nucleation and growth of the alloyed core QDs was allowed to proceed after which a ZnO solution containing in OA and ODE was injected into the growth solution and this was followed immediately by the addition of the S precursor. The CdSeTe/ZnS QDs were allowed to react for around 40 min with continuous monitoring of the shell growth. Purification of the hydrophobic QDs was carried out using methanol followed by acetone.

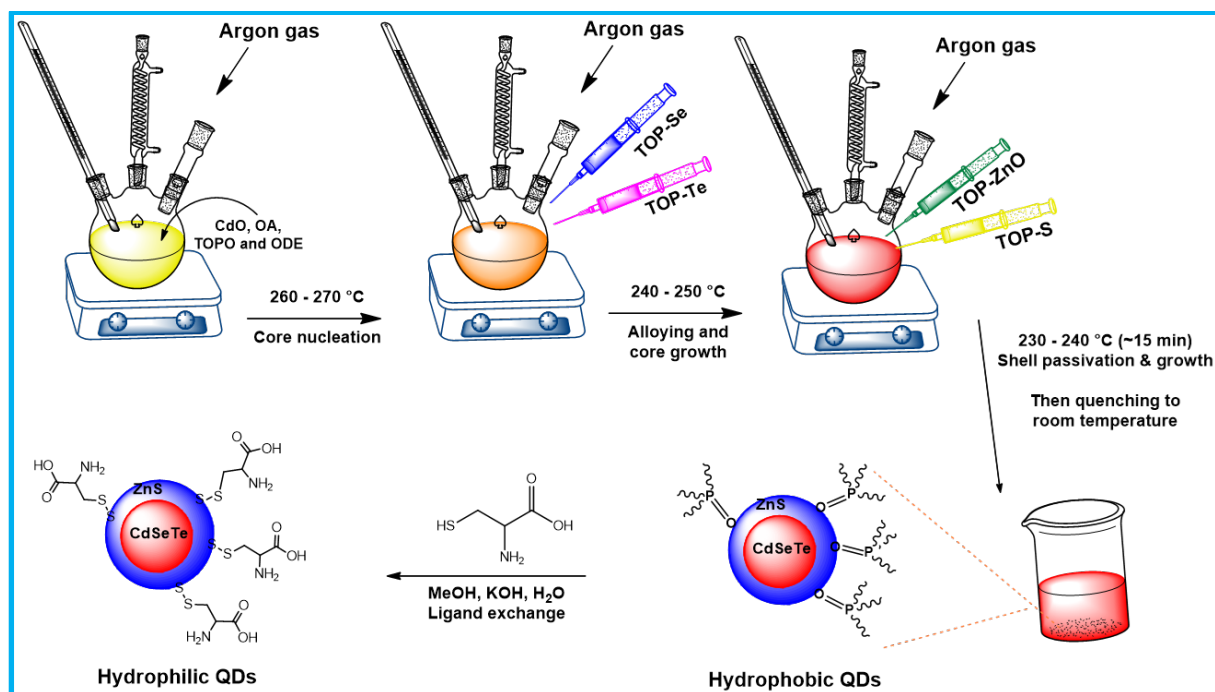


Figure 4.11 Schematic illustration of the synthesis of hydrophobic CdSeTe/ZnS QDs through stepwise hot injection of organometallic precursors. The reaction was continuously purged with argon while monitoring time and temperature. Water soluble QDs were obtained after ligand exchange with L-cysteine.

4.5.4 Functionalisation of CdSeTe/ZnS QDs with MIPs

Firstly, the L-cysteine capped QDs were functionalized with MPS through active condensation of the hydroxyl groups (Bressy *et al.*, 2012) in order to introduce polymerizable vinyl groups on the QD surface. The alkoxy groups in MPS were hydrolyzed due to presence of water in the reaction. This gave rise to silanol groups which then condensed with the OH- groups of L-cysteine on the QD surface. The silanol groups can also condense with one another to form a polymeric siloxane 'shell' around the QDs as shown Fig. 4.12. This results in encapsulation of the QD surface with silica groups and introduces the vinyl groups for polymerization. During the polymerisation step, atrazine was used as a template (2 mg), MAA was the functional monomer and EGDMA was added as a cross-linker. A few drops of AIBN were added to initiate the polymerisation reaction.

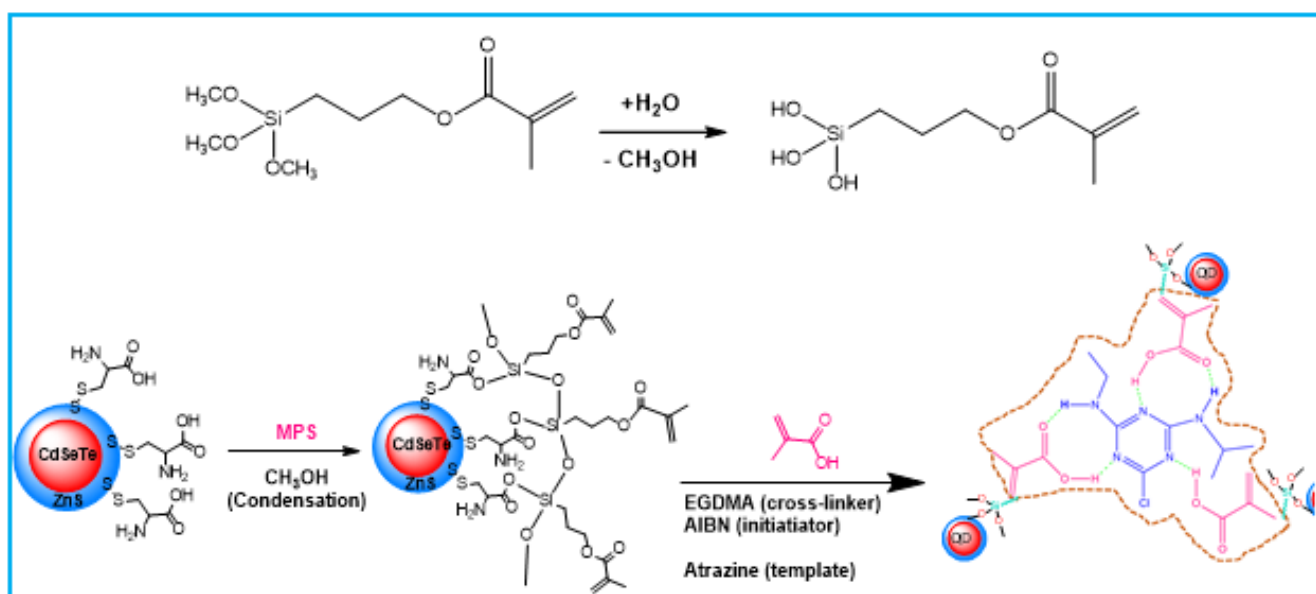


Figure 4.12 Schematic illustration of simultaneous silica encapsulation and vinyl modification of the L-Cys CdSeTe/ZnS QDs.

4.5.5 Procedure for fluorescence sensing of atrazine

The sensor solution was prepared by dissolving the CdSeTe/ZnS@MIP solution in ethanol and sonicating for several minutes to allow dispersion thereof. The concentration of the QD@MIP was optimized by dilution to 0.05 mg L^{-1} to avoid self-quenching during sensing. Also, the pH of the sensing solution was then adjusted to pH 8 using PBS buffer, as this was determined to be the optimum. To $500 \mu\text{L}$ of the buffered sensing solution, $100 \mu\text{L}$ atrazine standard solution ($2\text{-}20 \times 10^{-7} \text{ mol L}^{-1}$) was added and the mixture was incubated for 5 min before taking fluorescence measurements. This was to allow binding of atrazine to the cavities of the polymer. The interaction is mainly through hydrogen bonding with the $-\text{COOH}$ groups of the MAA monomer as shown in Fig. 4.13.

The selectivity of the QD@MIP sensor was investigated using terbuthylazine and simazine. To $500 \mu\text{L}$ (pH 8) of the sensor solution, $100 \mu\text{L}$ of $6 \times 10^{-7} \text{ mol L}^{-1}$ of each compound was added followed by a 5 min incubation time before taking PL measurements.

For all fluorescence measurements, 365 nm excitation wavelength was used and both the excitation and emission slit widths were set to 5 nm. To test the performance of the sensor in real water samples, these were collected from a local tap and from a lake at the University of Pretoria's Sports Campus. After collection the samples were placed in a cooler box and taken for storage in a refrigerator (at 4°C) in our lab. Before analysis, the water was centrifuged at 4000 rpm and filtered to remove excess humic matter and particulate suspensions.

These samples were spiked at three different concentrations (2×10^{-7} , 6×10^{-7} and 12×10^{-7} mol L⁻¹) and then 100 μ L of each spiked sample was mixed with 500 μ L of buffered CdSeTe/ZnS@MIP sensor solution and an incubation period of 5 min was allowed before taking fluorescence measurements.

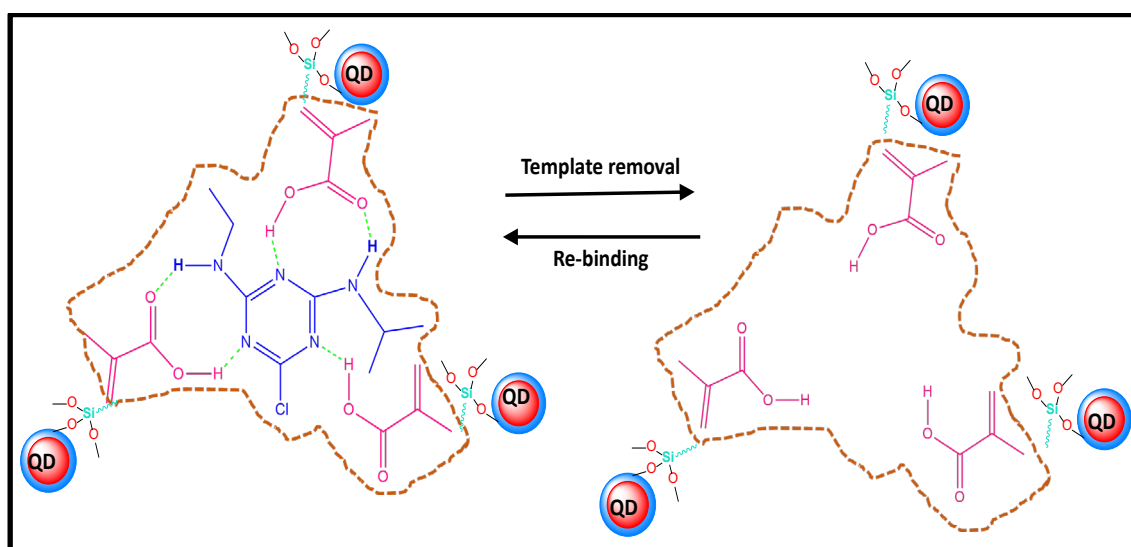


Figure 4.13 Schematic illustration of the binding of atrazine (template) carboxyl groups to MAA through hydrogen bonding (green dotted lines) on the MIP matrix and the specific site cavities left after removal of the template.



Figure 4.14 The theoretical interaction of atrazine with MAA monomers through hydrogen bonding. The numbers are the theoretical hydrogen bond lengths in Å (Han et al., 2017).

4.6 RESULTS AND DISCUSSION

4.6.1 Characterization

4.6.1.1 X-ray diffraction (XRD)

The powder XRD patterns that were obtained (Fig. 4.15) show the typical zinc blende crystal structure for the core and core/shell QDs corresponding to {111}, {220} and {311} planes. These confirm epitaxial growth and formation of the ZnS shell around the CdSeTe core whose crystalline form is retained during the synthesis (Liang *et al.*, 2010). This structure was also observed after functionalization of the QDs with MPS and MIP, thus confirming presence of the QD in the final sensor material (CdSeTe/ZnS@MIP).

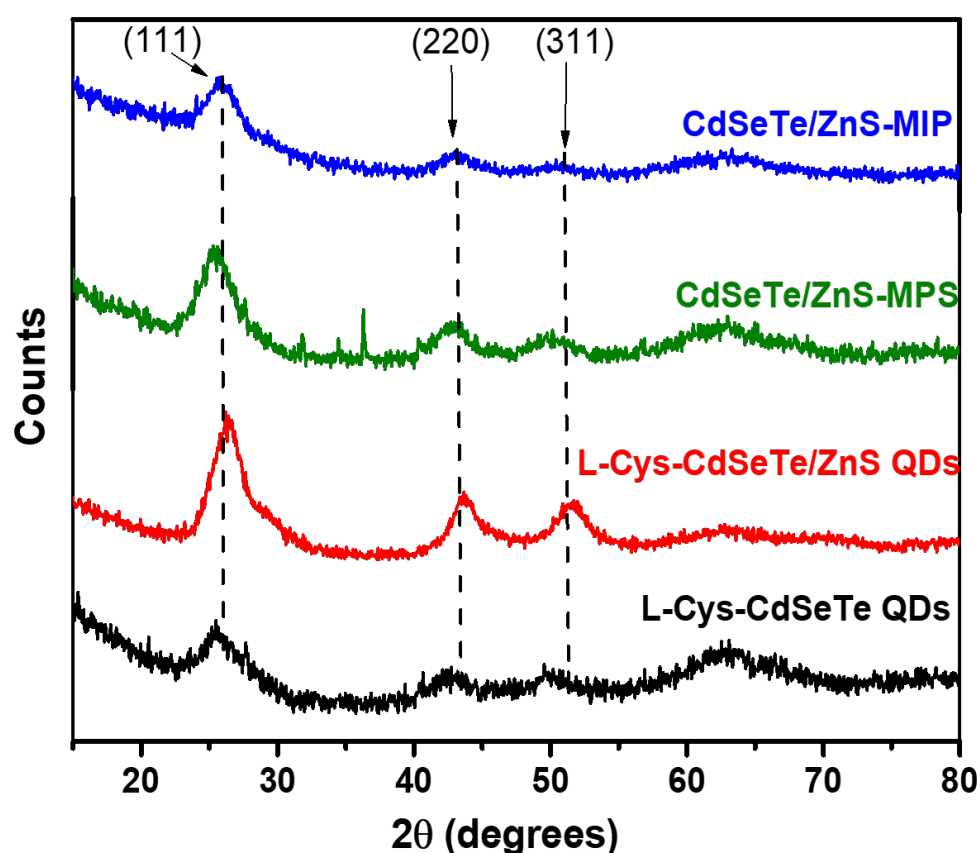


Figure 4.15 Powder X-ray diffraction patterns for CdSeTe QDs, CdSeTe/ZnS QDs, CdSeTe/ZnS-MPS and CdSeTe/ZnS@MIP showing the characteristic zinc blende crystal structure which was retained after polymerization.

4.6.1.2 FT-IR analysis

FTIR spectra were recorded for L-Cys, core and core/shell QDs as shown in Fig. 4.16. The stretching bands for C=O and C-O were observed at 1537 cm^{-1} and 1434 cm^{-1} , respectively. The bands at $2924\text{--}2850\text{ cm}^{-1}$ were attributed to N-H. A broad band at $\sim 3500\text{ cm}^{-1}$ was attributed to O-H stretching.

This FTIR data, together with disappearance of the S-H band at 2077 cm^{-1} indicated successful functionalization of the QD surface. The strong peak at 1094 cm^{-1} in both QD-MPS and QD-MIP is attributed to the polymeric siloxane (Si-O) groups.

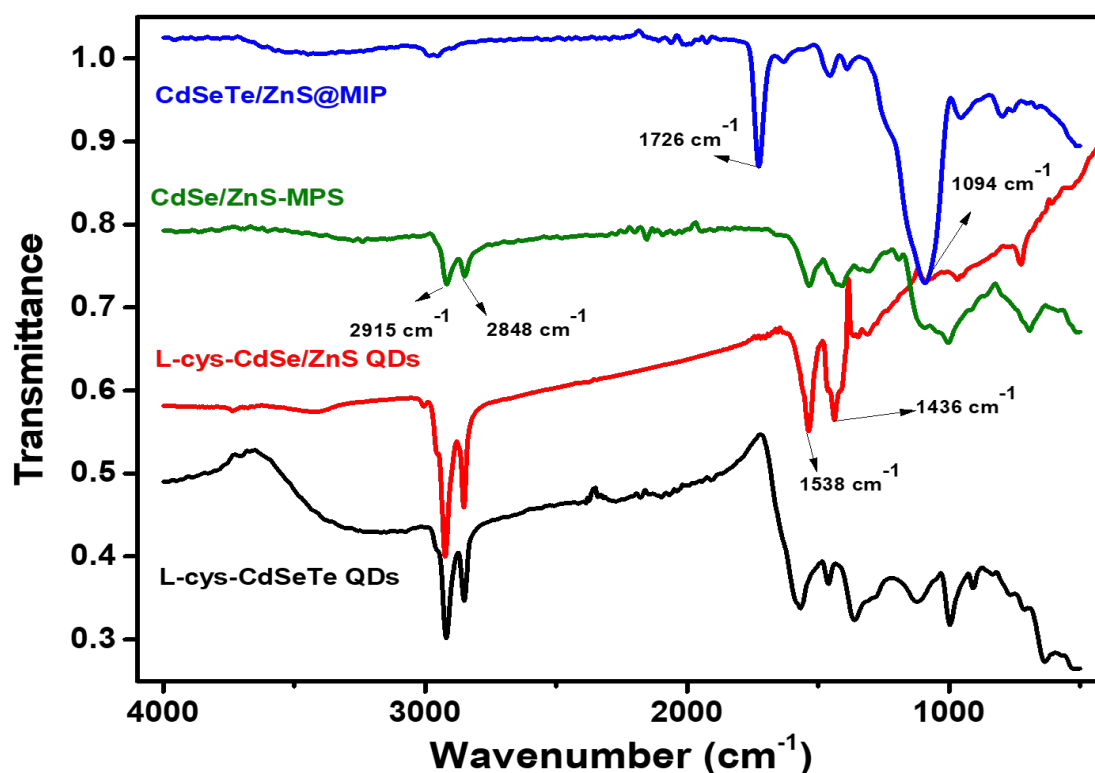


Figure 4.16 FTIR spectra of CdSeTe QDs, CdSeTe/ZnS QDs, CdSeTe/ZnS-MPS and CdSeTe/ZnS@MIP.

4.6.1.3 TEM analysis

TEM analysis was carried out to investigate the particle size and distribution of the different nanoparticles. As shown in Fig. 4.17, the L-Cys-CdSeTe core was mono dispersed in water and had an average particle size of $3.1 \pm 0.1\text{ nm}$, while the L-Cys-CdSeTe/ZnS core/shell QDs had an average size of $5.0 \pm 0.5\text{ nm}$, confirming coating of the core with the ZnS shell. On the other hand, the CdSeTe/ZnS@MIP TEM image (Fig. 4.17 C) showed that the QDs were successfully embedded inside the polymer matrix after functionalisation and the polymer had formed a web-like structure which could be due to the amount of monomer and/or cross-linker that was used.

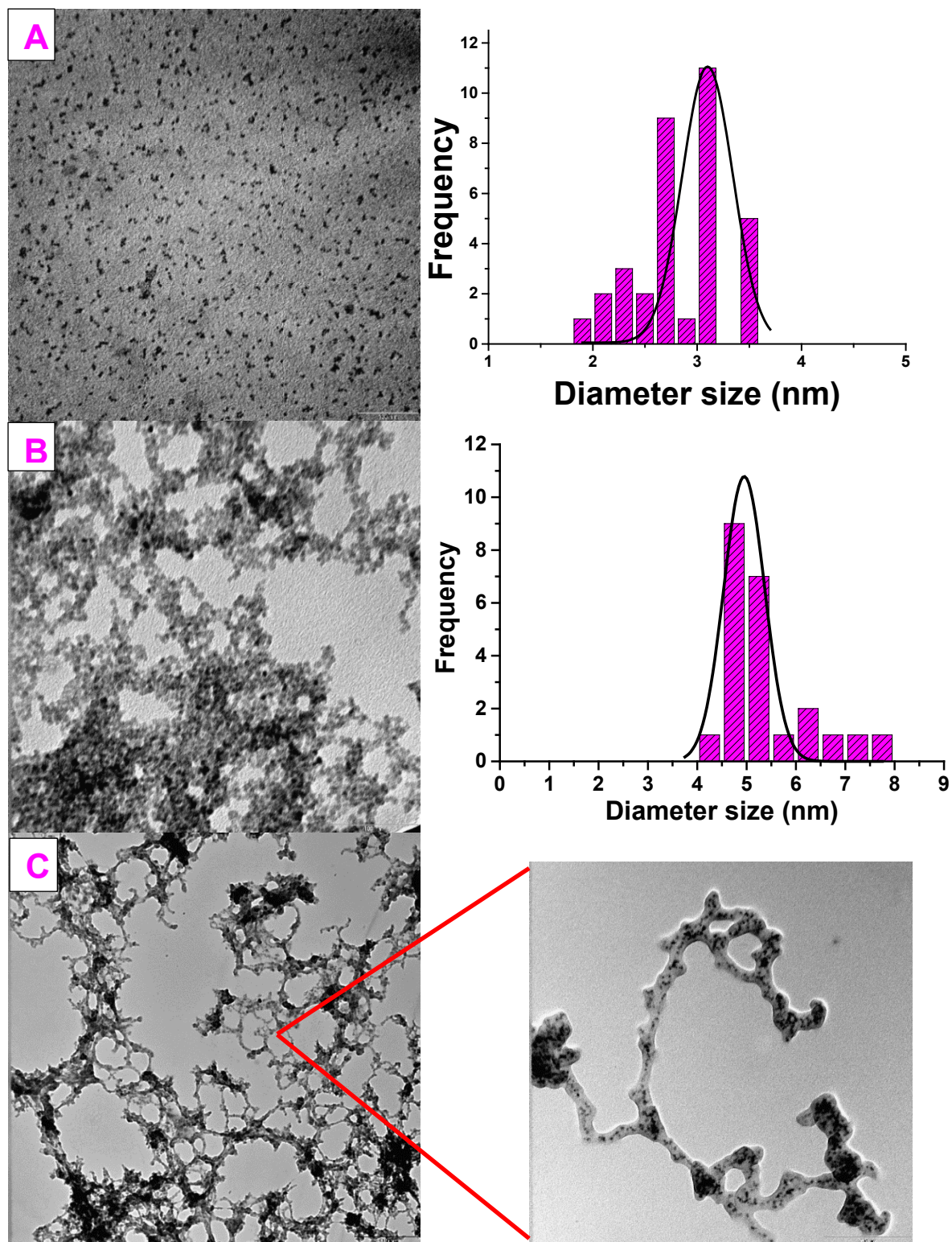


Figure 4.17 TEM images showing spherically shaped CdSeTe (A) and CdSeTe/ZnS (B) QDs dispersed in water. The insets show statistical size distributions with Gaussian fits (black curves). The average particle size (mean \pm HWHM) for the core was 3.1 ± 0.1 nm while the core/shell was 5.0 ± 0.5 nm. Images in (C) show the CdSeTe/ZnS@MIP material with the QDs imbedded inside the polymer's fiber-like network.

4.6.1.4 Optical properties

The normalized fluorescence spectra of core QDs, core/shell QDs and QD@MIP are shown in Fig. 4.18. During the synthesis of the core, it was allowed to grow until the fluorescence maximum was at 575 nm before adding the ZnS which allowed the QD to grow further resulting in a 30 nm red shift in fluorescence emission to 605 nm. It was observed that following the polymerization process, the emission of the QD slightly blue shifted 599 nm. Accordingly, the band gap for the core, core/shell, and QD@MIP were found to be 2.16, 2.05 and 2.07 eV, respectively. The characteristic broad absorption spectrum for each QD material is shown in Fig. 4.19 with the corresponding fluorescence emission spectrum.

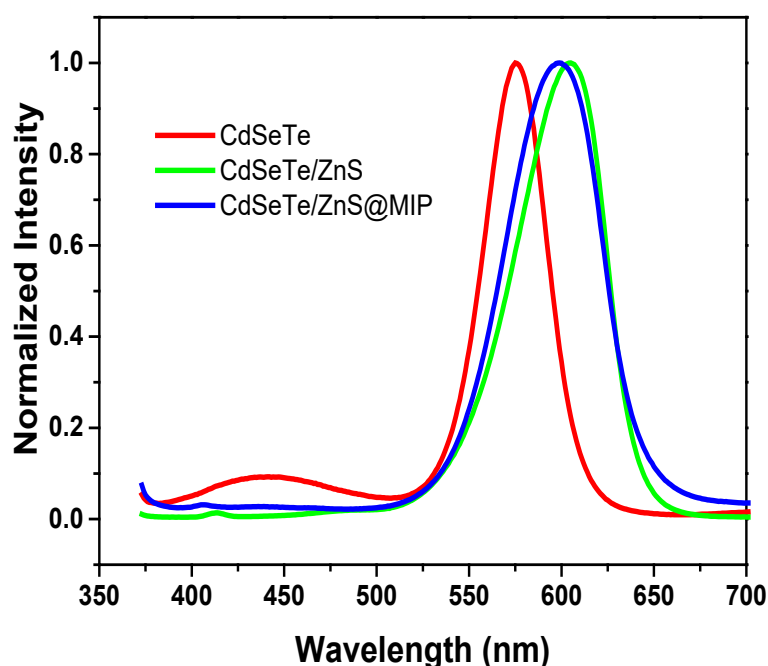


Figure 4.18 Fluorescence emission spectra of CdSeTe QDs at 575 nm, CdSeTe/ZnS QDs at 605 nm, and CdSeTe/ZnS@MIP at 599 nm. The excitation wavelength was 363 nm for all measurements.

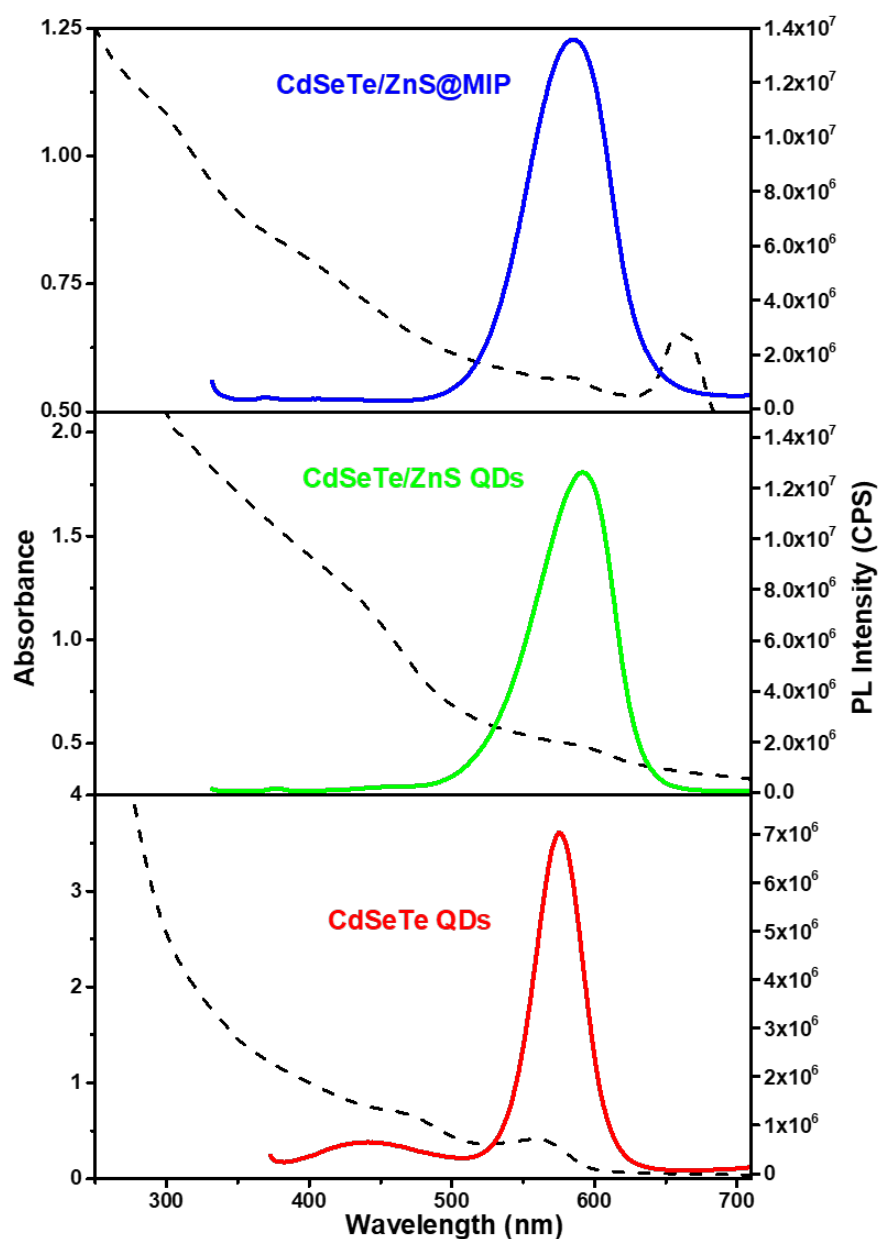


Figure 4.19 Absorption spectra (dotted lines) of CdSeTe QDs, CdSeTe/ZnS QDs and CdSeTe/ZnS@MIP along with corresponding emission spectra.

4.6.1.5 Sensing application

Sensing experiments were conducted for testing the response of the sensor to atrazine (Fig. 4.20). Stock solutions of atrazine were prepared over a range of concentrations from $2\text{--}20 \times 10^{-7} \text{ mol L}^{-1}$. A QD@MIP stock solution was also prepared by dissolving the QDs in water followed by dilution of the solution until the intensity was below $5 \times 10^6 \text{ CPS}$ to avoid saturation of the fluorescence detector. Upon interacting with the MIP, atrazine molecules would bind to the carboxylic groups of the MAA monomers through hydrogen bonding (Han *et al.*, 2017; Lakshmi *et al.*, 2013) resulting in quenching of the fluorescence intensity with increasing atrazine concentration.

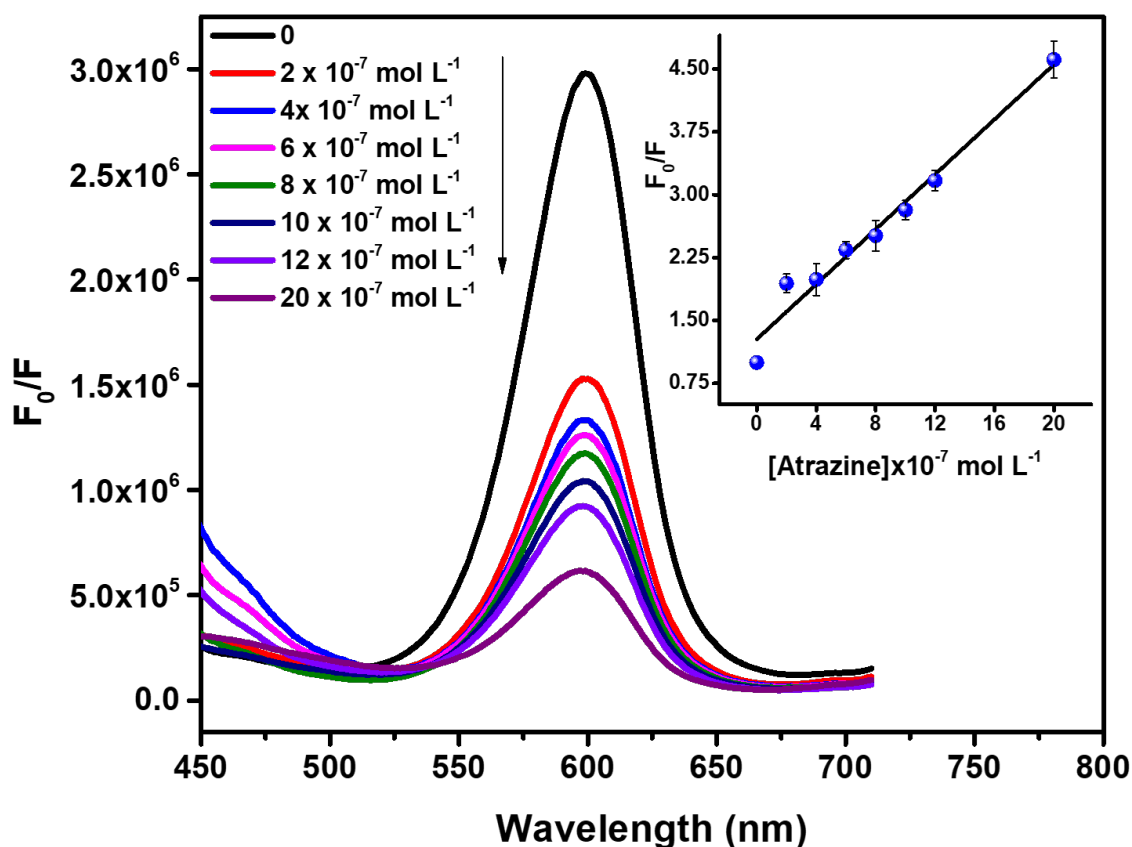


Figure 4.20 The fluorescence spectra of L-Cys-CdSeTe/ZnS@MIP in the presence of varying concentrations of atrazine ($2\text{--}20 \times 10^{-7}$ mol L $^{-1}$). The inset shows the linear response of F_0/F versus atrazine concentration where F_0 is the fluorescence intensity of CdSeTe/ZnS@MIP without atrazine and F is the fluorescence intensity after interaction with atrazine ($n = 3$).

4.6.1.6 Selectivity of the sensor to atrazine

The selectivity of the QD@MIP sensor was investigated using atrazine structural analogues, namely terbutylazine and simazine. These herbicides have similar uses to atrazine and therefore it is not uncommon that they occur simultaneously with atrazine in water systems. To 500 μL (pH 8) of the sensor solution, 100 μL of 6×10^{-7} mol L $^{-1}$ of each compound was added followed by a 5 min incubation time before taking PL measurements. As can be seen in **Figure 4.21**, the fluorescence intensity was quenched more in the case of atrazine than for terbutylazine and simazine, respectively

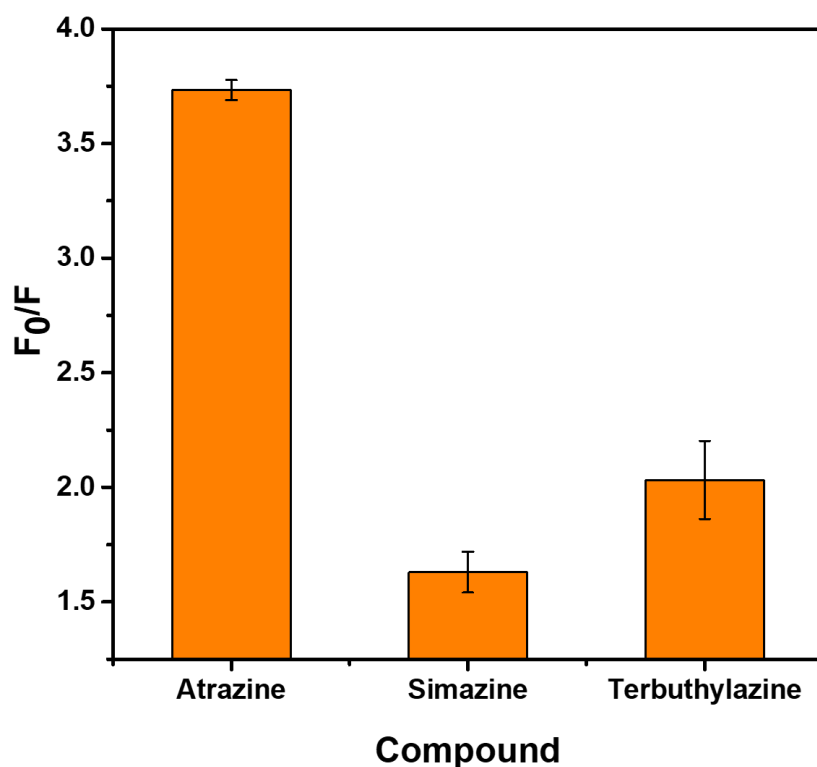


Figure 4.21 Quenching effects of atrazine, simazine and terbuthylazine on CdSeTe/ZnS@MIP sensor solution. 100 μL of $6 \times 10^{-7} \text{ mol L}^{-1}$ for each compound was used ($n = 3$).

4.6.1.7 Practical application

Water samples were collected from a local tap and from a lake at the University of Pretoria's Sports Campus. These samples were spiked at three different concentrations along the calibration curve and each concentration was analyzed, where 100 μL of the spiked sample was mixed with 500 μL of buffered CdSeTe/ZnS@MIP sensor solution and an incubation period of 5 min was allowed before taking fluorescence measurements. Table 4.2 shows the recoveries and these were found to be satisfactory ranging from 92-118%, showing that the performance of the sensor was not greatly affected by compounds which could be present in environmental water.

Table 4.2 Recovery test of atrazine spiked in tap water and lake water at three different concentrations (n = 3)

Water sample	Spiked atrazine (mol L ⁻¹)	Detected atrazine (mean ± RSD; n = 3, mol L ⁻¹)	Recovery (%)
Tap water	2 × 10 ⁻⁷	2.4 ± 0.2	119
	6 × 10 ⁻⁷	6.1 ± 0.1	101
	12 × 10 ⁻⁷	11.0 ± 0.04	92
Lake water	2 × 10 ⁻⁷	2.2 ± 0.1	111
	6 × 10 ⁻⁷	6.2 ± 0.2	103
	12 × 10 ⁻⁷	11.6 ± 0.2	97

The performance of the sensor was then compared to other atrazine sensors as shown in Table 4.3. It is important to note that these sensors are not based on quantum dot materials and some are not based on the fluorescence detection technique. Despite these differences, the CdSeTe/ZnS@MIP sensor still has a relatively low detection limit.

Table 4.3 Comparison of the performance of the CdSeTe/ZnS@MIP sensor with other sensors for atrazine detection.

Sensor material	Detection method	Matrix	Linear range (mol L ⁻¹)	LOD (mol L ⁻¹)	Reference
MICP on Pt electrode	CV	–	10 ⁻⁹ -1.5 × 10 ⁻²	1.0 × 10 ⁻⁶	Pardieu <i>et al.</i> (2009)
MIP film using o-PD	DPV	–	0.05-1.4 × 10 ⁻⁷	0.001 × 10 ⁻⁶	Li <i>et al.</i> (2015)
Ag/AgCl electrode @MIP	CV	–	1-10 × 10 ⁻⁶	–	Shoji <i>et al.</i> (2003)
Pt NPs/C ₃ N ₄ NTs	SWV	–	10 ⁻¹² -10 ⁻¹⁰	0.15 × 10 ⁻¹²	Liu <i>et al.</i> , (2016)
Fe ₃ O ₄ -Chitosan@MIP	Fluorescence	Water	2.32-185.4 × 10 ⁻⁶	0.86 × 10 ⁻⁶	Liu <i>et al.</i> (2016)
SiO ₂ @Zn protoporphyrin – MIP (core-shell)	Fluorescence	DI water & Lake water	0-1 × 10 ⁻⁴	1.8 × 10 ⁻⁶	Liu <i>et al.</i> (2011)
CdSeTe/ZnS@MIP	Fluorescence	Water	2-20 × 10 ⁻⁷	0.80 × 10 ⁻⁷	This work

4.7 CONCLUSION

MIPs were successfully used to functionalise QDs in this study, which combined the sensitivity of QD fluorescence sensors with the selectivity of MIPs. The resulting novel materials were applied towards the sensing of two emerging chemical pollutants (ECPs), namely acetaminophen (a pharmaceutical) and atrazine (a pesticide) in water.

The nano-molar level fluorescence detection of acetaminophen was achieved with the utilization of L-Cys-CdSe/ZnS QDs embedded in a MIP, likely via a charge transfer induced fluorescence quenching process from MIP@QDs to AC. The structures of QDs, MIP@QDs and NIP@QDs were characterized by fluorescence spectroscopy, FTIR and TEM. Quenching of the photoluminescence of the synthesized MIP@QDs enabled the determination of AC at concentrations as low as 0.34 nmol L^{-1} & over the linear concentration range of $1.0\text{-}300 \text{ nmol L}^{-1}$. The prepared MIP@QDs were highly selective to AC with outstanding reproducibility (3.7%). The simple and economical preparation of the MIP@QDs, good photostability as well as selectivity towards AC, allowed for this novel sensor material to be successfully applied in the analysis of nanomolar concentrations of AC in water samples with recoveries of 95% to 114%.

The development of alternative methods for detection of atrazine is also necessary due to the cost of sample analysis by conventional chromatographic methods. Here we reported on a CdSeTe/ZnS@MIP fluorescence sensor which was synthesized and characterized using various techniques to confirm functionalization of the QDs with the MIP polymer. Application of the sensor towards atrazine detection showed a linear response (fluorescence quenching) with increasing atrazine concentration in the range from $2\text{-}20 \times 10^{-7} \text{ mol L}^{-1}$. The performance of the sensor compared to other methods showed that the sensitivity needs to be improved in order to lower the detection limit ($0.80 \times 10^{-7} \text{ mol L}^{-1}$). A low detection limit is crucial for atrazine monitoring in environmental water samples, where the concentrations can be as low as 0.01 to $0.19 \mu\text{g L}^{-1}$ (Patterton, 2013). The World Health Organization (WHO) guideline limit for atrazine in water is 0.1 mg L^{-1} ($4.6 \times 10^{-7} \text{ mol L}^{-1}$) hence the sensor has potential in regulatory applications. The performance was further tested in tap and lake water samples and showed satisfactory recoveries ranging between 92-118%.

CHAPTER 5: THE IMMOBILIZATION OF QUANTUM DOTS

5.1 INTRODUCTION

Quantum dots have been applied in a range of real devices such as sensors (Biju *et al.*, 2005; Wuister, de Mello Donegá, & Meijerink, 2004), light emitting diodes (Coe, Woo, Bawendi, & Bulović, 2002) and photovoltaic cells (Bruchez, Moronne, Gin, Weiss, & Alivisatos, 1998). In order to have a high-density homogeneous distribution of QDs compatible for real device use, the QDs should be supported in host matrices. Although this leads to some degree of quenching of the photoluminescence quantum yield, it is of great importance to select a host matrix which provides an intact band gap of the QDs and photoluminescence efficiency (Selmarten *et al.*, 2005).

The development of luminescence based sensing devices ideally requires immobilization of the sensing indicators, in this case the quantum dots, onto or into solid supports to form active solids for working in flowing solutions and allowing for re-use. Forming such active materials also brings the advantage of reducing the potential for leaching of the QDs into the solution while equilibrium with the target analyte is being established. The immobilization process, however, may reduce the luminescence efficiencies of the QDs due to aggregation, oxidation and poor adhesion on the support material. The challenge therefore, is to retain the properties of the QDs after the immobilization process.

Different polymers and strategies have been utilized for the preparation of supporting host matrices for QDs including covalent and non-covalent conjugation of QDs to polymers (Zhang *et al.*, 2005; Zucolotto *et al.*, 2005) and simple mixing of QDs and polymers (Choudhury, Sahoo, Ohulchanskyy, & Prasad, 2005; Qi, Fischbein, Drndić, & Šelmić, 2005). Covalent conjugation of QDs to host materials is preferable so as to reduce the phase segregation of QDs. QDs which are directly mixed with polymers (epoxy or silicone matrices), typically form large agglomerates which constrains their application. For example, it decreases the power efficiency of QD based LEDs (Wang, Li, & Sun, 2011).

Poly(dimethylsiloxane) (PDMS) provides advantages compared to poly(vinyl pyrrolidone) (PVP) such as optical transparency, electrical and thermal insulation, easy molding into various structural forms, structural flexibility when molded, and efficient covalent conjugation to silanes which can bridge other molecules/systems to PDMS. More importantly, PL properties of QDs remain intact in the presence of PDMS (Hammond, 1999; McDonald & Whitesides, 2002).

Tao *et al.* (2013) used a silicone matrix to prepare highly transparent luminescent CdSe-silicone nanocomposites. In comparison with epoxies, silicones as encapsulant materials provide better thermo-mechanical stabilities for high brightness LEDs. In 2012, researchers modified poly(acrylic acid) (PAA) with both N-octylamine and 5-amino-1-pentanol to make a covalent conjugation with CdSe/ZnS nanocrystals (NCs). They then used NC encapsulated with the modified PAA for sensing of rhodamine

isothiocyanate. This strategy not only provided water solubilization but also functionalization of the NCs (Somers, Snee, Bawendi, & Nocera, 2012).

Here we focus on PDMS because of its advantages which include low cost, low toxicity, flexibility, as well as its ability to absorb organic non-polar analytes. We therefore sought to fabricate thin films of PDMS embedded with QDs and to study the properties of the resulting PDMS-QD material with the intention to use it to detect emerging chemical pollutant (ECP) compounds in future work.

5.2 PREPARATION OF QUANTUM DOT PDMS FILMS

5.2.1 Chemicals and equipment

Poly(acrylic) acid solution (25% from Polysciences, Inc), and Sylgard™ 184 silicone elastomer kit (Dow™) consisting of base and curing agent were used for thin film manufacture using a Laurell WS-650MZ-23NPPB spin coater from Laurell Technologies Corporation (USA). All chemicals, consumables and the spin coater were supplied by Black Hole Labs (Paris, France). QDs synthesized using methods reported in previous chapters, specifically CdSeTe/ZnS and graphene QDs, were immobilized in the thin films.

5.2.2 Preparation of PDMS@QD films

The procedure for preparing the PDMS@QD thin films by spin coating is shown in Fig. 5.1. 20.6 g of PDMS was mixed with 2.0 g of curing agent by stirring to form a ~ 10:1 elastomer. To this mixture, 0.041 g mL⁻¹ of CdSeTe/ZnS (0.0123 g dissolved in 3 mL chloroform) was added and mixed with a glass stirring rod. The air bubbles in the resulting mixture were removed by placing the mixture under vacuum for ~30 min.

A 4 inch silicon wafer substrate was prepared and cleaned with acetone and isopropanol followed by drying with compressed air. Then, 6 mL of diluted PAA (12.5%) was placed on the whole of the wafer and spun at 300 rpm for 15 s (acceleration of 1000 rpm/s).

The resulting PAA film was heated on a hot plate at 150°C for 1 min and then cooled to room temperature. 5 mL of the degassed QD@PDMS mixture was placed at the center of the PAA coated wafer and spin coated firstly at 500 rpm (300 rpm/s for 10 s) to disperse it on the wafer, then at 1200 rpm for 5 min to form a thin membrane on the wafer. The resulting PDMS membrane was heated at 150°C on a hot plate to complete the polymerization before cooling to room temperature. The edges were scraped with a scalpel to provide an opening for water to dissolve the PAA film. The membrane was then left overnight in water to completely dissolve the PAA sacrificial layer and to lift off the PDMS film from the substrate. The resulting fluorescent film was viewed under UV-light and the fluorescence properties were observed using a spectrofluorometer after transferring a portion of the film onto a glass microscope slide.

Similarly, a PDMS@GQDs film was prepared using GQDs synthesized from citric acid precursor. After dispersion of the GQDs in the PDMS base and curing agent mix, the mixture was spun on the substrate to form a blue fluorescent film.

5.2.3 Sensing of atrazine using the PDMS@QDs thin film

A small piece of the PDMS@QDs thin film (prepared using CdSeTe/ZnS QDs) was cut and was placed on a glass microscope slide. Initial fluorescence measurements were taken using the fluorescence spectrometer. The thin film was then immersed in a 1.5×10^{-5} mol L⁻¹ standard solution of atrazine for 15 min before fluorescence measurements were repeated.

5.3 RESULTS AND DISCUSSION

5.3.1 Previous work

In our previous study, PDMS@QD films were produced by spin coating on microscope glass slides, using a spin coater from another department at the University of Pretoria. The PL peaks were, however, very broad and had greatly reduced intensities compared to the pure QDs in solution. The dispersion of the QDs in the polymer matrix was very poor and the concentration of the QDs on the matrix was too low. Thus optimization of these parameters was needed. In addition, means to better remove small bubbles in the films and to produce a more homogeneous thin film of constant thickness required investigation.

We therefore purchased a spin coater assembly which has the necessary components to effectively and efficiently prepare thin films, including a de-gassing setup to prevent air bubble defects. This turnkey complete spin coater assembly consists of the spin coater, vacuum pump, degassing assembly, chemicals and consumables. Unfortunately the first spin coater which was delivered was found to be faulty after much trouble shooting, which delayed progress initially. The supplier subsequently sent a new spin coater, which was successfully commissioned and allowed for the preparation of excellent quality thin films in which QDs were homogeneously embedded.

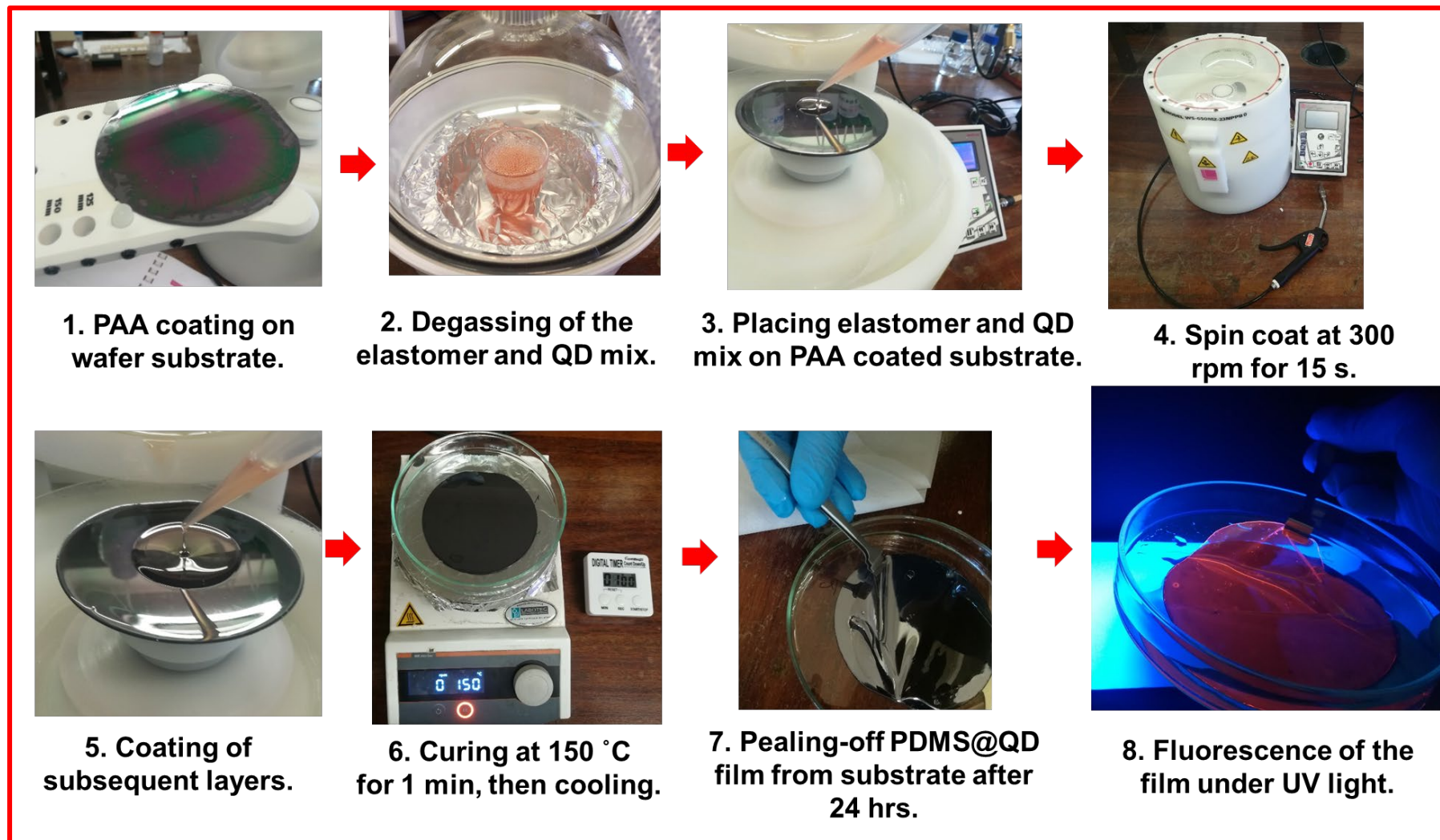


Figure 5.1 Preparation of a fluorescent PDMS@CdSeTe/ZnS QD thin film by means of spin coating (PAA: poly(acrylic) acid).

5.3.2 Optical properties of the PDMS@QD films

To study the fluorescence properties of the PDMS@QD film, a small piece was cut and placed on a glass microscope slide before being analyzed by fluorescence spectrometry using a solid sample holder. The fluorescence spectrum of the PDMS@QD film is shown in Fig. 5.2 and is compared with that of the CdSeTe/ZnS QDs in solution. It was observed from the normalized spectra that the strong emission peak of CdSeTe/ZnS QDs at 580 nm was slightly redshifted (to 594 nm) upon incorporating them onto the PDMS. This could be due to the passivating effect that the PDMS has on the QDs thus affecting their surface states. The PDMS@QDs films had a strong fluorescence as seen visually when illuminating the film under UV light (Fig. 5.3 & 5.4) where red fluorescence was evident for the PDMS@CdSeTe/ZnS film and blue fluorescence was seen from the PDMS@GQD film. This indicates their potential use in portable, re-usable sensor devices for target analytes, where different fluorescence emission wavelengths are required.

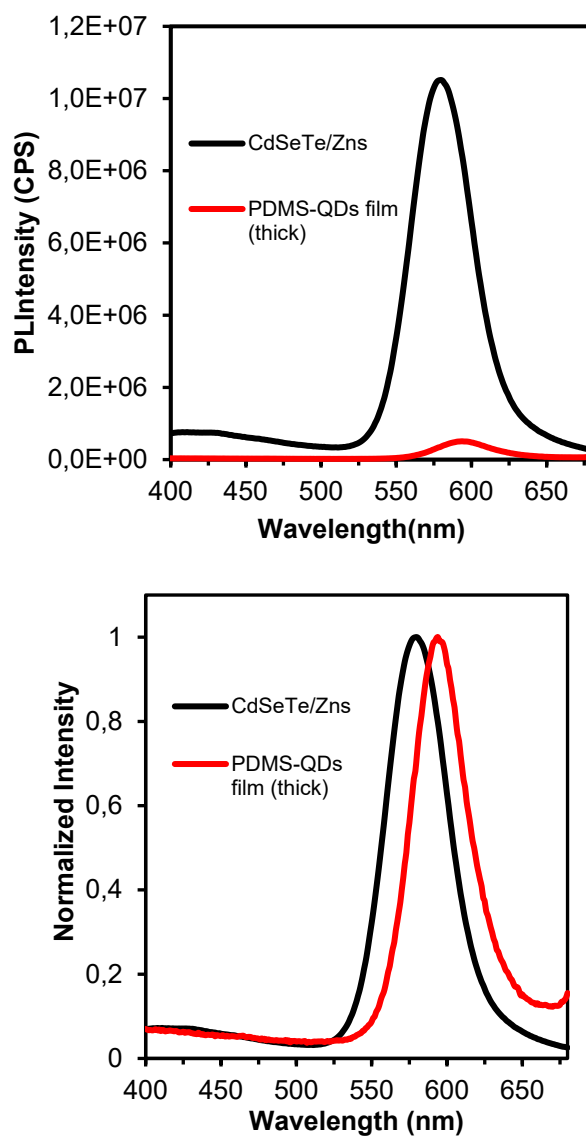


Figure 5.2 Fluorescence emission spectra of CdSeTe/ZnS QDs in chloroform and PDMS@QDs films. (Excitation wavelength = 350 nm, emission and excitation slit widths = 5 nm).

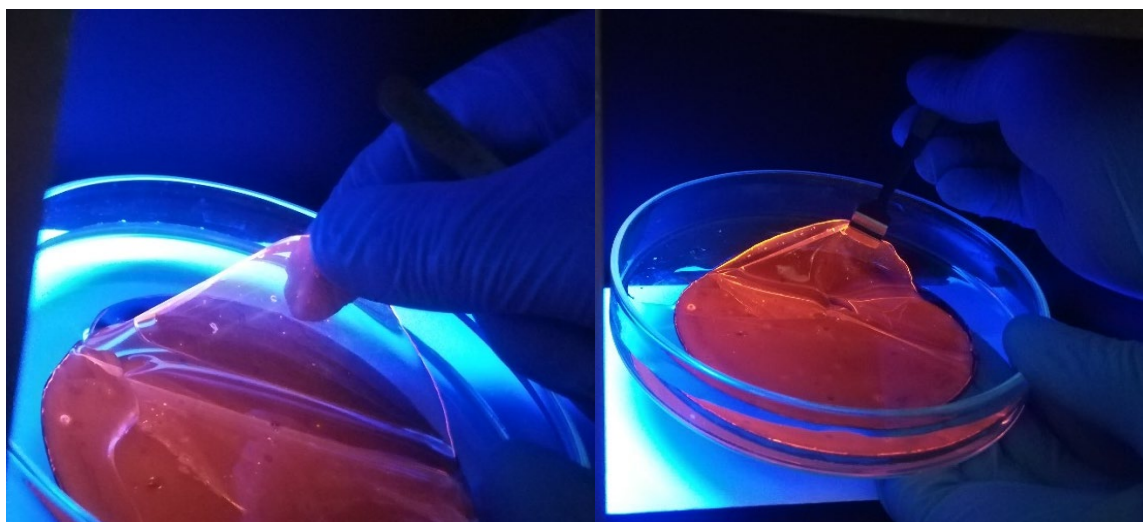


Figure 5.3 Images of PDMS@CdSeTe/ZnS film viewed under UV-light.

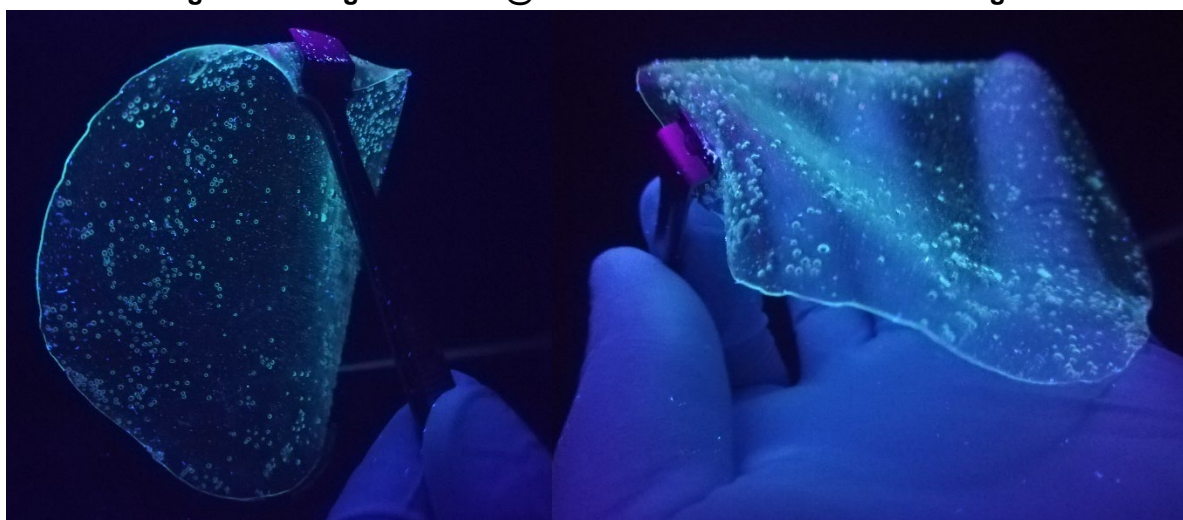


Figure 5.4 Images of PDMS@GQDs film viewed under UV-light.

5.3.3 Application of PDMS@QD thin films for atrazine sensing

The ability of the prepared PDMS@QD (using CdSeTe/ZnS QDs) thin film to detect one of the target compounds, namely atrazine, was tested. As shown in Fig. 5.5, a small piece of the PDMS@QDs thin film was placed on a glass microscope slide and initial fluorescence measurements were taken. The same piece of thin film was then immersed in 1.5×10^{-5} mol L⁻¹ atrazine a solution for 15 min before repeating the fluorescence measurements. This initial test experiment showed that the interaction of the PDMS@QDs with atrazine led to an increase in fluorescence intensity (Fig. 5.6). Future work will investigate the mechanism of this interaction as well as the effects of potential interfering ECP compounds.

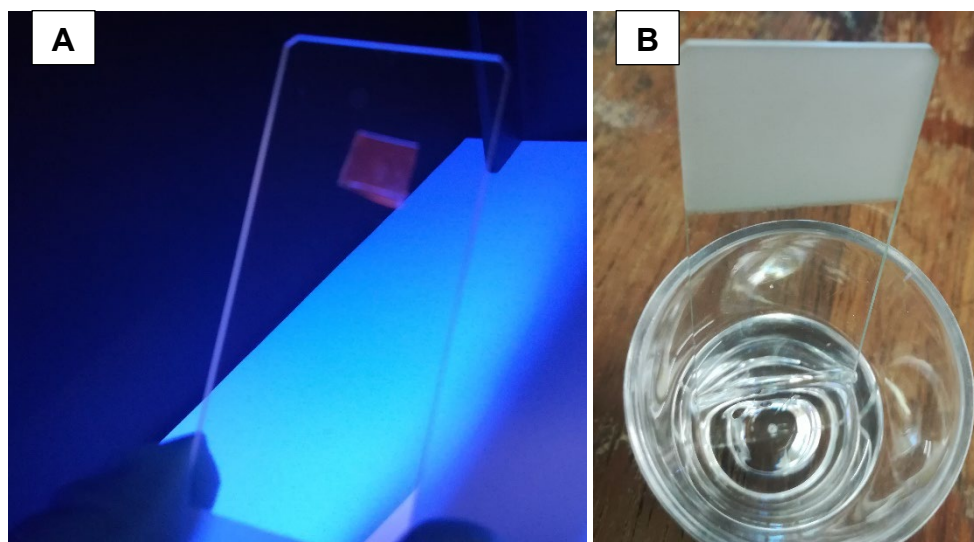


Figure 5.5 (A) Small piece of PDMS@QDs placed on a glass slide for sensing (viewed under UV light). (B) Sensing test where the glass slide with PDMS@QDs was placed in $1.5 \times 10^{-5} \text{ mol L}^{-1}$ atrazine solution before repeating PL measurements.

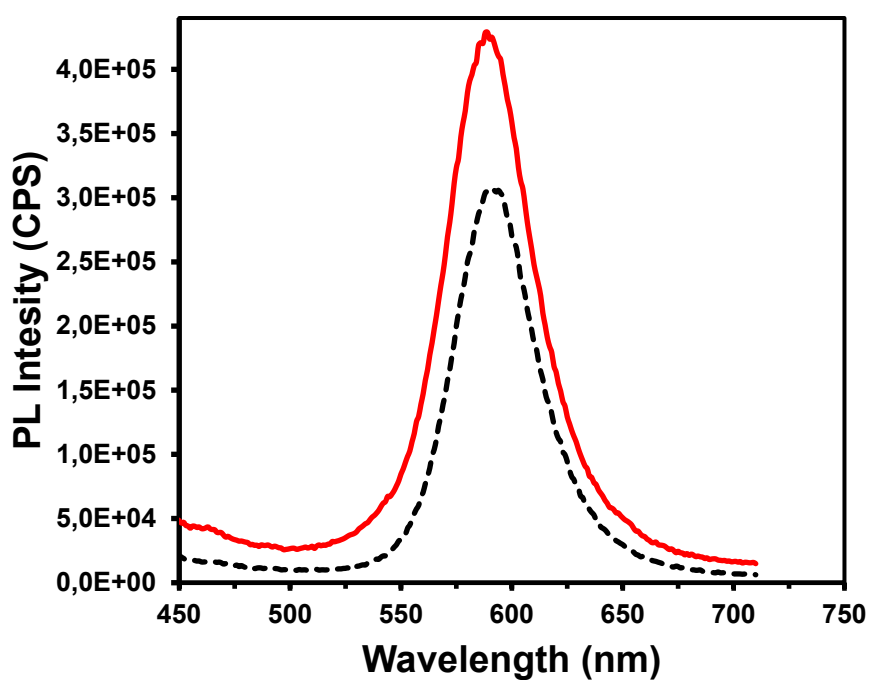


Figure 5.6 Fluorescence spectra showing the response of the PDMS@QD sensor to $1.5 \times 10^{-7} \text{ mol L}^{-1}$ of atrazine (black dashed line before exposure and red line after exposure to atrazine).

5.4 CONCLUSION

PDMS has been successfully used for the immobilization of QDs to produce thin fluorescent films. As proof of concept, CdSeTe/ZnS QDs and graphene quantum dots (GQDs) were incorporated into the PDMS through spin coating and red and blue fluorescent films were thus obtained. The CdSeTe/ZnS@PDMS thin film was tested for atrazine detection and an enhanced fluorescence signal was found. These fluorescent films hold great potential in designing reusable rapid field monitoring sensors for targeted ECP compounds in water systems. The sensitivity and stability of QDs combined with the inertness, flexibility, and ability of PDMS to pre-concentrate analytes will open doors for designing sensitive and robust fluorescence sensors for routine monitoring of ECPs.

CHAPTER 6: CONCLUSIONS & RECOMMENDATIONS

6.1 CONCLUSIONS

The reviewed literature showed that the target compounds included in this study (namely triclosan, acetaminophen, PAHs and atrazine) are constantly being released into the environment from various sources, mainly through human activities. A number of studies have also demonstrated that these substances have potential negative effects on the health of aquatic organisms and humans. Exposure to some of these compounds has been shown to disrupt reproductive cycles in some animals and has also been linked to carcinogenic effects. This, therefore, shows the importance of continuous monitoring and regulation of these compounds in the environment, including water resources, especially in water scarce countries such as South Africa.

Triclosan (TCS) is a biocide which is routinely added to a wide range of personal care, veterinary, industrial and household products. It can persist in the environment and shows toxicity towards various organisms. The continuous exposure of aquatic organisms to TCS and its bioaccumulation potential have led to detectable levels of this biocide in a wide array of aquatic species. Mammalian systemic toxicity studies have shown that TCS is neither acutely toxic, mutagenic, carcinogenic, nor a developmental toxicant, while endocrine disruption related to thyroid hormone homeostasis disruption and possibly the reproductive axis has been noted. Moreover, there is strong evidence that aquatic species such as algae, invertebrates and certain types of fish are much more sensitive to TCS than mammals. Specifically, algae is highly sensitive indicator organism that may be impacted by TCS occurrences in surface waters at levels of 200-2,800 ng L⁻¹, where the worldwide concentration has been found to range from 1.4-40,000 ng L⁻¹. The Minnesota Department of Health (MDH) has developed a guidance value of 50 ppb (50,000 ng L⁻¹) for triclosan in drinking water, whilst the Canadian Federal Water Quality Guideline (FWQG) for the protection of aquatic life from adverse effects of triclosan is 380 ng L⁻¹.

Acetaminophen (AC), or paracetamol, is an over-the-counter analgesic. Although acetaminophen is removed from wastewater by chemical oxidation processes, it has been detected in surface waters, wastewater and drinking water throughout the world. Concentrations of acetaminophen in surface water of over 10,000 ng L⁻¹ have been reported, including in Kenya and South Africa (107,000 ng L⁻¹ and 59,000 ng L⁻¹, respectively) which are higher than the predicted no-effect concentration (PNEC) of 9200 ng L⁻¹. Hence, AC might represent a threat to non-target organisms. A guidance value of 200 ppb (200,000 ng L⁻¹) for acetaminophen in drinking water has been set by the MDH.

PAHs are known to have generally low solubility in water hence they are typically found at very low concentrations in this medium, although they are ubiquitous environmental pollutants arising from combustion processes. Local studies have shown that PAHs occur in water systems at mean concentrations ranging from 0.035-532 $\mu\text{g L}^{-1}$. However, even at these low concentrations they are of concern, as some PAH compounds like benzo[a]pyrene have been shown to have LC50 of around 4 $\mu\text{g L}^{-1}$ towards cladoceran species. The reviewed literature shows that PAH exposure can lead to various toxicities leading to negative effects on some aquatic organisms.

The target pesticide, atrazine, is a commonly used herbicide that has been frequently detected in local water systems. The typical concentration that has been previously reported in WRC studies for this compound ranges from 0.01-0.19 $\mu\text{g L}^{-1}$. In this context, it is important to note that the World Health Organization (WHO) has set the guideline limit for atrazine in drinking water to 0.1 mg L^{-1} and the reported concentrations are well below this limit. However, it is also important to note that some studies have reported carcinogenic effects at much lower concentrations of 50-649 ng L^{-1} . Other negative toxicological effects that atrazine can cause to aquatic organisms have also been highlighted in the literature, making it a contaminant of environmental concern.

It needs to be remembered that ecotoxicity testing of compounds merely provides indications of acute effects *in vivo* in specific organisms of different trophic levels after short-term exposure, and only rarely after long-term (chronic) exposures. The results may thus not accurately reflect potential environmental toxic effects induced by long-term exposure to low levels of these pollutants. Moreover, in water systems a mixture of compounds is invariably present, therefore the risk of additive and synergistic toxic effects cannot be ignored. Local hotspots of elevated concentrations of contaminants near sources may also occur, which are outside the ranges of expected environmental levels reported in the literature. It is therefore important to monitor the levels of the target compounds in South African water systems as widely as possible in order to effectively and proactively manage our resources and to minimize potential negative toxicological effects.

Water soluble L-Cys functionalized CdSe/ZnS QDs were successfully synthesised and employed as a fluorescence sensor for the determination of acetaminophen in water samples. The operating mechanism of the designed probes was based on the fluorescence “turn-on” mode. Under optimum conditions, with the addition of acetaminophen to QDs in aqueous solution, the original PL intensity of the QDs was enhanced most likely due to fluorescence resonance energy transfer from analytes to QDs which was found to be linear within the concentration range of 3.0-100 nmol L^{-1} AC with a detection limit of 1.6 nmol L^{-1} . The method could therefore be applied to detect AC at nanomolar levels, which is environmentally relevant. Other advantages of this method include its simplicity, as well as stability and resistivity of QDs against photobleaching under ambient light conditions. The application of the sensor

to additionally related pharmaceuticals (such as ketoprofen, sulfamethoxazole, L-tryptophan, estradiol, L-Dopa and diclofenac sodium salt) may also be possible.

We also designed and synthesized core-shell structured GSH-CdSe/ZnS QDs via a one pot organometallic synthesis method. Transmission electron microscopy images, FTIR spectra and fluorescence spectra confirmed the successful synthesis of QDs and the formation of a GSH coating thereon. The fluorescence of QDs was effectively enhanced by TCS at an emission wavelength of 598 nm over the concentration range of 10-300 nmol L⁻¹ with a detection limit of 3.7 nmol L⁻¹ which confirmed the applicability of the method to detect TCS at nanomolar levels. The turn-on mechanism of the sensing process is likely associated with energy transfer from TCS to the QDs. The good response of this probe to TCS facilitates its application in the detection and determination of TCS in real water samples in the field of environmental monitoring.

Fluorescence sensor materials for detection of phenanthrene (GQDs) and atrazine (L-Cys-CdSeTe/ZnS QDs) were synthesized and initial tests were carried out to test their performance. Some of the important parameters that are crucial for the performance of the sensors were investigated and optimized. A low concentration of the sensor solution of 0.5 mg L⁻¹ was used and appears to give a good response to the target analytes. The interaction time (incubation time) between sensor solutions and target analytes was also investigated and 5 min was found to be sufficient for both atrazine and phenanthrene as a representative PAH compound, respectively. This short interaction time is ideal for application of the sensor in cases where there are a large number of samples for analysis. Upon interaction of the CdSeTe/ZnS QD sensor with atrazine, the fluorescence was quenched linearly within the 2-10 × 10⁻⁷ mol L⁻¹ range and the LOD was determined to be 1.8 × 10⁻⁷ mol L⁻¹. The GQDs were able to interact with PAHs through π-π interaction and for phenanthrene the sensor showed a linear response over 1-5 × 10⁻⁷ mol L⁻¹ and the LOD was found to be 2.5 × 10⁻⁸ mol L⁻¹.

MIPs were successfully used to functionalise QDs in this study, which combined the sensitivity of QD fluorescence sensors with the selectivity of MIPs. The resulting novel materials were applied towards the sensing of two emerging chemical pollutants, namely acetaminophen and atrazine in water.

The nano-molar level fluorescence detection of acetaminophen was achieved with the utilization of L-Cys-CdSe/ZnS QDs embedded in a MIP, likely via a charge transfer induced fluorescence quenching process from MIP@QDs to AC. The structures of QDs, MIP@QDs and NIP@QDs were characterized by fluorescence spectroscopy, FTIR and TEM. Quenching of the photoluminescence of the synthesized MIP@QDs enabled the determination of AC at concentrations as low as 0.34 nmol L⁻¹ & over the linear concentration range of 1.0-300 nmol L⁻¹. The prepared MIP@QDs were highly selective to AC with outstanding reproducibility (3.7%). The simple and economical preparation of the MIP@QDs, good photostability as well as selectivity towards AC, allowed for this novel sensor material to be successfully

applied in the analysis of nanomolar concentrations of AC in water samples with recoveries of 95% to 114%.

A CdSeTe/ZnS@MIP fluorescence sensor was synthesized and characterized using various techniques to confirm functionalization of the QDs with the MIP polymer. Application of the sensor towards atrazine detection showed a linear response (fluorescence quenching) with increasing atrazine concentration in the range from 2-20 $\times 10^{-7}$ mol L⁻¹. The performance of the sensor compared to other methods showed that the sensitivity needs to be improved in order to lower the detection limit (0.80 $\times 10^{-7}$ mol L⁻¹). A low detection limit is crucial for atrazine monitoring in environmental water samples, where the concentrations can be as low as 0.01 to 0.19 $\mu\text{g L}^{-1}$. The World Health Organization (WHO) guideline limit for atrazine in water is 0.1 mg L⁻¹ (4.6 $\times 10^{-7}$ mol L⁻¹) hence the sensor has potential in regulatory applications. The performance was further tested in tap and lake water samples and showed satisfactory recoveries ranging between 92-118%.

PDMS has been successfully used for the immobilization of QDs to produce thin fluorescent films. As proof of concept, CdSeTe/ZnS QDs and graphene quantum dots (GQDs) were incorporated into the PDMS through spin coating and red and blue fluorescent films were thus obtained. The CdSeTe/ZnS@PDMS thin film was tested for atrazine detection and an enhanced fluorescence signal was found. These fluorescent films hold great potential in designing reusable rapid field monitoring sensors for targeted ECP compounds in water systems. The sensitivity and stability of QDs combined with the inertness, flexibility, and ability of PDMS to pre-concentrate analytes will open doors for designing sensitive and robust fluorescence sensors for routine monitoring of ECPs.

Reliable and robust analytical techniques are needed for the detection of ECPs in surface waters. A fluorescence probe monitoring approach utilising quantum dots offers an alternative sensing technique to traditional methods, with clear advantages including easy operation, low cost, a fast and simple experimental process, and high sensitivity towards different molecular structures with different emission wavelengths. In addition, MIPs were successfully used to functionalise the QDs in order to combine the selectivity of MIPs with the sensitivity of QDs. A cost-benefit analysis of QD fluorescence sensors as compared to conventional analytical methods was included in our previous WRC project (Development of novel fluorescent sensors for the screening of emerging chemical pollutants in water, K5/2438), where it was shown that our sensors may provide a 100x cost saving per analysis over GC-MS, for example.

The synthesised fluorescent QD@PDMS thin films hold great potential in designing reusable rapid field monitoring sensors for targeted ECP compounds in water systems. The sensitivity and stability of QDs combined with the inertness, flexibility, and ability of PDMS to pre-concentrate analytes will open doors for designing sensitive and robust fluorescence sensors for routine monitoring of these compounds.

6.2 RECOMMENDATIONS

The development of South African guideline values or water quality limits for ECPs should receive attention from policy makers in order to safeguard human health. The Department of Health and the Department of Water and Sanitation are encouraged to partner with the Water Research Commission to invest in the further development and ultimate use of novel monitoring technologies which can enhance and complement the current *status quo* regarding water management.

As a result of the positive outcomes of this project, further work on the optimization studies of the sensor materials is recommended, particularly with respect to the testing thereof for real water samples in which the presence of the target ECPs has been confirmed by traditional (chromatographic-mass spectrometric) methods. A portable sensor device should also be developed based on these sensor materials, to allow for on-site real-time monitoring of ECPs in surface waters. A non-targeted screening method based on a mixture of different QDs should be investigated, as well additional compound class type sensors, to enable early detection of overall change in water quality with respect to ECPs.

REFERENCES

- Abdel-Shafy, H. I., & Mansour, M. S. M. (2016). A review on polycyclic aromatic hydrocarbons: Source, environmental impact, effect on human health and remediation. *Egyptian Journal of Petroleum*, 25(1), 107-123.
- Achilleos, A., Ines Vasquez Hadjilyra, M., Hapeshi, E., Michael, C., Monou, S. M., M., & Fatta Kassinos, D. (2008). Predicted environmental concentration of selected pharmaceutical active ingredients in urban wastewater in Cyprus. Paper presented at the International Conference on the Protection and Restoration of the Environment IX, Kefalonia, Greece.
- Adegoke, O., & Forbes, P. B. C. (2016). I-Cysteine-capped core/shell/shell quantum dot-graphene oxide nanocomposite fluorescence probe for polycyclic aromatic hydrocarbon detection. *Talanta*, 146, 780-788.
- Adegoke, O., Nyokong, T., & Forbes, P. B. (2017). Photophysical properties of a series of alloyed and non-alloyed water-soluble I-cysteine-capped core quantum dots. *Journal of Alloys and Compounds*, 695, 1354-1361.
- Adegoke, O., Nyokong, T., & Forbes, P. B. C. (2015). Deposition of CdS, CdS/ZnSe and CdS/ZnSe/ZnS shells around CdSeTe alloyed core quantum dots: effects on optical properties. *Luminescence*, 31(3), 694-703.
- Agunbiade, F. O., & Moodley, B. (2014). Pharmaceuticals as emerging organic contaminants in Umgeni River water system, KwaZulu-Natal, South Africa. *Environmental Monitoring and Assessment*, 186(11), 7273-7291.
- Ajao, C., Andersson, M. A., Teplova, V. V., Nagy, S., Gahmberg, C. G., Andersson, L. C., Hautaniemi, M., Kakasi, B., Roivainen, M., & Salkinoja-Salonen, M. (2015). Mitochondrial toxicity of triclosan on mammalian cells. *Toxicology Reports*, 2, 624-637.
- Allmyr, M., Adolfsson-Erici, M., McLachlan, M. S., & Sandborgh-Englund, G. (2006). Triclosan in plasma and milk from Swedish nursing mothers and their exposure via personal care products. *Science of the Total Environment*, 372(1), 87-93.
- Allmyr, M., Harden, F., Toms, L.-M. L., Mueller, J. F., McLachlan, M. S., Adolfsson-Erici, M., & Sandborgh-Englund, G. (2008). The influence of age and gender on triclosan concentrations in Australian human blood serum. *Science of the Total Environment*, 393(1), 162-167.
- Allmyr, M., McLachlan, M. S., Sandborgh-Englund, G., & Adolfsson-Erici, M. (2006). Determination of Triclosan as Its Pentafluorobenzoyl Ester in Human Plasma and Milk Using Electron Capture Negative Ionization Mass Spectrometry. *Analytical Chemistry*, 78, 6542-6546.
- Antunes, S. C., Freitas, R., Figueira, E., Goncalves, F., & Nunes, B. (2013). Biochemical effects of acetaminophen in aquatic species: edible clams *Venerupis decussata* and *Venerupis philippinarum*. *Environmental Science and Pollution Research Int*, 20(9), 6658-6666.
- Atar, N., Eren, T., Yola, M. L., & Wang, S. (2015). A sensitive molecular imprinted surface plasmon resonance nanosensor for selective determination of trace triclosan in wastewater. *Sensors and Actuators B: Chemical*, 216, 638-644.
- ATSDR, (2012). Case Studies in Environmental Medicine Toxicity of Polycyclic Aromatic Hydrocarbons (PAHs). Retrieved from <https://www.atsdr.cdc.gov/csem/pah/docs/pah.pdf>
- Bahram, M., Alizadeh, S., & Madrakian, T. (2015). Application of silver nanoparticles for simple and rapid spectrophotometric determination of acetaminophen and gentamicin in real samples. *Sensor Letters*, 13, 1-7.
- Barker, J. D., de Carle, D. J., & Anuras, S. (1977). Chronic excessive acetaminophen use and liver damage. *Annals of Internal Medicine*, 87(3), 299-301.
- Bedner, M., & MacCrehan, W. A. (2006). Transformation of acetaminophen by chlorination produces the toxicants 1, 4-benzoquinone and N-acetyl-p-benzoquinone imine. *Environmental Science & Technology*, 40(2), 516-522.
- Bendz, D., Paxeus, N. A., Ginn, T. R., & Loge, F. J. (2005). Occurrence and fate of pharmaceutically active compounds in the environment, a case study: Høje River in Sweden. *Journal of Hazardous materials*, 122(3), 195-204.
- Benítez-Martínez, S., & Valcárcel, M. (2015). Graphene quantum dots in analytical science. *TrAC Trends in Analytical Chemistry*, 72, 93-113.
- Bester, K. (2003). Triclosan in a sewage treatment process – balances and monitoring data. *Water Research*, 37(16), 3891-3896.
- Bester, K. (2005). Fate of triclosan and triclosan-methyl in sewage treatment plants and surface waters. *Archives of Environmental Contamination and Toxicology*, 49(1), 9-17.
- Bhargava, H., & Leonard, P. A. (1996). Triclosan: applications and safety. *American Journal of Infection Control*, 24(3), 209-218.

- Biju, V., Makita, Y., Sonoda, A., Yokoyama, H., Baba, Y., & Ishikawa, M. (2005). Temperature-sensitive photoluminescence of CdSe quantum dot clusters. *The Journal of Physical Chemistry B*, *109*(29), 13899-13905.
- Binelli, A., Cogni, D., Parolini, M., Riva, C., & Provini, A. (2009). Cytotoxic and genotoxic effects of in vitro exposure to triclosan and trimethoprim on zebra mussel (*Dreissena polymorpha*) hemocytes. *Comparative Biochemistry and Physiology Part C: Toxicology & Pharmacology*, *150*(1), 50-56.
- Binelli, A., Cogni, D., Parolini, M., Riva, C., & Provini, A. (2009). In vivo experiments for the evaluation of genotoxic and cytotoxic effects of triclosan in Zebra mussel hemocytes. *Aquatic Toxicology*, *91*(3), 238-244.
- Bingham, E., Cohrssen, B., & Powell, C. H. (2001). Patty's toxicology. Volume 2: toxicological issues related to metals, neurotoxicology and radiation metals and metal compounds: John Wiley and Sons.
- Bouabi, Y. E. L., Farahi, A., Labjar, N., El Hajjaji, S., Bakasse, M., & El Mhammedi, M. A. (2016). Square wave voltammetric determination of paracetamol at chitosan modified carbon paste electrode: application in natural water samples, commercial tablets and human urines. *Materials Science and Engineering: C*, *58*, 70-77.
- Bound, J. P., & Voulvoulis, N. (2006). Predicted and measured concentrations for selected pharmaceuticals in UK rivers: implications for risk assessment. *Water Research*, *40*(15), 2885-2892.
- Brausch, J. M., & Rand, G. M. (2011). A review of personal care products in the aquatic environment: environmental concentrations and toxicity. *Chemosphere*, *82*(11), 1518-1532.
- Bressy, C., Ngo, V. G., Ziarelli, F., & Margaillan, A. (2012). New Insights into the adsorption of 3-(trimethoxysilyl)propylmethacrylate on hydroxylated ZnO nanopowders. *Langmuir*, *28*(6), 3290-3297.
- Bruchez, M., Moronne, M., Gin, P., Weiss, S., & Alivisatos, A. P. (1998). Semiconductor nanocrystals as fluorescent biological labels. *Science*, *281*(5385), 2013-2016.
- Brun, G. L., Bernier, M., Losier, R., Doe, K., Jackman, P., & Lee, H. B. (2006). Pharmaceutically active compounds in Atlantic Canadian sewage treatment plant effluents and receiving waters, and potential for environmental effects as measured by acute and chronic aquatic toxicity. *Environmental Toxicology and Chemistry*, *25*(8), 2163-2176.
- Buser, H.-R., Müller, M. D., & Theobald, N. (1998). Occurrence of the pharmaceutical drug clofibrac acid and the herbicide mecoprop in various Swiss lakes and in the North Sea. *Environmental Science & Technology*, *32*(1), 188-192.
- Buser, H.-R., Poiger, T., & Müller, M. D. (1999). Occurrence and environmental behavior of the chiral pharmaceutical drug ibuprofen in surface waters and in wastewater. *Environmental Science & Technology*, *33*(15), 2529-2535.
- Calafat, A. M., Ye, X., Wong, L.-Y., Reidy, J. A., & Needham, L. L. (2008). Urinary concentrations of triclosan in the US population: 2003-2004. *Environmental Health Perspectives*, *116*(3), 303.
- Canadian Environmental Protection Act. (2017). Draft Federal Environmental Quality Guidelines: Triclosan. Retrieved from https://www.google.co.za/url?sa=t&rct=j&q=&esrc=s&source=web&cd=1&ved=0ahUKEwit3cvxx4HWAhVnJMAKHZzXAKoQFggmMAA&url=http%3A%2F%2Fwww.ec.gc.ca%2Fese-ees%2FF6CF7AA4-1403-4ED1-8DE8-0B42BC1AA852%2FTriclosan%2520Factsheet_En.pdf&usq=AFQjCNHr7FfON1_C_az8IS0Q-KvdJczqzA
- Canesi, L., Ciacci, C., Lorusso, L. C., Betti, M., Gallo, G., Pojana, G., & Marcomini, A. (2007). Effects of Triclosan on *Mytilus galloprovincialis* hemocyte function and digestive gland enzyme activities: possible modes of action on non target organisms. *Comparative Biochemistry and Physiology Part C: Toxicology & Pharmacology*, *145*(3), 464-472.
- Canosa, P., Morales, S., Rodriguez, I., Rubi, E., Cela, R., & Gomez, M. (2005). Aquatic degradation of triclosan and formation of toxic chlorophenols in presence of low concentrations of free chlorine. *Analytical and Bioanalytical Chemistry*, *383*(7-8), 1119-1126.
- Capdevielle, M., Van Egmond, R., Whelan, M., Versteeg, D., Hofmann-Kamensky, M., Inauen, J., Cunningham, V., & Woltering, D. (2008). Consideration of exposure and species sensitivity of triclosan in the freshwater environment. *Integrated Environmental Assessment and Management*, *4*(1), 15-23.
- Carlsson, C., Johansson, A.-K., Alvan, G., Bergman, K., & Kühler, T. (2006). Are pharmaceuticals potent environmental pollutants?: Part I: Environmental risk assessments of selected active pharmaceutical ingredients. *Science of the Total Environment*, *364*(1), 67-87.
- Carrillo-Carrion, C., Cardenas, S., Simonet, B. M., & Valcarcel, M. (2009). Selective quantification of carnitine enantiomers using chiral cysteine-capped CdSe(ZnS) quantum dots. *Analytical chemistry*, *81*(12), 4730-4733.
- Cha, J., & Cupples, A. M. (2009). Detection of the antimicrobials triclocarban and triclosan in agricultural soils following land application of municipal biosolids. *Water Research*, *43*(9), 2522-2530.

- Chalew, T. E., & Halden, R. U. (2009). Environmental exposure of aquatic and terrestrial biota to triclosan and triclocarban. *Journal of the American Water Resources Association*, 45(1), 4-13.
- Chau, W. C., Wu, J. L., & Cai, Z. (2008). Investigation of levels and fate of triclosan in environmental waters from the analysis of gas chromatography coupled with ion trap mass spectrometry. *Chemosphere*, 73(1 Suppl), S13-17.
- Chen, L., Wang, X., Lu, W., Wu, X., & Li, J. (2016). Molecular imprinting: perspectives and applications. *Chemical Society Reviews*, 45(8), 2137-2211.
- Chen, L., Xu, S., & Li, J. (2011). Recent advances in molecular imprinting technology: current status, challenges and highlighted applications. *Chemical Society Reviews*, 40(5), 2922-2942.
- Cheng, C.-T., Chen, C.-Y., Lai, C.-W., Liu, W.-H., Pu, S.-C., Chou, P.-T., Chou, Y.-H., & Chiu, H.-T. (2005). Syntheses and photophysical properties of type-II CdSe/ZnTe/ZnS (core/shell/shell) quantum dots. *Journal of Materials Chemistry*, 15(33), 3409-3414.
- Chevrier, C., Limon, G., Monfort, C., Rouget, F., Garlandé, R., Petit, C., Durand, G., & Cordier, S. (2011). Urinary biomarkers of prenatal atrazine exposure and adverse birth outcomes in the PELAGIE birth cohort. *Environmental Health Perspectives*, 119(7), 1034.
- Chimuka, L., Sibiya, P., Amdany, R., Cukrowska, E., & Forbes, P. B. C. (2015). Status of PAHs in environmental compartments of South Africa: A country report. *Polycyclic Aromatic Compounds*, 36, 376-394.
- Chong, Y., Ma, Y., Shen, H., Tu, X., Zhou, X., Xu, J., Dai, J., Fan, S., & Zhang, Z. (2014). The in vitro and in vivo toxicity of graphene quantum dots. *Biomaterials*, 35(19), 5041-5048.
- Choudhury, K. R., Sahoo, Y., Ohulchanskyy, T., & Prasad, P. (2005). Efficient photoconductive devices at infrared wavelengths using quantum dot-polymer nanocomposites. *Applied Physics Letters*, 87(7), 073110.
- Chu, S., & Metcalfe, C. D. (2007). Simultaneous determination of triclocarban and triclosan in municipal biosolids by liquid chromatography tandem mass spectrometry. *Journal of Chromatography A*, 1164(1), 212-218.
- Ciniglia, C., Cascone, C., Giudice, R. L., Pinto, G., & Pollio, A. (2005). Application of methods for assessing the geno- and cytotoxicity of triclosan to *C. ehrenbergii*. *Journal of Hazardous materials*, 122(3), 227-232.
- Coe, S., Woo, W.-K., Bawendi, M., & Bulović, V. (2002). Electroluminescence from single monolayers of nanocrystals in molecular organic devices. *Nature*, 420(6917), 800-803.
- Coogan, M. A., & Point, T. W. L. (2008). Snail bioaccumulation of triclocarban, triclosan, and methyltriclosan in a North Texas, USA, stream affected by wastewater treatment plant runoff. *Environmental Toxicology and Chemistry*, 27(8), 1788-1793.
- Coogan, M. A., Edziyie, R. E., La Point, T. W., & Venables, B. J. (2007). Algal bioaccumulation of triclocarban, triclosan, and methyl-triclosan in a North Texas wastewater treatment plant receiving stream. *Chemosphere*, 67(10), 1911-1918.
- Corporation, S. R., Substances, U. S. A. f. T., & Registry, D. (2003). Toxicological Profile for Atrazine. Retrieved from <https://www.atsdr.cdc.gov/ToxProfiles/tp153.pdf>
- Crane, M., Watts, C., & Boucard, T. (2006). Chronic aquatic environmental risks from exposure to human pharmaceuticals. *Science of the Total Environment*, 367(1), 23-41.
- Crofton, K. M., Paul, K. B., DeVito, M. J., & Hedge, J. M. (2007). Short-term in vivo exposure to the water contaminant triclosan: evidence for disruption of thyroxine. *Environmental Toxicology and Pharmacology*, 24(2), 194-197.
- Dabrowski, J. M. (2015a). Investigation of the contamination of water resources by Agricultural chemicals and the Impact on environmental health. Volume 1: Risk assessment of Agricultural chemicals to human and animal health. (1956/1/15). Water Research Commission. Pretoria, South Africa. Retrieved from <http://www.wrc.org.za/Pages/KnowledgeHub.aspx>
- Dabrowski, J. M. (2015b). Investigation of the contamination of water resources by agricultural chemicals and the impact on environmental health. Volume 2: Prioritising human health effects and mapping sources of agricultural pesticides used in South Africa. (TT 642/15). Water Research Commission. Pretoria, South Africa. Retrieved from <http://www.wrc.org.za/pages/KnowledgeHub.aspx>
- Dabrowski, J. M., & Balderacchi, M. (2013). Development and field validation of an indicator to assess the relative mobility and risk of pesticides in the Lourens River catchment, South Africa. *Chemosphere*, 93(10), 2433-2443.
- Dabrowski, J. M., & Schulz, R. (2003). Predicted and measured levels of azinphosmethyl in the Lourens River, South Africa: Comparison of runoff and spray drift. *Environmental Toxicology and Chemistry*, 22(3), 494-500.
- Dabrowski, J. M., Aneck-Hahn, N., Chamier, J., De Jager, C., Forbes, P., Genthe, B., Meyer, J. A., Pieters, R., Shadung, J., Thwala, M., & Van Zijl, M. C. (2013). Sampling and analysis of water and sediments for endocrine disrupting activity and concentrations of pesticide active ingredients. Water Research Commission. Pretoria, South Africa.

- Dabrowski, J. M., Shadung, J. M., & Wepener, V. (2014). Prioritizing agricultural pesticides used in South Africa based on their environmental mobility and potential human health effects. *Environment International*, *62*, 31-40.
- Dann, A. B., & Hontela, A. (2011). Triclosan: environmental exposure, toxicity and mechanisms of action. *Journal of Applied Toxicology*, *31*(4), 285-311.
- Daughton, C. G. (2001). Overview-1 Pharmaceuticals and personal care products in the environment: overarching issues and overview. Paper presented at the ACS Symposium Series.
- Daughton, C. G., & Ternes, T. A. (1999). Pharmaceuticals and personal care products in the environment: agents of subtle change? *Environmental Health Perspectives*, *107*(Suppl 6), 907.
- David, A., & Pancharatna, K. (2009). Effects of acetaminophen (paracetamol) in the embryonic development of zebrafish, *Danio rerio*. *Journal of Applied Toxicology*, *29*(7), 597-602.
- de García, S. A. O., Pinto, G. P., García-Encina, P. A., & Irusta-Mata, R. (2014). Ecotoxicity and environmental risk assessment of pharmaceuticals and personal care products in aquatic environments and wastewater treatment plants. *Ecotoxicology*, *23*(8), 1517-1533.
- de García, S. O., García-Encina, P., & Irusta-Mata, R. (2011). Environmental risk assessment (ERA) of pharmaceuticals and personal care products (PPCPs) using ecotoxicity tests. *Ecotoxicology*, *23*(8), 1-8.
- de Mello Donegá, C., Liljeroth, P., & Vanmaekelbergh, D. (2005). Physicochemical evaluation of the hot-injection method, a synthesis route for monodisperse nanocrystals. *Small*, *1*(12), 1152-1162.
- De Menezes, F. D., Brasil, A. G., Moreira, W. L., Barbosa, L. C., Cesar, C. L., Ferreira, R. d. C., De Farias, P. M. A., & Santos, B. S. (2005). CdTe/CdS core shell quantum dots for photonic applications. *Microelectronics Journal*, *36*(11), 989-991.
- Delgado-Perez, T., Bouchet, L. M., de la Guardia, M., Galian, R. E., & Perez-Prieto, J. (2013). Sensing chiral drugs by using CdSe/ZnS nanoparticles capped with N-acetyl-L-cysteine methyl ester. *A European Journal of Chemistry*, *19*(33), 11068-11076.
- DeLorenzo, M. E., & Fleming, J. (2008). Individual and mixture effects of selected pharmaceuticals and personal care products on the marine phytoplankton species *Dunaliella tertiolecta*. *Archives of Environmental Contamination and Toxicology*, *54*(2), 203-210.
- Delorenzo, M. E., Keller, J. M., Arthur, C. D., Finnegan, M. C., Harper, H. E., Winder, V. L., & Zdankiewicz, D. L. (2008). Toxicity of the antimicrobial compound triclosan and formation of the metabolite methyl-triclosan in estuarine systems. *Environmental Toxicology*, *23*(2), 224-232.
- Dhillon, G. S., Kaur, S., Pulicharla, R., Brar, S. K., Cledón, M., Verma, M., & Surampalli, R. Y. (2015). Triclosan: current status, occurrence, environmental risks and bioaccumulation potential. *International Journal of Environmental Research and Public Health*, *12*(5), 5657-5684.
- Dodd, M. C., Kohler, H.-P. E., & Von Gunten, U. (2009). Oxidation of antibacterial compounds by ozone and hydroxyl radical: elimination of biological activity during aqueous ozonation processes. *Environmental Science & Technology*, *43*(7), 2498-2504.
- Dong, W., Shen, H.-B., Liu, X.-H., Li, M.-J., & Li, L.-S. (2011). CdSe/ZnS quantum dots based fluorescence quenching method for determination of paeonol. *Spectrochimica Acta Part A: Molecular and Biomolecular Spectroscopy*, *78*(1), 537-542.
- Dong, Y., Shao, J., Chen, C., Li, H., Wang, R., Chi, Y., Lin, X., & Chen, G. (2012). Blue luminescent graphene quantum dots and graphene oxide prepared by tuning the carbonization degree of citric acid. *Carbon*, *50*(12), 4738-4743.
- Du Preez, J., & Yang, W. (2003). Improving the aqueous solubility of triclosan by solubilization, complexation, and in situ salt formation. *Journal of Cosmetic Science*, *54*, 537-550.
- Du Preez, L. H., Jansen van Rensburg, P. J., Jooste, A. M., Carr, J. A., Giesy, J. P., Gross, T. S., Kendall, R. J., Smith, E. E., Van Der Kraak, G., & Solomon, K. R. (2005). Seasonal exposures to triazine and other pesticides in surface waters in the western Highveld corn-production region in South Africa. *Environmental Pollution*, *135*(1), 131-141.
- Du, H., Fuh, R. C. A., Li, J., Corkan, L. A., & Lindsey, J. S. (1998). PhotochemCAD: A computer-aided design and research tool in photochemistry. *Photochemistry and Photobiology*, *68*(2), 141-142.
- Duong, H. D., Reddy, C. V. G., Rhee, J. I., & Vo-Dinh, T. (2011). Amplification of fluorescence emission of CdSe/ZnS QDs entrapped in a sol-gel matrix, a new approach for detection of trace level of PAHs. *Sensors and Actuators B: Chemical*, *157*(1), 139-145.
- Dussault, E. B., Balakrishnan, V. K., Sverko, E., Solomon, K. R., & Sibley, P. K. (2008). Toxicity of human pharmaceuticals and personal care products to benthic invertebrates. *Environmental Toxicology and Chemistry*, *27*(2), 425-432.
- Elangovan, M., Day, R., & Periasamy, A. (2002). Nanosecond fluorescence resonance energy transfer-fluorescence lifetime imaging microscopy to localize the protein interactions in a single living cell. *Journal of Microscopy*, *205*(1), 3-14.

- Ellenhorn, M. J., Schonwald, S., Ordog, G., & Wasserberger, J. (1997). *Ellenhorn's medical toxicology: diagnosis and treatment of human poisoning*: Williams & Wilkins.
- Engraff, M., Solere, C., Smith, K. E. C., Mayer, P., & Dahllöf, I. (2011). Aquatic toxicity of PAHs and PAH mixtures at saturation to benthic amphipods: Linking toxic effects to chemical activity. *Aquatic Toxicology*, *102*(3), 142-149.
- Escher, B. I., Baumgartner, R., Koller, M., Treyer, K., Lienert, J., & McArdell, C. S. (2011). Environmental toxicology and risk assessment of pharmaceuticals from hospital wastewater. *Water Research*, *45*(1), 75-92.
- Fair, P. A., Lee, H.-B., Adams, J., Darling, C., Pacepavicius, G., Alaei, M., Bossart, G. D., Henry, N., & Muir, D. (2009). Occurrence of triclosan in plasma of wild Atlantic bottlenose dolphins (*Tursiops truncatus*) and in their environment. *Environmental Pollution*, *157*(8), 2248-2254.
- Fan, L., Hu, Y., Wang, X., Zhang, L., Li, F., Han, D., Li, Z., Zhang, Q., Wang, Z., & Niu, L. (2012). Fluorescence resonance energy transfer quenching at the surface of graphene quantum dots for ultrasensitive detection of TNT. *Talanta*, *101*, 192-197.
- Fan, T., Zeng, W., Tang, W., Yuan, C., Tong, S., Cai, K., Liu, Y., Huang, W., Min, Y., & Epstein, A. J. (2015). Controllable size-selective method to prepare graphene quantum dots from graphene oxide. *Nanoscale Research Letters*, *10*, 55.
- Fan, W., Yanase, T., Morinaga, H., Gondo, S., Okabe, T., Nomura, M., Komatsu, T., Morohashi, K., Hayes, T., & Takayanagi, R. (2007). Atrazine-induced aromatase expression is SF-1 dependent: Implications for endocrine disruption in wildlife and reproductive cancers in humans. *Environmental Health Perspectives*, *115*(5), 720.
- Fang, C., Yi, C., Wang, Y., Cao, Y., & Liu, X. (2009). Electrochemical sensor based on molecular imprinting by photo-sensitive polymers. *Biosensors and Bioelectronics*, *24*(10), 3164-3169.
- Farré, M., Asperger, D., Kantiani, L., González, S., Petrovic, M., & Barceló, D. (2008). Assessment of the acute toxicity of triclosan and methyl triclosan in wastewater based on the bioluminescence inhibition of *Vibrio fischeri*. *Analytical and Bioanalytical Chemistry*, *390*(8), 1999-2007.
- Federle, T. W., Kaiser, S. K., & Nuck, B. A. (2002). Fate and effects of triclosan in activated sludge. *Environmental Toxicology and Chemistry*, *21*(7), 1330-1337.
- Fent, K. (2001). Fish cell lines as versatile tools in ecotoxicology: assessment of cytotoxicity, cytochrome P4501A induction potential and estrogenic activity of chemicals and environmental samples. *Toxicology in vitro*, *15*(4), 477-488.
- Fent, K., Weston, A. A., & Caminada, D. (2006). Ecotoxicology of human pharmaceuticals. *Aquatic Toxicology*, *76*(2), 122-159.
- Fort, D. J., Rogers, R. L., Gorsuch, J. W., Navarro, L. T., Peter, R., & Plautz, J. R. (2009). Triclosan and anuran metamorphosis: no effect on thyroid-mediated metamorphosis in *Xenopus laevis*. *Toxicological Sciences*, *113*(2), 392-400.
- Fraker, S. L., & Smith, G. R. (2004). Direct and interactive effects of ecologically relevant concentrations of organic wastewater contaminants on *Rana pipiens* tadpoles. *Environmental Toxicology*, *19*(3), 250-256.
- Frick, E.A., Henderson, A.K., Moll, D.M., Furlong, E.T., Meyer, M.T. In: K.J. Hatcher, editor. Proceedings of the 2001 Georgia Water Resources Conference, March 26-27, at the University of Georgia, Athens, Georgia: Institute of Ecology, The University of Georgia, 2001.
- Galus, M., Jeyaranjan, J., Smith, E., Li, H., Metcalfe, C., & Wilson, J. Y. (2013). Chronic effects of exposure to a pharmaceutical mixture and municipal wastewater in zebrafish. *Aquatic Toxicology*, *132*, 212-222.
- Galus, M., Kirischian, N., Higgins, S., Purdy, J., Chow, J., Rangaranjan, S., Li, H., Metcalfe, C., & Wilson, J. Y. (2013). Chronic, low concentration exposure to pharmaceuticals impacts multiple organ systems in zebrafish. *Aquatic Toxicology*, *132*, 200-211.
- Gao, R., Kong, X., Su, F., He, X., Chen, L., & Zhang, Y. (2010). Synthesis and evaluation of molecularly imprinted core-shell carbon nanotubes for the determination of triclosan in environmental water samples. *Journal of Chromatography A*, *1217*(52), 8095-8102.
- Gavrilescu, M., Demnerova, K., Aamand, J., Agathos, S., & Fava, F. (2014). Emerging pollutants in the environment: present and future challenges in biomonitoring, ecological risks and bioremediation. *New Biotechnology*, *32*(1), 147-156.
- Geyer, H. J., Schramm, K.-W., Feicht, E. A., Behecti, A., Steinberg, C., Brüggemann, R., Poiger, H., Henkelmann, B., & Ketrup, A. (2002). Half-lives of tetra-, penta-, hexa-, hepta-, and octachlorodibenzo-p-dioxin in rats, monkeys, and humans – a critical review. *Chemosphere*, *48*(6), 631-644.
- Gilliom, R. J. (2007). Pesticides in US streams and groundwater. *Environmental Science & Technology*, *41*(10), 3408-3414.
- Giusi, G., Facciolo, R., Canonaco, M., Alleva, E., Belloni, V., Dessi, F., & Santucci, D. (2006). The endocrine disruptor atrazine accounts for a dimorphic somatostatinergic neuronal expression pattern in mice. *Toxicological Sciences*, *89*(1), 257-264.

- Glassmeyer, S. T., Furlong, E. T., Kolpin, D. W., Cahill, J. D., Zaugg, S. D., Werner, S. L., Meyer, M. T., & Kryak, D. D. (2005). Transport of chemical and microbial compounds from known wastewater discharges: potential for use as indicators of human faecal contamination. *Environmental Science & Technology*, *39*(14), 5157-5169.
- Goldman, E. R., Medintz, I. L., Whitley, J. L., Hayhurst, A., Clapp, A. R., Uyeda, H. T., Deschamps, J. R., Lassman, M. E., & Mattoussi, H. (2005). A hybrid quantum dot-antibody fragment fluorescence resonance energy transfer-based TNT sensor. *Journal of the American Chemical Society*, *127*(18), 6744-6751.
- Gómez, M. J., Bueno, M. M., Lacorte, S., Fernández-Alba, A. R., & Agüera, A. (2007). Pilot survey monitoring pharmaceuticals and related compounds in a sewage treatment plant located on the Mediterranean coast. *Chemosphere*, *66*(6), 993-1002.
- Gorla, F. A., Duarte, E. H., Sartori, E. R., & Tarley, C. R. T. (2016). Electrochemical study for the simultaneous determination of phenolic compounds and emerging pollutant using an electroanalytical sensing system based on carbon nanotubes/surfactant and multivariate approach in the optimization. *Microchemical Journal*, *124*, 65-75.
- Gracia-Lor, E., Sancho, J. V., & Hernández, F. (2010). Simultaneous determination of acidic, neutral and basic pharmaceuticals in urban wastewater by ultra high-pressure liquid chromatography-tandem mass spectrometry. *Journal of Chromatography A*, *1217*(5), 622-632.
- Gros, M., Petrovic, M., & Barcelo, D. (2006). Development of a multi-residue analytical methodology based on liquid chromatography-tandem mass spectrometry (LC-MS/MS) for screening and trace level determination of pharmaceuticals in surface and wastewaters. *Talanta*, *70*(4), 678-690.
- Grujić, S., Vasiljević, T., & Laušević, M. (2009). Determination of multiple pharmaceutical classes in surface and ground waters by liquid chromatography-ion trap-tandem mass spectrometry. *Journal of Chromatography A*, *1216*(25), 4989-5000.
- Guo, J.-H., Li, X.-H., Cao, X.-L., Li, Y., Wang, X.-Z., & Xu, X.-B. (2009). Determination of triclosan, triclocarban and methyl-triclosan in aqueous samples by dispersive liquid-liquid microextraction combined with rapid liquid chromatography. *Journal of Chromatography A*, *1216*(15), 3038-3043.
- Halden, R. U., & Paull, D. H. (2005). Co-occurrence of triclocarban and triclosan in US water resources. *Environmental Science & Technology*, *39*(6), 1420-1426.
- Hammond, P. T. (1999). Recent explorations in electrostatic multilayer thin film assembly. *Current Opinion in Colloid & Interface Science*, *4*(6), 430-442.
- Han, G. H., Hur, H. G., & Kim, S. D. (2006). Ecotoxicological risk of pharmaceuticals from wastewater treatment plants in Korea: occurrence and toxicity to *Daphnia magna*. *Environmental Toxicology and Chemistry*, *25*(1), 265-271.
- Han, Y., Gu, L., Zhang, M., Li, Z., Yang, W., Tang, X., & Xie, G. (2017). Computer-aided design of molecularly imprinted polymers for recognition of atrazine. *Computational and Theoretical Chemistry*, *1121*, 29-34.
- Hardman, R. (2006). A toxicologic review of quantum dots: Toxicity depends on physicochemical and environmental factors. *Environmental Health Perspectives*, *114*(2), 165-172.
- Harnagea-Theophilus, E., Gadd, S. L., Knight-Trent, A. H., DeGeorge, G. L., & Miller, M. R. (1999). Acetaminophen-induced proliferation of breast cancer cells involves estrogen receptors. *Toxicology and Applied Pharmacology*, *155*(3), 273-279.
- Hayes, T. B., Khoury, V., Narayan, A., Nazir, M., Park, A., Brown, T., Adame, L., Chan, E., Buchholz, D., Stueve, T., & Gallipeau, S. (2010). Atrazine induces complete feminization and chemical castration in male African clawed frogs (*Xenopus laevis*). *Proceedings of the National Academy of Sciences USA*, *107*(10), 4612-4617.
- Heberer, T., Fuhrmann, B., Schmidt-Baumler, K., Tsipi, D., Koutsouba, V., & Hiskia, A. (2001). Occurrence of pharmaceutical residues in sewage, river, ground, and drinking water in Greece and Berlin (Germany) (pp. 70-83).
- Heberer, T., Reddersen, K., & Mechlinski, A. (2002). From municipal sewage to drinking water: fate and removal of pharmaceutical residues in the aquatic environment in urban areas. *Water Science & Technology*, *46*(3), 81-88.
- Heidler, J., & Halden, R. U. (2007). Mass balance assessment of triclosan removal during conventional sewage treatment. *Chemosphere*, *66*(2), 362-369.
- Henschel, K.-P., Wenzel, A., Diedrich, M., & Fliedner, A. (1997). Environmental hazard assessment of pharmaceuticals. *Regulatory Toxicology and Pharmacology*, *25*(3), 220-225.
- Hines, M. A., & Guyot-Sionnest, P. (1996). Synthesis and characterization of strongly luminescing ZnS-capped CdSe nanocrystals. *The Journal of Physical Chemistry*, *100*(2), 468-471.
- Holthoff, E. L., Stratis-Cullum, D. N., & Hankus, M. E. (2011). A nanosensor for TNT detection based on molecularly imprinted polymers and surface enhanced Raman scattering. *Sensors*, *11*(3), 2700-2714.

- Hrouzková, S., & Matisová, E. (2012). Endocrine disrupting pesticides. In R. P. Soundararajan (Ed.), *Pesticides – Advances in Chemical and Botanical pesticides* (pp. 99-126). Croatia: InTech.
- Hu, J., Zhou, L., Zhou, Q. W., Wei, F., Zhang, L. L., & Chen, J. M. (2012). Biodegradation of paracetamol by aerobic granules in a sequencing batch reactor (SBR). Paper presented at the Advanced Materials Research.
- Huang, H., & Zhu, J.-J. (2013). The electrochemical applications of quantum dots. *Analyst*, *138*(20), 5855-5865.
- Huang, S., Xiao, Q., Li, R., Guan, H.-L., Liu, J., Liu, X.-R., He, Z.-K., & Liu, Y. (2009). A simple and sensitive method for l-cysteine detection based on the fluorescence intensity increment of quantum dots. *Analytica Chimica Acta*, *645*(1), 73-78.
- Huber, M. M., Göbel, A., Joss, A., Hermann, N., Löffler, D., McArdell, C. S., Ried, A., Siegrist, H., Ternes, T. A., & von Gunten, U. (2005). Oxidation of pharmaceuticals during ozonation of municipal wastewater effluents: a pilot study. *Environmental Science & Technology*, *39*(11), 4290-4299.
- Hummers, W. S., & Offeman, R. E. (1958). Preparation of graphitic oxide. *Journal of the American Chemical Society*, *80*(6), 1339-1339.
- Huschek, G., Hansen, P. D., Maurer, H. H., Kregel, D., & Kayser, A. (2004). Environmental risk assessment of medicinal products for human use according to European Commission recommendations. *Environmental Toxicology*, *19*(3), 226-240.
- Ikenaka, Y., Sakamoto, M., Nagata, T., Takahashi, H., Miyabara, Y., Hanazato, T., Ishizuka, M., Isobe, T., Kim, J.-W., & Chang, K.-H. (2013). Effects of polycyclic aromatic hydrocarbons (PAHs) on an aquatic ecosystem: acute toxicity and community-level toxic impact tests of benzo[a]pyrene using lake zooplankton community. *The Journal of Toxicological Sciences*, *38*(1), 131-136.
- Ishibashi, H., Matsumura, N., Hirano, M., Matsuoka, M., Shiratsuchi, H., Ishibashi, Y., Takao, Y., & Arizono, K. (2004). Effects of triclosan on the early life stages and reproduction of medaka *Oryzias latipes* and induction of hepatic vitellogenin. *Aquatic Toxicology*, *67*(2), 167-179.
- Ithurria, S., Guyot-Sionnest, P., Mahler, B., & Dubertret, B. (2007). Mn²⁺ as a radial pressure gauge in colloidal core/shell nanocrystals. *Physical Review Letters*, *99*(26), 265501.
- Jia, M., Zhang, Z., Li, J., Shao, H., Chen, L., & Yang, X. (2017). A molecular imprinting fluorescence sensor based on quantum dots and a mesoporous structure for selective and sensitive detection of 2, 4-dichlorophenoxyacetic acid. *Sensors and Actuators B: Chemical*, *252*, 934-943.
- Jiang, L., Liu, H., Li, M., Xing, Y., & Ren, X. (2016). Surface molecular imprinting on CdTe quantum dots for fluorescence sensing of 4-nitrophenol. *Analytical Methods*, *8*(10), 2226-2232.
- Jin, S., Hu, Y., Gu, Z., Liu, L., & Wu, H.-C. (2011). Application of quantum dots in biological imaging. *Journal of Nanomaterials*, *2011*, 13.
- Jones, R. D., Jampani, H. B., Newman, J. L., & Lee, A. S. (2000). Triclosan: a review of effectiveness and safety in health care settings. *American Journal of Infection Control*, *28*(2), 184-196.
- Ju, J., & Chen, W. (2015). Graphene quantum dots as fluorescence probes for sensing metal ions: Synthesis and applications. *Current Organic Chemistry*, *19*(12), 1150-1162.
- Kanda, R., Griffin, P., James, H. A., & Fothergill, J. (2003). Pharmaceutical and personal care products in sewage treatment works. *Journal of Environmental Monitoring*, *5*(5), 823-830.
- Kantiani, L., Farré, M., Asperger, D., Rubio, F., González, S., López de Alda, M. J., Petrović, M., Shelver, W. L., & Barceló, D. (2008). Triclosan and methyl-triclosan monitoring study in the northeast of Spain using a magnetic particle enzyme immunoassay and confirmatory analysis by gas chromatography-mass spectrometry. *Journal of Hydrology*, *361*(1-2), 1-9.
- Kempe, M., & Mosbach, K. (1995). Molecular imprinting used for chiral separations. *Journal of Chromatography A*, *694*(1), 3-13.
- Kim, D., Han, J., & Choi, Y. (2013). On-line solid-phase microextraction of triclosan, bisphenol A, chlorophenols, and selected pharmaceuticals in environmental water samples by high-performance liquid chromatography-ultraviolet detection. *Analytical and Bioanalytical Chemistry*, *405*(1), 377-387.
- Kim, J., Park, J., Kim, P.-G., Lee, C., Choi, K., & Choi, K. (2010). Implication of global environmental changes on chemical toxicity-effect of water temperature, pH, and ultraviolet B irradiation on acute toxicity of several pharmaceuticals in *Daphnia magna*. *Ecotoxicology*, *19*(4), 662-669.
- Kim, J.-W., Ishibashi, H., Yamauchi, R., Ichikawa, N., Takao, Y., Hirano, M., Koga, M., & Arizono, K. (2009). Acute toxicity of pharmaceutical and personal care products on freshwater crustacean (*Thamnocephalus platyurus*) and fish (*Oryzias latipes*). *The Journal of Toxicological Sciences*, *34*(2), 227-232.
- Kim, S. D., Cho, J., Kim, I. S., Vanderford, B. J., & Snyder, S. A. (2007). Occurrence and removal of pharmaceuticals and endocrine disruptors in South Korean surface, drinking, and waste waters. *Water Research*, *41*(5), 1013-1021.
- Kim, Y., Choi, K., Jung, J., Park, S., Kim, P. G., & Park, J. (2007). Aquatic toxicity of acetaminophen, carbamazepine, cimetidine, diltiazem and six major sulfonamides, and their potential ecological risks in Korea. *Environment International*, *33*(3), 370-375.

- Kinney, C. A., Furlong, E. T., Zaugg, S. D., Burkhardt, M. R., Werner, S. L., Cahill, J. D., & Jorgensen, G. R. (2006). Survey of organic wastewater contaminants in biosolids destined for land application. *Environmental Science & Technology*, *40*(23), 7207-7215.
- Kolpin, D. W., Furlong, E. T., Meyer, M. T., Thurman, E. M., Zaugg, S. D., Barber, L. B., & Buxton, H. T. (2002). Pharmaceuticals, hormones, and other organic wastewater contaminants in US streams, 1999-2000: A national reconnaissance. *Environmental Science & Technology*, *36*(6), 1202-1211.
- Kolpin, D. W., Skopec, M., Meyer, M. T., Furlong, E. T., & Zaugg, S. D. (2004). Urban contribution of pharmaceuticals and other organic wastewater contaminants to streams during differing flow conditions. *Science of the Total Environment*, *328*(1), 119-130.
- Koneswaran, M., & Narayanaswamy, R. (2009). L-Cysteine-capped ZnS quantum dots based fluorescence sensor for Cu²⁺ ion. *Sensors and Actuators B: Chemical*, *139*(1), 104-109.
- K'Oreje K, O., Vergeynst, L., Ombaka, D., De Wispelaere, P., Okoth, M., Van Langenhove, H., & Demeestere, K. (2016). Occurrence patterns of pharmaceutical residues in wastewater, surface water and groundwater of Nairobi and Kisumu city, Kenya. *Chemosphere*, *149*, 238-244.
- Kosma, C. I., Lambropoulou, D. A., & Albanis, T. A. (2014). Investigation of PPCPs in wastewater treatment plants in Greece: occurrence, removal and environmental risk assessment. *Science of the Total Environment*, *466-467*, 421-438.
- Kumar, K. S., Priya, S. M., Peck, A. M., & Sajwan, K. S. (2010). Mass loadings of triclosan and triclocarban from four wastewater treatment plants to three rivers and landfill in Savannah, Georgia, USA. *Archives of Environmental Contamination and Toxicology*, *58*(2), 275-285.
- Kümmerer, K. (2001). Introduction: pharmaceuticals in the environment, *Pharmaceuticals in the Environment* (pp. 1-8): Springer.
- Lakowicz, J. (1999). *Principles of Fluorescence Spectroscopy*, Kluwer (2nd ed.). New York.
- Lakshmi, D., Akbulut, M., Ivanova-Mitseva, P. K., Whitcombe, M. J., Piletska, E. V., Karim, K., Güven, O., & Piletsky, S. A. (2013). Computational design and preparation of MIPs for atrazine recognition on a conjugated polymer-coated microtiter plate. *Industrial & Engineering Chemistry Research*, *52*(39), 13910-13916.
- Langford, K. H., & Thomas, K. V. (2009). Determination of pharmaceutical compounds in hospital effluents and their contribution to wastewater treatment works. *Environment International*, *35*(5), 766-770.
- Lee, G. F., & Morris, J. C. (1962). Kinetics of chlorination of phenol-chlorophenolic tastes and odors. *International Journal of Air and Water Pollution*, *6*, 419-431.
- Li, H., Li, Y., & Cheng, J. (2010). Molecularly imprinted silica nanospheres embedded CdSe quantum dots for highly selective and sensitive optosensing of pyrethroids. *Chemistry of Materials*, *22*(8), 2451-2457.
- Li, L., Bian, R., Ding, Y., Yu, M., & Yu, D. (2009). Application of functionalized ZnS nanoparticles to determinate uracil and thymine as a fluorescence probe. *Materials Chemistry and Physics*, *113*(2), 905-908.
- Li, L., Lu, Y., Ding, Y., Cheng, Y., Xu, W., & Zhang, F. (2012). Determination of paracetamol based on its quenching effect on the photoluminescence of CdTe fluorescence probes. *Journal of Fluorescence*, *22*, 591-596.
- Li, L., Wu, G., Yang, G., Peng, J., Zhao, J., & Zhu, J.-J. (2013). Focusing on luminescent graphene quantum dots: current status and future perspectives. *Nanoscale*, *5*(10), 4015-4039.
- Li, X., He, Y., Zhao, F., Zhang, W., & Ye, Z. (2015). Molecularly imprinted polymer-based sensors for atrazine detection by electropolymerization of o-phenylenediamine. *RSC Advances*, *5*(70), 56534-56540.
- Liang, G. X., Li, L. L., Liu, H. Y., Zhang, J. R., Burda, C., & Zhu, J. J. (2010). Fabrication of near-infrared-emitting CdSeTe/ZnS core/shell quantum dots and their electrogenerated chemiluminescence. *Chemical Communications*, *46*(17), 2974-2976.
- Lin, C. I., Joseph, A. K., Chang, C. K., & Der Lee, Y. (2004). Molecularly imprinted polymeric film on semiconductor nanoparticles: analyte detection by quantum dot photoluminescence. *Journal of Chromatography A*, *1027*(1), 259-262.
- Lin, L., Rong, M., Luo, F., Chen, D., Wang, Y., & Chen, X. (2014). Luminescent graphene quantum dots as new fluorescent materials for environmental and biological applications. *TrAC Trends in Analytical Chemistry*, *54*, 83-102.
- Lindström, A., Buerge, I. J., Poiger, T., Bergqvist, P.-A., Müller, M. D., & Buser, H.-R. (2002). Occurrence and environmental behavior of the bactericide triclosan and its methyl derivative in surface waters and in wastewater. *Environmental Science & Technology*, *36*(11), 2322-2329.
- Lishman, L., Smyth, S. A., Sarafin, K., Kleywegt, S., Toito, J., Peart, T., Lee, B., Servos, M., Beland, M., & Seto, P. (2006). Occurrence and reductions of pharmaceuticals and personal care products and estrogens by municipal wastewater treatment plants in Ontario, Canada. *Science of the Total Environment*, *367*(2), 544-558.

- Liu, G., Li, T., Yang, X., She, Y., Wang, M., Wang, J., Zhang, M., Wang, S., Jin, F., Jin, M., Shao, H., Jiang, Z., & Yu, H. (2016). Competitive fluorescence assay for specific recognition of atrazine by magnetic molecularly imprinted polymer based on Fe₃O₄-chitosan. *Carbohydrate Polymers*, *137*, 75-81.
- Liu, Q., Wang, K., Huan, J., Zhu, G., Qian, J., Mao, H., & Cai, J. (2014a). Graphene quantum dots enhanced electrochemiluminescence of cadmium sulfide nanocrystals for ultrasensitive determination of pentachlorophenol. *Analyst*, *139*(11), 2912-2918.
- Liu, Q., Zhou, Q., & Jiang, G. (2014b). Nanomaterials for analysis and monitoring of emerging chemical pollutants. *TrAC Trends in Analytical Chemistry*, *58*, 10-22.
- Liu, R., Guan, G., Wang, S., & Zhang, Z. (2011). Core-shell nanostructured molecular imprinting fluorescent chemosensor for selective detection of atrazine herbicide. *Analyst*, *136*(1), 184-190.
- Liu, Z.-h., Wang, Z.-M., Yang, X., & Ooi, K. (2002). Intercalation of organic ammonium ions into layered graphite oxide. *Langmuir*, *18*(12), 4926-4932.
- Lopez-Avila, V., & Hites, R. A. (1980). Organic compounds in an industrial wastewater. Their transport into sediments. *Environmental Science and Technology*, *14*(11), 1382-1390.
- Lourencao, B. C., Medeiros, R. A., Rocha-Filho, R. C., Mazo, L. H., & Fatibello-Filho, O. (2009). Simultaneous voltammetric determination of paracetamol and caffeine in pharmaceutical formulations using a boron-doped diamond electrode. *Talanta*, *78*(3), 748-752.
- MacBean, C. (2012). *The Pesticide Manual* (16th ed.). Omega Park, Alton, Hampshire, GU34 2QD, UK: British Crop Production Council.
- Manoli, E., & Samara, C. (1999). Polycyclic aromatic hydrocarbons in natural waters: sources, occurrence and analysis. *TrAC Trends in Analytical Chemistry*, *18*(6), 417-428.
- Matongo, S., Birungi, G., Moodley, B., & Ndungu, P. (2015). Occurrence of selected pharmaceuticals in water and sediment of Umgeni River, KwaZulu-Natal, South Africa. *Environmental Science and Pollution Research*, *22*(13), 10298-10308.
- Matongo, S., Birungi, G., Moodley, B., & Ndungu, P. (2015). Pharmaceutical residues in water and sediment of Msunduzi River, KwaZulu-Natal, South Africa. *Chemosphere*, *134*, 133-140.
- McAvoy, D. C., Schatowitz, B., Jacob, M., Hauk, A., & Eckhoff, W. S. (2002). Measurement of triclosan in wastewater treatment systems. *Environmental Toxicology and Chemistry*, *21*(7), 1323-1329.
- McDonald, J. C., & Whitesides, G. M. (2002). Poly(dimethylsiloxane) as a material for fabricating microfluidic devices. *Accounts of Chemical Research*, *35*(7), 491-499.
- Medintz, I. L., Clapp, A. R., Mattoussi, H., Goldman, E. R., Fisher, B., & Mauro, J. M. (2003). Self-assembled nanoscale biosensors based on quantum dot FRET donors. *Nature Materials*, *2*(9), 630-638.
- Memmert, U. (2006). Triclosan: Effects on the Development of Sediment-dwelling Larvae of Chironomus Riparius in a Water-sediment System with Spiked Sediment. RCC Ltd., Itingen, Switzerland.
- Méndez-Albores, A., Tarin, C., Rebollar-Pérez, G., Dominguez-Ramirez, L., & Torres, E. (2015). Biocatalytic spectrophotometric method to detect paracetamol in water samples. *Journal of Environmental Science and Health, Part A*, *50*(10), 1046-1056.
- Miller, T. R., Heidler, J., Chillrud, S. N., DeLaquil, A., Ritchie, J. C., Mihalic, J. N., Bopp, R., & Halden, R. U. (2008). Fate of triclosan and evidence for reductive dechlorination of triclocarban in estuarine sediments. *Environmental Science & Technology*, *42*(12), 4570-4576.
- Morales, S., Canosa, P., Rodríguez, I., Rubí, E., & Cela, R. (2005). Microwave assisted extraction followed by gas chromatography with tandem mass spectrometry for the determination of triclosan and two related chlorophenols in sludge and sediments. *Journal of Chromatography A*, *1082*(2), 128-135.
- Morasch, B., Bonvin, F., Reiser, H., Grandjean, D., De Alencastro, L. F., Perazzolo, C., Chèvre, N., & Kohn, T. (2010). Occurrence and fate of micropollutants in the Vidy Bay of Lake Geneva, Switzerland. Part II: micropollutant removal between wastewater and raw drinking water. *Environmental Toxicology and Chemistry*, *29*(8), 1658-1668.
- Moyo, M., Florence, L. R., & Okonkwo, J. O. (2015). Improved electro-oxidation of triclosan at nano-zinc oxide-multiwalled carbon nanotube modified glassy carbon electrode. *Sensors and Actuators B: Chemical*, *209*, 898-905.
- Muir, N., Nichols, J., Stillings, M., & Sykes, J. (1997). Comparative bioavailability of aspirin and paracetamol following single dose administration of soluble and plain tablets. *Current Medical Research and Opinion*, *13*(9), 491-500.
- Munger, R., Isacson, P., Hu, S., Burns, T., Hanson, J., Lynch, C. F., Cherryholmes, K., Van Dorpe, P., & Hausler Jr, W. J. (1997). Intrauterine growth retardation in Iowa communities with herbicide-contaminated drinking water supplies. *Environmental Health Perspectives*, *105*(3), 308.
- Murphy, C. J., & Coffey, J. L. (2002). Quantum Dots: A Primer. *Applied Spectroscopy*, *56*(1), 16-27.

- Naidenko, O., Leiba, N., Sharp, R., & Houlihan, J. (2008). Bottled water quality investigation: 10 major brands, 38 pollutants. Washington, DC, Environmental Working Group: <http://www.ewg.org/reports/bottledwater> [Accessed 08/17/2010].
- Nassef, M., Kim, S. G., Seki, M., Kang, I. J., Hano, T., Shimasaki, Y., & Oshima, Y. (2010). In ovo nanoinjection of triclosan, diclofenac and carbamazepine affects embryonic development of medaka fish (*Oryzias latipes*). *Chemosphere*, *79*(9), 966-973.
- Nassef, M., Matsumoto, S., Seki, M., Kang, I. J., Moroishi, J., Shimasaki, Y., & Oshima, Y. (2009). Pharmaceuticals and personal care products toxicity to Japanese medaka fish (*Oryzias latipes*). *Journal of the Faculty of Agriculture Kyushu University*, *54*(2), 407-411.
- NICNAS. (2009). Triclosan. Retrieved from Sydney, Australia: http://www.nicnas.gov.au/_data/assets/pdf_file/0017/4391/PEC_30_Triclosan_Full_Report_PDF.pdf
- Nisbet, I. C., & LaGoy, P. K. (1992). Toxic equivalency factors (TEFs) for polycyclic aromatic hydrocarbons (PAHs). *Regulatory Toxicology and Pharmacology*, *16*(3), 290-300.
- Nozik, A. J., Beard, M. C., Luther, J. M., Law, M., Ellingson, R. J., & Johnson, J. C. (2010). Semiconductor quantum dots and quantum dot arrays and applications of multiple exciton generation to third-generation photovoltaic solar cells. *Chemical Reviews*, *110*(11), 6873-6890.
- Nsibande, S. A., & Forbes, P. B. C. (2016). Fluorescence detection of pesticides using quantum dot materials – A review. *Analytica Chimica Acta*, *945*, 9-22.
- Ochoa-Acuña, H., Frankenberger, J., Hahn, L., & Carbajo, C. (2009). Drinking-water herbicide exposure in Indiana and prevalence of small-for-gestational-age and preterm delivery. *Environmental Health Perspectives*, *117*(10), 1619.
- Okumura, T., & Nishikawa, Y. (1996). Gas chromatography – mass spectrometry determination of triclosans in water, sediment and fish samples via methylation with diazomethane. *Analytica Chimica Acta*, *325*(3), 175-184.
- Oliveira, R., Domingues, I., Koppe Grisolia, C., & Soares, A. M. (2009). Effects of triclosan on zebrafish early-life stages and adults. *Environmental Science and Pollution Research Int*, *16*(6), 679-688.
- Orvos, D. R., Versteeg, D. J., Inauen, J., Capdevielle, M., Rothenstein, A., & Cunningham, V. (2002). Aquatic toxicity of triclosan. *Environmental Toxicology and Chemistry*, *21*(7), 1338-1349.
- Palenske, N. M., Nallani, G. C., & Dzialowski, E. M. (2010). Physiological effects and bioconcentration of triclosan on amphibian larvae. *Comparative Biochemistry and Physiology Part C: Toxicology & Pharmacology*, *152*(2), 232-240.
- Pan, Z., Zhao, K., Wang, J., Zhang, H., Feng, Y., & Zhong, X. (2013). Near infrared absorption of CdSexTe1-x alloyed quantum dot sensitized solar cells with more than 6% efficiency and high stability. *ACS Nano*, *7*(6), 5215-5222.
- Paneth, N. S. (1995). The problem of low birth weight. The future of children, 19-34.
- Pardieu, E., Cheap, H., Vedrine, C., Lazerges, M., Lattach, Y., Garnier, F., Remita, S., & Pernelle, C. (2009). Molecularily imprinted conducting polymer based electrochemical sensor for detection of atrazine. *Analytica Chimica Acta*, *649*(2), 236-245.
- Parolini, M., Pedriali, A., & Binelli, A. (2013). Application of a biomarker response index for ranking the toxicity of five pharmaceutical and personal care products (PPCPs) to the bivalve *Dreissena polymorpha*. *Archives of Environmental Contamination and Toxicology*, *64*(3), 439-447.
- Parrott, J., & Bennie, D. (2009). Life-cycle exposure of fathead minnows to a mixture of six common pharmaceuticals and triclosan. *Journal of Toxicology and Environmental Health, Part A*, *72*(10), 633-641.
- Patterton, H. (2013). Scoping study and research strategy development on currently known and emerging contaminants influencing drinking water quality. (WRC Report No. 2093/1/13). Water Research Commission. Retrieved from <http://goo.gl/qy9R9X>
- Perazzolo, C., Morasch, B., Kohn, T., Magnet, A., Thonney, D., & Chèvre, N. (2010). Occurrence and fate of micropollutants in the Vidy Bay of Lake Geneva, Switzerland. Part I: priority list for environmental risk assessment of pharmaceuticals. *Environmental Toxicology and Chemistry*, *29*(8), 1649-1657.
- Petrović, M., Gonzalez, S., & Barceló, D. (2003). Analysis and removal of emerging contaminants in wastewater and drinking water. *TrAC Trends in Analytical Chemistry*, *22*(10), 685-696.
- Phillips, P. J., Smith, S. G., Kolpin, D., Zaugg, S. D., Buxton, H. T., Furlong, E. T., Esposito, K., & Stinson, B. (2010). Pharmaceutical formulation facilities as sources of opioids and other pharmaceuticals to wastewater treatment plant effluents. *Environmental Science & Technology*, *44*(13), 4910-4916.
- Pick, F. E., van Dyk, L. P., & Botha, E. (1992). Atrazine in ground and surface water in maize production areas of the Transvaal, South Africa. *Chemosphere*, *25*(3), 335-341.
- Pintado-Herrera, M. G., González-Mazo, E., & Lara-Martín, P. A. (2014). Determining the distribution of triclosan and methyl triclosan in estuarine settings. *Chemosphere*, *95*, 478-485.

- Pomati, F., Castiglioni, S., Zuccato, E., Fanelli, R., Vigetti, D., Rossetti, C., & Calamari, D. (2006). Effects of a complex mixture of therapeutic drugs at environmental levels on human embryonic cells. *Environmental Science & Technology*, *40*(7), 2442-2447.
- Qi, D., Fischbein, M., Drndić, M., & Šelmić, S. (2005). Efficient polymer-nanocrystal quantum-dot photodetectors. *Applied Physics Letters*, *86*(9), 093103.
- Ratnesh, R. K., & Mehata, M. S. (2017). Investigation of biocompatible and protein sensitive highly luminescent quantum dots/nanocrystals of CdSe, CdSe/ZnS and CdSe/CdS. *Spectrochimica Acta Part A: Molecular and Biomolecular Spectroscopy*, *179*, 201-210.
- Ratola, N., Homem, V., Silva, J. A., Araujo, R., Amigo, J. M., Santos, L., & Alves, A. (2014). Biomonitoring of pesticides by pine needles – Chemical scoring, risk of exposure, levels and trends. *Science of the Total Environment*, *476-477*, 114-124.
- Raut, S. A., & Angus, R. A. (2010). Triclosan has endocrine-disrupting effects in male western mosquitofish, *Gambusia affinis*. *Environmental Toxicology and Chemistry*, *29*(6), 1287-1291.
- Reddy, S. M., Hawkins, D. M., Phan, Q. T., Stevenson, D., & Warriner, K. (2013). Protein detection using hydrogel-based molecularly imprinted polymers integrated with dual polarisation interferometry. *Sensors and Actuators B: Chemical*, *176*, 190-197.
- Roberts, P. H., & Thomas, K. V. (2006). The occurrence of selected pharmaceuticals in wastewater effluent and surface waters of the lower Tyne catchment. *Science of the Total Environment*, *356*(1-3), 143-153.
- Rodricks, J. V., Swenberg, J. A., Borzelleca, J. F., Maronpot, R. R., & Shipp, A. M. (2010). Triclosan: a critical review of the experimental data and development of margins of safety for consumer products. *Critical Reviews in Toxicology*, *40*(5), 422-484.
- Rossner, A., Snyder, S. A., & Knappe, D. R. (2009). Removal of emerging contaminants of concern by alternative adsorbents. *Water Research*, *43*(15), 3787-3796.
- Sabaliunas, D., Webb, S. F., Hauk, A., Jacob, M., & Eckhoff, W. S. (2003). Environmental fate of triclosan in the River Aire Basin, UK. *Water Research*, *37*(13), 3145-3154.
- Samsøe-Petersen, L., Winther-Nielsen, M., & Madsen, T. (2003). Fate and effects of triclosan. Danish Environmental Protection Agency, 47.
- Sanderson, J. T., Seinen, W., Giesy, J. P., & van den Berg, M. (2000). 2-Chloro-s-triazine herbicides induce aromatase (CYP19) activity in H295R human adrenocortical carcinoma cells: A novel mechanism for estrogenicity? *Toxicological Sciences*, *54*(1), 121-127.
- Santos, T. G., & Martinez, C. B. R. (2012). Atrazine promotes biochemical changes and DNA damage in a Neotropical fish species. *Chemosphere*, *89*(9), 1118-1125.
- Sapsford, K. E., Berti, L., & Medintz, I. L. (2006). Materials for fluorescence resonance energy transfer analysis: beyond traditional donor-acceptor combinations. *Angewandte Chemie International Edition*, *45*(28), 4562-4589.
- SCCS. (2010). Opinion on triclosan – Antimicrobial resistance. (SCCP/1251/09). Scientific Committee on Consumer Safety. Retrieved from http://ec.europa.eu/health/scientific_committees/consumer_safety/index_en.htm
- Schultz, M. M., Furlong, E. T., Kolpin, D. W., Werner, S. L., Schoenfuss, H. L., Barber, L. B., Blazer, V. S., Norris, D. O., & Vajda, A. M. (2010). Antidepressant pharmaceuticals in two US effluent-impacted streams: occurrence and fate in water and sediment, and selective uptake in fish neural tissue. *Environmental Science & Technology*, *44*(6), 1918-1925.
- Selmarten, D., Jones, M., Rumbles, G., Yu, P., Nedeljkovic, J., & Shaheen, S. (2005). Quenching of semiconductor quantum dot photoluminescence by a π -conjugated polymer. *The Journal of Physical Chemistry B*, *109*(33), 15927-15932.
- Shen, J. Y., Chang, M. S., Yang, S. H., & Wu, G. J. (2012b). Simultaneous determination of triclosan, triclocarban, and transformation products of triclocarban in aqueous samples using solid-phase micro-extraction-HPLC-MS/MS. *Journal of Separation Science*, *35*(19), 2544-2552.
- Shen, J., Zhu, Y., Yang, X., & Li, C. (2012a). Graphene quantum dots: emergent nanolights for bioimaging, sensors, catalysis and photovoltaic devices. *Chemical Communications*, *48*(31), 3686-3699.
- Shoji, R., Takeuchi, T., & Kubo, I. (2003). Atrazine sensor based on molecularly imprinted polymer-modified gold electrode. *Analytical Chemistry*, *75*(18), 4882-4886.
- Singer, H., Müller, S., Tixier, C., & Pillonel, L. (2002a). Triclosan: occurrence and fate of a widely used biocide in the aquatic environment: field measurements in wastewater treatment plants, surface waters, and lake sediments. *Environmental Science & Technology*, *36*(23), 4998-5004.
- Smith, G. R., & Burgett, A. A. (2005). Effects of three organic wastewater contaminants on American toad, *Bufo americanus*, tadpoles. *Ecotoxicology*, *14*(4), 477-482.

- Snyder, S., Wert, E., Lei, H., Westerhoff, P., & Yoon, Y. (2007). Removal of EDCs and pharmaceuticals in drinking and reuse treatment processes (91188). Denver, CO, USA: American Water Works Association Research Foundation (AWWARF).
- Sojini, O. S. S., Wang, J.-Z., Sonibare, O. O., & Zeng, E. Y. (2010). Polycyclic aromatic hydrocarbons in sediments and soils from oil exploration areas of the Niger Delta, Nigeria. *Journal of Hazardous Materials*, *174*(1), 641-647.
- Somers, R. C., Snee, P. T., Bawendi, M. G., & Nocera, D. G. (2012). Energy transfer of CdSe/ZnS nanocrystals encapsulated with Rhodamine-dye functionalized poly(acrylic acid). *Journal of Photochemistry and Photobiology A: Chemistry*, *248*, 24-29.
- Son, H.-S., Ko, G., & Zoh, K.-D. (2009). Kinetics and mechanism of photolysis and TiO₂ photocatalysis of triclosan. *Journal of Hazardous Materials*, *166*(2), 954-960.
- Stackelberg, P. E., Gibs, J., Furlong, E. T., Meyer, M. T., Zaugg, S. D., & Lippincott, R. L. (2007). Efficiency of conventional drinking-water-treatment processes in removal of pharmaceuticals and other organic compounds. *Science of the Total Environment*, *377*(2), 255-272.
- Stanisavljevic, M., Krizkova, S., Vaculovicova, M., Kizek, R., & Adam, V. (2015). Quantum dots-fluorescence resonance energy transfer-based nanosensors and their application. *Biosensors and Bioelectronics*, *74*, 562-574.
- Stasinakis, A. S., Petalas, A. V., Mamais, D., Thomaidis, N. S., Gatidou, G., & Lekkas, T. D. (2007). Investigation of triclosan fate and toxicity in continuous-flow activated sludge systems. *Chemosphere*, *68*(2), 375-381.
- Stevens, K. J., Kim, S. Y., Adhikari, S., Vadapalli, V., & Venables, B. J. (2009). Effects of triclosan on seed germination and seedling development of three wetland plants: *Sesbania herbacea*, *Eclipta prostrata*, and *Bidens frondosa*. *Environmental Toxicology and Chemistry*, *28*(12), 2598-2609.
- Stickler, D. J., & Jones, G. L. (2008). Reduced susceptibility of *Proteus mirabilis* to triclosan. *Antimicrobial Agents and Chemotherapy*, *52*(3), 991-994.
- Suarez, S., Dodd, M. C., Omil, F., & von Gunten, U. (2007). Kinetics of triclosan oxidation by aqueous ozone and consequent loss of antibacterial activity: relevance to municipal wastewater ozonation. *Water Research*, *41*(12), 2481-2490.
- Sun, H., Wu, L., Wei, W., & Qu, X. (2013). Recent advances in graphene quantum dots for sensing. *Materials Today*, *16*(11), 433-442.
- Sung, H. H., Chiu, Y. W., Wang, S. Y., Chen, C. M., & Huang, D. J. (2014). Acute toxicity of mixture of acetaminophen and ibuprofen to Green Neon Shrimp, *Neocaridina denticulata*. *Environmental Toxicology and Pharmacology*, *38*(1), 8-13.
- Swan, S. H. (2006). Semen quality in fertile US men in relation to geographical area and pesticide exposure. *International Journal of Andrology*, *29*(1), 62-68.
- Szczeklik, A., Szczeklik, J., Galuszka, Z., Musial, J., Kolarzyk, E., & Targosz, D. (1994). Humoral immunosuppression in men exposed to polycyclic aromatic hydrocarbons and related carcinogens in polluted environments. *Environmental Health Perspectives*, *102*(3), 302.
- Tan, Y., Zhou, Z., Wang, P., Nie, L., & Yao, S. (2001). A study of a bio-mimetic recognition material for the BAW sensor by molecular imprinting and its application for the determination of paracetamol in the human serum and urine. *Talanta*, *55*(2), 337-347.
- Tao, P., Li, Y., Siegel, R. W., & Schadler, L. S. (2013). Transparent luminescent silicone nanocomposites filled with bimodal PDMS-brush-grafted CdSe quantum dots. *Journal of Materials Chemistry C*, *1*(1), 86-94.
- Tatarazako, N., Ishibashi, H., Teshima, K., Kishi, K., & Arizono, K. (2004). Effects of triclosan on various aquatic organisms. *Environmental Sciences: an International Journal of Environmental Physiology and Toxicology*, *(11)*, 133-140.
- Ternes, T. A. (1998). Occurrence of drugs in German sewage treatment plants and rivers. *Water Research*, *32*(11), 3245-3260.
- Ternes, T. A. (2006). Human pharmaceuticals, hormones and fragrances: The challenge of micropollutants in urban water management: International Water Association.
- Thomas, K. V., Dye, C., Schlabach, M., & Langford, K. H. (2007). Source to sink tracking of selected human pharmaceuticals from two Oslo city hospitals and a wastewater treatment works. *Journal of Environmental Monitoring*, *9*(12), 1410-1418.
- Thompson, A., Griffin, P., Stuetz, R., & Cartmell, E. (2005). The fate and removal of triclosan during wastewater treatment. *Water Environment Research*, *77*(1), 63-67.
- Thurman, E. M., & Cromwell, A. E. (2000). Atmospheric transport, deposition, and fate of triazine herbicides and their metabolites in pristine areas at Isle Royale National Park. *Environmental Science & Technology*, *34*(15), 3079-3085.

- Tixier, C., Singer, H. P., Canonica, S., & Müller, S. R. (2002). Phototransformation of triclosan in surface waters: A relevant elimination process for this widely used biocide laboratory studies, field measurements, and modeling. *Environmental Science & Technology*, *36*(16), 3482-3489.
- Togola, A., & Budzinski, H. (2008). Multi-residue analysis of pharmaceutical compounds in aqueous samples. *Journal of Chromatography A*, *1177*(1), 150-158.
- Toxicological Summary for: Acetaminophen. (2010). Retrieved from www.health.state.mn.us/divs/eh/risk/guidance/dwec/sumacetamin.pdf
- Toxicological Summary: Triclosan. (2010). Retrieved from www.health.state.mn.us/divs/eh/risk/guidance/gw/triclosan.pdf
- USEPA. (2010). Existing Water Quality Standards. Retrieved from <https://www3.epa.gov/region1/npdes/remediation/Appendix-A.pdf>
- USEPA. (2015). Basic information on CCL and regulatory determinations Retrieved from <http://www2.epa.gov/ccl/regulatory-determination-3>
- USEPA. (21 July 2015). Pharmaceuticals and Personal Care Products (PPCP). Retrieved from <http://www.epa.gov/ppcp/>
- Van Leeuwen, J. A., Waltner-Toews, D., Abernathy, T., Smit, B., & Shoukri, M. (1999). Associations between stomach cancer incidence and drinking water contamination with atrazine and nitrate in Ontario (Canada) agroecosystems, 1987-1991. *International Journal of Epidemiology*, *28*(5), 836-840.
- Veldhoen, N., Skirrow, R. C., Osachoff, H., Wigmore, H., Clapson, D. J., Gunderson, M. P., Van Aggelen, G., & Helbing, C. C. (2006). The bactericidal agent triclosan modulates thyroid hormone-associated gene expression and disrupts postembryonic anuran development. *Aquatic Toxicology*, *80*(3), 217-227.
- Versteegh, J., Van Der Aa, N., & Dijkman, E. (2007). Pharmaceuticals in drinking water and sources of drinking water-results of monitoring campaign 2005/2006 (geneesmiddelen in drinkwater en drinkwaterbronnen-resultaten van het meetprogramma 2005/2006). Retrieved from 53, RIVM, Bilthoven, The Netherlands: Number: R.
- Vidal, L., Chisvert, A., Canals, A., Psillakis, E., Lapkin, A., Acosta, F., Edler, K. J., Holdaway, J. A., & Marken, F. (2008). Chemically surface-modified carbon nanoparticle carrier for phenolic pollutants: Extraction and electrochemical determination of benzophenone-3 and triclosan. *Analytica Chimica Acta*, *616*(1), 28-35.
- Waller, S. A., Paul, K., Peterson, S. E., & Hitti, J. E. (2010). Agricultural-related chemical exposures, season of conception, and risk of gastroschisis in Washington State. *American Journal of Obstetrics and Gynecology*, *202*(3), 241.
- Waltman, E. L., Venables, B. J., & Waller, W. T. (2006). Triclosan in a North Texas wastewater treatment plant and the influent and effluent of an experimental constructed wetland. *Environmental Toxicology and Chemistry*, *25*(2), 367-372.
- Wang, C., Ma, Q., Dou, W., Kanwal, S., Wang, G., Yuan, P., & Su, X. (2009). Synthesis of aqueous CdTe quantum dots embedded silica nanoparticles and their applications as fluorescence probes. *Talanta*, *77*(4), 1358-1364.
- Wang, H., Zhang, A., Wang, W., Zhang, M., Liu, H., & Wang, X. (2013). Separation and determination of triclosan and bisphenol A in water, beverage, and urine samples by dispersive liquid-liquid microextraction combined with capillary zone electrophoresis-UV detection. *Journal of AOAC International*, *96*(2), 459-465.
- Wang, L., Huang, Z., Gao, Q., Liu, Y., Kou, X., & Xiao, D. (2015). A novel pyrene fluorescent sensor based on the π - π interaction between pyrene and graphene of graphene-cadmium telluride quantum dot nanocomposites. *Spectroscopy Letters*, *48*(10), 748-756.
- Wang, L., Zhu, S.-J., Wang, H.-Y., Qu, S.-N., Zhang, Y.-L., Zhang, J.-H., Chen, Q.-D., Xu, H.-L., Han, W., Yang, B., & Sun, H.-B. (2014). Common origin of green luminescence in carbon nanodots and graphene quantum dots. *ACS Nano*, *8*(3), 2541-2547.
- Wang, S., Cole, I. S., & Li, Q. (2016). The toxicity of graphene quantum dots. *RSC Advances*, *6*(92), 89867-89878.
- Wang, X., Li, W., & Sun, K. (2011). Stable efficient CdSe/CdS/ZnS core/multi-shell nanophosphors fabricated through a phosphine-free route for white light-emitting-diodes with high color rendering properties. *Journal of Materials Chemistry*, *21*(24), 8558-8565.
- Wang, X., Yu, J., Kang, Q., Shen, D., Li, J., & Chen, L. (2016a). Molecular imprinting ratiometric fluorescence sensor for highly selective and sensitive detection of phycocyanin. *Biosensors and Bioelectronics*, *77*, 624-630.
- Wang, X., Yu, J., Wu, X., Fu, J., Kang, Q., Shen, D., Li, J., & Chen, L. (2016b). A molecular imprinting-based turn-on ratiometric fluorescence sensor for highly selective and sensitive detection of 2, 4-dichlorophenoxyacetic acid (2, 4-D). *Biosensors and Bioelectronics*, *81*, 438-444.

- Weber, F. A., Bergmann, A., Hickmann, S., Ebert, I., Hein, A., & Küster, A. (2016). Pharmaceuticals in the environment – Global occurrences and perspectives. *Environmental Toxicology and Chemistry*, 35(4), 823-835.
- Wei, W., Zhang, D. M., Yin, L. H., Pu, Y. P., & Liu, S. Q. (2013). Colorimetric detection of DNA damage by using hemin-graphene nanocomposites. *Spectrochimica Acta Part A: Molecular and Biomolecular Spectroscopy*, 106, 163-169.
- Wert, E. C., Rosario-Ortiz, F. L., & Snyder, S. A. (2009). Effect of ozone exposure on the oxidation of trace organic contaminants in wastewater. *Water Research*, 43(4), 1005-1014.
- Westerhoff, P., Yoon, Y., Snyder, S., & Wert, E. (2005). Fate of endocrine-disruptor, pharmaceutical, and personal care product chemicals during simulated drinking water treatment processes. *Environmental Science & Technology*, 39(17), 6649-6663.
- WHO. (2011). Guidelines for Drinking-water Quality 4th Edition. Retrieved from http://apps.who.int/iris/bitstream/10665/44584/1/9789241548151_eng.pdf
- William, W. Y., Chang, E., Drezek, R., & Colvin, V. L. (2006). Water-soluble quantum dots for biomedical applications. *Biochemical and Biophysical Research Communications*, 348(3), 781-786.
- Wilson, B. A., Smith, V. H., deNoyelles, F., & Larive, C. K. (2003). Effects of three pharmaceutical and personal care products on natural freshwater algal assemblages. *Environmental Science & Technology*, 37(9), 1713-1719.
- Wilson, W. L., Szajowski, P. F., & Brus, L. E. (1993). Quantum confinement in size-selected, surface-oxidized silicon nanocrystals. *Science*, 262(5137), 1242-1242.
- Wu, S., Zhang, L., & Chen, J. (2012). Paracetamol in the environment and its degradation by microorganisms. *Applied Microbiology and Biotechnology*, 96(4), 875-884.
- Wuister, S. F., de Mello Donegá, C., & Meijerink, A. (2004). Luminescence temperature anti-quenching of water-soluble CdTe quantum dots: role of the solvent. *Journal of the American Chemical Society*, 126(33), 10397-10402.
- Xie, R., Kolb, U., Li, J., Basché, T., & Mews, A. (2005). Synthesis and characterization of highly luminescent CdSe-Core CdS/ZnO.5Cd0.5S/ZnS multishell nanocrystals. *Journal of the American Chemical Society*, 127(20), 7480-7488.
- Xie, Z., Ebinghaus, R., Flöser, G., Caba, A., & Ruck, W. (2008). Occurrence and distribution of triclosan in the German Bight (North Sea). *Environmental Pollution*, 156(3), 1190-1195.
- Xu, H., Miao, R., Fang, Z., & Zhong, X. (2011). Quantum dot-based “turn-on” fluorescent probe for detection of zinc and cadmium ions in aqueous media. *Analytica Chimica Acta*, 687(1), 82-88.
- Yang, J., Wang, J., Zhao, K., Izuishi, T., Li, Y., Shen, Q., & Zhong, X. (2015). CdSeTe/CdS Type-I Core/Shell Quantum Dot Sensitized Solar Cells with Efficiency over 9%. *The Journal of Physical Chemistry C*, 119(52), 28800-28808.
- Yang, L. H., Ying, G. G., Su, H. C., Stauber, J. L., Adams, M. S., & Binet, M. T. (2008). Growth-inhibiting effects of 12 antibacterial agents and their mixtures on the freshwater microalga *pseudokirchneriella subcapitata*. *Environmental Toxicology and Chemistry*, 27(5), 1201-1208.
- Yang, Y., Yi, C., Luo, J., Liu, R., Liu, J., Jiang, J., & Liu, X. (2011). Glucose sensors based on electrodeposition of molecularly imprinted polymeric micelles: A novel strategy for MIP sensors. *Biosensors and Bioelectronics*, 26(5), 2607-2612.
- Ying, G.-G., & Kookana, R. S. (2007). Triclosan in wastewaters and biosolids from Australian wastewater treatment plants. *Environment International*, 33(2), 199-205.
- Yola, M. L., & Atar, N. (2017). Electrochemical detection of atrazine by platinum nanoparticles/carbon nitride nanotubes with molecularly imprinted polymer. *Industrial & Engineering Chemistry Research*, 56(27), 7631-7639.
- Yong, K. T., Law, W. C., Roy, I., Jing, Z., Huang, H., Swihart, M. T., & Prasad, P. N. (2011). Aqueous phase synthesis of CdTe quantum dots for biophotonics. *Journal of Biophotonics*, 4(1-2), 9-20.
- Young, T. A., Heidler, J., Matos-Pérez, C. R., Sapkota, A., Toler, T., Gibson, K. E., Schwab, K. J., & Halden, R. U. (2008). Ab initio and in situ comparison of caffeine, triclosan, and triclocarban as indicators of sewage-derived microbes in surface waters. *Environmental Science & Technology*, 42(9), 3335-3340.
- Yu, C., & Mosbach, K. (1997). Molecular imprinting utilizing an amide functional group for hydrogen bonding leading to highly efficient polymers. *The Journal of Organic Chemistry*, 62(12), 4057-4064.
- Yu, J., Wang, X., Kang, Q., Li, J., Shen, D., & Chen, L. (2017). One-pot synthesis of a quantum dot-based molecular imprinting nanosensor for highly selective and sensitive fluorescence detection of 4-nitrophenol in environmental waters. *Environmental Science: Nano*, 4(2), 493-502.
- Yuan, L., Zhang, J., Zhou, P., Chen, J., Wang, R., Wen, T., Li, Y., Zhou, X., & Jiang, H. (2011). Electrochemical sensor based on molecularly imprinted membranes at platinum nanoparticles-modified electrode for determination of 17 β -estradiol. *Biosensors and Bioelectronics*, 29(1), 29-33.

- Zeledón-Toruño, Z. C., Lao-Luque, C., de las Heras, F. X. C., & Sole-Sardans, M. (2007). Removal of PAHs from water using an immature coal (leonardite). *Chemosphere*, *67*(3), 505-512.
- Zhang, F., Liu, F., Wang, C., Xin, X., Liu, J., Guo, S., & Zhang, J. (2016). Effect of lateral size of graphene quantum dots on their properties and application. *ACS Applied Materials & Interfaces*, *8*(3), 2104-2110.
- Zhang, H., Wang, C., Li, M., Zhang, J., Lu, G., & Yang, B. (2005). Fluorescent nanocrystal-polymer complexes with flexible processability. *Advanced Materials*, *17*(7), 853-857.
- Zhang, H., Wang, L.-P., Xiong, H., Hu, L., Yang, B., & Li, W. (2003). Hydrothermal synthesis for high-quality CdTe nanocrystals. *Advanced Materials*, *15*(20), 1712-1715.
- Zhang, S., Zhang, Q., Darisaw, S., Ehie, O., & Wang, G. (2007). Simultaneous quantification of polycyclic aromatic hydrocarbons (PAHs), polychlorinated biphenyls (PCBs), and pharmaceuticals and personal care products (PPCPs) in Mississippi river water, in New Orleans, Louisiana, USA. *Chemosphere*, *66*(6), 1057-1069.
- Zhao, G., Yang, L., Wu, S., Zhao, H., Tang, E., & Li, C. P. (2017). The synthesis of amphiphilic pillar [5] arene functionalized reduced graphene oxide and its application as novel fluorescence sensing platform for the determination of acetaminophen. *Biosensors and Bioelectronics*, *91*, 863-869.
- Zhao, J.-L., Zhang, Q.-Q., Chen, F., Wang, L., Ying, G.-G., Liu, Y.-S., Yang, B., Zhou, L.-J., Liu, S., & Su, H.-C. (2013). Evaluation of triclosan and triclocarban at river basin scale using monitoring and modeling tools: implications for controlling of urban domestic sewage discharge. *Water Research*, *47*(1), 395-405.
- Zhao, X. (1990). Effects of benzo (a) pyrene on the humoral immunity of mice exposed by single intraperitoneal injection. *Zhonghua yu fang yi xue za zhi [Chinese Journal of Preventive Medicine]*, *24*(4), 220-222.
- Zheng, X. T., Ananthanarayanan, A., Luo, K. Q., & Chen, P. (2015). Glowing graphene quantum dots and carbon dots: Properties, syntheses, and biological applications. *Small*, *11*(14), 1620-1636.
- Zhu, S., Song, Y., Zhao, X., Shao, J., Zhang, J., & Yang, B. (2015). The photoluminescence mechanism in carbon dots (graphene quantum dots, carbon nanodots, and polymer dots): current state and future perspective. *Nano Research*, *8*(2), 355-381.
- Zor, E., Morales-Narváez, E., Zamora-Gálvez, A., Bingol, H., Ersoz, M., & Merkoçi, A. (2015). Graphene quantum dots-based photoluminescent sensor: A multifunctional composite for pesticide detection. *ACS Applied Materials & Interfaces*, *7*, 20272-20279.
- Zucolotto, V., et al. (2005). Nanoscale manipulation of CdSe quantum dots in layer-by-layer films: influence of the host polyelectrolyte on the luminescent properties. *Applied Surface Science*, *246*(4), 397-402.

APPENDIX: CAPACITY BUILDING & KNOWLEDGE DISSEMINATION

CAPACITY BUILDING

The students and their research topics listed below have contributed directly to the objectives of this project:

Hons research project report:

Miss Raquel da Costa (Graduated April 2017):

Synthesising molecularly imprinted polymers (MIPs) to use as sorbents in the solid phase extraction (SPE) of polycyclic aromatic hydrocarbons (PAHs).

BSc Hons Chemistry, University of Pretoria.

Supervisor: Prof Patricia Forbes

MSc students:

Miss Kedibone Mashale (in progress):

Monitoring of selected pesticide concentrations in South African aquatic systems using the Chemcatcher passive sampler.

MSc Chemistry, University of Pretoria.

Supervisor: Prof Patricia Forbes

Co-Supervisor: Dr Yvette Naudé

Mr Basil Munjanja (in progress):

Comparison of pesticide deposition sampling methods for spray drift of atrazine.

MSc Chemistry, University of Pretoria.

Supervisor: Prof Patricia Forbes

Co-Supervisor: Dr Yvette Naudé

Mr Paul Myburgh (in progress):

Development of analytical methods for pesticide determinations.

MSc Chemistry, University of Pretoria.

Supervisor: Prof Patricia Forbes

PhD theses:

Mr Sifiso Nsibande (in progress):

Novel fluorescence sensors for pesticides and polycyclic aromatic hydrocarbons.

PhD Chemistry, University of Pretoria.

Supervisor: Prof Patricia Forbes

Miss Hanieh Montaseri (Completed December 2018):

Quantum dot – molecularly imprinted polymer nanomaterials for the fluorescence sensing of selected pharmaceutical and personal care products.

PhD Chemistry, University of Pretoria.

Supervisor: Prof Patricia Forbes

KNOWLEDGE DISSEMINATION

Published journal papers:

1. Sifiso A. Nsibande and Patricia B.C. Forbes, Development of a quantum dot molecularly imprinted polymer sensor for fluorescence detection of atrazine, *Luminescence*, 2019, *accepted for publication*.
2. Oluwasesan Adegoke, Hanieh Montaseri, Sifiso Nsibande and Patricia B.C. Forbes, Passivating effect of ternary alloyed AgZnSe shell layer on the structural and luminescent properties of CdS quantum dots, *Materials Science in Semiconductor Processing*, 2019, 90, 162-170.
3. H. Montaseri and P.B.C. Forbes, Molecularly imprinted polymer coated quantum dots for fluorescence sensing of acetaminophen, *Materials Today Communications*, 2018, 17, 480-492.
4. H. Montaseri and P.B.C. Forbes, Analytical techniques for the determination of acetaminophen: A review, *TrAC Trends in Analytical Chemistry*, 2018, 108, 122-134.
5. H. Montaseri and P.B.C. Forbes, A triclosan turn-ON fluorescence sensor based on thiol-capped core/shell quantum dots, *Spectrochimica Acta Part A: Molecular and Biomolecular Spectroscopy*, 2018, 204, 370-379.
6. Oluwasesan Adegoke, Hanieh Montaseri, Sifiso Nsibande and Patricia B.C. Forbes, Alloyed quaternary/binary core/shell quantum dot-graphene oxide nanocomposite: Preparation, characterization and application as a fluorescence “switch ON” probe for environmental pollutants, *Journal of Alloys and Compounds*, 2017, 720, 70-78.
7. Oluwasesan Adegoke, Tebello Nyokong and Patricia B.C. Forbes, Photophysical properties of a series of alloyed and non-alloyed water-soluble L-cysteine-capped core quantum dots, *Journal of Alloys and Compounds*, 2017, 695, 1354-1361.

8. Oluwasesan Adegoke, Tebello Nyokong and Patricia B.C. Forbes, Deposition of CdS, CdS/ZnSe and CdS/ZnSe/ZnS shells around CdSeTe alloyed core quantum dots: effects on optical properties, *Luminescence*, 2016, 31, 694-703.
9. Oluwasesan Adegoke, Philani Mashazi, Tebello Nyokong and Patricia B.C. Forbes, Fluorescence properties of alloyed ZnSeS quantum dots overcoated with ZnTe and ZnTe/ZnS shells, *Optical Materials*, 2016, 54, 104-110.

Conference oral and invited presentations:

1. *Guest presentations:* P. Forbes, "An overview of nanoparticle analysis", PerkinElmer Innovation Tour, Johannesburg, Durban and Cape Town, 7-9 March 2017.
2. *Guest lecture:* P. Forbes, "Addressing the challenges of monitoring organic environmental pollutants", Laboratory Services Branch of the Ontario Ministry of the Environment and Climate Change, Toronto Canada, 2 June 2017.
3. *Plenary lecture:* P.B.C. Forbes, "Quantum dot based photonic sensor materials for emerging chemical pollutants in water", International Symposium on Luminescence Spectrometry (ISLS), 19-22 June 2018, Brest, France.
4. *Keynote address:* P.B.C. Forbes, "Seeing the invisible: Fluorescence sensors for detecting emerging chemical pollutants in water", SACI National Convention 2018, 2-7 December 2018, CSIR ICC, Pretoria.
5. Nsibandé, S.A. and Forbes, P.B.C., "Synthesis of graphene quantum dots and their application as fluorescence sensors for polycyclic aromatic hydrocarbons", 7th International Conference on Nanoscience and Nanotechnology in Africa, 22-25 April 2018, Salt Rock, KwaZulu-Natal.
6. Nsibandé, S.A. and Forbes, P.B.C. "Development of a quantum dot molecularly imprinted polymer sensor for fluorescence detection of atrazine", International Symposium on Luminescence Spectrometry (ISLS), 19-22 June 2018, Brest, France.
7. H Montaseri, PBC Forbes, "A novel fluorescence sensor for acetaminophen", Analitika 2018 Conference, 22-25 July 2018, Limpopo, South Africa.
8. K.N. Mashale, Y. Naudé, J.M. Dabrowski and P.B.C. Forbes, "Monitoring of pesticide concentrations in South African aquatic systems through the use of a Chemcatcher passive sampler", SACI National Convention 2018, 2-7 December 2018, CSIR ICC, Pretoria.

Conference poster presentations:

1. Hanieh Montaseri and Patricia Forbes, "Synthesis and characterization of L-cysteine capped CdSe/ZnS quantum dots coated with a molecularly imprinted polymer", SACI Inorganic 2017 Conference, 25-29 June 2017, Hermanus, South Africa.
2. Sifiso Nsibande and Patricia Forbes, "Preparation of graphene quantum dots for fluorescence sensing of polycyclic aromatic hydrocarbons", SACI Inorganic 2017 Conference, 25-29 June 2017, Hermanus, South Africa.
3. Hanieh Montaseri and Patricia Forbes, "Synthesis and characterization of L-cysteine capped CdSe/ZnS quantum dots coated with a molecularly imprinted polymer", South African Nanotechnology Initiative, 7th Annual Gauteng Nanosciences Young Researchers' Symposium, 20 October 2017, Tshwane University of Pretoria, Pretoria, South Africa.
4. Hanieh Montaseri and Patricia Forbes, "Fluorescence sensor probe for the detection of acetaminophen using L-cysteine CdSe/ZnS quantum dots and molecular imprinted polymer@quantum dots", IEEE Sensors 2017, 29 October-1 November 2017, Glasgow, Scotland.
5. KN Mashale, Y Naudé, JM Dabrowski, PBC Forbes, "Calibration of the Chemcatcher passive sampler for the monitoring of pesticide concentrations in South African aquatic systems", Analitika 2018 Conference, 22-25 July 2018, Limpopo, South Africa.
6. SA Nsibande and PBC Forbes, "Development of a quantum dot fluorescence sensor for detection of atrazine", Analitika 2018 Conference, 22-25 July 2018, Limpopo, South Africa.
7. BK Munjanja, Y Naude, J Dabrowski, E Van de Walt, PBC Forbes, "Comparison of pesticide deposition samplers for spray drift determination: A case study of atrazine", Analitika 2018 Conference, 22-25 July 2018, Limpopo, South Africa.